

University of Southampton Research Repository ePrints Soton

Copyright © and Moral Rights for this thesis are retained by the author and/or other copyright owners. A copy can be downloaded for personal non-commercial research or study, without prior permission or charge. This thesis cannot be reproduced or quoted extensively from without first obtaining permission in writing from the copyright holder/s. The content must not be changed in any way or sold commercially in any format or medium without the formal permission of the copyright holders.

When referring to this work, full bibliographic details including the author, title, awarding institution and date of the thesis must be given e.g.

AUTHOR (year of submission) "Full thesis title", University of Southampton, name of the University School or Department, PhD Thesis, pagination

UNIVERSITY OF SOUTHAMPTON

FACULTY OF MEDICINE

Cancer Sciences Unit

Chronic Lymphocytic Leukaemia and the
microenvironment: Investigating the
interplay between CLL cells, fibroblasts and
myofibroblasts

by

Samantha Damayanthi Dias

Thesis for the degree of Doctor of Philosophy (PhD)

September 2014

UNIVERSITY OF SOUTHAMPTON

ABSTRACT

FACULTY OF MEDICINE

Doctor of Philosophy

Thesis for the degree of Doctor of Philosophy

CHRONIC LYMPHOCYTIC LEUKAEMIA AND THE
MICROENVIRONMENT: INVESTIGATING THE INTERPLAY BETWEEN
CLL CELLS, FIBROBLASTS AND MYOFIBROBLASTS

by Samantha Damayanthi Dias

Chronic lymphocytic leukaemia (CLL) is a common B-cell malignancy characterised by the accumulation of malignant B cells in the blood, bone marrow and secondary lymphoid organs. CLL cells rapidly undergo apoptosis when removed from the body, indicating they are dependent on supporting cells within tissue microenvironments. This study investigated potential supporting interactions of CLL cells with fibroblasts and myofibroblasts (activated fibroblasts), important components of the tumour stroma in solid cancers. The overarching hypothesis is that CLL cells alter fibroblast to myofibroblast transdifferentiation and that this, in turn, creates an optimal protective niche through modulation of Bcl-2 family proteins and apoptotic pathways.

The first experiments characterised the presence of myofibroblasts in the CLL lymph node microenvironment *in vivo*, and evaluated various co-culture systems prior to detailed analysis of CLL cell/(myo)fibroblast interactions *in vitro*. **Immunohistochemical analysis of α -smooth muscle actin (α -SMA)**, a hallmark of myofibroblasts, demonstrated that myofibroblasts were present within the CLL microenvironment but with substantial variation between individual patients. The human foetal foreskin fibroblast (HFFF2) cell line was selected as a suitable experimental model for this project. Then the effect of CLL cells on myofibroblast transdifferentiation was investigated and showed that CLL cells can prevent myofibroblast transdifferentiation. Next the effect of fibroblasts and myofibroblasts on CLL cell viability was investigated and demonstrated that fibroblasts and myofibroblasts protect CLL cells from apoptosis, but fibroblasts have a greater protective effect. Additionally fibroblasts and myofibroblasts increased expression of the anti-apoptotic protein MCL-1 within CLL cells, yet fibroblasts had a greater effect. Following this the intracellular signalling pathways responsible for fibroblast-mediated protection of CLL cells was investigated and suggested that SYK, PI3K signalling and BTK are involved.

Overall the results are consistent with the initial hypothesis as CLL cells may block myofibroblast transdifferentiation therefore retaining these stromal cells as fibroblasts in order to create an optimal protective niche within which CLL cells evade undergoing apoptosis via SYK-dependent up-regulation of MCL-1.

Table of Contents

ABSTRACT	i
Table of Contents	iii
List of tables	ix
List of figures	xi
DECLARATION OF AUTHORSHIP	xix
Acknowledgements	xxi
Definitions and Abbreviations	xxiii
Chapter 1:	1
Introduction	1
1.1 Introduction	2
1.2 Chronic lymphocytic leukaemia	2
1.2.1 Chronic lymphocytic leukaemia	2
1.2.2 CLL epidemiology	5
1.2.3 Aetiology of CLL	5
1.2.4 Symptoms and diagnosis	10
1.2.5 Treatment strategies	10
1.3 The microenvironment and stromal cells: healthy versus malignant states	13
1.3.1 The healthy ‘non-malignant’ microenvironment	13
1.3.2 The bone marrow microenvironment	14
1.3.3 Secondary lymphoid organ microenvironment	16
1.3.4 Microenvironment in solid tumours	19
1.3.5 Microenvironment in blood cancers	20
1.4 CLL and the microenvironment	21
1.4.1 CLL cell infiltration	21
1.4.2 Effect of the microenvironment on CLL cells	22
1.5 Fibroblasts and myofibroblasts	30

1.5.1	Fibroblasts	30
1.5.2	Myofibroblasts	31
1.5.3	Myofibroblasts in cancer	34
1.5.4	Fibroblast-to-myofibroblast transdifferentiation	35
1.5.5	Differentiation versus transdifferentiation.....	37
1.6	TGF- β signalling	38
1.6.1	TGF- β structure and activation	38
1.6.2	TGF- β signalling	38
1.6.3	Effect of TGF- β under normal and malignant conditions	40
1.7	CLL and apoptosis	42
1.8	B-cell receptor signalling.....	43
1.9	PI3K/AKT signalling pathway	46
1.10	MAPK signalling pathway	48
1.11	NFκB signalling pathway	48
1.12	Hypothesis	50
1.13	Aims	50
Chapter 2:	53
Materials and methods	53
2.1	Cell culture	54
2.1.1	Primary cells	54
2.1.2	Cell lines.....	55
2.1.3	Cell culture	55
2.1.4	Freezing cells for long-term storage.....	57
2.1.5	Defrosting cells for culture	57
2.1.6	Co-cultures.....	57
2.1.7	Counting viable cells	58
2.1.8	Generating conditioned media from CLL cells	58
2.1.9	Generating conditioned media from HFFF2 cells	58
2.2	SDS-PAGE and western blotting	59
2.2.1	Cell lysate preparation.....	59

2.2.2	Bicinchoninic acid (BCA) protein assay	59
2.2.3	Preparing polyacrylamide gels	60
2.2.4	Western blotting.....	60
2.2.5	Stripping membranes	63
2.3	Treatment with small molecule inhibitors.....	63
2.4	TGF-beta (TGF- β) luciferase assays	63
2.5	Immunofluorescence	66
2.6	Induction of myofibroblast transdifferentiation	66
2.7	Adhesion assays.....	69
2.8	Annexin V assays	69
2.9	Reactive oxygen species (ROS) analysis	70
2.10	Exosome extraction.....	70
2.11	Statistical analysis	71
2.12	Solutions.....	71
Chapter 3:.....		75
Analysis of CLL/SLL tissues and selection of an appropriate experimental model for studies in vitro		75
3.1	Introduction	76
3.2	Analysis of α-SMA expression in normal and CLL/SLL tissues...	76
3.3	Analysis of palladin expression in CLL/SLL tissue.....	82
3.4	Determining if there is a link between α -SMA, ZAP-70 and Ki-67 in CLL/SLL tissue	83
3.5	Selecting a suitable experimental model system.....	94
3.5.1	Human Caucasian Foetal Foreskin Fibroblast (HFFF2) cell line	94
3.5.2	Characterising fibroblasts isolated from CLL lymph node tissue.....	95
3.5.3	Characterisation of STRO-1 positive cells.....	98
3.6	Discussion.....	101
3.6.1	Presence of myofibroblasts within unaffected and CLL/SLL-affected LNs	104
3.6.2	Variability in α-SMA expression.....	106

3.6.3	Selecting a suitable experimental model	108
3.6.4	Summary.....	110
Chapter 4:	113
Investigation of the effect of CLL cells on myofibroblast transdifferentiation.....		113
4.1 Introduction		114
4.2 Investigating the effect of CLL cells on myofibroblast transdifferentiation		114
4.2.1 Determining the effect of co-culture with CLL samples on HFFF2 cells.....		114
4.2.2 Determining the effect of CLL cell-derived soluble factors on HFFF2 fibroblasts		123
4.3 Investigating the effect of CLL cells on TGF- β directed myofibroblast transdifferentiation		125
4.4 Determining if CLL cells can activate TGF-β		132
4.5 Correlating the effect of CLL cells on HFFF2 α-SMA expression with their ability to activate TGF-β1		135
4.6 Preliminary analysis of effects of CLL cell-derived exosomes on myofibroblast transdifferentiation.		140
4.7 Discussion		144
4.7.1 Effect of CLL cells on myofibroblast transdifferentiation		146
4.7.2 Intrasample variation.....		148
4.7.3 Effect of soluble factors and exosomes on transdifferentiation		149
4.7.4 CLL cells can activate TGF- β 1		151
4.7.5 Summary.....		153
Chapter 5:		155
Investigation of the impact of stromal cells on CLL viability and adhesion		155
5.1 Introduction.....		156
5.2 Comparing the protective effect of fibroblasts and myofibroblasts on CLL cells		156

5.3	Investigating the effect of fibroblasts on caspase activity	168
5.4	Comparing CLL cell adhesion to fibroblasts and myofibroblasts	170
5.5	Effect of HFFF2 fibroblasts on reactive oxygen species (ROS) signalling in CLL cells	180
5.6	Investigating the effects of HFFF2 fibroblasts on Bcl-2 family proteins in CLL cells	186
5.6.1	Analysis of MCL-1 and BIMEL expression in CLL cells ..	186
5.6.2	Analysis of MCL-1 expression at earlier time-points ...	192
5.6.3	Comparing the effect of fibroblasts and myofibroblasts on MCL-1 expression	192
5.7	Discussion.....	196
5.7.1	Fibroblasts have a greater protective effect on CLL cells than myofibroblasts	199
5.7.2	HFFF2 fibroblasts do not protect CLL cells by reducing intrinsic ROS.....	201
5.7.3	Fibroblasts and myofibroblasts alter Bcl-2 family proteins in CLL cells.....	201
5.7.4	Effect of soluble factors on CLL viability.....	204
5.7.5	Variation in CLL viability	205
5.7.6	CLL cells preferentially bind to fibroblasts than to myofibroblasts	206
5.7.7	Summary.....	207
Chapter 6:	209
Investigation of the effect of fibroblasts on intracellular signalling pathways in CLL		209
6.1	Introduction	210
6.2	Determining which intracellular signal transduction pathways are activated within CLL cells by HFFF2 fibroblasts.....	210
6.3	Investigating the effect of small molecule inhibitors on fibroblast-induced protection of CLL cells.....	219
6.4	Investigating the effect of small molecule inhibitors on MCL-1 expression	233

6.5 Discussion	239
6.5.1 Determining which signalling pathways effect fibroblast- induced CLL survival	241
6.5.2 Summary.....	247
Chapter 7:	250
Final Discussion.....	250
7.1 Basis of project	251
7.2 Summary of key findings	251
7.3 Overview of key findings	253
7.4 Further work to extend current data	256
7.4.1 Chapter 3.....	256
7.4.2 Chapter 4.....	257
7.4.3 Chapter 5.....	258
7.4.4 Chapter 6.....	258
7.5 Future work.....	259
7.5.1 Gene expression profiling (GEP) study	259
7.5.2 <i>In vivo</i> studies.....	260
7.5.3 Drug-induced apoptosis	261
Appendices.....	263
Appendix A.....	265
A.1 CLL samples.....	265
A.2 Effect of HFFF2 fibroblast CM on CLL cell viability	268
List of References.....	269

List of tables

Table 1.1: Stromal cell surface expression markers.....	27
Table 2.1: Primary cells and cell lines	56
Table 2.2: Recipe for preparing separating and stacking gels	61
Table 2.3: Primary antibodies used for western blotting	62
Table 2.4: Secondary antibodies used for western blotting.....	64
Table 2.5: Small molecule inhibitors used to inhibit intracellular signalling pathways	65
Table 2.6: Primary antibodies used for immunofluorescence	67
Table 2.7: Secondary antibodies used for immunofluorescence	68
Table 3.1: Summary of α-SMA, ZAP-70 and Ki-67 expression in CLL/SLL lymph node tissue	81
Table 3.2: Summary of α-SMA and ZAP-70 expression in CLL/SLL patients	90
Table 3.3: Summary of α-SMA and ZAP-70 expression in Richter's patients	92
Table 3.4: Summary of positive and negative characteristics of the stromal cell types	111
Table 4.1: Summary of effect of CLL sample co-culture on HFFF2 α-SMA expression for 13 CLL samples analysed	120
Table 4.2: Effect of CLL cells on HFFF2 α-SMA expression correlated with their ability to activate TGF-β	141
Table 5.1: Summary of statistical analysis performed on annexin V assay data	165
Table A.1: CLL samples	265

List of figures

Figure 1.1: The structure of the B- cell receptor	4
Figure 1.2: Diagram showing the hierarchy of haematopoietic stem cells, progenitor cells and their differentiation progeny.....	15
Figure 1.3: Diagram of stromal cell origin	17
Figure 1.4: Diagram showing the structure of the lymph nodes	18
Figure 1.5: Diagram showing how CLL cells access the tissue microenvironment from the peripheral blood	24
Figure 1.6: Diagram showing the various sources of myofibroblasts	32
Figure 1.7: Diagram highlighting the key stages of myofibroblast transd ifferentiation	36
Figure 1.8: TGF- β signalling pathway	39
Figure 1.9: B-cell receptor signal transduction pathway	45
Figure 1.10: PI3K/AKT signal transduction pathway	47
Figure 1.11: MAPK signal transduction pathway	49
Figure 1.12: NFκB signal transduction pathway	51
Figure 3.1: Immunohistochemical analysis of non-CLL/SLL lymph nodes for α-SMA and CD21 expression	78
Figure 3.2: Expression of α-SMA within CLL/SLL lymph node tissue	79
Figure 3.3: α-SMA expression within a PC of CLL/SLL lymph node tissue	80
Figure 3.4: Immunohistochemical staining of CLL/SLL lymph nodes for α-SMA and palladin	84
Figure 3.5: Expression of ZAP-70 in CLL/SLL lymph nodes	85
Figure 3.6: Expression of Ki-67 in CLL/SLL lymph nodes	86

Figure 3.7: Comparison of α-SMA and ZAP-70 expression in CLL/SLL LNs.....	91
Figure 3.8: Comparison of α-SMA and ZAP-70 expression in Richter's LNs.....	93
Figure 3.9: Analysis of α-SMA expression in HFFF2 fibroblasts and HFFF2-derived myofibroblasts.....	96
Figure 3.10: Analysis of α-SMA expression in HFFF2 fibroblasts and HFFF2-derived myofibroblasts.....	97
Figure 3.11: Analysis of α-SMA expression in fibroblast-like cells derived from CLL LN.....	99
Figure 3.12: α-SMA expression in STRO-1 cells.....	100
Figure 3.13: STRO-1 and α -SMA expression in STRO-1 cells.....	102
Figure 3.14: Effect of TGF- β on α -SMA expression in STRO-1 cells.....	103
Figure 4.1: α-SMA expression in CLL cells.....	116
Figure 4.2: Effect of co-culture with CLL samples on α -SMA expression in HFFF2 cells.....	117
Figure 4.3: Effect of co-culture with CLL samples on HFFF2 α -SMA expression.....	118
Figure 4.4: Comparison of effects of co-culture with M-CLL or U-CLL samples on HFFF2 α -SMA expression.....	121
Figure 4.5: Comparison of effect of co-culture on sIgM signal responsive and non-responsive CLL samples on HFFF2 α -SMA expression.....	122
Figure 4.6: Effect of conditioned media derived from a CLL sample at different CLL densities on HFFF2 α -SMA expression.....	124
Figure 4.7: Effect of conditioned media derived from a CLL sample for different times on HFFF2 α -SMA expression.....	126

Figure 4.8: Effect of CLL sample- derived CM on HFFF2 α-SMA expression	127
Figure 4.9: TGF- β titration on α-SMA expression of HFFF2 cells.....	129
Figure 4.10: Effect of conditioned media derived from a CLL sample on TGF- β induced α-SMA expression in HFFF2 cells.....	130
Figure 4.11: Effect of CLL-derived conditioned media on TGF- β induced α-SMA expression in HFFF2 cells	131
Figure 4.12: Schematic representation of TGF- β1 responsive reporter construct	133
Figure 4.13: Diagram showing basis from quantitation of active TGF- β1 using the MLEC reporter assay	134
Figure 4.14: Typical TGF- β dose-dependent curve generated from MLEC cells.....	136
Figure 4.15: Typical result generated from a single TGF- β luciferase assay	137
Figure 4.16: TGF- β1 activation by CLL samples	138
Figure 4.17: Effect of IGHV mutational status on TGF- β1 activation	139
Figure 4.18: Correlation of CLL samples ability to activate TGF- β1 and effect α-SMA expression	142
Figure 4.19: Effect of CLL cell-derived exosomes on HFFF2 cell α-SMA expression	145
Figure 4.20: Diagram on key findings in chapter 4.....	154
Figure 5.1: Analysis process of annexin V FACS data	158
Figure 5.2: FACS plots comparing CLL viability when cultured in the absence or presence of fibroblasts and myofibroblasts.....	159
Figure 5.3: Graphs showing annexin V/PI staining data	161
Figure 5.4: Graphs showing annexin V/PI staining data	162

Figure 5.5: Graph summarising the effect of fibroblasts and myofibroblasts on CLL cell viability	164
Figure 5.6: comparison of spontaneous apoptosis in U-CLL and M-CLL samples.....	166
Figure 5.7: Comparison of the protective effect of stromal cells on U-CLL and M-CLL samples	167
Figure 5.8: Comparison of fibroblast and myofibroblast confluency	169
Figure 5.9: Effect of fibroblast CM on caspase 3 and PARP cleavage in CLL cells	171
Figure 5.10: Effect of HFFF2 fibroblast-derived CM on un-cleaved caspase 3 expression	172
Figure 5.11: Effect of HFFF2 fibroblast-derived CM on PARP cleavage in CLL cells	173
Figure 5.12: Converting fluorescent microscopy images into binary images	175
Figure 5.13: Method by which bound CLL cells were counted	176
Figure 5.14: Variation of bound CLL cells per condition	177
Figure 5.15: Summary graph of CLL cell adhesion to fibroblasts and myofibroblasts.....	178
Figure 5.16: CLL sample adhesion to fibroblasts and myofibroblasts at earlier time points	179
Figure 5.17: Analysis process of ROS data	181
Figure 5.18: Comparison of CM- H₂DCFDA labelled and unlabelled samples	183
Figure 5.19: Intracellular ROS levels in CLL cells cultured alone and co-cultured with fibroblasts	184
Figure 5.20: Comparison of intrinsic ROS levels in CLL samples cultured alone or co-cultured with fibroblasts	185

Figure 5.21: Effect of fibroblast conditioned media on Bcl-2 expression	187
Figure 5.22: Effect of fibroblast conditioned media on MCL-1 and BIM _{EL} expression.....	189
Figure 5.23: Effect of fibroblast CM on MCL-1 expression in CLL samples	190
Figure 5.24: Effect of fibroblast conditioned media on BIM _{EL} expression in CLL cells	191
Figure 5.25: Graphical representation of the BIM _{EL} /MCL-1 ratio	193
Figure 5.26: Effect of fibroblast conditioned media on MCL-1 expression in CLL samples at earlier time- points	194
Figure 5.27: Effect of fibroblast conditioned media on MCL-1 expression at earlier time- points	195
Figure 5.28: Comparison of fibroblast and myofibroblast conditioned media on MCL-1 expression in CLL samples	197
Figure 5.29: Effect of fibroblast and myofibroblast conditioned media on MCL-1 expression in CLL samples	198
Figure 5.30: Summary of survival data	208
Figure 6.1: Effect of HFFF2 fibroblasts on pERK expression in CLL cells and analysis of pERK expression in HFFF2 fibroblasts	212
Figure 6.2: α-SMA expression in CLL cells after co-culture with HFFF2 fibroblasts.....	213
Figure 6.3: pERK and pAKT ⁴⁷³ expression in CLL cells in response to HFFF2-derived conditioned media	215
Figure 6.4: Effect of HFFF2-derived conditioned media on pERK expression	216
Figure 6.5: Effect of HFFF2-derived conditioned media on pAKT ⁴⁷³ expression	217

Figure 6.6: Effect of HFFF2 CM and HFFF2 direct contact on pSYK ³⁵² expression in CLL cells.....	218
Figure 6.7: Correcting for inhibitor- induced apoptosis	221
Figure 6.8: Effect of AZD on HFFF2 fibroblast-mediated protection of CLL cells	222
Figure 6.9: Comparison of the effect of AZD pre-treatment with continuous AZD treatment on CLL cells	224
Figure 6.10: Effect of R406 on HFFF2 fibroblast-mediated protection of CLL cells	226
Figure 6.11: Effect of ibrutinib on HFFF2 fibroblast-mediated protection of CLL cells	227
Figure 6.12: Effect of CAL-101 on HFFF2 fibroblast-mediated protection of CLL cells	228
Figure 6.13: Effect of LY294002 on HFFF2 fibroblast-mediated protection of CLL cells	229
Figure 6.14: Effect of AZD6244 on HFFF2 fibroblast-mediated protection of CLL cells	230
Figure 6.15: Effect of small molecule inhibitors on HFFF2 fibroblast mediated protection of CLL samples at 24 and 48 hours	231
Figure 6.16: Expression of SYK and AKT in HFFF2 cells	232
Figure 6.17: Effect of blocking the NFκB and JAK/STAT signalling pathways on HFFF2 fibroblast-mediated protection of CLL cells	234
Figure 6.18: Effect of small molecule inhibitors on MCL-1 expression in CLL cells	236
Figure 6.19: Effect of inhibitors on MCL- 1 expression in CLL samples ...	237
Figure 6.20: Comparison of the effect of inhibitors on MCL-1 expression in CLL samples	238
Figure 6.21: effect of R406 on pERK expression in CLL cells.....	240

Figure 6.22: Effect of HFFF2 fibroblasts on intracellular signalling within CLL cells	248
Figure 7.1: Diagram summarising key findings	254
Figure A.2: Effect of HFFF2 fibroblast CM on CLL cell viability	268

DECLARATION OF AUTHORSHIP

I, SAMANTHA DIAS

Declare that this thesis and the work presented in it are my own and has been generated by me as the result of my own original research.

Chronic lymphocytic leukaemia and the microenvironment: Investigating the interplay between CLL cells, fibroblasts and myofibroblasts

I confirm that:

1. This work was done wholly or mainly while in candidature for a research degree at this University;
2. Where any part of this thesis has previously been submitted for a degree or any other qualification at this University or any other institution, this has been clearly stated;
3. Where I have consulted the published work of others, this is always clearly attributed;
4. Where I have quoted from the work of others, the source is always given. With the exception of such quotations, this thesis is entirely my own work;
5. I have acknowledged all main sources of help;
6. Where the thesis is based on work done by myself jointly with others, I have made clear exactly what was done by others and what I have contributed myself;
7. None of this work has been published before submission

Signed:.....

Date: 25-09-14

Acknowledgements

Numerous people have contributed in a variety of different ways to the realisation of this work. First and foremost, I am indebted to Professor Graham Packham, my supervisor for his ever present guidance, encouragement and generous support without whom this work would never have been a reality. He created the space for me to start my research career and continue progressing towards my dream goals.

I would also like to express my sincerest gratitude to Dr Serge Krysov for mentoring me in the lab and always lending his assistance and direction when needed.

I am most grateful to Professor Gareth Thomas, Dr Andrew Steele and Dr Veronika Jenei for their valuable advice and guidance given to me throughout the course of this project. I would also like to thank Dr Rahul Tare for providing me with cells and his assistance when required.

I also want to express my deepest gratitude to my research team, all of whom created an enjoyable work atmosphere, but specifically special thanks to Elizabeth Lemm, Dr Alison Yeomans, Dr Samantha Drennan and Dr Lindsay Smith for all their support and providing me with a pleasant work environment within which to conduct my studies.

Also, importantly I would like to thank both my parents and Phillip Eagles for their unending moral support, guidance and encouragement. Without them I would not have been able to achieve completing my PhD.

Finally I would like to acknowledge and thank the University of Southampton for providing me with a scholarship to pursue my studies, and Southampton Cancer Research UK centre for providing funding for consumables.

Definitions and Abbreviations

α -SMA	Alpha-smooth muscle actin
β -actin	Beta-actin
ALL	Acute lymphoblastic leukaemia
AML	Acute myeloid leukaemia
ATM	Ataxia telangiectasia
BCR	B-cell receptor
BL	Burkitt's lymphoma
BM	Bone marrow
BMMNC	Bone marrow mononuclear cells
CAF	Carcinoma associated fibroblast
CFSE	Carboxyfluorescein succinimidyl ester
CLL	Chronic lymphocytic leukaemia
CM	Conditioned media
CML	Chronic myeloid leukaemia
CMP	Common myeloid progenitor
CLP	Common lymphoid progenitor
DC	Dendritic cell
DLBCL	Diffuse large B-cell lymphoma
ECM	Extracellular matrix
EMT	epithelial-mesenchymal transition
FCS	Foetal calf serum
FDC	Follicular dendritic cell

FISH	Fluorescence in situ hybridisation
FRC	Fibroblastic reticular cell
FSC	Forward scatter
GC	Germinal centre
GSH	Glutathione
HEV	High endothelial venule
HFFF2	Human Caucasian foetal foreskin fibroblast
HSC	Haematopoietic stem cell
HSC70	Heat shock cognate protein 70
<i>IGHV</i>	Immunoglobulin heavy chain variable region
<i>IGLV</i>	Immunoglobulin light chain variable region
IHC	Immunohistochemistry
IKK	I kappa B kinase
ILV	Intraluminal vesicle
ITAM	Immunoreceptor tyrosine-based activation motif
LN	Lymph node
M-CLL	<i>IGHV</i> mutated CLL
MAPK	Mitogen-activated protein kinase
MBL	Monoclonal B-cell lymphocytosis
MM	Multiple myeloma
MRC	Marginal reticular cell
MRD	Minimal residual disease
MSC	Mesenchymal stromal cell
MVE	Multivesicular endosome

MZ	Marginal zone
NFκB	Nuclear factor kappa B
NHL	Non-Hodgkin's lymphoma
NK cell	Natural killer cell
NLC	Nurse-like cell
PBMC	Peripheral Blood Mononuclear Cell
PBS	Phosphate buffered saline
PC	Proliferation centre
PI	Propidium iodide
PI3K	Phosphoinositide 3-kinase
RB1	Retinoblastoma 1
ROS	Reactive oxygen species
SCS	Subcapsular sinus
SD	Standard deviation
SDF-1	Stromal cell-derived factor 1
SHM	Somatic hypermutation
sIgM	Surface IgM
SLL	Small lymphocytic leukaemia
SLO	Secondary lymphoid organ
SSC	Side scatter
TGF-β	Transforming growth factor beta
TMA	Tissue microarray
U-CLL	IGHV un-mutated CLL
ZAP-70	Zeta-chain-associated protein kinase 70

Chapter 1:

Introduction

Chapter 1

1.1 Introduction

The main aim of this project was to investigate the interplay between chronic lymphocytic leukaemia (CLL) cells, and fibroblasts and myofibroblasts. Therefore, the introduction to my thesis initially details an overview of CLL, including disease epidemiology, aetiology, symptoms, diagnosis and treatment strategies. This is followed by a detailed review of the microenvironment in both healthy and malignant states; the CLL microenvironment is explained in further detail. An introduction to fibroblasts, myofibroblasts and the major signal transduction pathway involved in myofibroblast transdifferentiation, the **TGF- β signalling pathway**, is described. Part of this project involved investigating the impact of fibroblasts and myofibroblasts on CLL cell survival and intracellular signalling pathways, thus an overview of apoptosis, B-cell receptor signalling and the signal transduction pathways which were investigated are provided.

1.2 Chronic lymphocytic leukaemia

1.2.1 Chronic lymphocytic leukaemia

CLL is an incurable B-cell malignancy caused by the clonal expansion of abnormal CD5⁺CD19⁺CD23⁺ B cells [1, 2]. CLL was initially thought to be a disease of failed apoptosis, but now several lines of evidence suggest that the malignant cells have a previously overlooked proliferative capacity. Possibly the most recognised work demonstrating this was generated from a series of **deuterated 'heavy'** water experiments, described by Messemer et al. In these studies, water containing a non-radioactive hydrogen isotope was used to measure CLL cell kinetics, in 19 separate patients. The data showed that CLL birth rates were much higher than originally thought, and varied between 0.1-1.0% of the entire clone per day [3]. Additional evidence for higher CLL proliferation rates arose from a study by Damle et al, which analysed CLL cell telomere length and telomerase activity. These data showed that telomeres in CLL cells are shorter than telomeres from healthy individuals; additionally, telomerase activity was shown to be higher in a CLL subgroup with poor outcome, compared to counterparts with favourable outcome [4]. Moreover, short telomere length in CLL cells correlates with poor prognosis [4, 5]. The combination of reduced apoptosis and increased proliferation, results in the

characteristic accumulation of resting B-CLL cells in the peripheral blood, and proliferating B-CLL cells within proliferation centres (PC) found in the lymph nodes (LN), and to a lesser extent within the bone marrow (BM) and spleen [6, 7]. CLL cells are constantly migrating between the peripheral blood and these microenvironment tissue sites, based on chemokine gradients (described further in section 1.3.2).

CLL is a highly heterogeneous disorder and clinical course varies between patients. For instance, some patients do not present with any symptoms and will survive for many years without requiring treatment (e.g. >20 years). Alternatively, in others the disease may progress rapidly and thus patients will require aggressive treatment strategies, yet only survive a few years (e.g. 2-3 years). There are however a number of prognostic markers in CLL which aid in determining disease progression, one of which includes immunoglobulin heavy chain variable region/immunoglobulin light chain variable region (*IGHV/IGLV*) mutations. *IGHV* and *IGLV* genes encode part of the BCR. The BCR, whose function will be discussed later (section 1.7), is composed of an antigen binding subunit and a signalling subunit, the former of which comprises 2 heavy chains and 2 light chains which are linked by disulphide bonds; each chain comprises a constant region and a variable region (Figure 1.1). In normal non-pathologic conditions, B cells undergo somatic hypermutation (SHM), where they acquire mutations within their immunoglobulin variable region (*IGV*) genes, and undergo affinity maturation (increase in antigen affinity) [8]. This process occurs in germinal centres (GC), which are specialised structures within the secondary lymphoid organs (SLOs), and is crucial for the production of memory B cells and effector plasma cells, which generate high affinity antibodies. Follicular dendritic cells (FDCs) are stromal cells present within the GC light zones and function to support survival and proliferation of GC B cells, as well as trap and retain antigens [9]. In CLL, all patients fall into two key subsets based on the presence or absence of somatic mutations, within their *IGHV* and *IGLV* genes. CLL cells that acquire *IGHV/IGLV* mutations are classified as mutated (M-CLL), whereas those which retain less than 98% similarity to germline sequences are classified as un-mutated (U-CLL) [10]. This highlights that there are 2 different cells of origin for CLL. One is a naïve B cell which has likely encountered antigen, due to the presence of activation markers (i.e. CD23), yet lacks sufficient stimulus to form a GC and therefore has not

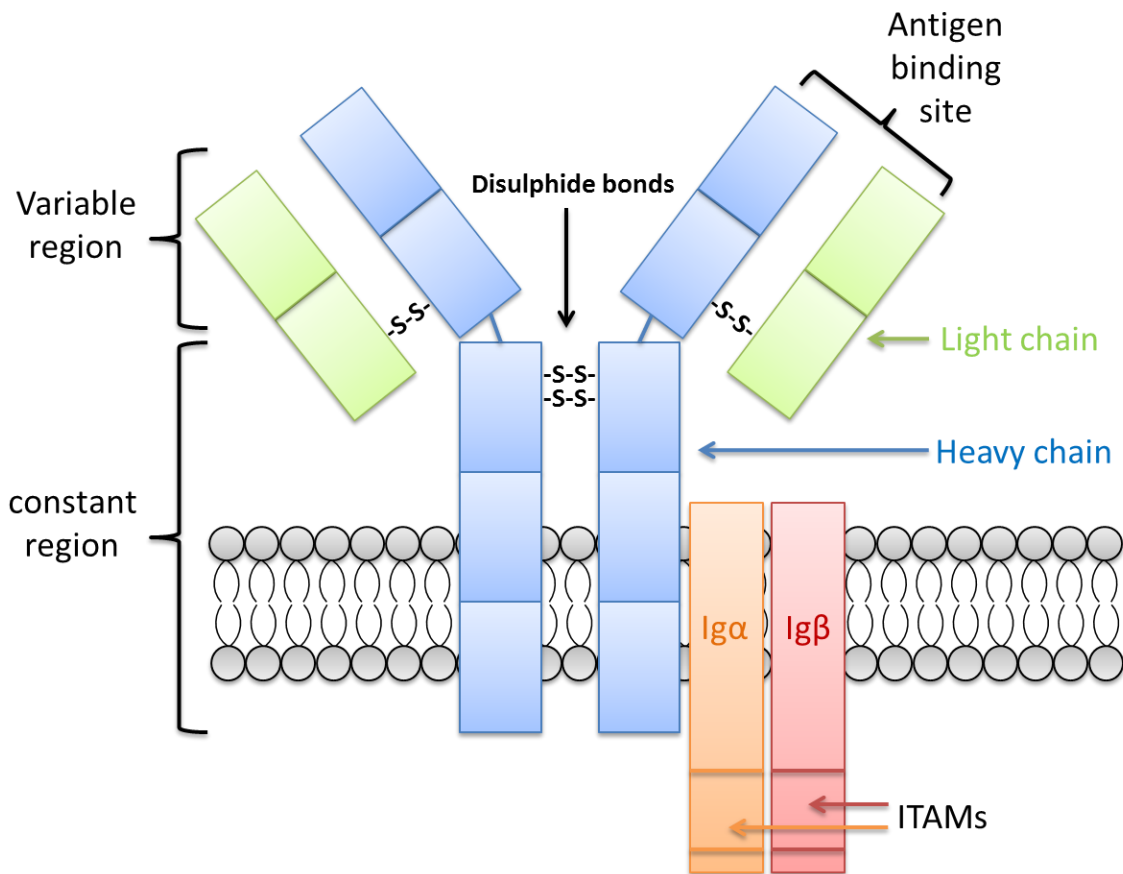


Figure 1.1: The structure of the B-cell receptor.

The BCR is composed of an antigen binding subunit and a signalling subunit. The antigen binding subunit is comprised of a heavy chain (blue) and a light chain (green), which are linked by disulphide (-S-S-) bonds. Both the heavy and light chains comprise variable and constant regions. The signalling subunit contains a conserved amino acid sequence motif known as the immunoreceptor tyrosine-based activation motif (ITAM) within its cytoplasmic tail.

undergone SHM; this is the cell of origin U-CLL is derived from. Whereas M-CLL is derived from a cell believed to have undergone SHM within a GC. These two subsets are characterised by very different clinical behaviour. M-CLL manifests as an indolent version of the disease and median survival of patients is 24 years, while U-CLL generally presents as a more aggressive form of CLL and patients have a median survival of 8 years [11]. Other prognostic markers include CD38 and ZAP-70, both of which are well-known to negatively impact disease progression. The presence of CD38 positive CLL cells correlates with a poor prognosis; this manifests as a more advanced stage of the disease as well as a reduction in both responsiveness to treatment and a reduction in survival [12]. Additionally, the presence of ZAP-70 is strongly associated with U-CLL [13], but is also independently associated with poor patient outcome [14].

1.2.2 CLL epidemiology

CLL is the most common form of adult leukaemia in the western world, and it comprises over 30% of all types of leukaemia [15]. According to cancer research UK statistics, around 2,800 people are diagnosed with CLL in the UK every year. As most patients with CLL do not actually present with any symptoms, it is likely that the true incidence of CLL is unknown and underestimated [15, 16]. CLL is mainly prevalent in Australia, North America and Europe; conversely, it is least prevalent in Asia and South America [17]. The disease affects approximately twice as many men as it does women, and increases dramatically with age giving it the reputation of being a disease of the elderly [17]. CLL mainly affects individuals over the age of 60; the median age at diagnosis is 64-70 years [17].

1.2.3 Aetiology of CLL

The cause of CLL is currently unknown. However, there is evidence that genetic factors play a role in disease onset. As mentioned above, CLL is prevalent in certain ethnicities, specifically western societies, compared to individuals of Asian descent, who are at low risk of the disease. Of course this could be due to cultural differences i.e. variances in diet, however individuals of Japanese descent, who relocate to America remain at low risk to CLL [17]. Additionally, there is a higher prevalence of CLL in individuals with first degree relatives who have been diagnosed with the disease [18]. Furthermore, there is some

Chapter 1

evidence that the phenomenon of anticipation, where successive generations suffer from a more severe form of the disease with earlier onset, presents in CLL [19]. Monoclonal B-cell lymphocytosis (MBL) was first described as an **'indolent' form of CLL**. The criteria for MBL is a B lymphocyte count in the peripheral blood of $<5.0 \times 10^9/L$, where the circulating lymphocytes have a CLL phenotype (i.e. CD5+, CD19+, CD23+) [20]. Data generated from large population-based studies have shown that MBL prevalence increases with age and affects up to 14% of the population over 62 years [21]. Although the risk of developing CLL from MBL is around 1% per year, the majority of patients diagnosed with CLL have a preceding MBL [22]. Multiple environmental factors have also been suspected to cause CLL, such as exposure to ionising radiation, chemicals such as benzene, and various drugs [23, 24]. However there is no definitive link between any of these factors and CLL onset.

Despite the use of B cell mitogens such as TPA, the low *in vitro* mitotic activity of CLL cells hinders the efficacy of conventional cytogenetic analysis, which in the past has only revealed chromosomal aberrations in 40-50% of CLL cases. However in more recent years the utilisation of fluorescence *in situ* hybridization (FISH) has allowed the detection of almost double the amount of genetic abnormalities in CLL cases, as was previously detected. This was demonstrated by a single centre study conducted by Döhner et al which analysed 325 CLL cases via FISH and found aberrations in 268 (82%) of samples within this cohort [25]. The most frequent being a deletion at 13q14 (55%), a deletion at 11q22-q23 (18%), trisomy 12q13 (16%), deletion at 17p13 (7%) and deletion at 6q21 (7%). A more recent study analysed these aberrations within 65 CLL patients and found that the deletion at 13q14 is the most frequent aberration within older patients (>60 years; 36.6%), whereas trisomy 12 is the most frequent aberration within younger patients (<60 years; 31.3%) [26].

Chromosome 13q14 maps to the Retinoblastoma gene (RB1) which is a well-known tumour suppressor gene, thus it was initially believed that aberrations within this gene promote CLL progression. However various studies have shown that disruption of both RB1 alleles is rare in CLL [27]. Furthermore studies have shown that patients with a single 13q14 aberration (i.e. no other aberration detected) have the longest estimated survival time (median survival 133 months) including that of patients with no detected genetic abnormalities (normal karyotype; median survival 111 months), indicating 13q14 deletions

correlate with favourable patient outcome [25, 28]. However more recently it has been found that not all 13q14 deletions correlate with favourable prognosis, and these patients can be divided into 2 groups classed as good prognosis type 1 (exclusive of RB1, approximately 30%) and poor prognosis type 2 (inclusive of RB1, approximately 20%) [29]. Additionally, miR-15a and miR-16-1 are encoded on chromosome 13q14, and are known to target the tumour suppressor gene TP53, and the anti-apoptotic protein Bcl-2. Lin et al revealed that loss of these 2 microRNAs at chromosome 13q14 associates with poor prognosis, as a result of de-repression of Bcl-2 (i.e loss of repression), and up-regulation of TP53 mRNA as a subsequent effect [30].

Aberrations in 11q22-q23 generally correlate with progressive disease and reduced patient survival times compared to patients with normal karyotype [31]. Overall, patients with this genetic abnormality have a median survival of 79 months [25]. Additionally these patients tend to present with extensive lymphadenopathy [32]. Initially it was unclear which gene(s) primarily affect this aberration. However more recently, studies have highlighted that the Ataxia Telangiectasia Mutated (ATM) tumour suppressor gene, which is implicated in cell cycle control and DNA repair, is a key target of 11q deletions. Recent studies have shown that ATM mutations occur in 30-40% of CLL patients with 11q deletions [33, 34]. Rose-Zerilli et al screened 166 patients with known 11q deletions for ATM mutations [35]. 105 were successfully screened for ATM mutations and were detected in 36 patients (34%). Furthermore they observed that ATM mutation (in patients with 11q deletion) correlated with reduced overall progression-free survival. Several lines of evidence have also indicated that ATM deficiency or somatic mutations within the ATM gene correlates with extensive LN involvement, aggressive disease and poor patient survival [33, 36, 37].

Trisomy 12 was the first genetic aberration to be reported in CLL by conventional cytogenetic analysis [38]. However the clinical consequence of this genetic abnormality remains controversial. Some studies have shown that trisomy 12 correlates with shorter patient survival times [39], yet this was not observed in other single centre cytogenetic studies which found that this aberration had no correlation with poor prognosis [40]. Thus trisomy 12 is thought to confer an intermediate prognosis in CLL and median survival for these patients is 114 months [25]. However, emerging data indicates an

Chapter 1

association between trisomy 12 and NOTCH1 mutations which correlate with U-CLL and thus an unfavourable prognosis [41].

The tumour suppressor TP53 (p53) gene is located at 17p13. A previous study analysing 126 different CLL patients found that most patients (approximately 81%) with 17p deletions also have p53 mutations [42]. Multiple studies have demonstrated that 17p deletions and p53 mutations associate with poor prognosis and outcome in CLL. In fact patients with these aberrations have the worst prognosis compared to patients harbouring the aforementioned mutations (median survival 32 months) [25]. Rouby et al reported that p53 mutations correlate with aggressive disease characterised by advanced disease stage and resistance to chemotherapy, compared to the majority of patients without p53 who achieved partial remission [43]. Döhner et al observed that patients with 17p deletion had significantly shorter survival times compared to patients without the aberration [44]. These studies indicate p53 gene deletion predicts non-response to therapy. Furthermore, Thornton et al conducted a study on 115 separate CLL patients and found that p53 abnormalities are significantly more frequent in refractory groups compared to untreated patients [45]. A recent study by Zenz et al assessed p53 mutations in 328 separate CLL patients [46]. The mutation was detected in 28 patients (8.5%), and 4.5% of these patients did not have 17p deletion. Furthermore they observed a significantly lower median progression-free survival and overall survival in patients with p53 mutation compared to those without it.

More recently, advances in next generation sequencing have revealed mutations in other genes that may have clinical consequence in CLL, such as NOTCH1, SF3B1 and BIRC3. The NOTCH1 gene encodes a transmembrane protein, and constitutive NOTCH1 signalling has been found to be implicated in disease progression as it sustains CLL cell survival [47]. In CLL, NOTCH1 mutations generally occur within its PEST domain, which is required for the proteasomal degradation of NOTCH1, thus resulting in impaired NOTCH1 degradation leading to aberrant NOTCH1 signalling. These mutations are associated with progressive disease as studies have shown a higher prevalence of NOTCH1 mutations in U-CLL [48]. The SF3B1 gene encodes a component of the spliceosome which is involved in forming mature mRNA by removing introns from the protein-encoding gene. Mutations within the SF3B1 gene are usually missense nucleotide changes within the HEAT domain of the protein

and are associated with poor prognosis in CLL [49]. Additionally SF3B1 mutations preferentially occur within tumours with 11q deletions which, as mentioned earlier, correlate with poor patient prognosis and outcome [34]. Furthermore these mutations confer alterations in pre-mRNA splicing within the host malignant sample [34]. BIRC3 negatively regulates non-canonical NF κ B signalling, by inhibiting its major activator, MAP3K14 [50]. Thus mutations in BIRC3 lead to constitutive NF κ B signalling which confers pro-survival signals to the malignant cells and associates with disease progression [7]. Previous work has shown that BIRC3 mutations are present within fludarabine-refractory patients, however they were absent in patients with progressive disease that were sensitive to fludarabine, thus indicating that BIRC3 mutations correlate with chemorefractory cases [50].

The TGF- β signalling pathway mediates a wide variety of biological effects, including cell growth, differentiation and apoptosis. It is well documented that this pathway has an inhibitory effect on cell proliferation and growth, in various cell lineages including haematopoietic, mesenchymal and epithelial cells [51]. Various reports have revealed that mutational inactivation of components within the TGF- β pathway can predispose cells to malignant transformation. Inactivating mutations in both alleles of the TGF- β type 2 gene abolishes the growth inhibitory effect of TGF- β , in many types of cancer, including cutaneous T-cell lymphoma [52]. One study found that a deletion in exon 1 of the TGF- β receptor 1 gene, in the tumour cell line, JK cells, resulted in the loss of their resistance to the growth inhibitory effects of TGF- β [53]. Additionally, mutations in SMAD proteins, which are critical components in TGF- β signalling, can, also lead to leukemogenesis. Data by Imai et al revealed that missense mutations in the SMAD 4 gene, of acute myelogenous leukaemia cells (AML) disrupt TGF- β signalling, thus leading to disease progression [54]. In CLL, TGF- β is also well known to have a growth inhibitory effect on these cells. However, some B-CLL cells are in-sensitive to this effect of the cytokine. A previous study identified 2 mutations within the TGF- β type 1 receptor gene, which are linked to resistance of the anti-proliferative effects of TGF- β , in the in-sensitive CLL cells [55].

MicroRNAs (miRNAs) are small non-coding RNA molecules of approximately 22 nucleotides which can regulate gene expression, usually by inducing gene silencing. Initial studies which highlighted the clinical relevance of miRNAs in

Chapter 1

CLL were conducted by Calin et al. They performed genome wide expression profiling of CLL miRNAs in 38 different CLL samples utilising microarray technology and discovered miRNA signatures which associate with the poor prognostic marker ZAP-70 [56]. Following this they analysed the miRNA profiles of 94 CLL samples and discovered a unique miRNA signature composed of 13 genes which associates with CLL prognostic markers including ZAP-70 and *IGHV* mutation status [57]. Since then various studies have implicated miRNAs in CLL disease progression and outcome. Mraz et al demonstrated that miRNA-150 is associated with favourable prognosis [58]. They found that ZAP-70 positive and U-CLL cells had a significantly lower median expression of miR-150 compared to ZAP-70 negative and M-CLL cells. Additionally high expression of miR-150 associated with a longer treatment-free survival of patients. A study by Stamatopoulos et al demonstrated that miR-29c and miR-223 expression associates with ZAP-70 expression and U-CLL [59]. They observed that expression of these 2 miRNAs was lower in patients with advanced disease stage and they were expressed at lower levels in poor prognostic subgroups.

1.2.4 Symptoms and diagnosis

The most common symptom in CLL is swelling of the LNs (lymphadenopathy) which presents in approximately 80% of patients [17]. Other symptoms include splenomegaly (approximately 50%), hepatomegaly (approximately 10%), weakness, fatigue, night sweats and fever [17]. Some patients may present with other infections or autoimmune disorders such as Coombs-positive autoimmune haemolytic anaemia (10%), hypogammaglobulinaemia (10%) or hypergammaglobulinaemia (15%) [60]. However approximately 25 % of patients are asymptomatic at diagnosis [17]. According to the 2008 World Health Organisation (WHO) guidelines, a diagnosis of CLL requires a count of $>5.0 \times 10^9/L$ of monoclonal B cells with a CLL phenotype circulating within the peripheral blood [61]. Additionally CLL cell infiltration must be $>30\%$ within the BM, however this is rarely required in general clinical practice for diagnosis.

1.2.5 Treatment strategies

As CLL is mostly an indolent disease, most patients can go several months or even years without requiring treatment after diagnosis. Some patients never

require any treatment. Guidelines have been set in place for treatment initiation by the National Cancer Institute Working Group (NCIWG) which includes patients losing over 10% weight within 6 months, continuous fevers lasting for 2 weeks, suffering from extreme fatigue, worsening anaemia, progressive splenomegaly and doubling of lymphocyte count within 6 months; these are just a few examples [62]. The type of treatment strategy used depends on the age of the patient, how far the disease has progressed and prognostic factors of the patient (i.e. CD38, ZAP-70). Younger patients or those suffering from a later stage of CLL may benefit from more aggressive treatment. Conversely older patients or those with a more indolent form of the disease may only require treatment which reduces the disease symptoms using a strategy with minimal adverse effects from treatment based toxicity.

1.2.5.1 Chemotherapy

The frontline treatment strategy in CLL is currently chemotherapy, except for patients with 17p deletion, as this small subgroup of patients have poor response to chemoimmunotherapy [63]. The alkylating **agents'** chlorambucil and cyclophosphamide were the standard treatment of CLL for several decades, used either as single agents, or in combination with corticosteroids; yet complete remission was rare. Chlorambucil is a low toxicity drug, low cost, oral administration and complete response rates are 50-60%. Cyclophosphamide is generally administered to patients who are unresponsive or cannot tolerate chlorambucil. More recently, fludarabine has been identified as a stronger candidate for the treatment of CLL. Fludarabine is a purine nucleoside analog which acts by inhibiting DNA synthesis, and is used as a first- and second-line treatment in CLL. It has been shown to be more effective than chlorambucil in terms of better response rates and a longer disease-free period for patients [64]. Furthermore the effects of fludarabine are superior when incorporated into certain combination therapies including CAP (cyclophosphamide, doxorubicin and prednisone) and ChOP (cyclophosphamide, vincristine, prednisone and doxorubicin) in advanced stage, previously untreated, CLL patients [65]. Incorporating fludarabine into a combination regime with cyclophosphamide has also been shown to produce higher response rates in patients [66]. Fludarabine, cyclophosphamide and rituximab (FCR) is the preferred choice of therapy for younger patients, who are able to tolerate chemoimmunotherapy, as progression-free survival is

Chapter 1

higher with this combination. For older patients (>65 years) who are frail, chlorambucil plus obinutuzumab is the favoured choice of treatment.

1.2.5.2 Immunotherapy

Immunotherapy is another treatment strategy used in CLL. Rituximab is a chimeric humanised murine monoclonal antibody which binds the surface antigen CD20 with high affinity; CD20 is expressed by both normal B lymphocytes and CLL B lymphocytes. Treatment with rituximab by itself has limited effects on response rates [67], this is likely due to the low expression of CD20 on CLL cells [68]. However incorporating rituximab into combination regimens with fludarabine, cyclophosphamide and pentostatin have significantly improved patient response rates as well as induced longer disease free intervals [69-71]. Previous data has indicated that rituximab can down-modulate CD20 expression on CLL cells, which may partly explain resistance to this drug by some patients [72]. More recently it has been shown that the **inhibitory Fc gamma receptor IIb (FcγRIIb) expressed by target cells promotes** this internalisation process, thus suggesting **FcγIIb as a potential biomarker to** determine patient response to rituximab [73].

Alemtuzumab is a humanised monoclonal antibody against CD52 which is expressed by normal and malignant lymphocytes (including CLL cells) as well as monocytes and natural killer cells (NK cells). It can also be used as a first line treatment in CLL and is highly effective at clearing the disease in the peripheral blood, BM and spleen but is limited at reducing lymphadenopathy [74, 75]. It is generally used to treat patients who have relapsed or are refractory to fludarabine [76].

1.2.5.3 Haematopoietic stem cell transplantation

Even with major advances being made in treatment strategies CLL remains an incurable disease. Haematopoietic stem cell transplantation (HSCT) is the only potential curative strategy for CLL; however its use in CLL remains controversial. The use of this therapy is limited due to advanced age of patients and high mortality rates, and should only be considered in younger patients or those with adverse prognostic markers early in the disease. Most patients who successfully undergo this treatment enter complete remission; however this is inevitably followed by disease relapse [77, 78].

1.2.5.4 Kinase inhibitors

Kinase inhibitors are an emerging treatment strategy for CLL, which target specific kinases within intracellular signalling pathways that promote CLL cell survival. Idelalisib and ibrutinib, **which inhibit PI3K γ and BTK, are now** approved in the USA [79, 80]. In a multicentre phase 3 study conducted on 220 patients, the overall response rate and overall survival of patients receiving rituximab plus idelalisib (81% and 92% respectively) was higher compared to patients receiving rituximab plus placebo (13% and 80%) [81]. Another recent multicentre phase 3 study conducted on 391 patients comparing the effects of ibrutinib and the anti-CD20 antibody ofatumumab, showed that patients who received ibrutinib had a higher overall survival rate and a significantly higher overall response rate (90% and 42.6% respectively) compared to patients who received ofatumumab (81% and 4.1%) [82].

1.3 The microenvironment and stromal cells: healthy versus malignant states

The microenvironment is important in CLL disease progression. Here will discuss the microenvironment, in normal and malignant states, before moving onto CLL specifically.

1.3.1 **The healthy 'non-malignant' microenvironment**

Tissue microenvironments are composed of various types of accessory cells. These cells, collectively, create a supportive environment for the functioning cells of the organ or tissue within which they reside, through both direct cell-cell interactions and the release of soluble factors. The structure and the types of cells which comprise each microenvironment vary between organs and are finely tuned in order for that specific organ to carry out its appropriate functions. For instance, immature B cells develop in the BM from committed progenitor cells via a highly ordered process called lymphopoiesis. This process is dependent on osteoblasts and stromal cells which provide support for the B-cell progenitors as they develop into pro-B cells, pre-B cells and finally immature B cells [83, 84]; loss of these cells leads to defective lymphopoiesis [85]. This demonstrates that the bone provides a microenvironment that is essential for haematopoiesis. The immature B cells

Chapter 1

then migrate towards the SLOs where they encounter antigen resulting in their proliferation, maturation and differentiation into effector plasma cells and memory B cells [86]. The differing roles of these two organs define the requirements for the structure of the microenvironment; therefore the BM microenvironment differs considerably from that of the SLOs.

1.3.2 The bone marrow microenvironment

The BM is a well-organised tissue which resides within the central compartment of long and axial bones. It is one of the largest organs in the body and constitutes approximately 5% of the total body weight. The inner surface of the bone is lined by a single layer of bone lining cells which are supported by reticular connective tissue, as well as osteoblasts and osteoclasts; together this is known as the endosteal lining [87]. The BM is highly innervated by myelinated and non-myelinated nerves, and is also extensively vascularised, but lacks lymphatic vessels. The blood flow circulates between the centre of the marrow cavity and the periphery.

Two main cellular components reside within the BM. The first are haematopoietic cells. The BM is the main site of haematopoiesis in the body and is a reservoir for haematopoietic stem cells (HSCs), which have been found to localise to the endosteal region [88]. HSCs are pluripotent and generate all haematopoietic lineages (erythrocytes, granulocytes, monocytes, lymphocytes and platelets). Haematopoiesis must be supported by the BM microenvironment in order to progress. This vital process relies on the microenvironment to recognise and retain HSCs within the BM, as well as secrete factors which act to support the progenitor cells to differentiate and mature into their correct differentiated cell type. Haematopoiesis is a continuous process which can be divided into stages. Initially the HSCs undergo self-renewal in order to maintain cell numbers. In response to appropriate signals this is followed by differentiation into either a common myeloid progenitor (CMP) or a common lymphoid progenitor (CLP); these are committed stem cells [89, 90] (Figure 1.2). Their ability for self-renewal is limited but they give rise to all myeloid and lymphoid lineages, respectively. The final stage involves CMPs and CLPs further differentiating into their lineage-specific progenitor cell, which eventually develops into their committed cell type, i.e. B lymphocyte T lymphocyte, red blood cell etc.

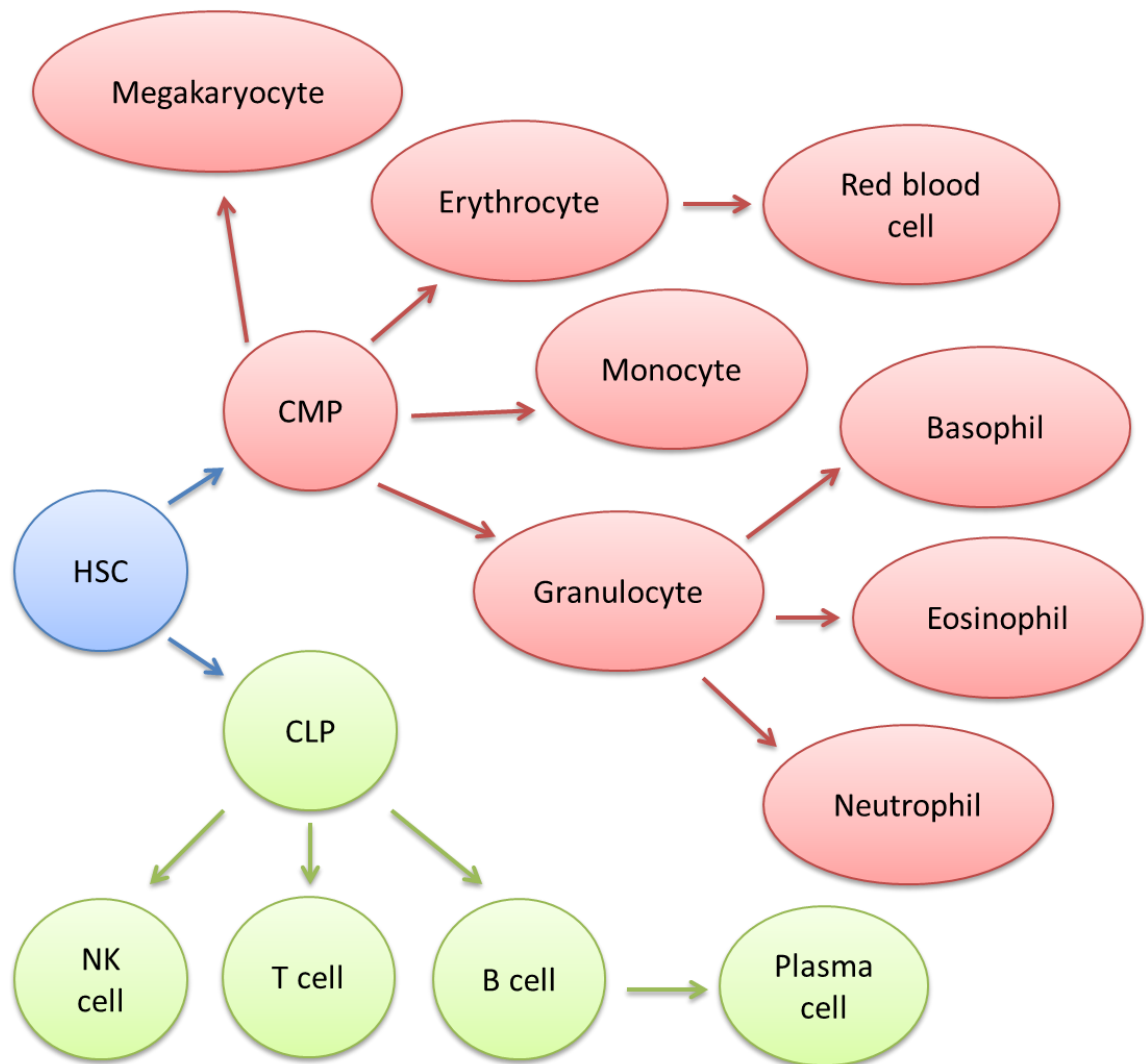


Figure 1.2: Diagram showing the hierarchy of haematopoietic stem cells, progenitor cells and their differentiation progeny.

Pluripotent HSCs (blue) undergo self-renewal to maintain cell numbers. They then give rise to CMPs (red) and common lymphoid progenitor CLPs (green). CMPs have the potential to differentiate into any myeloid cell (green), including erythrocytes, megakaryocytes, monocytes and granulocytes; erythrocytes can subsequently undergo erythropoiesis to generate red blood cells. Granulocytes undergo granulopoiesis to generate basophils, eosinophils and neutrophils. CLPs give rise to all lymphocytes (red) which include B cells, T cells and NK cell; B cells can then go onto generate plasma cells.

Chapter 1

Haematopoiesis is a compartmentalised process and the different cell types develop in distinct anatomical sites. For instance erythrocytes develop into red blood cells in erythroblastic islands, and megakaryopoiesis takes place in the sinus endothelium [91].

The second cellular component within the BM is stromal cells of mesenchymal origin. There is a lot of confusion within the literature in regards to mesenchymal nomenclature. The terms Mesenchymal stromal cells, mesenchymal stem cells, bone marrow stromal cells and bone marrow mesenchymal stem cells are just a few which are used to define a heterogeneous subset of multipotent stem cells which were first discovered over 40 years ago by A.J. Friedenstein [92]. From this point on they will be referred to as mesenchymal stromal cells (MSCs). When MSCs were first isolated they rapidly formed adherent fibroblast-like colonies, which are now known as colony forming unit-fibroblasts (CFU-F); thus distinguishing them from the haematopoietic population. These cells have the ability for self-renewal and upon exposure to the appropriate signals they can differentiate into various cell types including osteoblasts, adipocytes and chondrocytes which subsequently give rise to multiple mesenchymal tissues (bone, fat, and cartilage respectively) [93, 94] (Figure 1.3). BM-derived MSCs were the first type of stromal cell shown to support CLL cell survival [95].

1.3.3 Secondary lymphoid organ microenvironment

The SLOs comprise the LNs, spleen, thymus, tonsils, peyers patches and mucosa-associated lymphoid tissues (MALT). These structures, form a network of heterogeneous tissues, which create a filtration and surveillance system, responsible for detecting and presenting pathogens to appropriate cells of the immune system [96]. The structures of the LNs and the spleen are the best characterised of all the SLOs and both contain various types of stromal cell subsets.

The LNs are encased by a capsule and is comprised of lobules, the basic anatomical and functional unit of the LNs, which are arranged side-by-side (Figure 1.4). The lymphatic vessels drain the body's **tissues and organs of lymph** (an interstitial fluid containing lymphocytes, antigens and microorganisms) and transport it to the LNs. The afferent lymphatic vessels drain into the subcapsular sinus (SCS) which lies directly beneath the LN

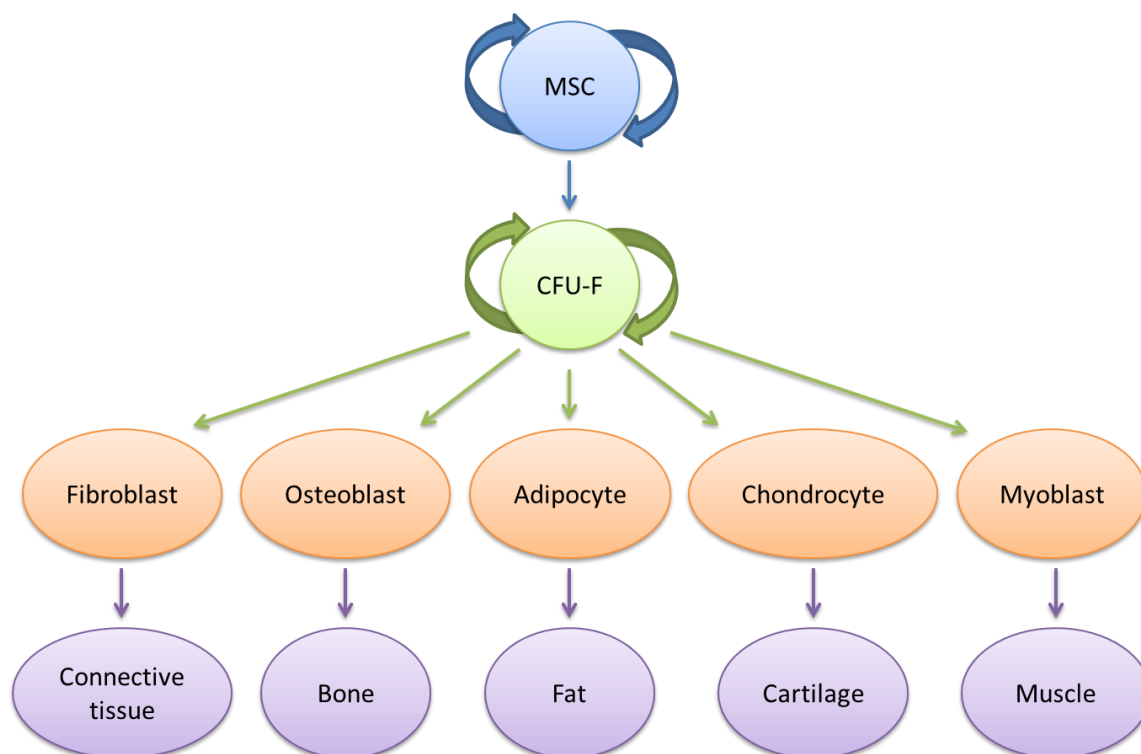


Figure 1.3. Diagram of stromal cell origin.

MSCs rapidly form adherent fibroblast-like colonies (CFU-F), post-isolation from the BM. These cells have the ability for self-renewal and can differentiate into various other stromal cell types including osteoblasts, adipocytes, chondrocytes and myoblasts, which subsequently give rise to multiple mesenchymal tissues (bone, fat, cartilage and muscle, respectively).

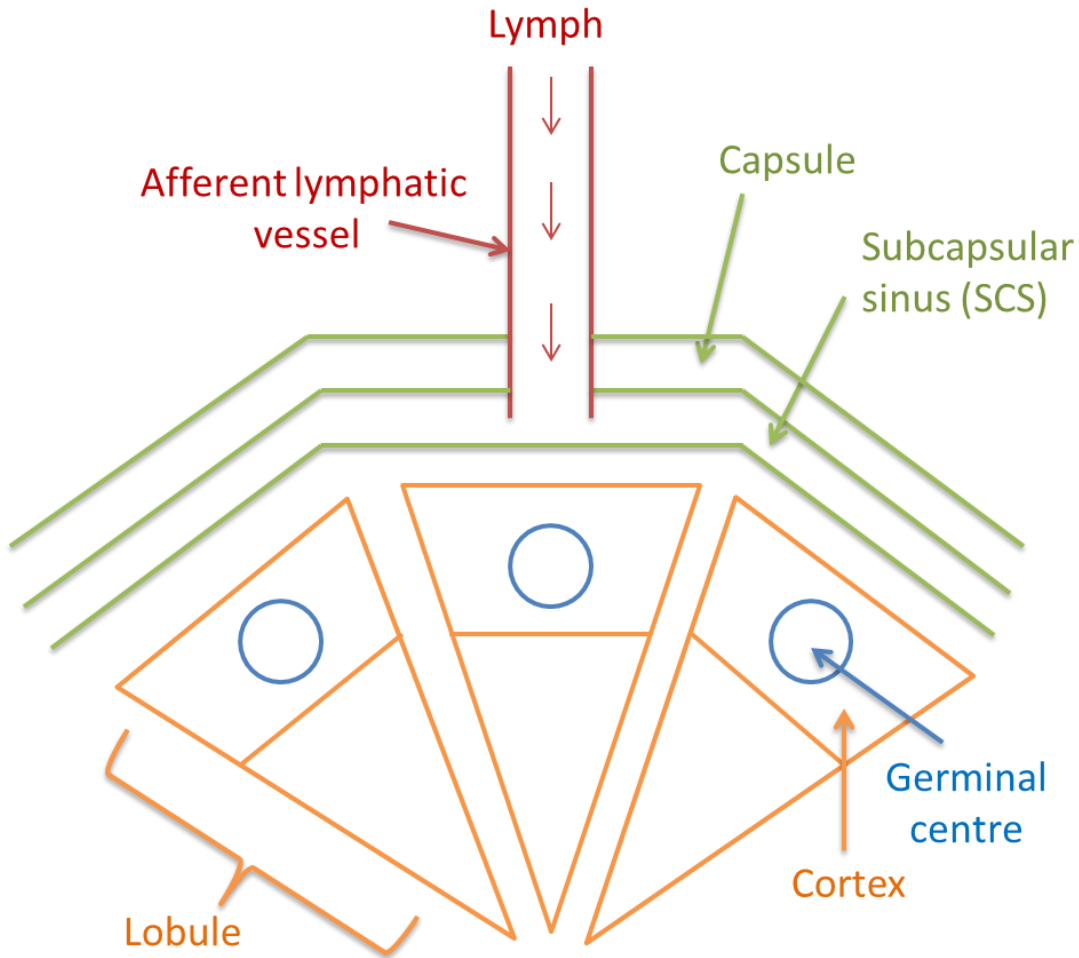


Figure 1.4. Diagram showing the structure of the lymph nodes.

The LNs are encased by a capsule. Beneath the capsule is the SCS which is the region where lymph enters the LNs via the afferent lymphatic vessels. Beneath the SCS lies the functional units of the LNs, the lobule; directly beneath the SCS is the cortex. GCs, sites within which B cells undergo SHM of their *IGV* genes and affinity maturation, are located within the LN cortex. Additionally the cortex is the region within which lymphocytes enter the LNs, through high endothelial venules (HEVs) (not shown).

capsule; the SCS is lined with macrophages which detect antigens within the incoming lymph [97, 98]. Beneath the SCS is the cortex; the main route of entry for lymphocytes is through high endothelial venules (HEV) within this region [99]. The LNs also contain B and T cell zones. B cell zones contain B lymphocytes, FDCs and stromal cells, while T cell zones contain CD4⁺ and CD8⁺ T lymphocytes and dendritic cells (DCs). Other stromal subsets that are found within the LNs include marginal reticular cells (MRCs), fibroblastic reticular cells (FRCs) and LN medullary fibroblasts [100, 101].

The spleen is one of the main filters of blood in the body and is enclosed by a fibrous capsule. It is supplied by blood vessels which enter at the hilum and branch out into central arterioles. The central arterioles are surrounded by splenic white pulp and terminate at a region called the marginal zone (MZ). The MZ is surrounded by a perifollicular zone; this separates the white pulp from the splenic red pulp [102]. The main route of lymphocyte entry is at the MZ. Similar to the LNs, the spleen also contains B and T cell zones. Both zones comprise similar cells as in the LNs (i.e. FDCs, stromal cells and DCs). Additionally the spleen contains MRCs, FRCs and red pulp fibroblasts [100, 102].

1.3.4 Microenvironment in solid tumours

Alterations can occur in these complex microenvironmental systems leading to the breakdown in cell-cell communication resulting in a shift of the delicate balance that keeps vital processes, such as cell proliferation and apoptosis, in check. This can lead to the development of a microenvironment that favours tumorigenesis. In solid tumours the microenvironment is altered by the invading cells to promote survival of the malignant cells. Therefore the microenvironment in solid tumours differs from that of the non-malignant microenvironment. For instance the components and organisation of the tumour extracellular matrix (ECM) promotes tumour cell invasion and hinders therapeutic drug delivery. Fibroblasts are more abundant within the tumour microenvironment; a study by Aznavoorian et al demonstrated that laminin, fibronectin and type IV collagen, all of which are produced by fibroblasts, stimulated chemotaxis of the A2058 human melanoma cell line [103]. Additionally a study by Bredin et al demonstrated that various major lung cancer cell lines also showed chemotactic motility to the aforementioned ECM

Chapter 1

proteins [104]. Netti et al measured the interstitial diffusion rate of the macromolecule IgG within four different tumour types (human colon adenocarcinoma, human glioblastoma, human soft tissue sarcoma and murine mammary carcinoma) to determine if assembly of the solid tumour ECM hinders the penetration of therapeutic agents [105]. Their data revealed that the more penetration-resistant tumours comprised an extended collagen network, and collagenase treatment significantly increased the IgG diffusion rate. Additionally, Brekken et al measured the interstitial fluid pressure (IFP) within human osteosarcoma xenografts and found that the IFP within the tumour microenvironment is elevated, and may therefore hinder anticancer drug administration [106]. It is also well known that in the majority of cases, the solid tumour microenvironment contains regions of hypoxia [107, 108]. Prolonged hypoxia can lead to necrosis and necrotic lesions are characteristic within the solid tumour microenvironment [109]. As oxygen can only diffuse across tissue 1-2 mm from the blood vessels, tumours cannot grow larger than this diameter in the absence of blood circulation [110]. Therefore, tumour induced angiogenesis is an important process for cancer progression. However the blood vessels that form within tumours differ from those within normal tissue. For instance they do not conform to the normal vascular organisation, whereby blood flows through large arteries, to small arteries, to arterioles and so on; instead the tumour-induced vessels share features of all these structures. Additionally these vessels are generally **'leaky'** due to a defective luminal endothelial monolayer, poorly connected overlapping cells and unfused regions [111, 112]. Cancer associated fibroblasts (CAFs) are another important component of the tumour stroma. They have multiple sources of origin (discussed in section 1.5.2) including fibroblasts, MSCs and can be generated through epithelial-mesenchymal transition (EMT), although the latter is controversial; they promote tumour progression and correlate with poor clinical outcome in various types of cancers (discussed in section 1.5.3) [113].

1.3.5 Microenvironment in blood cancers

Alternatively, blood cancers tend to develop within specialised tissue microenvironments such as the BM. The relationship between the neoplastic cells and the cells of the microenvironment differs depending on the type of malignancy. Some types of leukaemia develop a genetic abnormality which allows the neoplastic cells more independence from the microenvironment.

This is the case for Burkitts lymphoma where virtually all (approximately 80%) malignant cells undergo a translocation of the c-myc oncogene to one of the immunoglobulin loci, leading to activation of c-myc which supports their proliferation [114]. For these lymphomas, and in the case of Burkitts lymphoma, targeting the microenvironment as a therapeutic strategy would be limited. For other types of leukaemia the microenvironment supports the malignant cells by promoting cell growth and protecting the cells from spontaneous and drug-induced apoptosis. This has been shown for many types of leukaemia. Garrido et al co-cultured primary acute myeloid leukaemia (AML) cells with the HS-5 human BM stromal cell line and found that the stromal cells significantly protected AML cells from both spontaneous and drug-induced apoptosis. This protection was consistent with increased expression of the anti-apoptotic protein Bcl-2 within the AML cells [115]. Manabe et al co-cultured primary acute lymphoblastic leukaemia (ALL) cells with BM-derived stromal cells and found that ALL cell survival was extended compared to cells cultured alone [116]. Another study by Wang et al demonstrated that stromal cells can protect ALL cells from chemotherapy-induced apoptosis [117]. Vianello et al showed that human MSCs protected primary chronic myeloid leukaemia (CML) cells from imatinib induced apoptosis. This was consistent with a reduction in caspase 3 activity and an induction of the anti-apoptotic protein Bcl-XL [118]. Multiple studies have demonstrated the ability of various microenvironment-derived signals and cells to support CLL cell survival, and are described below (section 1.4.2). For these lymphomas, targeting the interactions between the stroma and the malignant cells could potentially create novel effective treatment strategies.

1.4 CLL and the microenvironment

1.4.1 CLL cell infiltration

BM and SLO involvement is characteristic in CLL. CLL LN histology is heterogeneous. Infiltration of the LNs generally results in complete effacement of the LN tissue architecture which is replaced diffusely by, predominantly, lymphocytes [119]. Histologically the infiltrating cells are interspersed in a pseudofollicular pattern, or paler areas containing larger cells (prolymphocytes or paraimmunoblasts) surrounded by a darker background of smaller cells, which are now defined as PCs [120]. Schmid et al utilised

Chapter 1

immunohistochemistry to analyse LN tissue from 30 different CLL patients and found that PCs contain a higher proliferation fraction and more T cells compared to the surrounding infiltrate [121]. Additionally most cases contained a delicate FDC network. Other studies have shown that cells within these sites express higher levels of the proliferation markers Ki-67 and CD71 [120]. A study conducted by Gine et al analysed tissue biopsies from 78 patients diagnosed with CLL and correlated the size of PCs and rate of proliferation, with patient survival [120]. The tissues were analysed by immunohistochemistry and they identified expanded PCs which were characterised as being broader than a 20x magnification field, and high proliferation rate was defined as either >2.4 mitoses/PC, or $Ki-67 > 40\%/PC$. 23 of the cases were classed as accelerated disease due to the presence of expanded PCs and/or high proliferation rates within the PCs. Patients with accelerated CLL expressed higher levels of the poor prognostic marker ZAP-70 and had a shorter median survival time (34 months) compared to patients with small or absent PCs (76 months). Additionally, FDCs are present within GCs of normal tissue [122] however they are generally absent within GCs from CLL-affected tissue, as observed by Shi et al who previously detected absent or scattered FDC clusters within CLL human tissue utilising immunohistochemistry [123], thus aiding differential diagnosis of CLL with other types of small B-cell lymphomas, such as follicular lymphoma, marginal zone lymphomas and mantle cell lymphomas.

CLL cells accumulate in the BM in 4 distinct histologic patterns; these are displayed as nodular, interstitial, diffuse or mixed (interstitial and nodular) infiltrates of small lymphoid cells [124]. CLL cells can also infiltrate the BM in an interfollicular pattern (infiltration in BM GCs) however this is rare as GCs are not usually present within the BM [125]. Infiltration pattern has been correlated with disease progression. Diffuse BM infiltration has been correlated with poor clinical outcome compared to a nodular and mixed infiltration pattern [126]. Additionally PCs may also be present within the BM but this is common in cases with extensive BM involvement.

1.4.2 Effect of the microenvironment on CLL cells

CLL cells readily accumulate *in vivo* however once they are removed from the body and cultured *in vitro* they rapidly undergo apoptosis [127, 128]. This

indicates that the survival advantages expressed by these cells, such as their resistance to apoptosis, are not innate and is likely due, at least in part, to signals derived from the microenvironment.

CLL cells appear to co-exist with their surrounding microenvironment; in fact many of the interactions between the neoplastic cells and the microenvironment are similar to those seen by the microenvironment and healthy B cells. For instance, CLL cells appear to imitate the homing and migratory mechanisms of healthy B lymphocytes in order to enter the protective microenvironment niche of the BM and SLOs (Figure 1.5). Normal B lymphocytes express the chemokine receptor CXCR4, which binds to the chemokine CXCL12 (also known as SDF-1; stromal cell-derived factor-1). During early development of B lymphocytes, stromal cells within the BM release SDF-1 in order to retain early progenitor B cells (pro-B cells, pre-B cells) within the microenvironment; this keeps the progenitors within close contact with BM stromal cells that will promote their growth and maturation [129]. A study by Burger et al showed that CLL cells express functional CXCR4 receptors [130]. CXCR4 mRNA was detected within primary CLL cells followed by detection of high levels of CXCR4 receptor expression using flow cytometry to analyse CLL cells pre-stained with anti-CXCR4-PE. Receptor sensitivity to SDF-1 was indicated by conducting endocytosis assays whereby CLL cell CXCR4 expression was down-regulated in response to SDF-1 treatment. Calcium mobilisation is a characteristic response to chemokine receptor ligation, thus intracellular calcium flux within CLL cells in response to SDF-1 treatment was analysed and shown to be induced after treatment. Chemotaxis assays were conducted utilising 5µM pore polycarbonate filters which demonstrated that a higher number of CLL cells migrated in response to SDF-1 compared to untreated control cells. Additionally this migration was significantly reduced when cells were pre-treated with a monoclonal antibody against CXCR4. Furthermore this study showed that SDF-1 secreted by a murine BM-derived stromal cell line induced CLL cell migration into the stromal cell layer. Additionally, a study by Herishanu et al utilised flow cytometry to analyse CXCR4 expression on CLL cells isolated from the peripheral blood, LNs and BM of 24 patients [7]. Lower levels of CXCR4 expression was detected on LN and BM-derived CLL cells compared to counterparts derived from the blood, indicating receptor down-modulation in response to SDF-1 ligation within the microenvironment. Together these data confirm the ability of CLL cells to

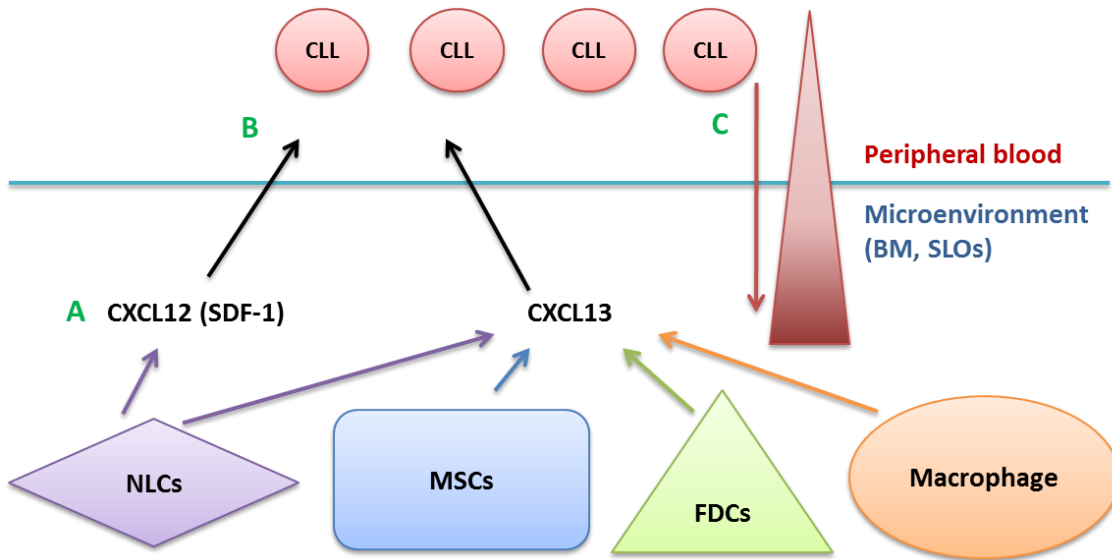


Figure 1.5: Diagram showing how CLL cells access the tissue microenvironment from the peripheral blood.

Various stromal cell types within the microenvironment, including NLCs (purple), MSCs (blue), FDCs (green) and macrophages (orange) release the chemokines CXCL12 and CXCL13 (A). These chemokines travel into the peripheral blood where they bind to their specific receptor that is expressed by CLL cells (red circles) (B); CXCL12 binds to CXCR4, and CXCL13 binds to CXCR5. This causes the CLL cells to migrate down a chemokine gradient towards the source of chemokine release (C, red arrow) (C). Once within the microenvironment CLL cells are protected by multiple types of stromal cells within the microenvironment.

migrate towards stromal cells releasing SDF-1, both *in vitro* and *in vivo*. Additionally CXCL13 (also known as B-cell attracting chemokine 1 (BCA-1)) is another key chemokine involved in lymphocyte homing to the microenvironment. A study by Bürkle et al demonstrated that CLL cells express high levels of functional CXCR5 receptors [131]. Similar to the investigations by Burger et al, this study utilised flow cytometry to detect expression of CXCR5 on CLL cells labelled with anti-CXCR5-PE. Endocytosis assays were performed to confirm receptor sensitivity to its cognate ligand; CXCR5 was down-modulated on CLL cells after treatment with CXCL13. Moreover co-culture with stromal cells also reduced CLL CXCR5 expression. Actin polymerisation, a prerequisite for cell motility, was induced within CLL cells treated with CXCL13. Also, chemotaxis assays were conducted which demonstrated that CLL cells migrated in response to CXCL13 and this chemokine-induced migration was significantly reduced when CLL cells were pre-treated with monoclonal antibodies against CXCR5. Overall this study showed that CLL cells can migrate towards CXCR13, *in vitro*. Both SDF-1 and CXCL13 are released by a variety of different stromal cells within the bone marrow and SLOs organs. SDF-1 has been previously detected within the supernatant of a murine BM stromal cell line (MS-5), and induced actin polymerisation within lymphocytes [132]. Burger *et al* showed that a subset of PBMCs isolated from the blood of CLL patients can spontaneously differentiate, *in vitro*, into large adherent cells with stromal cell characteristics; these cells were termed nurse-like cells (NLCs) and were shown to express the stromal cell marker vimentin as well as low levels of the stem cell marker STRO-1 [133]. NLCs have been shown to express CXCL13 mRNA and high levels of this chemokine was also detected within the supernatant of NLCs derived from 10 separate CLL patients [131]. Evidence for the presence of NLCs *in vivo* was demonstrated by Tsukada et al [134]. They observed that among other markers, NLCs were shown to express CD14 and CD68. Mononuclear cells were isolated from the spleens of patients with or without CLL and analysed for CD14 and CD68 by flow cytometry. It was observed that CLL-derived CD14⁺ splenocytes expressed significantly higher levels of CD68 than counterparts from non-CLL patients. Additionally FDCs, present within SLO GC light zones, are known to be a major source of CXCL13 which accumulates on their processes [135]. Macrophages have been detected within CLL LNs, by immunohistochemistry, which express CXCL13. Also, data obtained from immunohistochemical analysis and laser capture microscopy

Chapter 1

found that the GC dark zones contains higher amount of SDF-1 than the GC light zone [136], thereby attracting lymphocytes to the LNs. Upon receptor ligation these chemokines drive B lymphocyte migration out of the peripheral blood and into the microenvironment. Within these supportive niches CLL cells are kept in close proximity to various accessory cells such as NLCs, FDCs, MSCs and macrophages.

The surface expression markers of the aforementioned stromal cells are described here (Table 1.1). NLCs have been shown to express SDF-1 and CD14 [134]. Previous work by Tsukada et al revealed that NLCs failed to differentiate from CD14-mononuclear cells, indicating the significance of this marker for these cells [134]. Additionally they have been found to express CD11b, CD33, CD40, CD45RO, CD68, CD80, CD86, HLA-DQ, HLA-DR and c-MET [134, 137]. FDCs have been shown to express high levels of the complement receptors CR1 (CD35) and CR2 (CD21) [138]. They also express the fc-receptor, CD32 [139], and the TNF family member, CD137 [140]. Generally, MSCs do not express haematopoietic or endothelial cell markers (i.e. CD11b, CD31, CD45) [141]. They do however express various adhesion molecules such as CD44, CD49e and CD62 [141]. Additionally they express multiple other cell surface markers including CD73, CD105, CD90, stro-1, CD271 (LNGFR) and the neural molecule GD2 [142]. Macrophages express CD14, CD11b, CD11c, CD40, CD68, CD163 and F4/80 [143-145]. These microenvironment-based cells have been shown to confer survival of CLL cells *in vitro*, either by direct cell-cell contact, binding to soluble factors or a combination of both (described below).

Numerous studies have shown that multiple stromal cell types can protect CLL cells from apoptosis via various mechanisms; key studies which have demonstrated this are described here. Burger et al showed that co-culturing CLL cells with NLCs significantly protected the malignant cells from spontaneous apoptosis [128]. Additionally NLCs were found to express SDF-1 mRNA and it was demonstrated through the utilisation of SDF-1 neutralising antibodies, that SDF-1 released by NLCs protects CLL cells from spontaneous apoptosis. NLCs have also been implicated in inducing expression of potent chemoattractants within CLL cells. A gene expression microarray showed elevated expression of the T cell chemokines, CCL3 and CCL4, within CLL cells after co-culture with NLCs [146]. Furthermore high levels of both chemokines were detected in CLL-NLC co-cultures supernatant; interestingly higher levels

Cell type	Surface expression markers
Nurse-like cells	SDF-1, CD14, CD11b, CD33, CD40, CD45RO, CD68, CD80, CD86, HLA-DQ, HLA-DR
Follicular dendritic cells	CR1 (CD35), CR2 (CD21), CD32, CD137
Mesenchymal stromal cells	CD73, CD105, stro-1, CD271, GD2, CD44, CD49e, CD62
Macrophages	CD14, CD11b, CD11c, F4/80, CD40, CD68, CD163

Table 1.1: Stromal cell surface expression markers.

Table shows the surface expression markers expressed by nurse-like cells, follicular dendritic cells, mesenchymal stromal cells and macrophages.

Chapter 1

of these chemokines were detected in supernatants from ZAP-70^{+ve} patients (poor prognosis) compared to ZAP-70^{-ve} patients. A study by Pedersen et al demonstrated the protective effect of FDCs on CLL cells. Co-culture of primary CLL cells with the FDC cell line, HK cells, was shown to protect CLL cells from both spontaneous and drug-induced apoptosis [147]. Immunoblot analysis revealed that CLL-HK cell co-culture up-regulated expression of the anti-apoptotic protein MCL-1 within the malignant cells. Furthermore this study demonstrated that inhibiting MCL-1 expression within CLL cells, by utilising MCL-1 anti-sense oligonucleotides, significantly blocked HK cell-mediated protection of the malignant cells, indicating a primary role for MCL-1 in FDC-mediated protection. Additionally, neutralising antibodies against various adhesion molecules were used to demonstrate that direct cell-to-cell contact between CLL and HK cells, through CD44 interaction, is involved in both HK-mediated protection and induction of MCL-1 expression in CLL cells. A study by Kurtova et al demonstrated the ability of various MSCs to protect primary CLL cells, including murine cells lines (M210B4, KUM4, KUSA-H1 and ST2), human cell lines (stromalNKtert, UE6E7T-1 and UCB408E6E7TERT-33) and primary human MSCs isolated from the BM of patients with CLL [127]. Direct co-culture of CLL cells and MSCs showed that both murine and human MSCs protect CLL cells from both spontaneous apoptosis and apoptosis induced by fludarabine, dexamethasone and cyclophosphamide. Similar to the Pedersen et al paper, this study also showed that direct cell-to-cell contact was required for sufficient MSC-mediated protection of CLL cells, as separating these two cells using micro-pore filters prevented the stromal-cell induced protection. Furthermore immunoblot analysis revealed that the MSCs maintained MCL-1 expression within CLL cells. Additionally higher levels of cleaved MCL-1 and PARP were detected within fludarabine-treated CLL cells, however this cleavage was reduced upon co-culture with MSCs, indicating that these stromal cells protect CLL cells from apoptosis by maintaining MCL-1 expression and preventing PARP cleavage. Additionally it has been shown that T cells can release interleukin 4 (IL-4) which protects CLL cells for apoptosis through the up-regulation of the anti-apoptotic protein Bcl-2 [148].

Investigations have also been made into determining which intracellular signalling pathways are involved in stromal cell-mediated protection of CLL cells. Kamdje et al demonstrated that NOTCH signalling is involved in promoting stromal cell-mediated protection and chemoresistance to CLL cells

[149]. This study utilised primary human BM derived stromal cells and primary CLL cells. Co-culture of the two cell types prevented spontaneous and drug induced apoptosis of the malignant cells. Treatment of CLL cells with anti-Notch-1, 2 and 4 antibodies, as well as the Notch-specific neutralising antibody, GSI XII, prevented this protection, both in the absence and presence of various chemotherapy drugs. Furthermore Hedgehog signalling has also been implicated in promoting CLL cell survival. Hedge et al utilised a hedgehog signalling inhibitor, cyclopamine, in CLL-BM stromal cell co-cultures, and observed a reduction in stromal cell-mediated protection of CLL cells [150].

Furthermore the LN microenvironment has been shown to be a primary site for promoting BCR activation, NF κ B signalling and proliferation of CLL cells, all of which promote disease progression [7]. This was demonstrated by Herishanu et al who isolated CLL cells from the peripheral blood, BM and LNs of 24 treatment-naive patients and analysed the cells by gene expression profiling. Expression of genes involved in BCR and NF κ B activation was strongly detected in CLL cells isolated from the LNs, therefore indicating induction of BCR and NF κ B signalling. Expression of phosphorylated SYK (downstream event of BCR activation; described in section 1.8) was analysed in CLL cells by flow cytometry and found to be higher within LN-derived CLL cells compared to counterparts from the peripheral blood. Immunoblot analysis detected higher expression of phosphorylated I κ B α (indicates NF κ B pathway induction; NF κ B pathway described in section 1.11) in LN-derived cells compared to cells derived from the blood. Additionally a set of proliferation-related genes, E2F and c-Myc, were found to be up-regulated within LN-derived CLL cells compared to cells derived from the peripheral blood and BM. Furthermore flow cytometry was utilised to analyse expression of the proliferation marker Ki-67, which was found to be higher in LN-derived samples compared to those derived from the peripheral blood.

Interactions between CLL cells and the ECM can also modulate survival of the malignant cells. The glycoprotein receptor CD44 is expressed at high levels by CLL cells [151]. The main ligand for this receptor is hyaluronic acid (HA) [152], however other ECM components can interact with CD44 including fibronectin and collagen, both of which are expressed by stromal cells, specifically fibroblasts and myofibroblasts [153]. Herishanu et al showed that engagement of CD44, utilising HA or an anti-CD44 monoclonal antibody promoted CLL cell

Chapter 1

survival by inducing PI3K/AKT and MAPK/ERK signalling, as well as up-regulating MCL-1 expression [154]. Further to this, activation of CD44 was also shown to protect CLL cells from both spontaneous and fludarabine-induced apoptosis. Overall there is a vast amount of data in the literature which demonstrate that the microenvironment is vital for the survival of CLL cells both *in vivo* and *in vitro* [7, 127, 133].

1.5 Fibroblasts and myofibroblasts

This project focusses on investigating what effect fibroblasts and myofibroblasts have on CLL cells, and vice versa. Therefore this section will discuss fibroblasts, myofibroblasts and process by which fibroblasts transdifferentiate into myofibroblasts.

1.5.1 Fibroblasts

Fibroblasts are stromal cells of mesenchymal origin; they are non-contractile, spindle-shaped cells that express low basal levels of alpha smooth muscle actin (α -SMA), an isoform of actin associated with contractility [155]. They are present in virtually every organ and tissue within the body, and thus it has been shown that fibroblasts are a heterogeneous population whose characteristics vary depending on their anatomical site. Evidence for this comes from a study conducted by Chang et al who utilised cDNA microarray technology to analyse the gene expression patterns of various types of primary human fibroblasts from 10 distinct anatomical sites and 16 different donors [156]. These sites included the arm, abdomen, back, scalp, foreskin, thigh, gum and toe. This study demonstrated that fibroblasts from different anatomical sites express distinct transcriptional patterns thus indicating the diversity of these cells. Unfortunately confirming the presence of these cells *in vitro* can be difficult mainly because fibroblast-specific markers are poorly defined. Generally fibroblasts are identified based on their spindle-shaped morphology, ability to adhere to tissue culture plastic, expression of the mesenchymal cell marker vimentin and absence of markers for other cell lineages such as epithelial or muscle cells [156, 157]. However this is not a definitive method of identification as vimentin is not exclusive to fibroblasts and multiple other cell types, including pericytes and smooth muscle cells, have been found to express this marker [158, 159]. Fibroblasts are mainly

involved in producing and maintaining the ECM of the organ or tissue within which they are located; the endoplasmic reticulum and Golgi are found in abundance within fibroblasts and are required to synthesise various ECM proteins such as fibronectin. They also play a role in wound healing when they transdifferentiate into myofibroblasts upon activation.

1.5.2 Myofibroblasts

The myofibroblast phenotype appears to be intermediate between that of fibroblasts and smooth muscle cells. **They express high levels of α -SMA** (a hallmark of myofibroblasts) as well as contain an abundant amount of stress fibres (discussed in section 1.5.4). Myofibroblasts have been shown to express the marker vimentin, which is expressed by fibroblasts, and the 4Ig isoform of palladin which is present within myofibroblast stress fibres [160-162]. These cells are also negative for smooth muscle markers such as smoothelin, desmin and caldesmon [160].

The origin of myofibroblasts is heterogeneous (Figure 1.6). Primarily myofibroblast precursors appear to be locally recruited fibroblasts from adjacent intact dermal and subcutaneous tissue. Evidence for this has emerged from multiple studies. One of the earliest studies to demonstrate this came from Grillo et al who quantitatively analysed fibroblast proliferation within the local area of a wound (using male guinea pigs), which had been x-irradiated both before and after wound healing [163]. The cells were labelled with tritiated thymidine, which incorporates into replicating DNA, and analysed by autoradiography. They observed that the primary site of origin for fibroblasts involved in wound healing (i.e. myofibroblasts) was within the connective tissue adjacent to the wound. A further study by Stewart et al studied a patient following BM transplantation and observed that fibroblast-like cells emigrating from a 5 day old skin wound explant had host karyotype, compared to emigrating macrophages which expressed donor markers [164]. These data indicated that the wound fibroblasts were of local tissue whereas the myofibroblasts were of haematopoietic tissue origin. Local mesenchymal stem

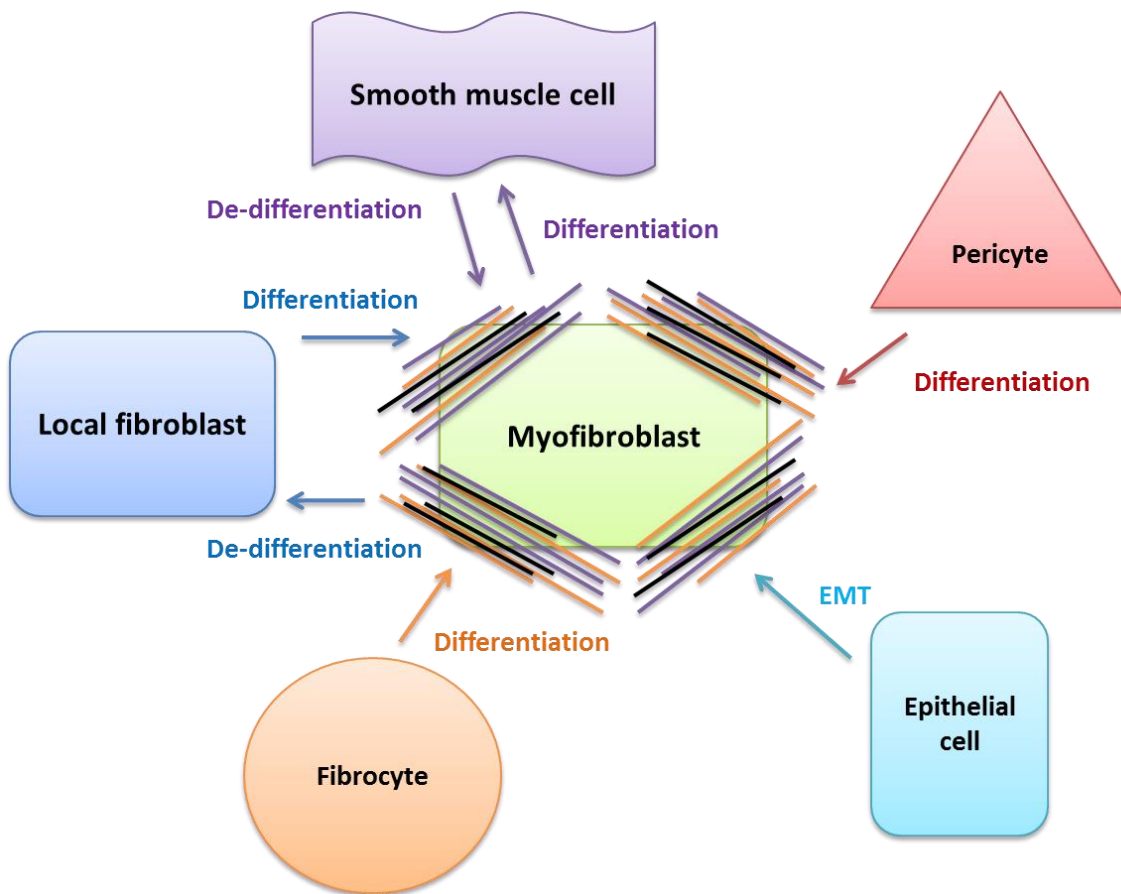


Figure 1.6: Diagram showing the various sources of myofibroblasts.

Primarily myofibroblasts originate from local fibroblasts in response to wound healing. However there is evidence for other potential sources; Epithelial cells can undergo EMT to develop the myofibroblast phenotype, smooth muscle cells may de-differentiate into myofibroblasts and fibrocytes and pericytes can differentiate into myofibroblasts.

cells have also been implicated as a potential myofibroblast precursor. Jahoda et al investigated the ability of progenitor cells residing within the dermal sheath that surrounds the hair follicle to express the myofibroblast phenotype, and observed their ability to transdifferentiate into myofibroblasts after the induction of a lesion [165]. Additionally the ability for a sub-population of BM-derived circulating leukocytes with fibroblast characteristics, termed fibrocytes, have been studied for their ability to acquire the myofibroblast phenotype and aid in wound healing. Abe et al showed that treatment of peripheral blood mononuclear cell (PBMC) cultures with transforming growth factor beta (TGF- β) induced fibrocyte differentiation as observed by the accumulation of cells with spindle-shaped morphology [166]. Additionally these cells were found to rapidly migrate into the wound sites of mice injected with enriched murine fibrocyte preparations. Furthermore fibrocytes were found to express both α -SMA mRNA and protein, and were able to significantly contract collagen gels which is an ability shared by myofibroblasts. Another source of myofibroblasts involves EMT, a process by which epithelial or endothelial cells undergo phenotypic conversion into mesenchymal cells, such as fibroblasts and myofibroblasts. A study by Yang et al demonstrated that the treatment of human renal tubular epithelial cells with TGF- β (main cytokine responsible for myofibroblast transdifferentiation; discussed below) induced expression of α -SMA and the formation of stress fibres [167]. Additionally, TGF- β treated cells also expressed the mesenchymal marker vimentin and were able to produce the ECM molecules fibronectin and collagen. Furthermore the transformed cells underwent complete loss of the epithelial cell marker E-cadherin. Kim et al studied lung biopsies from patients with idiopathic pulmonary fibrosis and found that the alveolar epithelial cells within these tissues underwent dramatic phenotypic alterations as observed by the formation of stress fibres and α -SMA expression, indicating that the cells transformed into expressing a myofibroblast phenotype [168]. Additionally studies have also shown that pericytes and smooth muscles cells are also potential sources of myofibroblasts. Rajkumar et al analysed skin biopsies from individuals with or without diffuse cutaneous systemic sclerosis (dcSSc), for the myofibroblast markers α -SMA and the ED-A splice variant of fibronectin (discussed below) by immunohistochemistry and dual immunofluorescence [169]. They observed the presence of myofibroblasts within dcSSc tissue but not within normal tissue. Additionally, both myofibroblasts and pericytes within dcSSc tissue expressed

Chapter 1

ED-A fibronectin. Hao et al analysed the phenotypic characteristics of coronary artery smooth muscle cells within stenotic plaques, erosions, stable plaques and in-stent restenosis, by analysing expression of α -SMA, smooth muscle myosin heavy chains (SMMHCs), and smoothelin, the latter two being smooth muscle cell markers, by immunohistochemistry [170]. α -SMA expression was detected within the different lesions, and interestingly within the same location there was a significant reduction in SMMHCs and smoothelin, indicating a possible conversion of smooth muscle cells towards the myofibroblast phenotype.

1.5.3 Myofibroblasts in cancer

Myofibroblasts are present within the stroma of multiple types of solid tumours and many groups have studied their impact on disease progression. **Yamashita et al analysed α -SMA expression within the stroma of 60 different patients diagnosed with invasive breast cancer, by immunohistochemistry [171]. They found that α -SMA expression was significantly higher in patients with metastasis compared to those with no metastasis. Additionally, patients were divided into low and high α -SMA expression groups, with 8.48% as the cut-off, and patients in the high α -SMA groups had a significantly worse overall survival rate compared to patients in the low α -SMA group.** Hwang et al studied the effect of pancreatic stellate cells, which are myofibroblast-like cells (express vimentin and α -SMA) on pancreatic tumour progression [172]. Two pancreatic tumour cell lines, BxPC3 and Panc1, were cultured in conditioned media derived from human pancreatic stellate cells; an increase in tumour cell proliferation, migration, invasion and colony formation was observed. **Another study by Fujita et al analysed α -SMA mRNA levels by quantitative PCR of tissue samples from 109 different patients diagnosed with pancreatic ductal adenocarcinoma, and observed that patients expressing high levels of α -SMA had a significantly shorter survival rate than patients with low α -SMA expression [173].** Olumi et al studied the effect of human prostate cancer associated fibroblasts (CAFs) on prostatic epithelial cells and demonstrated that the CAFs were able to stimulate growth of initiated human prostatic epithelial cells but had no effect on normal prostatic epithelial cells [174]. Additionally normal prostatic fibroblasts did not promote cell growth of initiated epithelial cells. **Lee et al analysed α -SMA expression in 263 patients with primary lung adenocarcinoma by immunohistochemistry and observed**

that patients with high α -SMA expression associated with significantly enhanced metastasis and poor prognosis compared to patients with low α -SMA expression [175]. Additionally, down-regulating α -SMA utilising siRNA reduced malignant cell migration and invasion *in vitro*, indicating that myofibroblasts promote metastasis in lung adenocarcinoma. Collectively these **data, as well as numerous other studies, indicate that the presence of α -SMA-positive cells** (i.e. myofibroblasts) within the solid tumour stroma promote progression of multiple types of cancer, a few of which include breast cancer, pancreatic adenocarcinoma, prostate cancer and lung adenocarcinoma, resulting in poor patient outcome.

1.5.4 Fibroblast-to-myofibroblast transdifferentiation

Myofibroblasts were first detected within the granulation tissue of healing wounds; this led to the idea, which is now widely accepted, that they are contractile cells responsible for wound contraction and subsequent wound closure [176]. It was then shown that α -SMA expression within the granulation tissue of an open wound progressively increased as the wound healed; α -SMA expression declined thereafter upon completion of wound closure [177]. This indicated that myofibroblasts express high levels of the contractile protein α -SMA. Their ability to contract is a vital characteristic required for the closure and subsequent healing of cutaneous wounds. Furthermore it has been demonstrated that transforming growth factor beta (TGF- β) **induces expression of α -SMA** in granulation tissue, indicating that this cytokine coordinates myofibroblast transdifferentiation both *in-vivo* and *in-vitro* [178].

The first stage of myofibroblast transdifferentiation involves the differentiation of fibroblasts into proto-myofibroblasts (Figure 1.7). For this to occur, fibroblasts must attach to a surface so they can spread and migrate in order to induce mechanical tension. Evidence for this was demonstrated when increasing mechanical tension within granulation tissue induced the formation of stress fibres [179]. Conversely, releasing the granulation tissue of mechanical stress resulted in the reduction of stress fibres [179]. These data strongly suggest that mechanical tension generated from this adherent step is essential for inducing the proto-myofibroblast phenotype. Characteristics of the proto-myofibroblast phenotype include formation of stress fibres, focal adhesions, extracellular fibronectin fibrils and expression of the ED-A splice

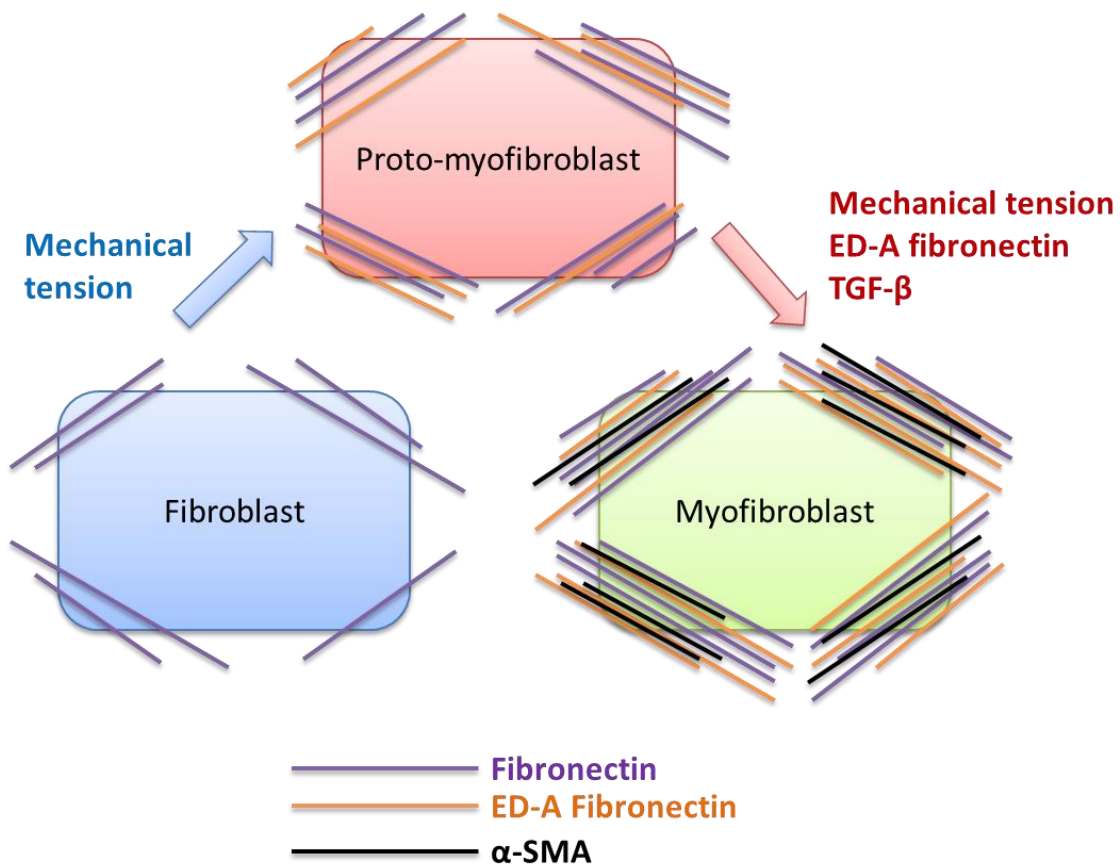


Figure 1.7: Diagram highlighting the key stages of myofibroblast transdifferentiation.

Mechanical stress is required to induce fibroblasts (blue) to develop into proto-myofibroblasts (red). Proto-myofibroblasts express higher levels of fibronectin (purple) including the ED-A splice variant of fibronectin (orange). TGF- β , ED-A fibronectin and mechanical stress are required for proto-myofibroblast differentiation into myofibroblasts (green), which express higher levels of fibronectin and ED-A fibronectin compared to proto-myofibroblasts. Additionally myofibroblasts express high levels of α -SMA.

variant of fibronectin. ED-A fibronectin has been shown to be essential for promoting further myofibroblast transdifferentiation. Previous data showed that stimulating granulation tissue with TGF- β **induced the deposition of ED-A fibronectin, which preceded α -SMA expression** [180]. Furthermore blocking ED-A expression inhibited TGF- β **induced α -SMA expression** [180].

The proto-myofibroblast phenotype can now be stimulated to develop into the myofibroblast phenotype, which **typically expresses high α -SMA** and increased levels of ED-A fibronectin (compared to proto-myofibroblasts). TGF- β is the key stimulus required to induce the myofibroblast phenotype. Many studies have shown that TGF- β **induces α -SMA expression** and promotes generation of contractile force in myofibroblasts [181]. Additionally, various cytokines have been tested yet were unable to produce the responses induced by TGF- β [182]. **High levels of α -SMA expression and fibronectin organisation into fibrils within myofibroblasts relays the ability to generate stronger contractile force than their proto-myofibroblast counterparts.**

1.5.5 Differentiation versus transdifferentiation

Differentiation and transdifferentiation, although similar, are 2 distinct processes. Differentiation is the process by which a less specialised cell type undergoes genetic and phenotypic changes, to become a more specialised cell type. For example, this is the case in haematopoiesis, during which the un-specialised, progenitor cell type, the HSC, which has pluripotent potential, develops in a step-wise manner towards becoming any haematopoietic lineage. At each stage of development the progenitor cell becomes more specialised, and successively loses its cell potency as it becomes further committed to a specific cell lineage. Transdifferentiation, on the other hand, is a subset of metaplasias, which involves the conversion of a differentiated cell, into another differentiated cell type [183]. Examples of transdifferentiation, other than myofibroblast transdifferentiation, include the formation of a complete lens from the iris, which occurs in the eye of an adult newt [183]. Another example of this phenomenon occurs between the pancreas and liver, where it has been documented that pancreatic cells can convert into hepatocytes, and vice versa [183].

1.6 TGF- β signalling

1.6.1 TGF- β structure and activation

The TGF- β superfamily is comprised of two subfamilies: the TGF- β /Activin/Nodal subfamily and the BMP/GDF/MIS subfamily. The members of this family all share common structural features and are characterised by six conserved cysteine residues in humans; yet they all induce diverse biological effects. TGF- β exists as three separate isoforms; TGF- β 1, TGF- β 2 and TGF- β 3. TGF- β 1 has been the most extensively studied and it has been shown to be released from most cell types in a latent form which requires activation in order to induce TGF- β signalling [184, 185]. TGF- β is synthesised as a dimer whose monomer subunits are connected via disulphide bridges. This TGF- β dimer is cleaved by the enzyme furin convertase resulting in the non-covalent association of the mature TGF- β dimer with latency associated peptide (LAP) [186]; this is known as the small latent TGF- β complex (SLC). LAP confers latency to the mature TGF- β subunit of the SLC, rendering this cytokine biologically inactive. Additionally, a large protein known as latent TGF- β binding protein (LTBP) is covalently attached thus forming the large latent TGF- β complex (LLC); LTBP facilitates secretion of the latent TGF- β complex [187]. Dissociation of TGF- β with LAP and LTBP results in the activation of the cytokine allowing it to carry out its diverse range of biological functions.

1.6.2 TGF- β signalling

Active TGF- β dimers bind to the serine/threonine kinase receptor family. Within the human genome this family is formed of 12 members: 7 are type 1 receptor serine/threonine kinases and the remaining 5 are type 2 receptor serine/threonine kinases. All of these receptors are committed to the TGF- β signalling pathway which is dependent on the formation of heteromeric complexes comprising the type 1 and type 2 receptors [188]. TGF- β has a high affinity for type 2 receptors and little interaction occurs with type 1. The type 1 receptor contains the GS domain, which is absent in type 2 receptors; this is a 30 amino acid sequence containing a highly conserved SGSGSG sequence in the middle [188]. Upon cytokine binding the type 2 receptor recruits the type 1 receptor and phosphorylates multiple serine and threonine residues within its cytoplasmic GS region resulting in receptor activation (Figure 1.8). This

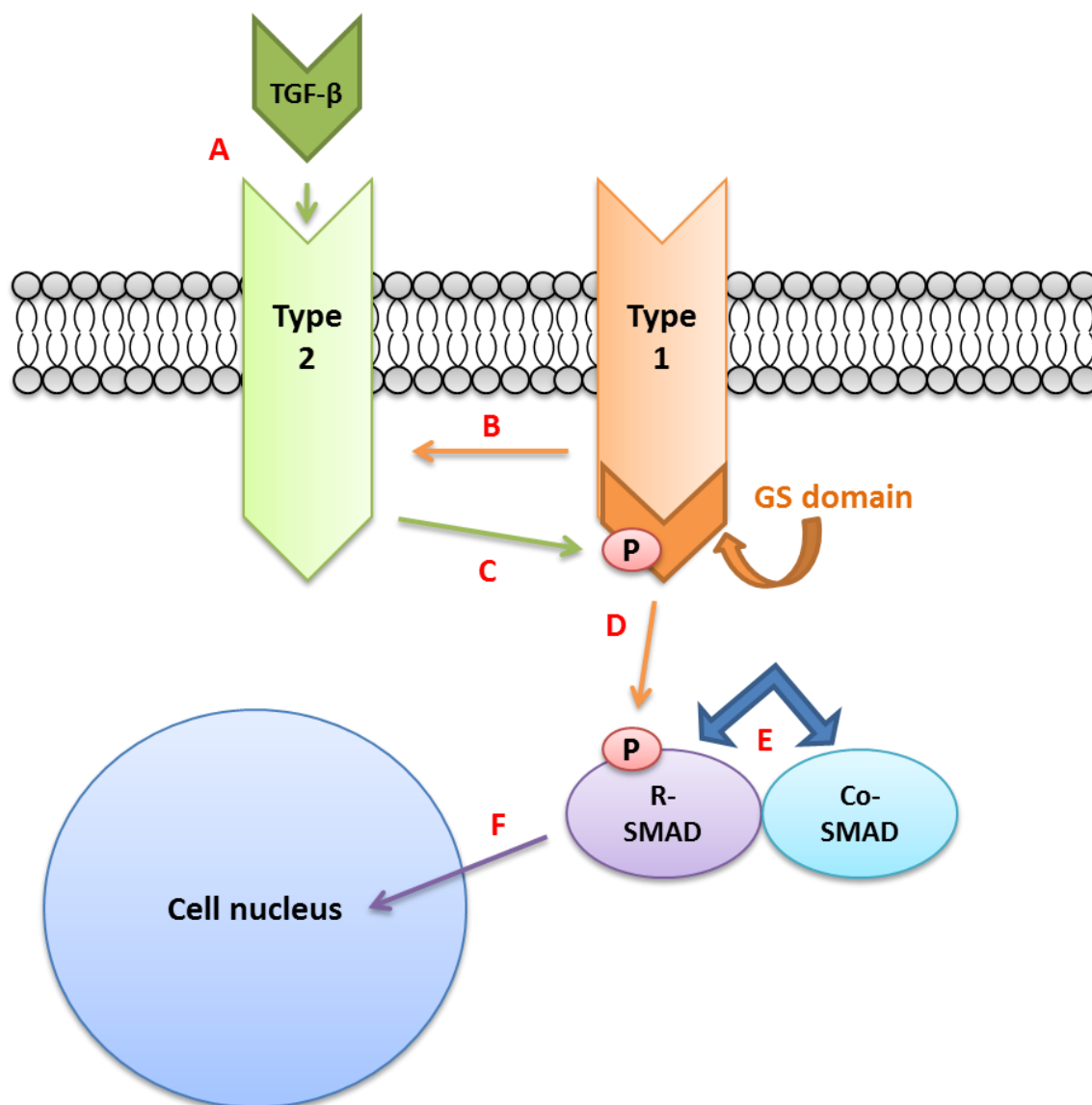


Figure 1.8: TGF- β signalling pathway

TGF- β has a high affinity for type 2 receptors (green) and little interaction occurs with type 1 (orange). The type 1 receptor contains a 30 amino acid sequence containing a highly conserved SGSGSG sequence (GS domain), which is absent in type 2 receptors. Upon cytokine binding (A) the type 2 receptor recruits the type 1 receptor (B) and phosphorylates multiple serine and threonine residues within its cytoplasmic GS region resulting in receptor activation (C). The activated receptor type 1 kinases phosphorylate and subsequently activate R-Smads (D) which consequently form heteromeric complexes with Co-Smad 4 (E). The Smad complexes then translocate to the cell nucleus (F) where they mediate transcriptions of target genes.

Chapter 1

initiates the TGF- β signalling cascade involving the phosphorylation of multiple Smad transcription factors. Initial identification of Smad proteins was through the detection of mothers against Dpp (MAD) in drosophila followed by identifying sma proteins that were closely related to MAD in c.elegans; thus far 8 mammalian Smad proteins have been identified which fall into 3 distinct functional groups [189, 190]. Firstly there are the receptor-regulated Smads (R-Smads) which comprise Smad 1, 2, 3, 5 and 8. The second group are co-mediator Smads (Co-Smads) which is solely composed of Smad 4. The final group are inhibitory Smads (I-Smads) which include Smad 6 and 7. Activated receptor type 1 kinases phosphorylate and subsequently activate R-Smads. Consequently R-Smads form heteromeric complexes with Co-Smad 4. The newly formed Smad complexes subsequently translocate to the cell nucleus where they bind cellular DNA and mediate transcription of target genes to induce various biological effects.

1.6.3 Effect of TGF- β under normal and malignant conditions

TGF- β signalling mediates a range of diverse cellular functions including cell proliferation, differentiation, apoptosis, migration and extracellular matrix production. Therefore this cytokine can induce various biological effects under both normal and tumorigenic conditions. It has been previously mentioned that TGF- β is a key stimulus for inducing myofibroblast transdifferentiation (section 1.4). Under normal conditions myofibroblasts develop within granulation tissue to aid in wound healing. However myofibroblasts have been detected within the stroma of multiple types of solid tumour and their presence correlate with a more severe disease progression and poor clinical outcome; a few examples include prostate, pancreatic and breast cancer [171, 172, 174].

As well as playing a vital role in promoting fibroblast-to-myofibroblast transdifferentiation, **TGF- β also plays a crucial role in regulating** differentiation, within various other cell types. For instance, previous data have shown that the treatment of human cardiomyocyte progenitor cells, with TGF- β , **can induce their differentiation into functional beating myocytes** [191]. TGF- β is also known to play a role in the formation of bone. **An earlier study revealed that TGF- β promotes the differentiation of human mesenchymal stem cells into osteoblasts, through the activation of β -catenin signalling** [192]. Previous work has also highlighted the importance of TGF- β in

oligodendrocyte differentiation. Oligodendrocyte-type-2 astrocyte (O-2A) progenitor cells proliferate in response to the mitogens, PDGF and bFGF, however, upon removal of these growth factors, the progenitor cells differentiate into oligodendrocytes. O-2A cells have been shown to release TGF- β , **which acts to inhibit PDGF-**, and to a lesser extent, bFGF-induced proliferation, resulting in the differentiation of O-2A into oligodendrocytes [193].

TGF- β is also known to be a potent inhibitor of cell proliferation in multiple cell types. Previous work has shown that TGF- β can inhibit proliferation of skin keratinocytes by suppressing c-Myc transcription, which is required to induce proliferation of these cells [194]. Additionally TGF- β has been shown to significantly inhibit N-Myc expression in lung bud epithelia thus preventing tracheobronchial epithelial development [195]. These are just a few examples of the inhibitory effect of this cytokine on cell proliferation. As a result inactivation of TGF- β signalling can contribute to tumorigenesis, and resistance to TGF- β mediated growth inhibition has been seen in multiple types of cancer including breast cancer, colon carcinoma and B and T lymphomas [196-198]. This resistance could be a consequence of TGF- β receptor mutation. Previous work in colon cancer cell lines has demonstrated that the type 2 TGF- β receptor acquires truncating mutations leading to the absence of its expression at the cell surface thus resulting in TGF- β resistance [199]. Conversely another study demonstrated that overexpression of TGF- β may suppress development of mammary neoplasia during its early stages. This work suggested that TGF- β may play a dual role by preventing development of carcinomas but then enhance tumorigenesis upon complete neoplastic transformation and loss of TGF- β responsiveness [200].

Previous work has shown that CLL cells release endogenous TGF- β which acts in an autocrine fashion to reduce proliferation of the malignant cells [201]. It is thought this may account for the low proliferative rate of the cells and therefore slow progression of the disease. Additionally neutralising antibodies against TGF- β increase the rate of CLL proliferation [201]. Furthermore it has been demonstrated that TGF- β inhibits DNA synthesis in B lymphocytes from **both 'normal' donors and CLL patients; however the reduction in DNA synthesis induced by TGF- β was greater in the B cells of normal donors** [202]. These data suggest that TGF- β may allow selective accumulation of CLL cells

Chapter 1

thus providing a survival advantage over normal B lymphocytes. However CLL cells from some patients are resistant to the growth-inhibiting effect of TGF- β and previous data has shown that this may be due to loss of expression of functional type 1 TGF- β receptors on the CLL cell surface [203].

1.7 CLL and apoptosis

Apoptosis is programmed cell death; it is a critical homeostatic process involved in maintaining the balance between cell survival and death to maintain cell numbers and discard damaged or diseased cells. It is characterised by the induction of a series of controlled biochemical events and morphological changes which differs from necrosis in that the latter is a form of cell death caused by injury to the cell. The initial phase of apoptosis involves distinct condensation processes resulting in cell shrinkage which is visible by light microscopy. Firstly chromatin condensation (pyknosis) occurs within the nucleus followed by cytoplasmic condensation [204]. Next the cytoskeleton disintegrates resulting in the presence of blebs on the cell surface which is followed by the accumulation of apoptotic bodies due to the cells breaking down [205]. Phagocytosis is the final stage resulting in the removal of apoptotic bodies by normal surrounding cells. There are two main pathways that initiate apoptosis; they are the extrinsic and intrinsic pathways. The extrinsic pathway involves ligation of death receptors belonging to the tumour necrosis factor (TNF) receptor superfamily. This results in the induction of the caspase cascade which leads to cell death. The intrinsic pathway involves an increase in mitochondrial membrane permeability resulting in release of various pro-apoptotic proteins such as cytochrome c, Smac/DIABLO or HtrA2, which enter the cytosol. Cytochrome c forms part of a multi-protein complex known as the apoptosome, while Smac/DIABLO and Htr2A inhibit IAPs (inhibitors of apoptosis proteins).

To date the Bcl-2 family constitute over 25 different proteins which share sequence homology that display anti-apoptotic or pro-apoptotic function. There are 6 known anti-apoptotic proteins in human which are Bcl-2, Mcl-1, Bcl-xL, Bcl-B, Bcl-W and Bfl-1 [206]. There are far more pro-apoptotic proteins, a few of which include Bim, Bad, Bax, Bak and Bid [207]. These proteins regulate apoptosis, and the balance between pro-apoptotic and anti-apoptotic proteins, in response to specific signals, determine whether or not

apoptosis will be initiated. For instance, under normal non-pathological conditions, cell damage up-regulates the expression of pro-apoptotic proteins leading to the execution of apoptosis [208]. Previous work has shown that the majority of CLL cases overexpress Bcl-2 indicating a potential mechanism by which CLL cells evade apoptosis [209]. Furthermore utilising inhibitors to block Bcl-2 expression has been shown to induce apoptosis in CLL cells *ex vivo* [210]. Additionally, other anti-apoptotic Bcl-2 proteins have been detected in CLL cells and contribute to apoptotic resistance; they include Bcl-XL, Mcl-1, Bcl-WL and Bfl-1 [211-213]. Higher levels of MCL-1 have been shown to correlate with poor clinical outcome [211]. A higher Bcl-2-Bax ratio was detected in CLL cells compared to normal lymphocytes [212]. Furthermore this ratio was reduced in cells undergoing spontaneous apoptosis.

One of the main reasons CLL cells accumulate within the microenvironment is due to stromal cell-mediated protection from apoptosis. Several lines of evidence indicate that various stromal cells can protect CLL cells from apoptosis by altering their expression of Bcl-2 family proteins. A previous study has shown that a FDC cell line, HK cells, can protect CLL cells from apoptosis through the up-regulation of anti-apoptotic MCL-1 expression [214]. Additionally bone marrow-derived stromal cells were shown to protect CLL cells from apoptosis through the activation of Notch signalling which consequently induced the up-regulation of Bcl-2 expression [149].

1.8 B-cell receptor signalling

A lot is known about the BCR and the signal transduction pathway induced downstream of it. Many of the molecules involved in BCR signalling are shared by other pathways and therefore they are good candidates for analysing the interplay between CLL cells, and fibroblasts and myofibroblasts. Both normal and CLL B lymphocytes express BCRs on their cell surface. These receptors do not have an exclusive ligand. The BCR for each individual B lymphocyte recognises a specific ligand which is different to what is bound by other BCRs expressed by different B lymphocytes. BCR signalling in normal B cells is involved in promoting B cell function such as antibody production, as well as mediating cell proliferation and differentiation. It is widely accepted that BCR signalling in CLL cells plays an important role in disease pathogenesis, due to

Chapter 1

its effect on CLL cell survival, proliferation and homing to specific tissue sites [215].

The BCR is composed of an antigen binding subunit which is non-covalently bound to a signalling subunit. The latter is a disulphide linked heterodimer comprising the transmembrane proteins CD79a (Ig α) and CD79b (Ig β) [216]. The cytoplasmic tail of Ig α and Ig β each contain a conserved amino acid sequence motif known as the immunoreceptor tyrosine-based activation motif (ITAM); phosphorylation of tyrosine residues within this motif is required for signal transduction initiation following BCR activation [217]. Ligation of the antigen binding subunit induces BCR aggregation (Figure 1.9). This induces phosphorylation of the ITAMs by src family protein tyrosine kinases (PTKs) such as Lyn, Fyn and Blk. The phosphorylated ITAMS serve as docking sites for proteins containing src homology 2 (SH2) domains, such as syk. Binding of syk to the ITAMs results in it being initially phosphorylated at its Tyr352 site (syk³⁵²) [218]. This phosphorylation step induces syk to undergo a conformational change which releases it from its autoinhibitory configuration [219]. Syk is then trans-autophosphorylated at its Tyr525 and Tyr526 sites

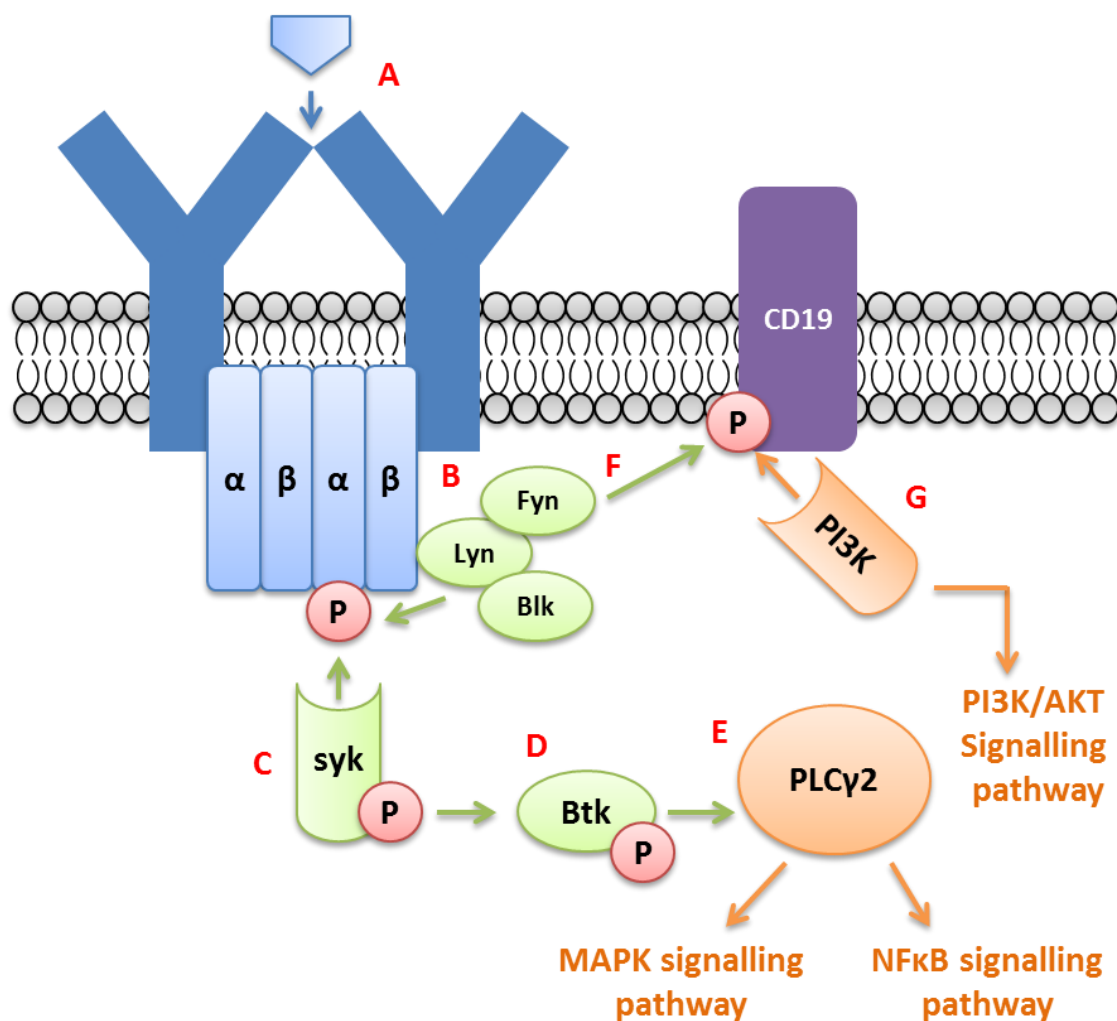


Figure 1.9: B-cell receptor signal transduction pathway.

Upon receptor ligation, the BCR undergoes dimerisation (A). This induces src family kinases, such as Lyn, to phosphorylate tyrosine residues within cytoplasmic ITAMs of the signalling subunit of the BCR (B). Syk is then able to bind to the phosphorylated tyrosine residues via its SH2 domain leading to its phosphorylation and consequent activation (C). Activated syk then phosphorylates and activates Btk (D) which subsequently activates PLC γ 2 (E). Through the generation of IP3 and DAG (not shown) the MAPK and NF κ B signalling pathways are activated. Lyn also phosphorylates tyrosine residues on CD19 (F). This recruits PI3K to the plasma membrane and allows it to bind to CD19 through its regulatory subunit (p85- not shown; (G)). This activates PI3K which mediates the PI3K/AKT signalling pathway.

(pSYK^{525/526}) resulting in full syk activity. Syk then phosphorylates and activates **Bruton's tyrosine kinase (Btk) which leads to the activation of key signalling** intermediate molecules such as phospholipase C gamma 2 (PLC γ 2).. Activation of PLC γ 2 enzymatic activity leads to the generation of the second messenger inositol 1, 4, 5-trisphosphate (IP3) and diacylglycerol (DAG) which subsequently induce the release of intracellular calcium and activation of protein kinase C (PKC), respectively. This causes the activation of multiple downstream signal transduction pathways such as the MAPK and NF κ B pathways (sections 1.9 and 1.10) [220]. Additionally Lyn phosphorylates the B cell surface marker CD19 allowing PI3K to bind to it; this consequently activates the PI3K/AKT pathway (section 1.8).

1.9 PI3K/AKT signalling pathway

The PI3K/AKT pathway acts downstream of various receptors including the BCR, T cell receptor, receptor tyrosine kinases, integrin receptors and G-protein-coupled receptors. PI3K is a heterodimer composed of a regulatory subunit (p85) and a catalytic subunit (p110). Upon BCR receptor activation in normal lymphocytes and CLL cells, the src family kinase Lyn phosphorylates CD19, a B cell specific cell surface marker, on multiple tyrosine residues (Figure 1.10). This allows the p85 subunit to bind to CD19 via its SH2 domain, therefore relocating PI3K to the plasma membrane [221]. The catalytic domain of PI3K then phosphorylates the membrane-associated phospholipid, phosphatidylinositol (4,5)-biphosphate (PIP2), converting it into phosphatidylinositol (3,4,5)-triphosphate (PIP3). PIP3 then recruits proteins containing pleckstrin homology (PH) domains to the membrane, such as the serine/threonine kinase Akt (protein kinase B; PKB) and PDK1 and PDK2. There are 3 main isoforms of Akt (Akt1, Akt2 and Akt3). PDK1 phosphorylates Akt at its threonine 308 (T308; pAK³⁰⁸) site which partially activates it [222]. For full activation Akt is phosphorylated at its serine 473 (S473; pAKT⁴⁷³) site by PDK2 [222]. AKT then goes on to activate its target substrates. Akt can regulate apoptosis by inhibiting pro-apoptotic proteins such as BAD. It has also been **implicated in activating the NF κ B pathway (section 1.10) by degrading I κ B**[223].

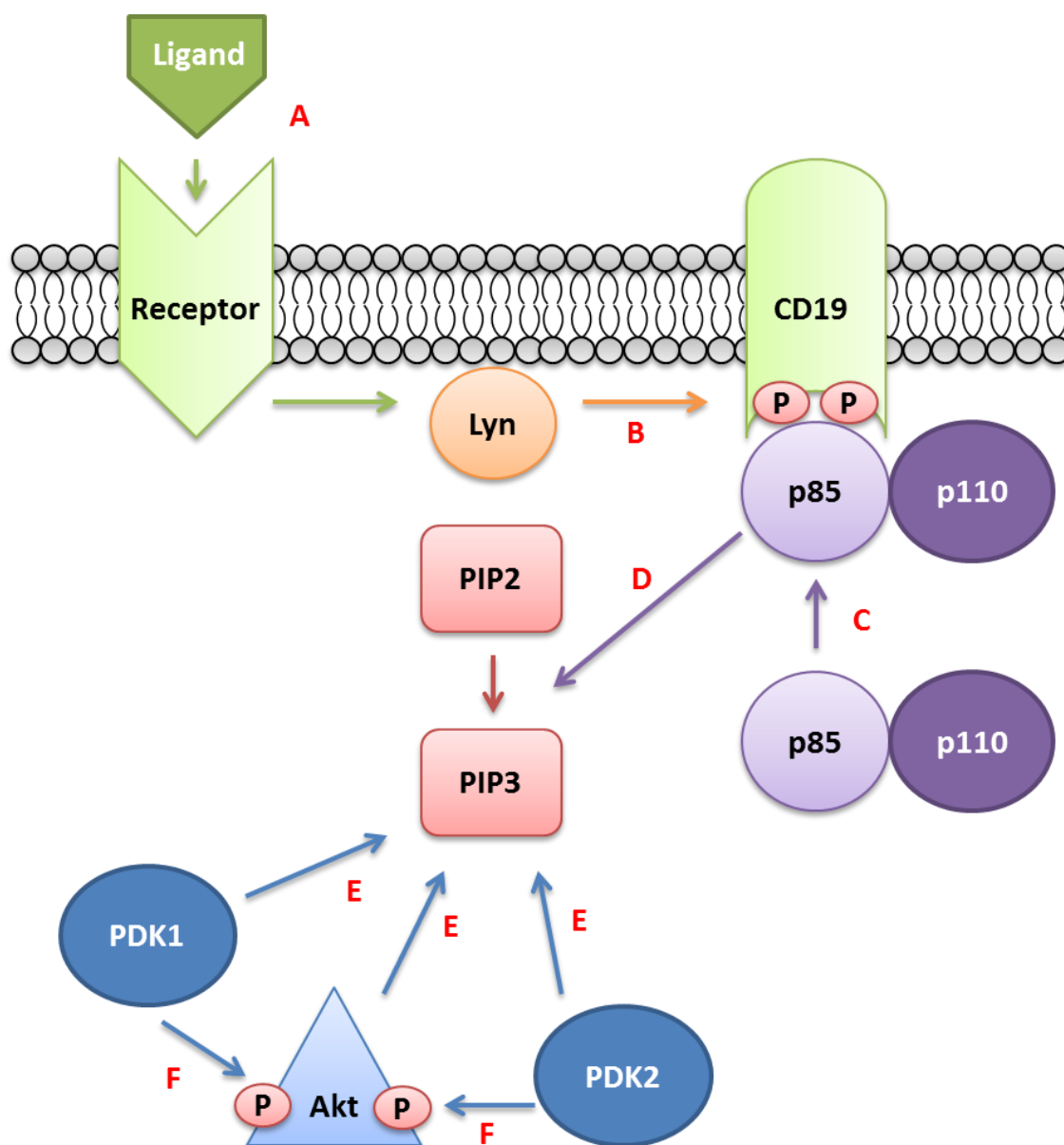


Figure 1.10: PI3K/AKT signal transduction pathway.

Upon receptor ligation (A) the src family kinase Lyn phosphorylates the B cell surface marker CD19 at specific tyrosine residues (B). PI3K is formed of a regulatory p85 subunit and a catalytic p110 subunit. p85 binds to the phosphorylated tyrosine residues of CD19 (C), therefore recruiting PI3K to the plasma membrane, as well as activating it. PI3K then phosphorylates the membrane phospholipid PIP₂, converting it into PIP₃ (D). PIP₃ recruits various proteins containing pleckstrin homology (PH) domains including AKT, PDK1 and PDK2 (E). PDK1 and PDK2 phosphorylate AKT at its threonine 308 site and its serine 473 site respectively, leading to full AKT activation.

1.10 MAPK signalling pathway

The mitogen-activated protein kinase pathway (MAPK) is activated downstream of multiple receptors including the BCR, receptor tyrosine kinases and integrin receptors. There are 3 main branches of the MAPK signalling pathway (Figure 1.11). They include the MAPK/ERK pathway, c-Jun N-terminal kinase (JNK) pathway and the p38 MAPK pathway. In CLL, the MAPK/ERK pathway has shown to be activated downstream of the BCR and the transmembrane glycoprotein, CD44 [154, 224-226]. It is less clear if the JNK and p38 MAPK pathways are active in CLL cells. Evidence has shown that BCR activation does not activate or enhance JNK and p38 MAPK activity; however p38 MAPK is constitutively expressed [225, 226]. The MAPK signalling pathway constitutes a vast amount of diverse signalling molecules therefore the exact signalling molecules involved in this pathway vary greatly depending on the stimuli and which branch of the MAPK pathway is activated; however the basic principle is fairly similar. The general MAPK pathway is described here, however only the signalling molecules involved in the MAPK/ERK pathway are mentioned. Adaptor proteins such as shc and Grb2 link the receptor to guanine nucleotide exchange factors such as son of sevenless (SOS). These factors then activate small GTPase-binding proteins such as RAS which act as molecular switch and induce the main signalling component of the signalling cascade which comprises a sequential series of phosphorylation steps. A MAPKKK (Raf) phosphorylates and activates a MAPKK (MEK) which in turn phosphorylates a MAPK (ERK). The activated MAPK subsequently translocates to the cell nucleus where it activates target transcription factors, such as Elk-1 and c-Myc, and thereby alter gene expression. Evidence has shown that the shc-Grb2-SOS-Ras-Raf-MEK-ERK pathway is induced downstream of the BCR [227].

1.11 NFκB signalling pathway

The nuclear factor- κ B (NFκB) signalling pathway is activated in response to various stimuli and acts downstream of various receptors such as the BCR, TNFR and growth factor receptors. The NFκB pathway has been shown to be activated in CLL cells though signalling via the BCR [228]. NFκB proteins act as dimeric transcription factors. The NFκB family comprises 5 members which include p50 (NFκB1), p52 (NFκB2), p65 (RelA), RelB and c-Rel. All members contain a Rel homology domain (RHD) which is necessary for DNA binding and

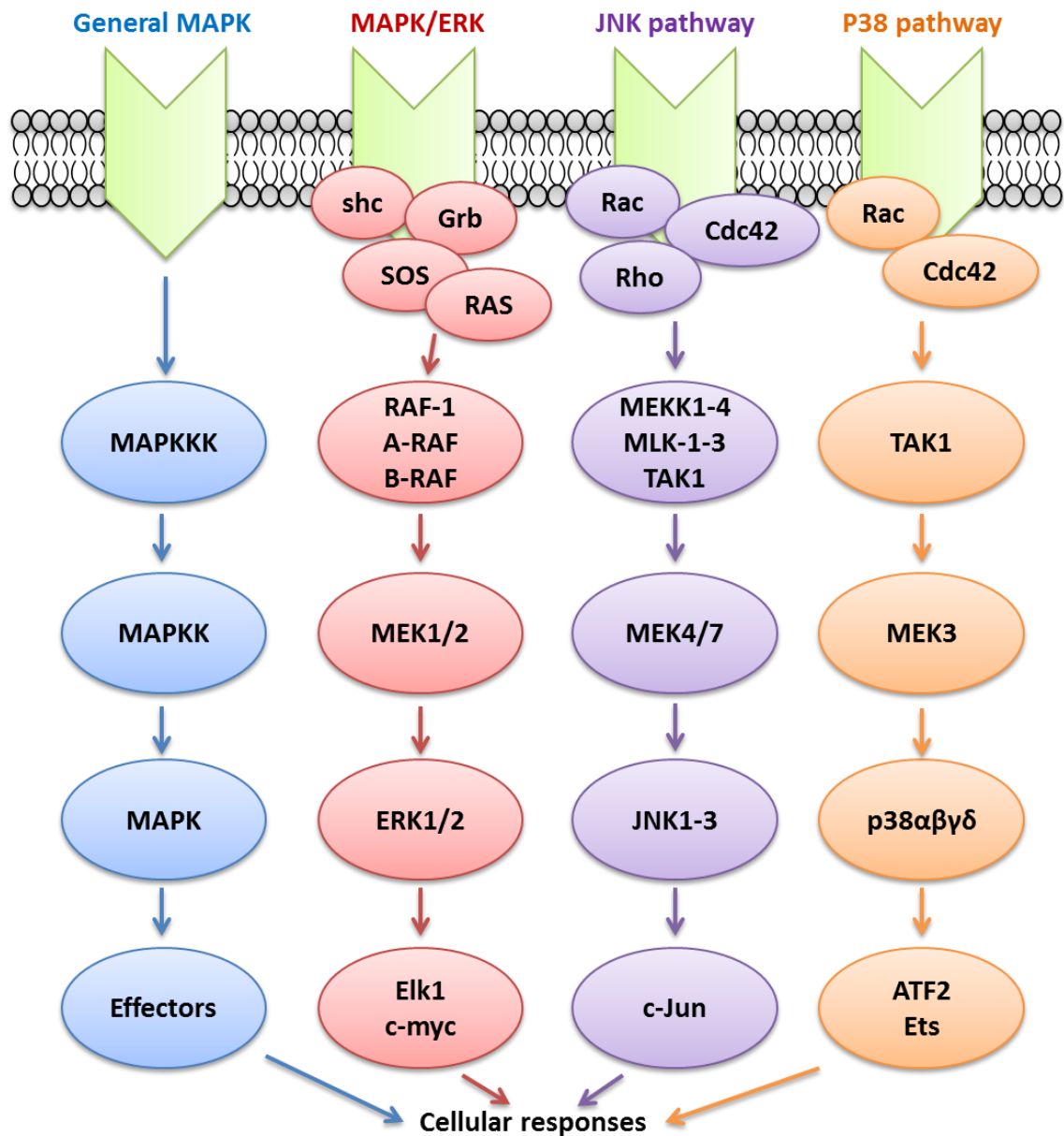


Figure 1.11: MAPK signal transduction pathway.

There are 3 main branches of the MAPK pathway; MAPK/ERK pathway (red), JNK signalling pathway (purple) and the p38 signalling pathway (orange). Upon receptor ligation adaptor proteins (e.g. shc and Grb) activate guanine nucleotide exchange factors (e.g. SOS), which activate small GTPase binding proteins (e.g. RAS). This induces a series of sequential phosphorylation steps in which a MAPKKK phosphorylates and activates a MAPKK which consequently phosphorylates and activates a MAPK. The MAPK then activates its target transcription factors to mediate various cellular responses.

Chapter 1

homodimerisation as well as heterodimerisation. The transcription activation domain (TAD) is required for inducing transcription of target genes; this domain is only present within the 3 Rel proteins (RelA, RelB and c-Rel). TAD is **absent in NFκB1 and NFκB2 and therefore these 2 proteins can repress transcription unless dimerised with a Rel subunit.** In its inactive form NFκB dimers are **constitutively bound to IκB (inhibitor of kappa B),** which retains them within the cell cytoplasm (Figure 1.12). **Degradation of IκB is caused by IKK (inhibitor kappa B kinase).** The IKK complex comprises 2 kinase subunits known as CHUK (IKKα) and IKBKB (IKKβ) as well as the regulatory subunit NEMO (IKKγ). **Upon** receptor ligation, IKK become activated by being phosphorylated **on 2 specific serine residues each for both IKKα and IKKβ; the mechanism by** which this occurs is currently unclear. Activated IKK then phosphorylates IκB on 2 critical serine residues, leading to its ubiquitination and subsequent **degradation by the proteasome.** NFκB is then **no longer inactive and** translocates to the cell nucleus where it binds to DNA of target genes and regulates transcription.

1.12 Hypothesis

This project investigates the interactions between CLL cells, fibroblasts and their differentiated counterpart, myofibroblasts. The overarching hypothesis is that CLL cells alter fibroblast to myofibroblast transdifferentiation and that this, in turn, creates an optimal protective niche through modulation of Bcl-2 family proteins and apoptotic pathways.

1.13 Aims

- Aim 1: **Ex vivo** analysis of normal and CLL/SLL tissue for myofibroblast markers
 - Analysis of the myofibroblast marker **α-SMA** in the LN of healthy individuals
 - **Analysis of α-SMA** and palladin in the affected LNs of CLL/SLL patients
 - Correlation **of α-SMA** with the CLL prognostic markers ZAP-70 and Ki-67

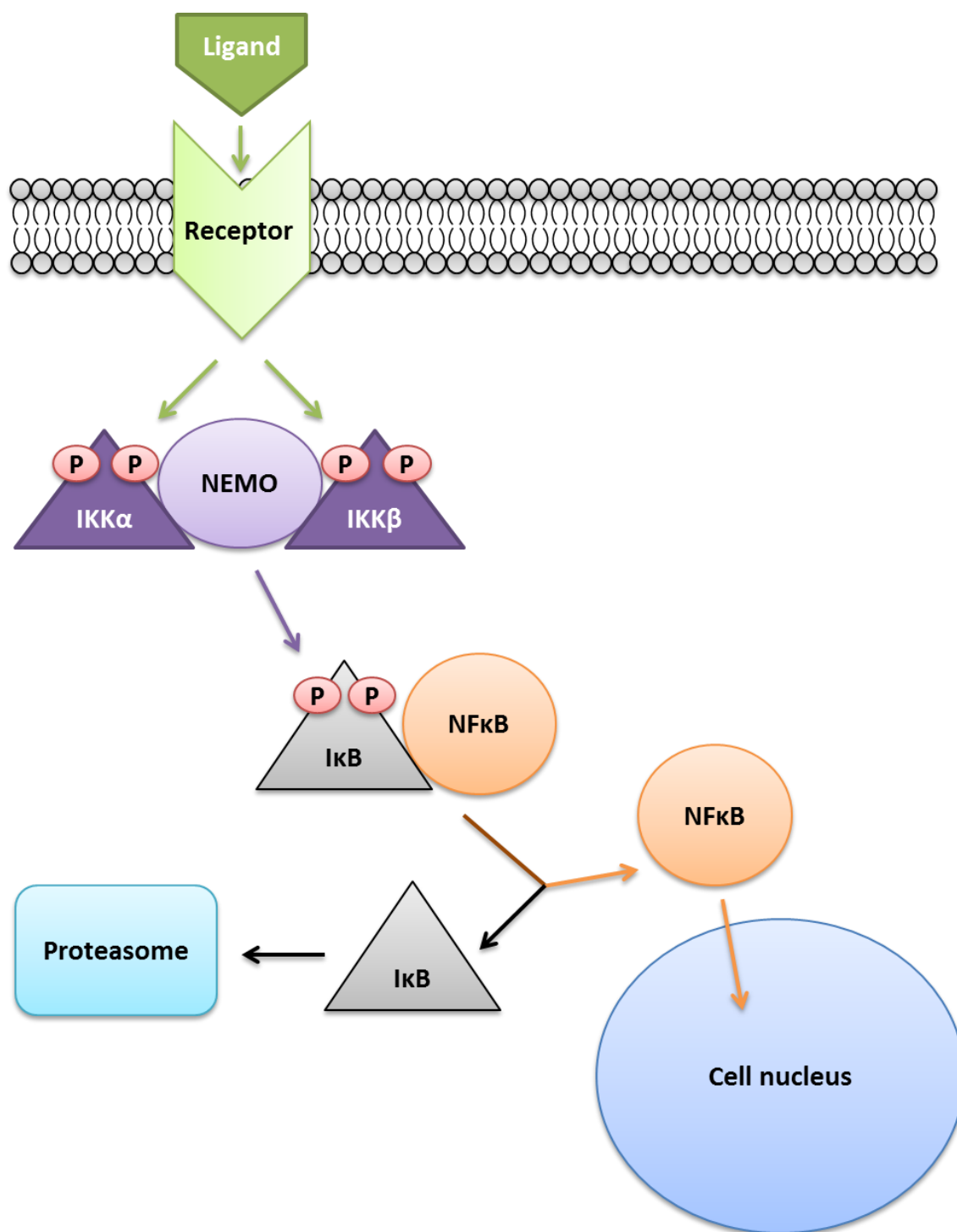


Figure 1.12: **NFκB signal transduction pathway.**

Upon receptor (green) ligation IKK (purple) is phosphorylated on specific serine residues within its IKK α and IKK β subunits. This leads to its activation. IKK then phosphorylates I κ B (grey) on 2 critical serine residues leading to its ubiquitination and degradation by the proteasome (black). NF κ B (orange) is then released from its state of inhibition and consequently translocates to the cell nucleus (blue) where it binds to DNA of target genes.

Chapter 1

- Aim 2: Characterisation of various stromal cell types for selection of a suitable experimental model
 - **Analysis of α -SMA** expression in HFFF2 cells \pm treatment with the main inducer of myofibroblast transdifferentiation, TGF- β
 - **Analysis of α -SMA** expression in LN-derived fibroblast-like cells \pm TGF- β treatment
 - Analysis of α -SMA and STRO-1 expression in BM-derived MSCs, STRO-1 cells, at various time-points post-isolation.
 - **Analysis of α -SMA** in STRO-1 cells \pm TGF- β treatment
- Aim 3: To investigate the effect of CLL samples on spontaneous and TGF- β -induced myofibroblast transdifferentiation
 - **Analysis of HFFF2 α -SMA** expression after co-culture with CLL samples or culture in CLL-derived conditioned media (CM)
 - Analysis of TGF- β activation by CLL cells
- Aim 4: To investigate the effect of fibroblasts and myofibroblasts on CLL cell survival
 - Analysis of CLL cell survival by flow cytometry after co-culture with fibroblasts and myofibroblasts
 - Analysis of caspase and PARP cleavage in CLL cells after culture in fibroblast CM by immunoblotting
 - Comparison of CLL cell binding to fibroblasts and myofibroblasts
 - Analysis of intrinsic ROS levels within CLL cells after co-culture with fibroblasts
 - Analysis of Bcl-2 family protein expression in CLL cells post-culture in fibroblast or myofibroblast CM
- Aim 5: To investigate the effect of fibroblasts on intracellular signalling pathways within CLL cells
 - Analysis of phospho-protein expression in CLL cells after culture in fibroblast CM
 - Analysis of CLL cell viability after co-culture with fibroblasts in the presence of various small molecule inhibitors
 - Analysis of MCL-1 expression in CLL cells post-culture in fibroblast CM supplemented with small molecule inhibitors.

Chapter 2:

Materials and methods

Chapter 2

2.1 Cell culture

2.1.1 Primary cells

All **patients' material was used following informed consent and Ethics Committee approval**, and in accordance with the Declaration of Helsinki.

Primary CLL peripheral blood mononuclear cells (PBMC) samples were obtained as vials of cryopreserved cells from the University of Southampton Lymphoproliferative Disease Tumour Bank. Cells were cultured in complete RPMI-1640 growth medium (RPMI-1640 media (Sigma-Aldrich) supplemented with 10% (v/v) fetal calf serum (FCS; PAA laboratories), 2 mM glutamine (PAA laboratories) and 1000 µg/ml penicillin-streptomycin (PAA laboratories). Cells were incubated at 37°C in atmosphere containing 5% CO₂. Cells were allowed to recover for 1 hour prior to use.

STRO-1 cells are a heterogeneous population of bone marrow-derived mononuclear cells (BMMNC) obtained from the bone marrow of individuals undergoing hip replacement surgery and were a generous gift from Dr Rahul Tare (University of Southampton, UK) [229]. Cells were isolated by immunolabelling with microbead-bound STRO-1 antibody followed by MACs isolation using a MACS separator. STRO-1 cells were cultured in complete minimum essential medium alpha media (α -MEM; GIBCO) supplemented with 10% (v/v) FCS and 1000 µg/ml penicillin-streptomycin) and incubated at 37°C in an atmosphere with 10% CO₂.

Primary fibroblast-like cells were grown out of tissue extracted from the affected lymph nodes of a patient diagnosed with CLL. The tissue sample was from the University of Southampton Lymphoproliferative Disease Tumour Bank. Briefly, the tissue specimen was transferred into a 6-well cell culture plate. 2-3ml of DMEM media, supplemented with 10%/20% (v/v) FCS, 2 mM glutamine and 1000 µg/ml penicillin-streptomycin, was added to the well to allow complete coverage of the tissue explant. The tissue specimen was incubated at 37°C in an atmosphere containing 10% CO₂ to allow outgrowth of fibroblast-like cells. Media was changed to be replaced by fresh media, twice weekly.

2.1.2 Cell lines

Human Caucasian Foetal Foreskin Fibroblast (HFFF2) cells were purchased from Health protection agency culture collections (UK). Mink Lung Epithelial Cells (MLEC) cells, stably transfected with a TGF-beta1 (TGF- β 1) responsive reporter construct were a kind gift from Dr Veronika Jenei (University of Southampton, UK) [230]. Both cell lines were grown in **complete Dulbecco's modified Eagle's** Medium (DMEM; Sigma-Aldrich) containing 10% FCS plus 2 mM glutamine and incubated in a 37°C incubator supplied with 10% CO₂. The media for the MLEC cells were also supplemented with 400 µg/ml Genetecin (G418; Life Technologies).

For list of primary cells and cell lines used see Table 2.1.

2.1.3 Cell culture

HFFF2 cells were grown in both 75cm² and 175cm² tissue culture flasks. Cells were routinely passaged twice a week; sub-confluent cultures were split 1:3 and kept at a confluency of approximately 70-80% to minimise spontaneous transdifferentiation. Media was removed by aspiration and the flask was washed with 5 ml of phosphate buffered saline (PBS; recipe in section 2.12) to remove any residual FCS. 3µl or 5µl of trypsin (sigma) was added, respectively, and cells were incubated at 37°C **in an atmosphere of 10% CO₂** for 10-15 minutes to detach cells. Complete DMEM medium was added to the flasks and cells were transferred into new flasks which were returned to a 37°C incubator **supplied with 10% CO₂**.

MLEC cells were cultured in 75cm² tissue culture flasks. Cells were routinely passaged twice a week; confluent cultures were split 1:2. Media was removed by aspiration and the flask was washed with 5 ml of PBS to remove any residual FCS. Trypsin was added and cells were incubated at 37°C in an atmosphere of **10% CO₂** for 10-15 minutes to detach cells. **Complete α -MEM** medium was added to the flasks and cells were transferred into new flasks which were returned to a 37°C **incubator supplied with 10% CO₂**.

STRO-1 cells were seeded into 6-well cell culture plates (2x10⁵/well; 2 ml/well) **in complete α -MEM** media and incubated at 37°C **in an atmosphere of 10% CO₂** until experimental use.

Chapter 2

Primary cells/cell lines	Origin	Supplier
Chronic lymphocytic leukaemia (CLL) cells	Human, peripheral blood of individuals diagnosed with CLL	Southampton lymphoproliferative disease tumour bank
STRO-1 cells	Human, bone marrow of individuals undergoing hip replacement. Not diagnosed with CLL.	Gift from Dr Rahul Tare
Fibroblast-like cells	Human, affected lymph nodes of individuals diagnosed with CLL	Southampton lymphoproliferative disease tumour bank
Human foetal foreskin fibroblast (HFFF2) cells	Human, skin	HPA collections (UK)
Mink lung epithelial cells (MLEC)	Mink, lung	Gift from Dr Veronika Jenei

Table 2.1: Primary cells and cell lines.

Table shows the origin and supplier of all the primary cells and cell lines utilised.

CLL-derived fibroblast-like cells were cultured in 75cm² tissue culture flasks. Cells were passaged depending on high confluency. However media was replaced twice a week; media was removed by aspiration and the flask was washed with 5 ml of PBS to remove non-adherent/dead cells and fresh complete DMEM media was added to the flask. Flasks were returned to a 37°C **incubator in an atmosphere of 10% CO₂**.

2.1.4 Freezing cells for long-term storage

Cells were trypsinised as in 2.1.3. Cells were collected for centrifugation (3 minutes; 1250 rpm in a Sorvall Legend RT centrifuge) and the cell pellet was suspended in freezing medium (10% (v/v) dimethyl sulphoxide (DMSO), 90% (v/v) FCS). Aliquots of cells (1 ml) were transferred into labelled cryovials (Greiner Bio-One Ltd) and stored overnight at -80°C in a NALGENE Mr Frosty (Thermo Fisher Scientific) containing 250 ml isopropanol. Cells were transferred to liquid nitrogen the following day.

2.1.5 Defrosting cells for culture

Cells were defrosted swiftly by hand to ensure maximum cell viability. Cells were transferred to a 15 ml falcon tube containing 9 ml of complete RPMI, or complete DMEM media. Cells were centrifuged at 1500 rpm for 5 minutes in a Sorvall Legend RT centrifuge and the supernatant was aspirated. CLL cells were re-suspended in 4 ml of complete RPMI media and then incubated at 37°C **in an atmosphere containing 5% CO₂, for 1 hour prior to experimentation**. HFFF2 and MLEC cells were re-suspended in 5 ml of complete DMEM media, and then transferred into a 75cm² tissue culture flask containing 15 ml complete DMEM media, and incubated at 37°C **in an atmosphere containing 10% CO₂**.

2.1.6 Co-cultures

HFFF2 cells were plated into 6-well cell culture plates (2x10⁵/well) or 48-well cell culture plates (5x10⁴/well) in complete DMEM and left overnight at 37°C/10% CO₂. Wells were washed with PBS to remove dead or detached HFFF2 cells. CLL cells were then added at a density of 1x10⁶/well (6-well plate) or 2x10⁵/well (48-well plated), in a volume of 2 ml/well or 500 µl/well of complete RPMI-1640 media, respectively. As controls, CLL cells were plated in wells at the same density in 2 ml/well complete RPMI-1640 media in the

Chapter 2

absence of HFFF2 cells, and HFFF2 cells were cultured with addition of 2 ml/well complete RPMI-1640 media without CLL cells. Cells were returned to a 37°C/10% CO₂ incubator.

2.1.7 Counting viable cells

All cells were counted by being mixed in a 1:1 (v/v) ratio with trypan blue (0.4% (w/v) Sigma-Aldrich). Prior to this CLL cells were diluted 1/10 in complete RPMI-1640 media to allow for more accurate counting. Cells were pipetted onto a Neubauer Haemocytometer Counting Chamber. Only cells which had excluded the dye were counted as viable cells. Cells within each 16-square grid were counted; all 4 grids were counted and averaged. The total amount of cells in the original suspension was calculated by multiplying the number of cells counted by multiplying the number of cells by 10,000 x dilution factor.

2.1.8 Generating conditioned media from CLL cells

CLL cells were plated into 6-well cell culture plates in serum-free DMEM (DMEM media supplemented with 1% (w/v) bovine serum albumin (BSA; Sigma-Aldrich), 2 mM glutamine) at a density of 5×10^6 /ml and incubated at 37°C for 72 hours **in atmosphere containing 5% CO₂**, unless stated otherwise. Tissue culture medium was collected and centrifuged at 1500 rpm for 5 minutes in a Sorvall Legend RT centrifuge to pellet cells and cell debris. Supernatant was collected and this centrifugation step was repeated to ensure optimal removal of CLL cells. Conditioned media was either used immediately or stored at -20°C until use.

2.1.9 Generating conditioned media from HFFF2 cells

HFFF2 cells were plated into 6-well cell culture plates in complete RPMI-1640 medium, at a density of 2×10^5 /ml and incubated at 37°C for 72 hours **in atmosphere containing 10% CO₂**. Media was collected and centrifuged as above. Supernatant was collected and utilised immediately for experiments.

2.2 SDS-PAGE and western blotting

2.2.1 Cell lysate preparation

2.2.1.1 Preparation of lysates for CLL cells

For co-culture experiments, cells were collected by washing the wells twice with ice-cold PBS 1 ml/well. The collected cells were then centrifuged for 5 minutes at 1500 rpm in a Sorvall Legend RT centrifuge and the supernatant was discarded. Cell pellets were re-suspended in 40 μ l of radio-immunoprecipitation assay (RIPA) buffer (Recipe in section 2.12) supplemented with protease inhibitor cocktail (1% (w/v); Sigma) and phosphatase inhibitor cocktails 2 and 3 (each 1% (w/v); Sigma). Cells were incubated on ice for 30 minutes and then centrifuged for 15 minutes at 13,000 rpm at 4°C in a Heraeus Fresco17 centrifuge (Thermo Scientific). The supernatant was collected and lysates were stored at -20°C.

2.2.1.2 Preparation of lysates for adherent cells

Once removed from the incubator, 6-well cell culture plates were kept on ice. Media was removed by aspiration and wells were washed twice with PBS 1 ml/well to remove dead or detached cells and excess media. RIPA buffer (80 μ l) supplemented with protease/phosphatase inhibitor cocktails (as above) was added to wells. Cells were then detached using a cell scraper and transferred into a 1.5 ml Eppendorf and incubated on ice for 30 minutes. Lysates were centrifuged for 15 minutes at 13,000 rpm at 4°C in a Heraeus Fresco17 centrifuge. The supernatant was collected and lysates were stored at -20°C.

2.2.2 Bicinchoninic acid (BCA) protein assay

Protein content of lysates was quantified using the BCA protein assay kit from Thermo Scientific Pierce. BSA standards (1000, 500, 250, 125, 62, 31, 15 μ g/ml) were prepared to create a concentration curve. Cell samples (4 μ l) were **diluted 1:12.5 in H₂O and 23 μ l of each diluted sample** was pipetted in duplicate into a 96-well cell culture plate. Reagent A was mixed with reagent B in a 1:50 dilution and 200 μ l of the combined reagents was added to all wells containing samples and BSA standards. Wells lacking sample/BSA were used as a blank control. The plate was incubated at 37°C/5% CO₂ for 30 minutes and

Chapter 2

absorbance (562 nm) was quantified using a Varioskan Flash multimode spectrophotometer. The protein concentration for each sample was calculated by extrapolating the absorbance values from the standard curve generated from the BSA standards.

2.2.3 Preparing polyacrylamide gels

The BioRad Mini-PROTEAN Tetra cell system was used to prepare 10% polyacrylamide gels. The recipes for both the separating and stacking gels are shown (Table 2.2). 30% acrylamide and TEMED were purchased from Sigma-Aldrich. Recipes for the Tris buffers are in section 2.12.

2.2.4 Western blotting

Samples were prepared by combining the lysate and one-half of the volume of 3x SDS sample buffer red (Cell signalling technology; recipe in Section 2.12) supplemented with 0.1 M dithiothreitol (DTT, Cell signalling technology). Samples were prepared to ensure equal protein loading for each track, typically 25 - 40 μg , depending on the protein being analysed. Samples were boiled for 5 minutes at 95°C. Molecular weight markers (Cell Signaling, pre-stained protein marker broad range) were prepared in parallel. Samples were centrifuged briefly at 13,000 rpm in a Heraeus Biofuge microfuge prior to loading into wells of an SDS-polyacrylamide gel. Proteins were resolved in a BioRad Mini-PROTEAN Tetra cell containing approximately 600 ml of 1x running buffer (recipe in section 2.12). The gel was resolved at 100 V until the dye-front entered the separating gel (approximately 15 minutes) and then at 150 V for an additional 60-90 minutes.

The transfer step involved assembling a “sandwich” consisting of a nitrocellulose membrane, 2 pieces of transfer filter paper and 2 sponges (BioRad) per gel. This sandwich was placed in a BioRad Mini-Trans Blot Cell containing approximately 600 1X transfer buffer (recipe in section 2.12) and run at 100 V for 70 minutes.

The membranes were incubated with 5 ml of blocking solution (3% (w/v) dried milk in 1X TBS-tween (1X TBS (recipe in section 2.12), 0.5% (v/v) Tween-20 (Fisher Scientific)) for 1 hour at room temperature. Membranes were then incubated overnight at 4°C in primary antibody (see Table 2.3) diluted in

Reagent	Volume for separating gel (v/v)	Volume for stacking gel (v/v)
H ₂ O	41.5%	60%
30% acrylamide	33%	14%
1.5M Tris pH 8.8	25%	-
1.0M Tris pH 6.8	-	25%
10% Ammonium persulphate	0.5%	1%
N,N,N',N'-Tetramethylethylenediamine (TEMED)	0.05%	0.1%

Table 2.2: Recipe for preparing separating and stacking gels.

Table shows the reagents and respective volumes (v/v) required to produce 10% separating and 10% stacking gels for western blotting.

Chapter 2

Primary antibody	Dilution	Species	Supplier
Anti-human α -SMA	1:5000	Mouse	Dako
Anti-Phospho-p44/42 MAPK (Erk1/2) (Thr202/Tyr204)	1:1000	Rabbit	Cell Signaling Technology
Anti- Phospho-Akt (Ser473)	1:1000	Rabbit	Cell Signaling Technology
Anti-p44/42 MAPK (Erk1/2)	1:1000	Rabbit	Cell Signaling Technology
Anti-Total AKT	1:1000	Rabbit	Cell Signaling Technology
Anti-Phospho-Zap-70 (Tyr319)/Syk (Tyr352)	1:1000	Rabbit	Cell Signaling Technology
Anti-HSC70	1:1000	Mouse	Santa Cruz Biotechnology
Anti- β -actin	1:5000	Rabbit	Sigma-Aldrich
Anti-PARP	1:1000	Mouse	BD Biosciences
Anti-caspase 3	1:2000	Mouse	Enzo Life Sciences
Anti-Mcl-1	1:2000	Rabbit	Santa Cruz Technology
Anti-Bim	1:1000	Rabbit	Cell Signaling Technology
Anti-Bcl-2	1:5000	Mouse	Dako

Table 2.3: Primary antibodies used for western blotting.

Table shows the concentrations at which the antibodies were diluted, the species they were derived from and the company which supplied them. All antibodies used for western blotting are shown. All antibodies were diluted in 3% milk solution (3% (w/v) dried milk in 1X TBS-tween).

blocking solution, on an automatic roller. The membranes were then washed twice with 1X TBS-tween, each for 10 minutes. Membranes were then incubated for 1-2 hours at room temperature in horse radish peroxidase (HRP) conjugated to secondary antibody (see Table 2.4) diluted in blocking solution. Membranes were washed twice for 15 minutes with 1X TBS-tween prior and then developed using Supersignal West Pico Chemilluminiscent substrate reagent (Thermo Scientific; 1 ml luminol enhancer and 1 ml peroxide solution) or Supersignal West Femto Chemilluminiscent substrate (Thermo Scientific; 800 μ l H₂O plus 100 μ l luminol enhancer and 100 μ l peroxide solution). Images were collected using a BioRad Fluor-S™ Multimager. Exposure times ranged between 5-30 seconds depending on the protein being analysed. Quantitation was performed using Quantity One 1-D analysis software (BioRad) and protein expression was normalised to expression of the loading control (β -actin or HSC70). For phosphorylated proteins, expression was normalised using **expression of the appropriate “total” protein control.**

2.2.5 Stripping membranes

To serially re-probe membranes, membranes were incubated for 3-5 minutes with stripping buffer (Section 2.12) on an automatic roller. Membranes were then washed with 1x TBS-tween twice for 10 minutes prior to treatment with new primary antibody in blocking solution.

2.3 Treatment with small molecule inhibitors

CLL cells were re-suspended in a volume of 1-2 ml of complete RPMI-1640 medium and pre-treated with small molecule inhibitors (Table 2.5) or incubated with the solvent control (DMSO) for 1 hour at 37°C/5% CO₂ **prior to** further experimentation, unless states otherwise.

2.4 TGF-beta (TGF- β) luciferase assays

MLEC stably transfected with a TGF- β 1 responsive reporter construct were plated into a sterile, white 96-well cell culture plate (Sigma-Aldrich; 5x10⁴/well) and incubated overnight at 37°C/10% CO₂ **to allow cells to adhere.** Cells were then serum-starved for 4 hours by washing wells with PBS and culturing cells in serum-free DMEM. This was done to eliminate the possibility

Chapter 2

Secondary antibody	Dilution	Species	Supplier
Anti-mouse conjugated to horse radish peroxidase	1:2000	Goat	Dako
Anti-rabbit conjugated to horse radish peroxidase	1:2000	Goat	Dako

Table 2.4: Secondary antibodies used for western blotting.

Table shows the concentrations at which the antibodies were diluted, the species they were derived from and the company which supplied them. All antibodies used for western blotting are shown. All antibodies were diluted in 3% milk solution (3% (w/v) dried milk in 1X TBS-tween).

Inhibitor	Final concentration	Target	Supplier
R406 (Tamatinib)	10 μ M	SYK	Selleckchem
PCI-32765 (Ibrutinib)	10 μ M	BTK	Selleckchem
CAL-101 (Idelalisib)	10 μ M	PI3K	Selleckchem
LY294002	10 μ M	PI3K	Selleckchem
AZD6244 (Selumetinib)	10 μ M	MEK1/2	Selleckchem
BAY-11-7082	50nM	IKK	Selleckchem
CP690550 (Tofacitinib)	10 μ M	JAK	Selleckchem

Table 2.5: Small molecule inhibitors used to inhibit intracellular signalling pathways.

Table shows the final concentration at which the inhibitor was used, the target molecule it inhibits, and the company which supplied it. CLL cells were treated with all inhibitors for 1 hour at 37°C/5% CO₂. R406 inhibits SYK and is the active form of fostamatinib [215], PCI-32765 inhibits BTK [80], CAL-101 and LY294002 block PI3K (PI3K/AKT pathway) [79, 231], AZD6244 blocks MEK (MAPK pathway) [232], BAY-11-7082 inhibits IKK (NF κ B pathway) [233] and CP690550 blocks JAK3 (JAK/STAT pathway) [234].

Chapter 2

of serum-induced activation of TGF- β . After 4 hours, media was removed and CLL cells were added (5×10^5 cells/well in serum-free RPMI-1640 medium; 100 μ l/well). Experiments with CLL samples were performed with six replicates per sample. A standard curve was also produced by adding increasing concentrations of recombinant TGF- β 1 (R&D systems; 100, 200, 300, 500, 750 and 1000 pg/ml) in serum free RPMI to MLEC cells in the absence of CLL cells, 100 μ l/well). Standard curve determinations were performed in triplicate. As a negative control, 100 μ l of serum-free RPMI-1640 medium (i.e. no CLL cells, no TGF- β 1) was added to MLEC cells in triplicate. Cells were incubated at 37°C/5% CO₂ for 24 hours. Wells were washed with PBS for optimal removal of CLL cells and adherent MLEC cells were lysed by adding 25 μ l of 1x reporter lysis buffer (Promega) and freezing at -80°C for a minimum of 30 minutes. Cells were defrosted and 50 μ l of luciferase assay reagent (Promega) was added to all wells. Luminescence was quantified by a Varioskan Flash multimode spectrophotometer.

2.5 Immunofluorescence

Cells were fixed and stained within the 6-well cell culture plate they were seeded in. Media was removed from wells and cells were washed twice in PBS to remove debris and detached cells. Cells were then fixed for 20 minutes at room temperature in PBS/4% (w/v) paraformaldehyde (300 μ l/well) and then washed 3 times in PBS/0.1% (w/v) TX-100. Cells were permeabilised for 10 minutes with PBS/0.5% (w/v) TX-100 and the reaction was neutralised using 50 mM NH₄Cl for 5 minutes. Cells were blocked for 20 minutes in 2% BSA buffer (0.1% (w/v) TX-100, 2% (w/v) BSA, in PBS) and incubated for 1 hour with the primary antibody (Table 2.6) diluted in 2% BSA buffer. Cells were washed and then incubated for 45 minutes in the dark with the secondary antibody diluted in 2% BSA buffer (Table 2.7). Subsequent steps were carried out in the dark. Cells were incubated with 4',6-diamidino-2-phenylindole (Sigma-Aldrich; DAPI, 1:10,000) for 10 minutes to visualise cell nuclei. Images were obtained using AxioVision software on the Zeiss microscopy system.

2.6 Induction of myofibroblast transdifferentiation

HFFF2 cells were plated into a 96-well cell culture plate (1×10^4 cells/well; 100 μ l/well), a 48-well cell culture plate (5×10^4 cells/well; 500 μ l/well) or a 6-well

Primary antibody	Dilution	Species	Supplier
Anti-human α -SMA	1:750	Mouse	Dako
STRO-1 supernatant. Monoclonal IgM	Neat	Mouse	In-house

Table 2.6: Primary antibodies used for immunofluorescence.

Table shows the dilution factor for the antibody, the species it was derived from and the company which supplied it. The STRO-1 supernatant was a kind gift from Dr Rahul Tare (University of Southampton, UK).

Chapter 2

Secondary Antibody	Dilution	Species	Supplier
Anti-mouse-Alexa-488	1:250	Goat	Invitrogen
Anti-mouse IgG-Cy3	1:400	Goat	Invitrogen

Table 2.7: Secondary antibodies used for immunofluorescence.

Table shows the dilution factor for the antibody, the species it was derived from and the company which supplied it.

cell culture plate (2×10^5 cells/well; 2 ml/well) in complete DMEM media and incubated overnight at $37^\circ\text{C}/10\% \text{CO}_2$. **The following day wells were treated** with 2 ng/ml TGF- $\beta 1$ [235] or vehicle control (DMSO) in complete DMEM medium and incubated for 48-72 hours at $37^\circ\text{C}/10\% \text{CO}_2$ **to allow TGF- $\beta 1$ -treated cells to transdifferentiate into myofibroblasts.** Media was then removed and wells were washed twice with PBS to remove all traces of TGF- $\beta 1$.

2.7 Adhesion assays

HFFF2 cells were plated into a 96-well cell culture plate (1×10^4 cells/well) and respective cells were treated with TGF- $\beta 1$ **as described above.** CLL cells (1×10^5 /well) were re-suspended in serum-free RPMI-1640 and added to both TGF- $\beta 1$ **treated and TGF- $\beta 1$ un-**treated HFFF2 cells; serum free media was used to prevent unknown components within the serum from affecting adhesion between CLL cells and HFFF2 cells. Prior to co-culture with HFFF2 cells, CLL cells were pre-treated with 15 μM CFSE (Invitrogen) in complete RPMI-1640 media at $37^\circ\text{C}/5\% \text{CO}_2$ **for 15 minutes to allow for easy detection.** Cells were incubated for various time points (1-48 hours) at $37^\circ\text{C} 10\% \text{CO}_2$. Media was gently removed and wells were washed once with PBS to remove unbound CLL cells. Cells were subsequently fixed with 10% (w/v) formalin and stored at 4°C in the dark until analysis. AxioVision software using the Zeiss microscopy system was used to capture 5 separate fields at x5 magnification per well. The number of adherent CLL cells within each field were counted using Image J software.

2.8 Annexin V assays

HFFF2 cells were plated into a 48-well cell culture plate (5×10^4 cells/well) in complete DMEM medium and left overnight at $37^\circ\text{C}/10\% \text{CO}_2$. **Respective wells** were treated with 2 ng/ml TGF- $\beta 1$ **as described above (section 2.6).** Control cells were left untreated (fibroblasts). Next, CLL cells were plated into all HFFF2-containing wells (2×10^5 /wells) in complete RPMI-1640 media, as well as into wells containing no HFFF2 cells as controls. A portion of CLL cells were isolated and analysed immediately (0 hr time-point), while the rest were incubated at $37^\circ\text{C} 10\% \text{CO}_2$ **for 24, 48 or 72 hours.** At each time-point CLL cells were collected and transferred into FACS tubes. All wells were washed once with PBS to collect excess CLL cells and then transferred into labelled FACS

Chapter 2

tubes which were centrifuged at 1500 rpm for 5 minutes in a Sorvall Legend RT centrifuge. Cells were re-suspended in 300 μ l of Annexin V buffer (Recipe in section 2.12) containing 2.5 μ g/ml of Annexin V-FITC (a kind gift from Dr Patrick Duriez, University of Southampton) and 1 μ g/ml of propidium iodide (PI; Life Technologies) per well. Cells were vortexed briefly and incubated for 15 minutes at room temperature in the dark prior to FACS analysis via FACSCanto I flow cytometer. 10,000 events were recorded per tube. Results were analysed using FlowJo version 7.6.5.

2.9 Reactive oxygen species (ROS) analysis

HFFF2 cells were plated into 24-well cell culture plates (1×10^5 /well) in complete DMEM media and incubated overnight at 37°C/10% CO₂ to allow cells to adhere. The following day, CLL cells (5×10^5 cells/well) were plated into all HFFF2-containing wells in complete RPMI-1640 media, as well as into wells containing no HFFF2 cells as a control. A portion of CLL cells were analysed immediately (0hr time-point) while the rest were incubated for 24 and 48 hours at 37°C 10% CO₂. At each time-point cells were transferred into FACS tubes and treated with 1 μ M CM-H₂DCFDA (Invitrogen) for 1 hour in the dark at 37°C/10% CO₂. Cells were then washed twice with PBS to remove excess CM-H₂DCFDA and re-suspended in 500 μ l of PBS. Cells were kept in the dark until FACS analysis by a FACSCanto 2 flow cytometer. 100,000 events were recorded per tube. Results were analysed using FlowJo version 7.6.5.

2.10 Exosome extraction

Conditioned media was derived from CLL cells as described in section 2.1.8. Half the conditioned media was stored at -20°C until use. The remaining conditioned media was treated with 0.5 volumes of Total Exosome Isolation Reagent (Invitrogen, Life Technologies) and mixed well. The mixture was incubated overnight at 4°C to allow the reagent to bind water molecules. The following day the conditioned media was centrifuged at 10,000 g for 1 hour at 4°C in a Heraeus Fresco17 centrifuge in order to pellet the exosomes. The exosome-depleted conditioned media was collected. The exosome sediment was re-suspended in an equivalent volume of serum-free DMEM.

2.11 Statistical analysis

Data was analysed using GraphPad Prism version 6. Statistical significance is shown as asterisks; the level of significance is signified by the number of asterisks, $p < 0.05^*$, $p < 0.01^{**}$, $p < 0.001^{***}$, $p < 0.0001^{****}$. Non-significant data is indicated by 'ns' when $p > 0.05$.

Data were analysed by various statistical tests. Wilcoxon's **matched**-pairs signed-rank test was utilised to compare 2 paired groups. Mann Whitney test was used to compare 2 un-paired groups. One-way ANOVA with Bonferroni correction was utilised to compare the means of 3 or more matched groups. Significance level for all tests was set at 0.05.

2.12 Solutions

Phosphate buffered saline (PBS)

137 mM NaCl

2.7 mM KCl

4.3 mM Na_2HPO_4

1.47 mM KH_2PO_4

Adjust to pH of 7.4 with HCL

5x Radioimmunoprecipitation assay buffer (RIPA)

250 mM Tris-HCl (pH 8.0)

750 mM NaCl

5% (v/v) Igepal CA-630

2.5% (w/v) Deoxychlorate (DOC)

0.5% (w/v) Sodium dodecylsulfate (SDS)

Tris buffer pH 8.8

1.5 M Tris-HCl (adjust to pH 8.8 with HCl)

Chapter 2

Tris buffer pH 6.8

1.0 M Tris-HCl (adjust to pH 6.8 with HCl)

3x SDS sample buffer red

187.5 mM Tris-HCl (pH 6.8)

6% (w/v) SDS

30% glycerol

0.03% (w/v) phenol red

10x Running buffer

250 mM Tris-base

1.92 M glycine

1% (w/v) SDS

Transfer buffer

192 mM glycine

25 mM Tris-base

10% (v/v) ethanol

10x Tris-buffered saline (TBS)

100 mM Tris-HCl (pH 8.0)

1.5 M NaCl

TBS-Tween

10 mM Tris-HCl (pH 8.0)

150 mM NaCl

0.1% Tween-20

Stripping buffer

25 mM glycine (2.0)

1% (w/v) SDS

10X Annexin V buffer

10 mM HEPES (Adjust to pH 7.4 with NaOH)

140 mM NaCl

2.5 mM CaCl₂

Chapter 3:

Analysis of CLL/SLL
tissues and selection of an
appropriate experimental
model for studies in vitro

3.1 Introduction

The overall goal of the project was to characterise the interactions between CLL cells and fibroblasts/myofibroblasts. Therefore, it was important to first analyse the presence of these cells within the stroma of CLL tissues *in vivo*. Immunohistochemical analysis was performed on tissue sections from affected LNs of patients diagnosed with CLL or small lymphocytic lymphoma (SLL), a variant of CLL with a predominant tissue-based presentation[61, 236]. Although CLL/SLL cells also accumulate in the BM and spleen, LN tissue sections were selected for study since these are the main sites of PCs, and samples were readily available from tissues taken for routine pathology analysis. Markers for the reliable identification of fibroblasts are not clearly defined and their detection is generally based on morphology (i.e. spindle shape) and presence of the positive marker vimentin and the absence of markers for other mesenchymal cells (i.e. muscle cells)[156]. Therefore this study focused on the identification of myofibroblasts, which are better defined histologically. This was followed by correlating the presence of potential myofibroblasts with ZAP-70 and Ki-67 expression, to probe potential relationships between the presence of myofibroblasts and variable clinical behaviour.

The second main aim of the results described in this chapter was to select a suitable cell type to use as an experimental model for follow-on mechanistic experiments. The main selection criteria were that cells (i) were of human fibroblast origin, (ii) retained the ability to reproducibly and robustly transdifferentiate into myofibroblasts under defined conditions, and (iii) were available in sufficient numbers for detailed molecular analysis. The following cells were characterised; (i) HFFF2, a human caucasian foetal foreskin fibroblast (HFFF2) cell line, (ii) fibroblasts derived from CLL/SLL LNs, and (iii) human STRO1-expressing mesenchymal stromal cells (STRO-1 cells).

3.2 **Analysis of α -SMA** expression in normal and CLL/SLL tissues

The goal of the experiments described in this section was to characterise myofibroblasts in LN samples derived from patients with CLL/SLL. Potential myofibroblasts were initially identified by immunohistochemical analysis using

an antibody that recognised alpha smooth muscle actin (α -SMA), a key hallmark of myofibroblasts [237], and a tissue-microarray (TMA) containing triplicate cores from 11 individual CLL/SLL samples obtained from UHS Pathology Department archives in Southampton. The anti- α -SMA antibody selected is used for routine diagnostic staining in the Pathology Department and is therefore highly validated for immunohistochemical analysis. The TMA was constructed by Dr Meg Ashton-Key (Consultant Pathologist) and staining was performed with the UHS Pathology Department. Evaluation of staining was performed with the assistance of Dr Meg Ashton-Key. The TMA additionally contained cores from reactive LNs of 6 individuals diagnosed with either inflammatory bowel disease or colon cancer, with uninvolved LNs, allowing comparison of α -SMA staining in 'normal' and CLL/SLL LN. For normal LN, I also analysed CD21 which is expressed at high levels by FDC within GC. Like the α -SMA antibody, the CD21 antibody is well validated and routinely used in the Pathology Department

Analysis of α -SMA and CD21 expression from a representative non-CLL/SLL LN is shown in Figure 3.1. CD21 staining clearly reveals the localisation of germinal centres, with abundant CD21 positive FDCs. By contrast, α -SMA positive cells are excluded from the germinal centres, but detected throughout the extrafollicular area. α -SMA positive cells appeared to be organised in a branch-like, interdigitating pattern.

Analysis of α -SMA expression in CLL/SLL LN tissue is illustrated in Figure 3.2. Data for all samples is summarised in Table 3.1. α -SMA positive cells were detected in all samples. However, the abundance of these cells was highly variable between individual samples. Where α -SMA positive cells were abundant, the overall distribution was similar to the extrafollicular regions of normal LN (ie interdigitating and branch-like); this arrangement was not clearly apparent **when** α -SMA expression was sparse. The images shown in Figure 3.2 were all taken outside PCs. In some cases α -SMA expression was higher within the PCs compared to the extrafollicular area; however, overall there was no clear distinction between these two sites (Figure 3.3). CD21 expression was not analysed within these tissues since it is known to be not expressed or expressed at low levels in most CLL/SLL tissues [123, 238].

Overall, these data clearly demonstrate **that** α -SMA positive cells are present within normal LN as well as within the affected LN of CLL/SLL patients,

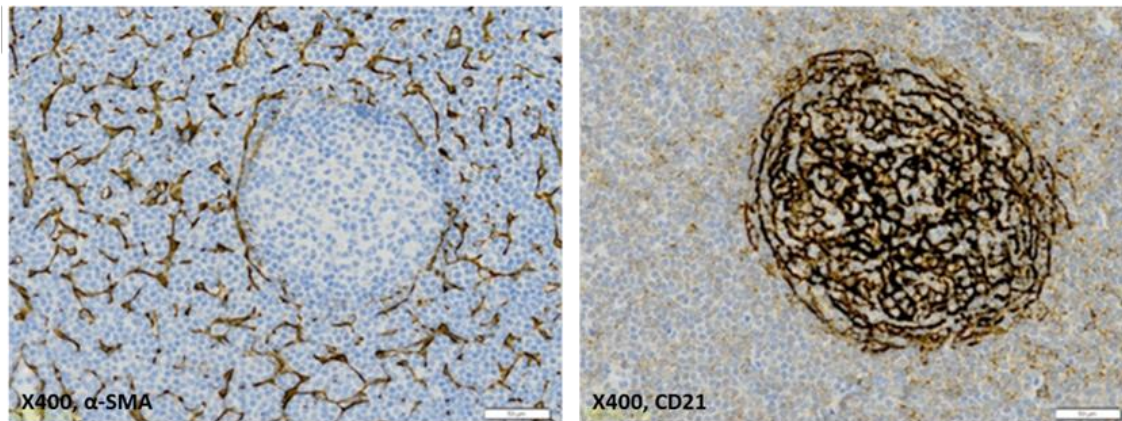


Figure 3.1: Immunohistochemical analysis of non-CLL/SLL **lymph nodes for α-SMA** and CD21 expression.

Tissue sections from the reactive LNs of 6 separate individuals unaffected with lymphoma were analysed for α -SMA and CD21 expression by immunohistochemistry. Figure shows staining from 1 of the 6 patients analysed. The left image displays the staining for the myofibroblast marker α -SMA, and the right image shows the respective staining for the follicular dendritic cell (FDC) marker CD21. Positive staining for either marker is shown in brown. Original magnification is at x400.

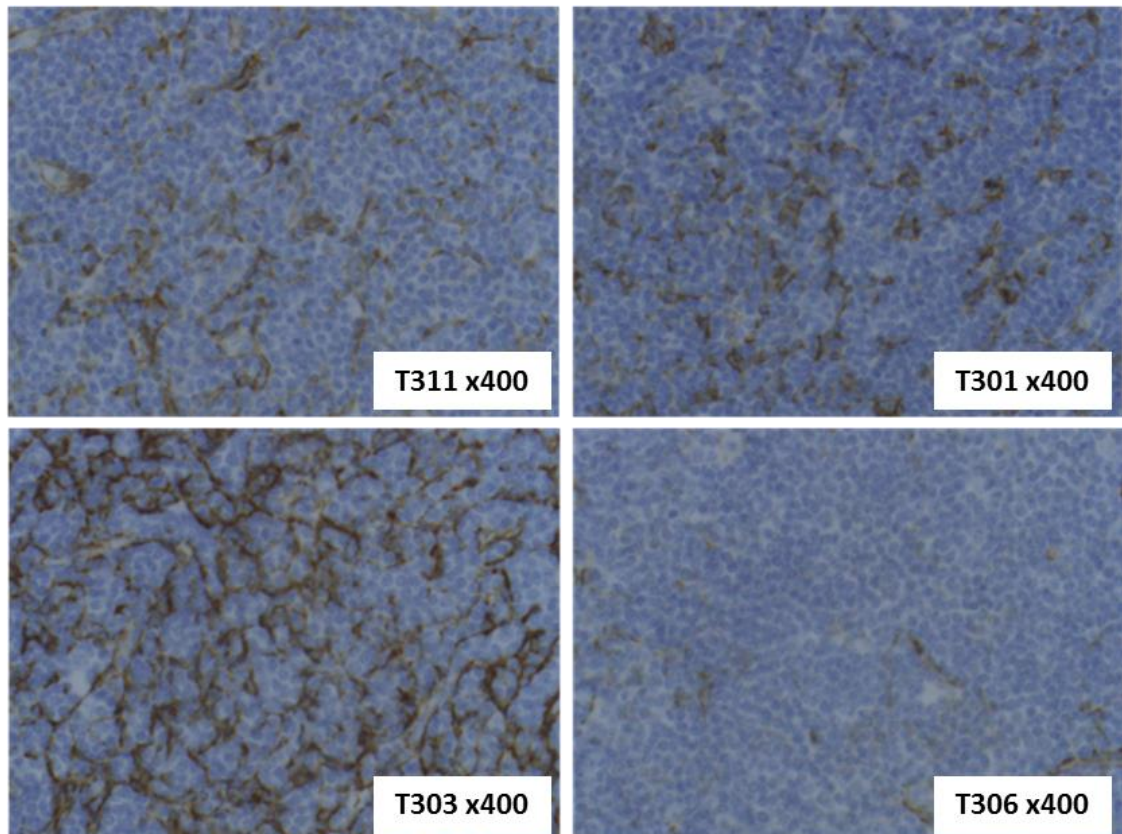


Figure 3.2: Expression of α -SMA within CLL/SLL lymph node tissue.

Tissue sections from the affected LNs of 11 separate patients diagnosed with CLL/SLL were incorporated into a TMA and Immunohistochemical staining was performed to analyse the presence of the myofibroblast marker α -SMA. **Figure shows** α -SMA expression in 4 of the 11 patients that were analysed. α -SMA expression is represented by the brown staining. All four images have been taken outside proliferation centres. Sample numbers correlate with description in Table 3.1. Original magnification is at x400.

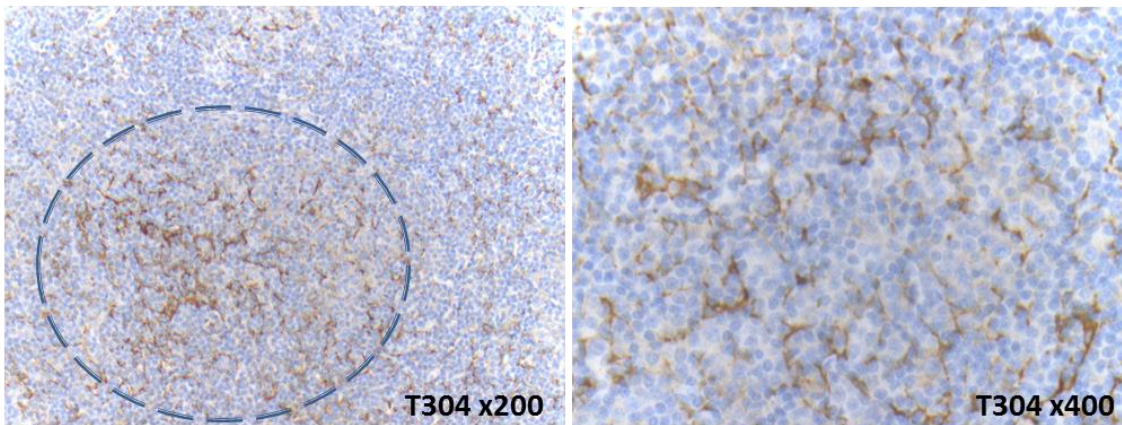


Figure 3.3: α -SMA expression within a PC of CLL/SLL lymph node tissue.

Tissue sections from the affected LNs of 11 different patients were incorporated into a TMA and analysed for α -SMA expression by immunohistochemical staining. Figure shows respective images of α -SMA expression within PCs from 1 patient at different magnifications. Left image shows α -SMA expression within a PC (represented within dashed circle) surrounded by extrafollicular region; original magnification was x200. Right image shows α -SMA expression within PC at higher magnification; original magnification was x400. α -SMA expression is represented by the brown staining.

CLL/SLL sample	α -SMA ^A	ZAP-70 ^B	Ki-67 ^C (%)
T301	Present in both PC and diffuse areas	Negative	<5
T302	Greater in PC	Negative	5-10
T303 (409) ^D	Prominent. Greater in PC	Negative	<5
T304	Greater in PC	Positive	10-15
T305	Variable	Negative	<5
T306	Low	Positive	10-15
T307	Present. Greater in PC	Positive	<5
T308 (421)	Low	Negative	<5
T309	Low, not present in PC	Positive	15-20
T310 (440)	Greater in PC	Positive	10-15
T311	Present with no pattern	Negative	>20

Table 3.1: Summary of α -SMA, ZAP-70 and Ki-67 expression in CLL/SLL lymph node tissue.

Tissue sections from the affected lymph nodes of 11 different patients diagnosed with CLL/SLL were incorporated into a TMA and analysed for α -SMA, Ki-67 and ZAP-70 expression. See Figures 3.2, 3.3, 3.5 and 3.6 for representative staining images. Only 3 of the above samples have been stored in the lymphoproliferative disease (LPD) database.

^ADescribes the presence of α -SMA positive cells within the tissue. PC; proliferation centre.

^BIndicates whether or not ZAP-70 positive cells are present within the tissue (negative/positive); weak expression isn't indicated.

^CDisplays an approximate percentage of Ki-67 positive cells present within the tissue as determined by eye.

^DThe corresponding LPD CLL sample number, assigned to that sample is shown in brackets.

although with clear differences in distribution within these tissues. In CLL/SLL, α -SMA expression was variable between individual patients.

3.3 Analysis of palladin expression in CLL/SLL tissue

Analysis of α -SMA provided encouraging evidence for the presence of myofibroblasts at variable levels within CLL/SLL LNs. However, although α -SMA is a well-established myofibroblast marker, it is also expressed by other stromal cells including pericytes and endothelial cells. Therefore it was important to analyse additional markers of myofibroblasts.

I initially studied vimentin, a type III intermediate filament protein that is expressed by myofibroblasts [160, 239]. LN tissue from 3 individual CLL/SLL samples were analysed for vimentin (data not shown). However, vimentin is a key cytoskeletal component of mesenchymal cells which is expressed by all mesenchymal-derived cells, and immunohistochemical analysis showed that most of the cells within the CLL/SLL LN tissue sections were positive for this marker. Therefore it was decided to examine a marker that was more specific for myofibroblasts.

I next analysed expression of palladin, a cytoskeletal protein which plays a role in controlling stress fibre integrity. Several isoforms of palladin exist including the 4Ig (140 kDa) isoform which is another well-known myofibroblast specific marker; TGF- β stimulation of fibroblasts strongly induces expression of this isoform within stress fibres [162]. Unfortunately antibodies against the 4Ig isoform of palladin were not available for immunohistochemical analysis. However a previous study suggested that co-expression of α -SMA and palladin (all isoforms) strongly indicates the presence of myofibroblasts [240]. I therefore used the antibody described in this previous study to characterise palladin expression in tissue sections from the LN of 3 different CLL/SLL patients. Additionally these samples were stained for α -SMA expression in parallel sections. As before, staining was performed within the UHS pathology department.

Immunohistochemical images from 1 of the 3 patients analysed are shown in Figure 3.4. As seen previously (Figure 3.2), α -SMA positive cells are present within CLL/SLL LNs. Although the staining for palladin is weak, palladin positive cells were also detected. Also, it appears that α -SMA positive cells may

co-express palladin as seen in the parallel tissue sections further suggesting the presence of myofibroblasts within CLL/SLL LNs. This was observed in the other two patients analysed, however the staining for palladin was even weaker in these tissue sections.

Overall, analysis of palladin appeared to confirm the presence of myofibroblasts within CLL/SLL LNs. However, staining for palladin was particularly weak so it is difficult to draw firm conclusions.

3.4 Determining if there is a link between α -SMA, ZAP-70 and Ki-67 in CLL/SLL tissue

The variable expression of α -SMA observed in CLL/SLL LN (Figure 3.2) may relate to distinct clinical behaviour. Clinical outcome data were not available for all of the samples used to generate the TMA, and we therefore also used immunohistochemistry to quantify expression of ZAP-70 and Ki-67. ZAP-70 belongs to the syk tyrosine kinase family and is generally associated with poor patient prognosis [13, 241]. Additionally there is usually a strong positive correlation between ZAP-70 expression and U-CLL cases [242]. Ki-67 is a marker of proliferation which tends to reside within PCs of CLL tissues. High levels of Ki-67 in CLL tissue biopsies (mainly LN), which presents as expanded or highly active proliferation centres, were shown to correlate with a more aggressive disease progression [120]. These prognostic markers were therefore used as surrogate markers of outcome. The ZAP-70 and Ki-67 antibodies are well validated and routinely used in the Pathology Department for analysis of CLL/SLL samples. Evaluation of the staining was assisted by Dr Meg Ashton-Key. Examples of ZAP-70 and Ki-67 staining are shown in Figures 3.5 and 3.6. The results are summarised in Table 3.1.

The scoring system for each marker in Table 3.1 was different. ZAP-70 was the only marker which was not present in all samples; therefore this was simply classed as positive or negative. Ki-67 and α -SMA were present in all 11 samples, but were expressed at variable levels. Therefore, an approximate percentage of Ki-67 positive cells were recorded, as determined by eye. In terms of α -SMA expression, for some samples the presence of α -SMA positive cells varied between the PCs and the extrafollicular region, and this was indicated for these samples, when applicable i.e. when PCs were present. For

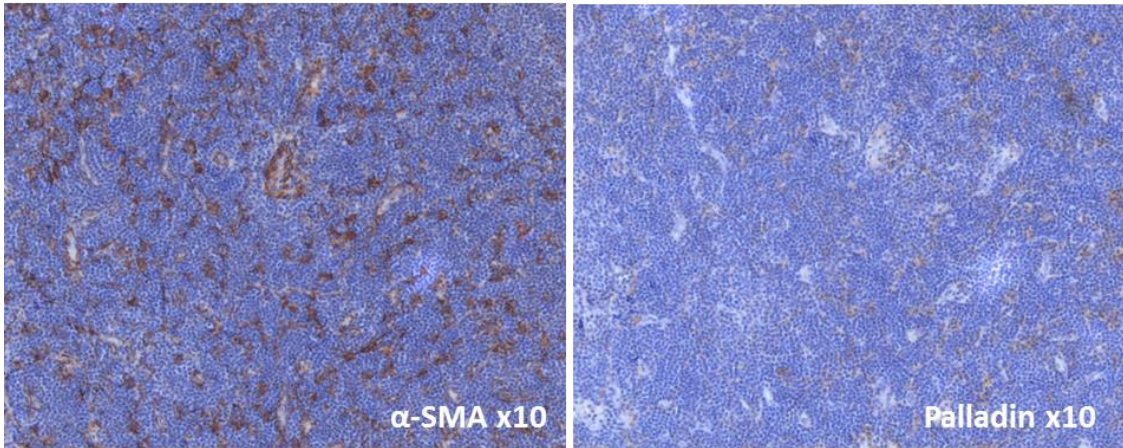


Figure 3.4: Immunohistochemical staining of CLL/SLL lymph nodes **for α-SMA** and palladin.

CLL/SLL LN sections from three individual patients were analysed by immunohistochemical staining for **α-SMA** and palladin expression. Images for **α-SMA** (left) and palladin (right) are shown at indicated original magnifications. Brown staining indicates **α-SMA** and palladin positive cells respectively. Images are obtained from a single sample; similar results were obtained for the other two samples, although expression of palladin was weaker.

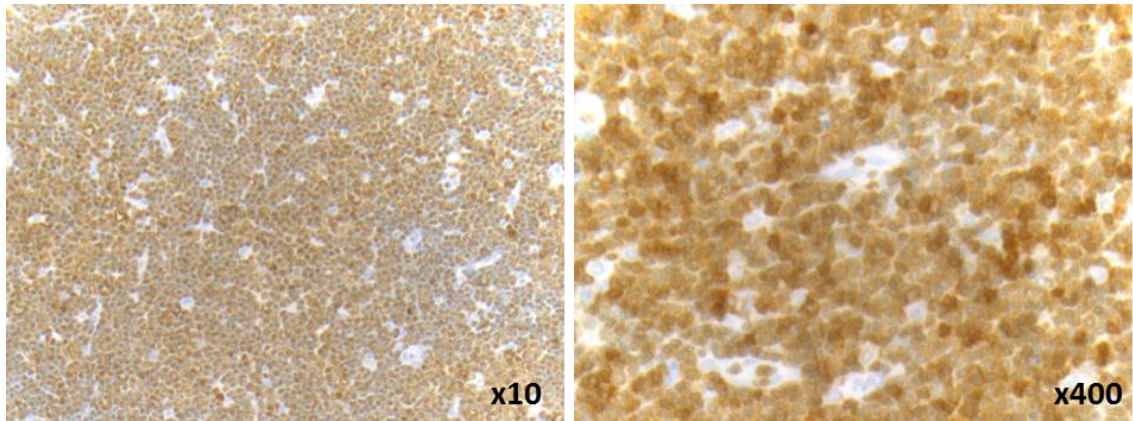


Figure 3.5: Expression of ZAP-70 in CLL/SLL lymph nodes.

Tissue sections from the affected LNs of 11 different CLL/SLL patients were incorporated into a TMA and immunohistochemical staining was performed to analyse expression of ZAP-70. Figure shows respective images of ZAP-70 expression from 1 patient at different magnifications. ZAP-70 expression is represented by the brown staining. Original magnification was x10 (left) or x400 (right).

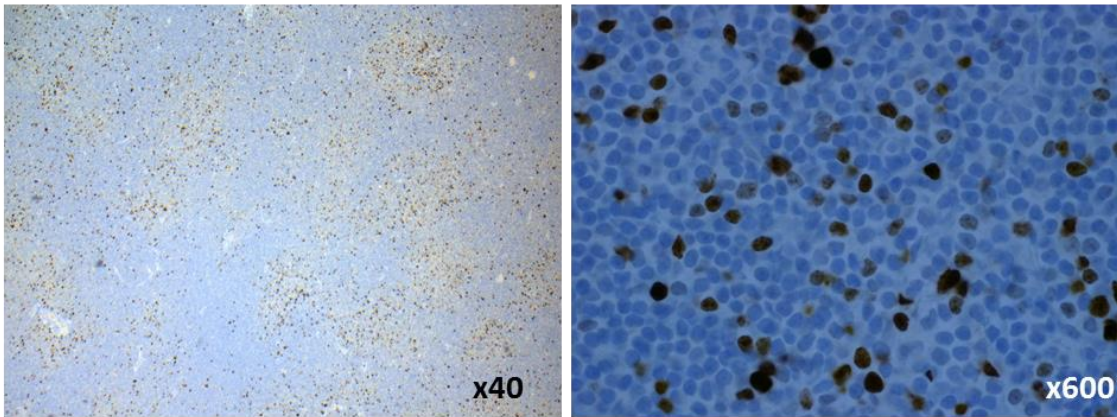


Figure 3.6: Expression of Ki-67 in CLL/SLL lymph nodes.

Tissue sections from the affected LNs of 11 different CLL/SLL patients were incorporated into a TMA and immunohistochemical staining was performed to analyse expression of Ki-67. Figure shows respective images of Ki-67 expression from 1 patient at different magnifications. Ki-67 expression is represented by the brown staining. Original magnification was x200 (left) or x400 (right).

instance, for samples T302, T303, T304, T307 and T310, α -SMA expression was greater in the PCs, compared to areas outside of this region. For sample T301, as no **difference in expression was indicated**, α -SMA expression was comparable between PCs and the extrafollicular region. Sample T309 was the **only sample which contained more α -SMA positive cells in the extrafollicular region compared to the PCs**, as no α -SMA positive cells were detected within the PCs. PCs were not detected within samples T305, T306, T308 and T311, **and therefore the extent of α -SMA expression was made as a general comment, i.e. low or variable. Variable expression indicates that α -SMA expression was not consistent throughout the sample, thus some areas may have contained low amounts of α -SMA positive cells**, whereas other areas would contain medium-high levels.

ZAP-70 positive cells were present in 5/11 (45%) samples whereas Ki-67 was detected within the PCs in all samples, but at variable levels. Most of the ZAP-70 negative samples contained low (<5-10%) numbers of Ki-67 expressing cells (T301, T302, T303, T305 and T308); in fact only one ZAP-70 negative sample expressed high levels of Ki-67 (>20 %, T311). Conversely, most of the ZAP-70 positive samples, appeared to contain higher levels of Ki-67 expression (>10%); only one ZAP-70 positive sample contained low Ki-67 expression (T307). Overall, for this cohort, there appears to be a close positive relationship between these two markers, whereby high Ki-67 expression correlates with ZAP-70 positive samples, and conversely, the absence of ZAP-70 appears to correlate with low levels of Ki-67 expression. This correlation makes sense, as both ZAP-70 and Ki-67 are associated with poor prognosis in CLL; therefore it is unsurprising that this correlation is synergistic. Additionally, it indicates that samples which are positive for ZAP-70, and contain a higher level of Ki-67, may have a worse prognosis and more advanced disease stage compared to ZAP-70 negative samples, which express low amounts of Ki-67 positive cells.

However for this small cohort there was no clear correlation between α -SMA, ZAP-70 and Ki-67. In general, negative expression of ZAP-70 correlated with low Ki-67 (i.e. <10%) expression. However this was not linked with a clear **trend in α -SMA expression**. For instance ZAP-70 and Ki-67 expression were **negative or low in samples T303, T305 and T308**, however α -SMA expression was prominent, variable and low, respectively. Moreover, when ZAP-70 and Ki-

67 expression were positive or high (i.e. $\geq 10\%$) in samples T309 and T310, α -SMA expression was not present within PCs or greater within PCs, respectively.

To extend this analysis, we examined expression of ZAP-70 and α -SMA in additional TMAs, kindly provided by Professor John Gribben (Barts and The London School of Medicine). These TMAs contained triplicate cores from the affected LNs of 108 separate CLL/SLL patients and 13 different patients with Richter's transformation. Richter's transformation is high grade non-Hodgkin's lymphoma (NHL) that develops in patients with CLL/SLL; this transformation occurs in approximately 2-8% of CLL cases and clinical outcome for patients is very poor [243].

Overall, staining patterns for α -SMA and ZAP-70 were similar to results obtained with the initial TMA (Figure 3.2 and 3.5). As shown earlier α -SMA expression varied greatly between individual patients. α -SMA positive cells were arranged in the previously seen interdigitating, branch-like pattern, but **only when α -SMA positive cells were abundant within the stroma; this pattern was not apparent when α -SMA positive cells were sparse.** Unlike before **however, α -SMA positive cells were not present in all samples and therefore it was decided to score α -SMA expression as positive and negative.**

Out of 108 different CLL/SLL LNs, **68/108 (63%) contained α -SMA positive cells** and 43/108 (40%) contained ZAP-70 positive cells (Table 3.2). The majority of **samples were positive for α -SMA and negative for ZAP-70 (α -SMA^{+ve}/ZAP^{-ve}; red)**; this group comprised 42/108 (38%) samples and contains almost double the amount of samples compared to the remaining 3 groups. The number of samples which fall into the other 3 groups are comparable. Cells that were positive for **both α -SMA and ZAP-70 (α -SMA^{+ve}/ZAP^{+ve}; yellow)**, negative for **both α -SMA and ZAP-70 (α -SMA^{-ve}/ZAP^{-ve}; green)** or **negative for α -SMA and positive for ZAP-70 (α -SMA^{-ve}/ZAP^{+ve}; purple)** comprised 16/108 (24%), 23/108 (21%) and 17/108 (16%), respectively. There was no statistically significant **correlation between α -SMA and ZAP-70 for this cohort (R=0.04; $p > 0.05$)** (Figure 3.7, left). **To further confirm whether α -SMA and ZAP-70 are inversely linked, I compared samples with concordant α -SMA and ZAP-70 expression (i.e. α -SMA^{+ve}/ZAP-70^{+ve}, α -SMA^{-ve}, ZAP-70^{-ve}) with non-concordant samples (i.e. α -SMA^{+ve}/ZAP-70^{-ve}, α -SMA^{-ve}/ZAP-70^{+ve}) for the CLL/SLL samples, however again this was not statistically significant (Figure 3.7, right).**

Following this I analysed the TMA comprising 13 different Richter's transformation LNs. 10/13 (77%) and 4/13 (31%) samples contained α -SMA and ZAP-70 respectively (Table 3.3). Similar to the CLL/SLL TMA, the majority of samples were α -SMA^{+ve}/ZAP^{-ve}. This group comprised 8/13 (61.5%) samples, and contained over twice as many samples as the remaining 3 groups. Again, the number of samples in the other 3 groups was comparable. α -SMA^{+ve}/ZAP^{+ve}, α -SMA^{-ve}/ZAP^{-ve} and α -SMA^{-ve}/ZAP^{+ve} comprise 2/13 (24%), 1/13 (21%) and 2/13 (15%) samples, respectively. For this cohort there was a statistically significant correlation between α -SMA and ZAP-70 indicating that one variable increases (α -SMA) as the other decreases (ZAP-70) ($R=-0.43$; $p<0.0001$) (Figure 3.8, left). However there was no statistical significance between concordant and non-concordant samples for the Richter's samples (Figure 3.8, right).

Overall these data suggest there may be a possible inverse correlation between α -SMA and ZAP-70. For CLL/SLL, 55% of samples were α -SMA^{+ve}/ZAP-70^{-ve} or α -SMA^{-ve}/ZAP-70^{+ve}, whereas 45% were concordant for expression of these two markers. For Richter's transformation, 77% of samples were α -SMA^{+ve}/ZAP-70^{-ve} or α -SMA^{-ve}/ZAP-70^{+ve}, whereas 23% were concordant. These differences were not statistically significant for either CLL/SLL or Richter's transformation samples. However, when α -SMA and ZAP-70 were correlated not based on concordance, there was a significant difference for the Richter's samples, but not the CLL/SLL samples. Since ZAP-70 expression in CLL/SLL LN is associated

SLL/CLL		α -SMA	
		Negative	Positive
ZAP-70	Negative	23	42
	Positive	17	26

Table 3.2: Summary of α -SMA and ZAP-70 expression in CLL/SLL patients.

Triplicate cores from the tissue sections extracted from the affected lymph nodes of 108 separate patients diagnosed with CLL/SLL were incorporated into a TMA and analysed by immunohistochemistry for α -SMA and ZAP-70 expression concomitantly. Table shows the number of samples that were divided into α -SMA^{-ve}/ZAP-70^{-ve} (green), α -SMA^{+ve}/ZAP-70^{-ve} (red), α -SMA^{-ve}/ZAP-70^{+ve} (purple) and α -SMA^{+ve}/ZAP-70^{+ve} (yellow).

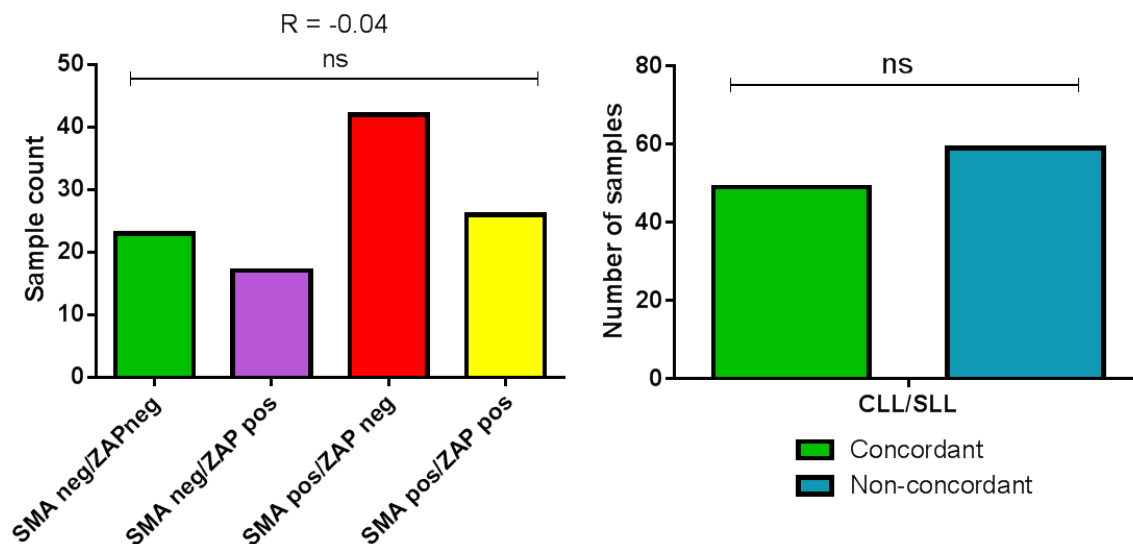


Figure 3.7: Comparison of α -SMA and ZAP-70 expression in CLL/SLL LNs.

Left- The graph shows the number of samples that were negative for both α -SMA and ZAP-70 (green), negative for α -SMA and positive for ZAP-70 (purple), positive for α -SMA and negative for ZAP-70 (red), or positive for both α -SMA and ZAP-70 (yellow). The 108 CLL/SLL LN samples are shown. Statistical significance of the difference was analysed using Spearman's correlation test; α -SMA and ZAP-70 expression were correlated by ranking each sample 1 for negative expression or 2 for positive expression. α -SMA^{-ve}/ZAP^{-ve} (1, 1), α -SMA^{-ve}/ZAP^{+ve} (1, 2), α -SMA^{+ve}/ZAP^{-ve} (2, 1) and α -SMA^{+ve}/ZAP^{+ve} (2, 2). R= correlation coefficient. Right- The graph shows the number of CLL/SLL samples that were concordant (green) for α -SMA and ZAP-70 expression (i.e. α -SMA^{+ve}/ZAP-70^{+ve}, α -SMA^{-ve}/ZAP-70^{-ve}) and non-concordant (blue) for expression (i.e. α -SMA^{+ve}/ZAP-70^{-ve}, α -SMA^{-ve}/ZAP-70^{+ve}). The 108 CLL/SLL samples are shown. The statistical significance of the difference was analysed using Fisher's exact test.

Richter's		α-SMA	
		Negative	Positive
ZAP-70	Negative	1	8
	Positive	2	2

Table 3.3: Summary of **α-SMA** and **ZAP-70** expression in **Richter's** patients.

Triplicate cores from the tissue sections extracted from the affected lymph nodes of 13 separate patients with Richter's transformation were incorporated into a TMA and analysed by immunohistochemistry for α-SMA and ZAP-70 expression. Tables shows the number of samples that were divided into SMA^{-ve}/ZAP-70^{-ve} (green), α-SMA^{+ve}/ZAP-70^{-ve} (red), α-SMA^{-ve}/ZAP-70^{+ve} (purple) and α-SMA^{+ve}/ZAP-70^{+ve} (yellow).

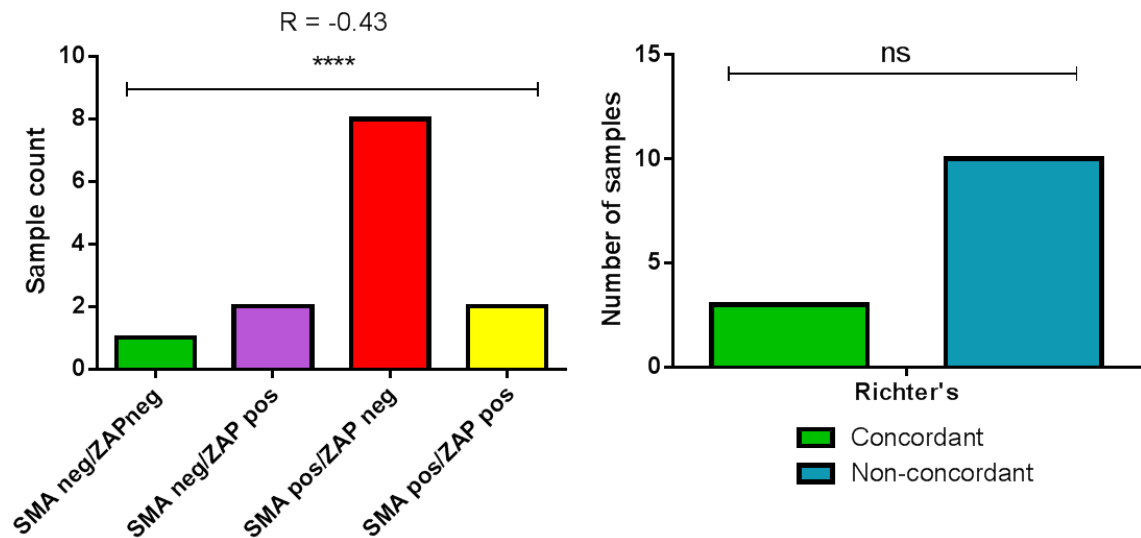


Figure 3.8: **Comparison of α -SMA and ZAP-70 expression in Richter's LNs.**

Left- The graph shows the number of samples that were negative for both α -SMA and ZAP-70 (green), negative for α -SMA and positive for ZAP-70 (purple), positive for α -SMA and negative for ZAP-70 (red), or positive for both α -SMA and ZAP-70 (yellow). The 13 Richter's LN samples are shown. Statistical significance of the difference was analysed using Spearman's correlation test; α -SMA and ZAP-70 expression were correlated by ranking each sample 1 for negative expression or 2 for positive expression. α -SMA^{-ve}/ZAP^{-ve} (1, 1), α -SMA^{-ve}/ZAP^{+ve} (1, 2), α -SMA^{+ve}/ZAP^{-ve} (2, 1) and α -SMA^{+ve}/ZAP^{+ve} (2, 2). R= correlation coefficient. Right- The graph shows the number of Richter's samples that were concordant (green) for α -SMA and ZAP-70 expression (i.e. α -SMA^{+ve}/ZAP-70^{+ve}, α -SMA^{-ve}/ZAP-70^{-ve}) and non-concordant (blue) for expression (i.e. α -SMA^{+ve}/ZAP-70^{-ve}, α -SMA^{-ve}/ZAP-70^{+ve}). The 13 Richter's samples are shown. The statistical significance of the difference was analysed using Fisher's exact test.

Chapter 3

with U-CLL this suggests that increased numbers of myofibroblasts may be associated with more indolent forms of disease. This would be particularly interesting since, in solid cancers, myofibroblasts are generally associated with aggressive disease [171, 172, 174]. However, given the variation in α -SMA expression between PC and non-PC regions in some samples, accurate quantitation of α -SMA expression is difficult and further confirmatory studies, including other markers and larger cohorts, are required.

3.5 Selecting a suitable experimental model system

The second main aim of the experiments described in this chapter was to select a suitable experimental model to use for the assays described in follow-on mechanistic experiments.

3.5.1 Human Caucasian Foetal Foreskin Fibroblast (HFFF2) cell line

The initial experiments investigated the potential utility of HFFF2 cells. These cells were derived from the foreskin of a human foetus and have a typical spindle-shaped morphology. It is an adherent cell line with a finite lifespan. HFFF2 cells express low basal levels of α -SMA, as expected of a typical fibroblast phenotype. However, with passaging in culture, these cells slowly begin to express **myofibroblast characteristics, including increased α -SMA** expression and formation of stress fibres. Additionally cells adhere more tightly to tissue culture plates. One key factor thought to induce this spontaneous transdifferentiation of HFFF2 cells is their confluency and to maintain these cells in their undifferentiated form it is best to keep them at around 60-80% confluency. Some degree of spontaneous transdifferentiation is inevitable in HFFF2 cells; however in my experience they can be maintained as fibroblasts for a few months prior to showing substantial signs of myofibroblast transdifferentiation.

It has been previously shown that when HFFF2 cells are treated with TGF- β , the main inducer of myofibroblast transdifferentiation, they consistently and robustly transdifferentiate into myofibroblasts within 48-72 hours [235, 244]. To confirm this, HFFF2 cells were cultured in complete DMEM media supplemented with 2 ng/ml of TGF- β , or left untreated as a control. After 72 hours expression of α -SMA was analysed by immunofluorescence (Figure 3.9)

and western blotting (Figure 3.10). Heat shock cognate protein 70 (HSC70) was used as the loading control in the western blot; it has been previously used as a reliable loading control for HFFF2 cells [235]. An isotype control **for the α -SMA** antibody was not used for the immunofluorescence staining, however this antibody has been utilised previously within our group and proven to be highly specific and reliable [235].

Both the immunofluorescence and western blot showed a clear up-regulation of α -SMA expression in HFFF2 cells that were treated with TGF- β **compared to** their control (TGF- β un-treated) counterparts (Figures 3.9 and 3.10). Additionally the immunofluorescence images show that TGF- β treatment induced the formation of stress fibres within HFFF2 cells, which is absent in control HFFF2 cells. These effects were highly reproducible and, with appropriate culture conditions, expression of α -SMA expression in control HFFF2 cells remained low in all assays.

These data confirm that HFFF2 cells can be easily and consistently induced to transdifferentiate into myofibroblasts as well as remain undifferentiated during long term cell culture.

3.5.2 Characterising fibroblasts isolated from CLL lymph node tissue

One potential drawback of HFFF2 cells is that they are an established cell line, and, although competent for regulated transdifferentiation, their properties may be affected by long-term culture. I therefore also investigated the potential utility of primary mesenchymal cells, initially focusing on fibroblasts obtained directly from affected LNs of CLL patients. The cells that grew out of the LN tissue were thin and spindle-shaped (not shown), similar to that of fibroblast morphology. Although it was possible to generate a culture of fibroblast-like cells from these tissues, these cells accumulated at an extremely slow rate in culture, even when the cells were cultured in media supplemented with a higher concentration of FCS (20% FCS). However after several months sufficient cells had accumulated for initial studies.

Similar to HFFF2 cells, cells were cultured in complete DMEM media in the presence or absence of 2 ng/ml of TGF- β for 72 hours. Cells were then analysed for α -SMA expression by immunoblotting. α -SMA is normally detected as a single band; this was seen in HFFF2 cells (Figure 3.10). However,

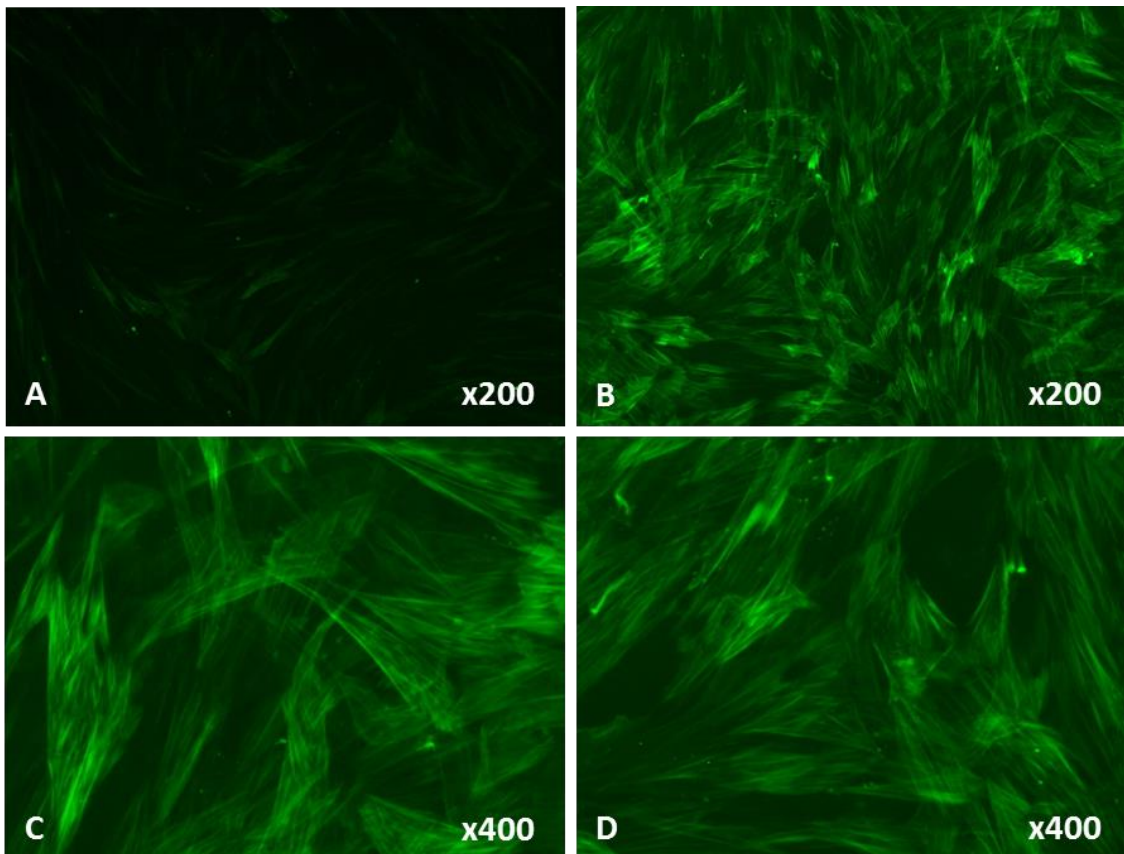


Figure 3.9: Analysis of α -SMA expression in HFFF2 fibroblasts and HFFF2-derived myofibroblasts.

Representative immunofluorescence image shows α -SMA expression in HFFF2 cells. HFFF2 cells were cultured in complete DMEM media in the absence of TGF- β (A) as a control or supplemented with TGF- β (2 ng/ml) (B-D). After 72 hours HFFF2 cells were **then analysed for α -SMA** expression by immunofluorescence. C and D show a higher magnification of HFFF2 cells treated with TGF- β , **to show stress fibres** more clearly. α -SMA is shown by the green immunofluorescence. Data is representative of 3 repeats.

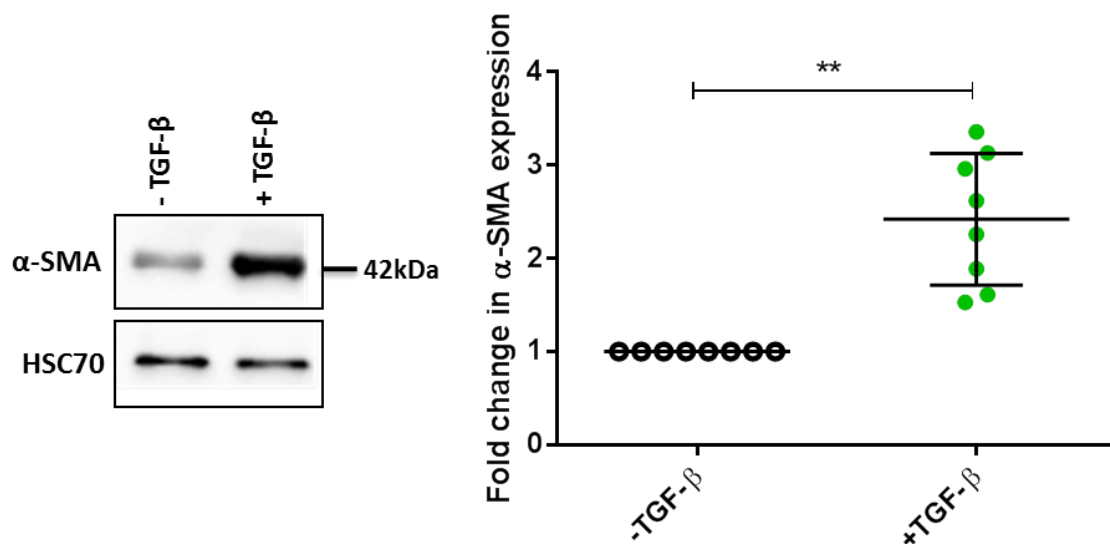


Figure 3.10: **Analysis of α -SMA** expression in HFFF2 fibroblasts and HFFF2-derived myofibroblasts.

HFFF2 cells were cultured in complete DMEM media supplemented with TGF- β (2 ng/ml) or in the absence of TGF- β as a control. After 72 hours cells were then collected and analysed for α -SMA and HSC70 (loading control) expression by immunoblotting. Figure shows results of Western blotting (left) with quantitation (right). For all individual repeats α -SMA expression in control cells was set to 1.0. Each dot represents results from an individual repeat with mean (\pm SD). The statistical significance of the differences was analysed by Wilcoxon's matched-pairs signed-rank test (n=8).

in the LN fibroblasts α -SMA was detected as 2 bands and it is unknown why this occurs. The LN-derived cells expressed low basal levels of α -SMA which was only increased slightly (~50%) following treatment with TGF- β for 72 hours (Figure 3.11). Given the difficulty in obtaining sufficient cells for thorough analysis, especially follow-on mechanistic experiments, no further studies were performed using CLL LN-derived cells.

3.5.3 Characterisation of STRO-1 positive cells

STRO-1 cells were analysed as an additional potential source of primary human stromal cells. These mesenchymal stromal cells (MSCs) are isolated from the bone marrow of patients undergoing hip replacements using an antibody specific for STRO-1, a cell surface protein expressed by undifferentiated mesenchymal stromal cells [245]. They are a relatively heterogeneous subset of MSCs within which fibroblast colony-forming units (CFU-F) are present [246]. A small fraction of the CFU-F population is capable of differentiating into multiple stromal lineages involved in producing bone [247]. Previous data has shown they can give rise to cells expressing a fibroblast, adipocyte and smooth muscle cell phenotype; STRO-1 cells have been used extensively to study osteogenic differentiation [248]. However, potential fibroblast to myofibroblast transdifferentiation has not been studied before using these cells. STRO-1 cells were a kind gift of Dr Rahul Tare (University of Southampton).

To begin to characterise potential transdifferentiation of STRO-1 cells, α -SMA expression was analysed using immunofluorescence at various time-points up to 15 days post-isolation (Figure 3.12). Cells were also stained with DAPI to visualise cell nuclei. At day 6 after isolation, STRO-1 cells were relatively sparse with low or undetectable α -SMA expression. However, by day 9, when cells began to accumulate, there was a clear increase in α -SMA expression. In addition, stress fibre formation was also detected in a proportion of cells. By days 12 and 15 there was significant accumulation of cells, but also α -SMA expression and stress fibre formation. Similar results were obtained with STRO-1 cells obtained from a further two separate donors.

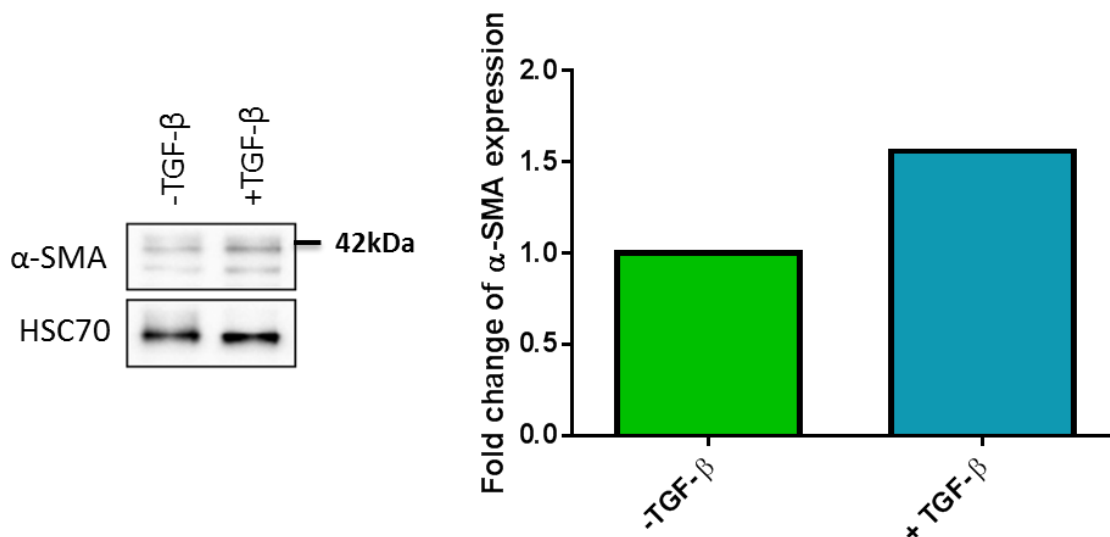


Figure 3.11: **Analysis of α -SMA** expression in fibroblast-like cells derived from a CLL LN.

Fibroblast-like cells derived from a CLL-affected LN were cultured in complete DMEM media supplemented with TGF- β (2 ng/ml) for 72 hours. Cells were also cultured in complete DMEM media in the absence of TGF- β as a control. Figure shows results of Western blotting (left) with quantitation (right), with relative expression in control cells set to 1.0. HSC70 was analysed as a loading control and used to normalise expression between samples. The experiment was performed once due to difficulty of obtaining sufficient cells.

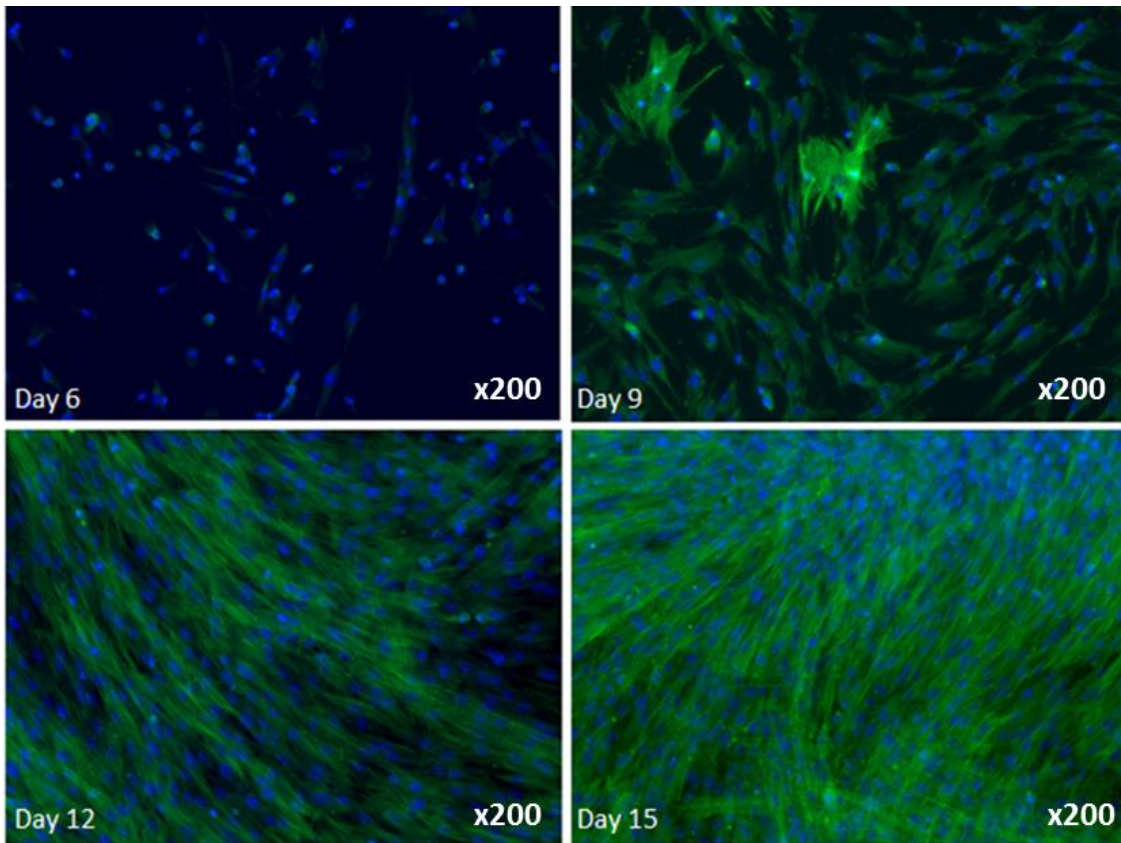


Figure 3.12: α -SMA expression in STRO-1 cells.

After isolation from the bone marrow, STRO-1 cells were immediately plated out and analysed for α -SMA expression (green) at days 6 (top left), 9 (top right), 12 (bottom left) and 15 (bottom right) by immunofluorescence. Cells were also stained with DAPI to visualise cell nuclei (blue). Experiment shown is representative of data obtained from a total of three individual donors.

An additional experiment was performed to probe this potential transdifferentiation of STRO-1 cells. In particular, I used dual-colour immunofluorescence to investigate STRO-1 in parallel with α -SMA (Figure 3.13). As shown previously (Figure 3.12), culture of STRO-1 cells was associated with accumulation of cells and increases in α -SMA expression and stress fibre formation. In parallel, there was a reduction in STRO-1 expression. By day 15, **the majority of cells expressed higher levels of α -SMA**, compared to STRO-1. Taken together, these data indicate that STRO-1 cells readily undergo spontaneous transdifferentiation in culture, associated with increased α -SMA expression and reduced expression of the stem cell marker, STRO-1

Having established that STRO-1 cells readily undergo spontaneous transdifferentiation, a final experiment was performed to investigate effects of TGF- β . **Cells were cultured for 6 days, at which time only a portion of cells have up-regulated α -SMA**, and then treated with TGF- β for an additional 3 days. STRO-1 cells were also cultured in complete α -MEM media in the absence of TGF- β for a total of 9 days as a control. α -SMA expression was analysed by immunofluorescence (Figure 3.14). However, there was no clear effect of TGF- β on α -SMA expression.

Overall these data demonstrate that STRO-1 cells readily undergo spontaneous transdifferentiation into myofibroblasts.

3.6 Discussion

The results described in this chapter had two main aims. The first was to determine if myofibroblasts are present within the CLL stroma as this project is based on understanding the interactions between CLL cells, fibroblasts and myofibroblasts. This was initially investigated using immunohistochemistry to analyse tissue extracted from the affected LNs of individuals diagnosed with **CLL/SLL for the key myofibroblast marker, α -SMA**, as well as another myofibroblast marker, palladin. Following this I investigated whether there is a **link between α -SMA**, the CLL prognostic marker ZAP-70, and the proliferation marker Ki-67.

The second main aim of this chapter was to select a suitable experimental model to utilise in the experiments outlined in the subsequent chapters. The HFFF2 cell line, fibroblasts derived from affected LNs of CLL/SLL patients, and

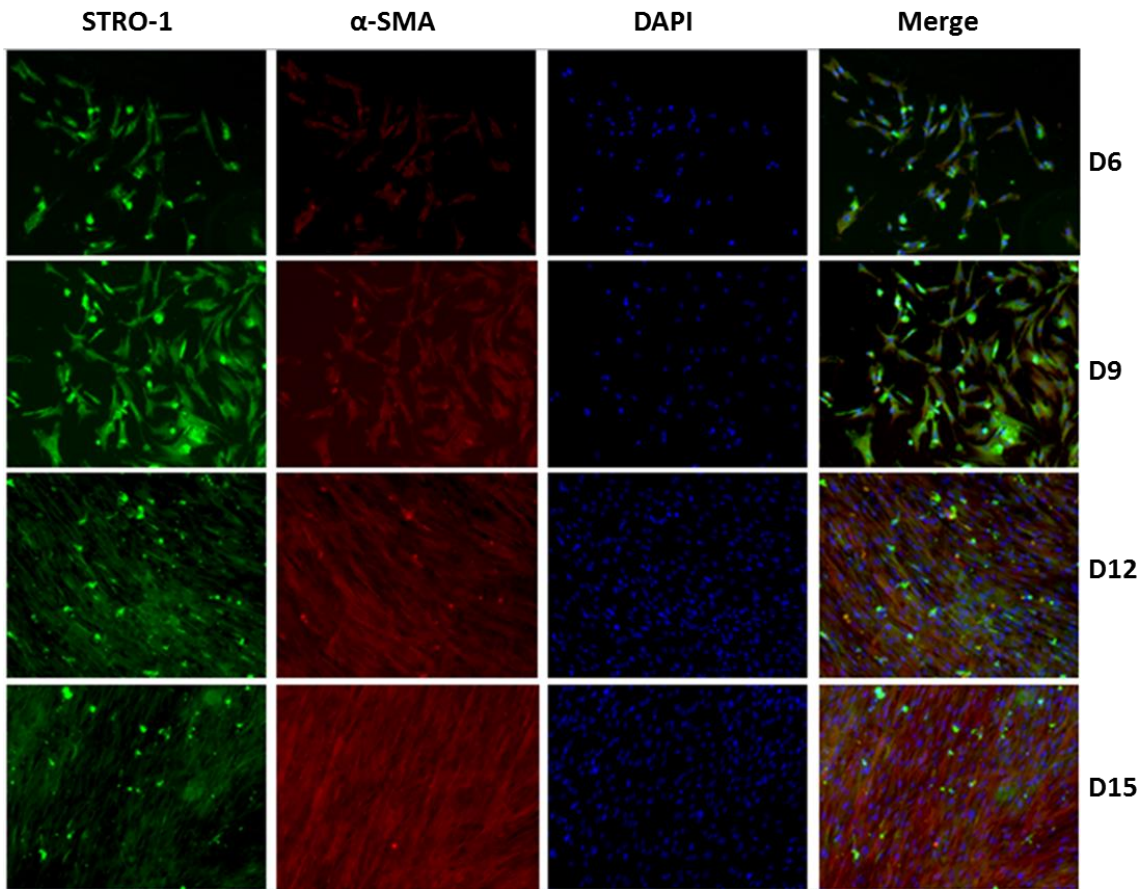


Figure 3.13: STRO-1 and α -SMA expression in STRO-1 cells.

STRO-1 cells were analysed for expression of STRO-1 (green) and α -SMA (red) at days 6 (D6), 9 (D9), 12 (D12) and 15 (D15) following isolation using immunofluorescence. Cells were also stained with DAPI (blue). Merged images are also shown.

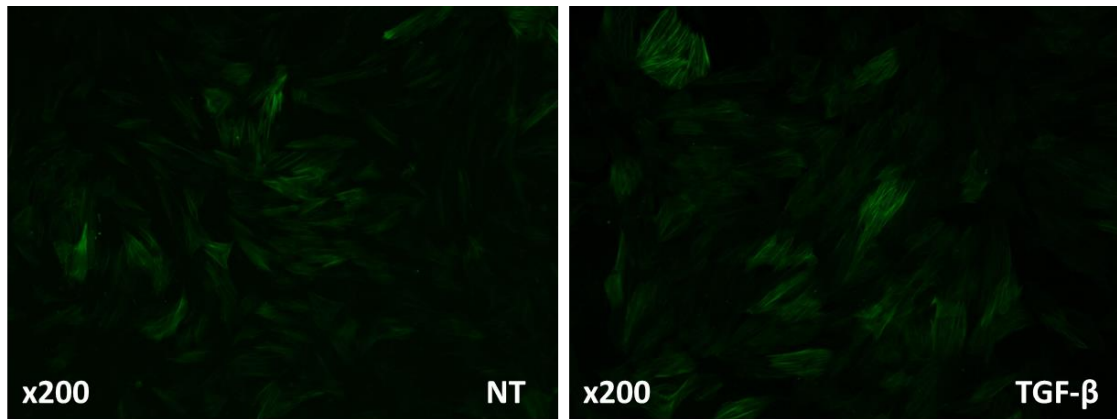


Figure 3.14: Effect of TGF- β on α -SMA expression in STRO-1 cells.

STRO-1 cells were cultured for 6 days in α -MEM media and then treated with TGF- β (2 ng/ml) for an additional 3 days, or cultured in the absence of TGF- β as a control. α -SMA expression (green) was then analysed by immunofluorescence. Data are derived from 1 STRO-1 sample and are representative of data obtained from two independent STRO-1 samples.

Chapter 3

primary STRO-1 cells (bone marrow-derived mesenchymal stromal cells) were characterised.

3.6.1 Presence of myofibroblasts within unaffected and CLL/SLL-affected LNs

Tissue from CLL/SLL unaffected LNs contained α -SMA positive cells which were arranged in an organised, interdigitating, branch-like pattern. α -SMA positive cells were absent within germinal centres (GCs), which are sites within SLO follicles where B lymphocytes undergo affinity maturation of their B-cell receptor genes and differentiate into plasma cells or memory B cells [249]. Conversely CD21 positive cells were found in abundance within these sites, but absent in the extrafollicular region, indicating that the presence of FDCs is exclusive to the GCs. This is consistent with previous data which has detected the presence of FDCs within murine SLO GCs [122]. Additionally the α -SMA staining is consistent with that of earlier studies which have detected α -SMA positive cells within normal LNs of human, rat and mouse [250, 251]. Furthermore α -SMA positive cells were also absent within both human and rat LN germinal centres [250]. However these studies, as well as the data presented here, do not confirm the presence of myofibroblasts within normal LN tissue. Various other cell types within the stroma express α -SMA including endothelial cells and pericytes therefore additional myofibroblast markers, such as the EDA splice variant of fibronectin, or the 4lg isoform of palladin, need to be analysed within these tissues to confirm their presence [161].

The main conclusion of the studies conducted in this section was that myofibroblasts are present within the CLL stroma. Affected LN tissue extracted from CLL/SLL patients contained α -SMA positive cells, which potentially co-express palladin. The presence of myofibroblasts within the CLL stroma has not been previously examined therefore **current data on α -SMA expression within CLL/SLL tissues is sparse. However, α -SMA positive cells have been previously detected within the CLL/SLL bone marrow stroma [252, 253].** Within the bone marrow these cells appear to be arranged in the similar interdigitating pattern observed here, within CLL/SLL LNs. Moreover it was discovered that the presence of α -SMA positive cells were significantly higher within the stroma of an indolent lymphoma subtype (i.e. CLL/SLL) compared to more aggressive lymphomas including Burkitt lymphoma and diffuse large B-

cell lymphoma [252]. However these studies do not confirm whether the **detected α -SMA** positive cells are myofibroblasts.

Palladin exists in multiple isoforms. One drawback of this study is that the palladin antibody used recognises all palladin isoforms, yet only the 4lg isoform is specifically expressed within myofibroblast stress fibres [162]. This is because there are no antibodies available for immunohistochemical analysis against the 4lg isoform. An alternative method to detect the 4lg isoform of palladin could be to utilise RNA *in situ hybridisation*. This technique uses nucleic acid probes to obtain gene expression information at the RNA level, in fixed tissues and cells. Therefore, it could potentially be used to detect 4lg palladin RNA expression, in fixed CLL/SLL LN tissue. However cells co-expressing α -SMA and palladin are encouraging of myofibroblast presence. Further analysis could include performing dual staining on CLL/SLL LNs for α -SMA and palladin expression opposed to staining separate parallel sections for the two markers. However both α -SMA and palladin are cytoskeletal proteins and are likely to co-localize in the same cellular region, therefore detecting their expression by immunofluorescence would allow us to accurately confirm co-expression upon merging the images. To further confirm the presence of the myofibroblasts other myofibroblast-specific markers should be analysed such as the EDA isoform of fibronectin which is vital for the induction of the myofibroblast phenotype by TGF- β [180]. Additionally it would be ideal to determine if the α -SMA/palladin positive cells lack expression of myofibroblast negative markers such as smoothelin and caldesmon to allow further confirmation of the myofibroblast phenotype [254].

Another drawback of this study is that the presence of fibroblasts within CLL/SLL tissues was not investigated. This is largely due to the fact that suitable fibroblast markers are poorly defined, thus making them difficult to positively identify. Generally fibroblasts are identified based on their spindle shaped morphology coupled with expression of vimentin. Unfortunately vimentin is not exclusive to fibroblasts and is expressed by multiple cell types [157]. Furthermore, although fibroblasts are conventionally spindle shaped their morphology can change within different tissues [157]. Moreover other cell types can express spindle-shaped morphology and vimentin, such as macrophages [255]. Additionally myofibroblasts can also express vimentin [255]. Due to these technical limitations, fibroblasts were not analysed.

Chapter 3

However fibroblasts exist within virtually every organ of the body and there are various types of fibroblast subsets within healthy bone marrow and SLOs. The bone marrow for instance is a reservoir of MSCs which can give rise to multiple mesenchymal lineages including fibroblasts. The SLOs comprise various fibroblast subsets such as fibroblastic reticular cells within the LN and spleen, LN medullary fibroblasts within the LN, and red pulp fibroblasts within the spleen. [100-102]. Therefore it is highly likely fibroblasts are present within CLL/SLL tissue. However, their abundance and localisation with CLL/SLL tissues remains unclear.

3.6.2 **Variability in α -SMA expression**

CLL is a highly heterogeneous disorder and clinical behaviour varies greatly between individual patients. Various markers aid in determining disease progression such as ZAP-70 and Ki-67. Both correlate with a more aggressive disease course and poor patient outcome [120, 241]. Furthermore all patients fall into one of two subsets based on *IGHV* mutation status; patients who acquire somatic mutations within their *IGHV* genes (M-CLL) suffer from a less severe form of the disease, compared to patients who do not acquire these mutations (U-CLL).

There was clear variation in the degree of α -SMA expression between individual patients. Of the 119 different CLL/SLL LN sections that were analysed, 79 were positive for α -SMA. Furthermore within these 79 samples the degree of α -SMA expression varied greatly between patients. **When α -SMA expression was high it retained the organised interdigitating pattern displayed within normal LNs; however this arrangement was lost within samples containing low α -SMA expression.**

The presence of myofibroblasts, and thus α -SMA positive cells, correlates with a more aggressive disease progression and poor patient outcome in a number of different solid tumours [171, 172, 174]. Therefore I investigated whether there **was a link between α -SMA expression and disease progression in CLL** by comparing expression of α -SMA, ZAP-70 and Ki-67 expression. There did appear to be a link between ZAP-70 and Ki-67, both of which are valuable markers of disease progression and patient outcome as their presence tends to correlate with poor patient prognosis. Higher levels of Ki-67 ($\geq 10\%$) were generally associated with ZAP-70 expression. This is consistent with previous

findings which have shown a significant correlation between ZAP-70 and Ki-67 in CLL cells isolated from the blood. However there was no clear correlation between α -SMA, ZAP-70 and Ki-67 from the initial TMA (Table 3.1), although a larger cohort may highlight more prominent differences.

Further to this α -SMA and ZAP-70 expression were correlated within a larger cohort comprising 108 CLL/SLL samples and **13 Richter's** samples. 68/108 (63%) of the CLL/SLL samples, and 10/13 (77%) **of the Richter's samples** contained α -SMA positive cells. Interestingly, in both disorders the majority of the α -SMA positive samples were also negative for ZAP-70; 42/68 and 8/10 for CLL/SLL and **Richter's** respectively, indicating a possible inverse correlation between α -SMA and ZAP-70. This correlation was not statistically significant for the CLL/SLL samples but was significant **for the Richter's samples**. To further determine if there was a link between the two markers, samples expressing α -SMA and ZAP-70 **concordance** (i.e. α -SMA^{+ve}/ZAP-70^{+ve}, α -SMA^{-ve}/ZAP-70^{-ve}) were grouped and compared against non-**concordant samples** (α -SMA^{+ve}/ZAP-70^{-ve}, α -SMA^{-ve}/ZAP-70^{+ve}). There was a trend towards inverse α -SMA and ZAP-70 correlation however this was not statistically significant. Overall from all the tissues analysed there is some supporting evidence for a trend of inverse α -SMA and ZAP-70 expression which becomes more apparent with further disease progression, as there was a significant inverse correlation **for the Richter's patients, yet not for CLL/SLL patients**. This suggests that α -SMA expression may correlate with a less aggressive disease progression and better patient outcome. **If indeed the α -SMA positive cells are myofibroblasts** then these data suggest that the presence of myofibroblasts within CLL stroma may encourage a more indolent disease course, which is the opposite of what is observed within solid tumours. Further studies are required comprising a larger cohort, preferably including disease stage and patient survival outcome to further analyse this relationship.

To further determine whether α -SMA associates with a favourable disease prognosis this data could be correlated with patient *IGHV* mutation status. Furthermore additional prognostic markers could be analysed such as Ki-67 and CD38, the latter of which is also known to negatively impact patient prognosis and survival [241].

3.6.3 Selecting a suitable experimental model

Overall it was decided that the HFFF2 cell line would be the most appropriate experimental model to use for this project. Firstly they can both maintain their un-differentiated fibroblast phenotype as well as reliably transdifferentiate in to myofibroblasts upon stimulation with TGF- β . They are easily accessible as they are a cell line and grow rapidly in culture and therefore should not negatively impact the rate at which experiments are conducted. However negative aspects include that although HFFF2 cells are of human origin they are not physiologically applicable as they are derived from the skin, which is not a common site of CLL cell infiltration. Also, HFFF2 cells have a finite life-span and slowly, over time, spontaneously transdifferentiate into myofibroblasts; however in my experience this occurs over a couple of months **and α -SMA expression is consistently checked to make sure the cells express relatively low levels of this protein compared to TGF- β treated counterparts.**

Fibroblast-like cells derived from the affected LNs of CLL patients would have been an ideal experimental model for this project. These cells are more physiologically relevant than HFFF2 cells and STRO-1 cells as they were isolated from the affected LNs of a patient diagnosed with CLL. They are more readily accessible than STRO-1 cells as they have already been isolated and stored within a tissue bank. However these cells grew extremely slowly and when treated with TGF- β they did not transdifferentiate into myofibroblasts as well as HFFF2 cells. Moreover although these cells had spindle shaped morphology they were not analysed for expression of vimentin, or any type of fibroblast marker, therefore it was not confirmed that they were fibroblasts.

STRO-1 cells would have been a good candidate for this project as they are primary human cells derived from the bone marrow, a major site of CLL cell infiltration. Therefore STRO-1 cells are more physiologically relevant than HFFF2 cells, as they are derived from the BM of individuals not diagnosed with CLL/SLL, yet, they are less physiologically applicable than the fibroblast-like cells which were isolated from the LNs of individuals diagnosed with CLL/SLL. Unfortunately once isolated and cultured *in vitro* they rapidly underwent transdifferentiation into myofibroblasts. By day 9 post-isolation cells began expressing α -SMA and stress fibre formation and by days 12 and 15 α -SMA expression and stress fibre formation were abundant, indicating a myofibroblast phenotype. Additionally **it was observed that as α -SMA**

expression increased over time, expression of the mesenchymal stem cell marker STRO-1 declined; further confirming that STRO-1 cells undergo rapid transdifferentiation. Due to their propensity to spontaneously transdifferentiate STRO-1 cells cannot be maintained in culture long-term, therefore I would need to be continuously supplied with them. Furthermore their isolation is dependent on patients undergoing hip replacement surgery; overall these cells would not be easy to access and could hinder the rate at which experiments were conducted. Additionally there is a limited window of opportunity within which these cells can be used. Although the cells are undifferentiated at day 6 their numbers are low and therefore unlikely to yield enough cells for an assay. By days 12 and 15 the cell numbers will have significantly increased but they will have also fully transdifferentiated into myofibroblasts. Therefore STRO-1 cells could only be used between days 7 and 11; ideally around day 9.

Moreover TGF- β did not appear to induce transdifferentiation of STRO-1 cells at day 6; this was odd as these cells have a high propensity to spontaneously transdifferentiate, yet when treated with the main inducer of myofibroblast transdifferentiation they maintain their fibroblast phenotype. A possible explanation for this is that over-confluency may be a strong inducer of myofibroblast transdifferentiation of STRO-1 cells; as the number of STRO-1 cells increase, so does the level of α -SMA expression. To test this, STRO-1 cultures could be split and maintained at low confluency up until days 12 or 15 at which point their expression of α -SMA could be analysed by immunoblotting or immunofluorescence. Although these cells spontaneously differentiate into myofibroblasts, they are widely used as a model for differentiation into adipocytes, chondrocytes and osteoblasts [248]. STRO-1 colonies can be induced to develop into the aforementioned cell types through manipulation of culture conditions. Culturing cells in the presence of dexamethasone, methyl isobutylxanthine, insulin and indomethacin favours the development of adipocytes [256], whereas culturing cells in serum supplemented with dexamethasone and ascorbic acid induces the formation of osteoprogenitors [257].

3.6.4 Summary

- α -SMA positive cells, which potentially co-express palladin, are present within the affected LNs of CLL/SLL patients, thus indicating the presence of myofibroblasts within the CLL stroma.
- **There was great variation in the degree of α -SMA expression between individual samples, however not all samples contained α -SMA positive cells.**
- **There may be a link between α -SMA and ZAP-70; the presence of α -SMA may correlate with the absence of ZAP-70 within the CLL stroma, indicating that α -SMA expression may favour a more indolent disease progression.**
- Fibroblast-like cells derived from the affected LNs of CLL/SLL patients grew extremely slowly in culture and did not respond effectively to TGF- β .
- STRO-1 cells rapidly transdifferentiate spontaneously, post-isolation from the bone marrow, and also do not respond effectively to TGF- β .
- HFFF2 cells grow rapidly, maintain their fibroblast phenotype in culture and reliably transdifferentiate into myofibroblasts when treated with TGF- β , **therefore they were chosen as the most appropriate experimental model for the assays conducted in this project.**

	Positive aspects	Negative aspects
HFFF2 cells	<ul style="list-style-type: none"> Easily accessible Grow rapidly Retain fibroblast phenotype Reliably transdifferentiate into myofibroblasts upon stimulation with TGF-β 	<ul style="list-style-type: none"> Derived from the skin Finite life-span (spontaneously transdifferentiate into myofibroblasts, extremely slowly)
LN fibroblasts	<ul style="list-style-type: none"> Derived from the lymph nodes of CLL patients 	<ul style="list-style-type: none"> Grow extremely slowly Poor transdifferentiation response to TGF-β
STRO-1 cells	<ul style="list-style-type: none"> Derived from the bone marrow 	<ul style="list-style-type: none"> Not easily accessible Rapidly transdifferentiate into myofibroblasts

Table 3.4: Summary of positive and negative characteristics of the stromal cell types.

The positive and negative attributes for the Human Caucasian Foetal Foreskin Fibroblast (HFFF2) cell line, fibroblasts derived from the affected lymph nodes of CLL/SLL patients, and mesenchymal stromal cells isolated from the BM of individuals not diagnosed with CLL/SLL (STRO-1) have been summarised.

Chapter 4:

Investigation of the effect of
CLL cells on myofibroblast
transdifferentiation

4.1 Introduction

It has been well documented that myofibroblasts play an important role in facilitating the development and progression of solid tumours, and their abundance within the stroma correlates with poor patient prognosis, including in prostate, pancreatic and breast cancer [171, 172, 174]. However, the communication between malignant cells and the stroma is bidirectional and, in addition to supporting growth of solid cancers, malignant cells have been shown to induce myofibroblast transdifferentiation [258, 259]. Data presented in Chapter 3 demonstrate that myofibroblasts are present within the CLL **stroma as α -SMA positive cells** were detected, potentially with co-expression of palladin. One possibility is that, similar to solid tumours, CLL cells promote myofibroblast transdifferentiation. Therefore the main aim of the experiments described in this chapter was to determine if CLL cells modulate the transdifferentiation of fibroblasts to myofibroblasts, using HFFF2 cells as a model system.

4.2 Investigating the effect of CLL cells on myofibroblast transdifferentiation

4.2.1 Determining the effect of co-culture with CLL samples on HFFF2 cells.

To investigate the effect of CLL cells on fibroblast transdifferentiation to myofibroblasts, I co-cultured primary CLL samples with HFFF2 fibroblasts and evaluated the effects on α -SMA expression using immunoblotting. These first experiments evaluated the effects of spontaneous transdifferentiation and were therefore performed in the absence of added TGF- β . However, HFFF2 cells were treated with TGF- β without CLL cells as a positive control for α -SMA induction. Although CLL samples may comprise a mixture of malignant and normal cells, I decided to use unsorted CLL PBMCs in my experiments, to avoid potential artefacts associated with cell sorting. However, all samples selected **for study contained $\geq 80\%$ CLL cells to minimise effects of contaminating, non-malignant cells.**

HFFF2 cells were **either cultured alone as a control for basal α -SMA** expression or co-cultured with CLL samples in DMEM media lacking serum, to minimise

potential transdifferentiation in response to serum factors. DMEM media was utilised opposed to RPMI, which is preferred by CLL cells, in order to optimise conditions for HFFF2 cells as transdifferentiation is being analysed within these cells. After 48 hours, cultures were washed thoroughly to remove CLL cells and α -SMA expression in the adherent cells was analysed by immunoblotting. This time point was selected since 48 hours is sufficient to induce complete myofibroblast transdifferentiation in response to TGF- β , but would hopefully minimise potential confounding effects on CLL cell death, especially as cells were cultured in serum-free media which would be detrimental to their survival.

Cultures were checked by light microscopy following washing to ensure optimal removal of CLL cells prior to lysis of HFFF2 cells. However, CLL cells can bind strongly to tissue culture surfaces/cells and complete removal of CLL cells was not possible. Therefore prior to analysis of α -SMA expression in **HFFF2 cells, I analysed expression of α -SMA** in CLL cells using 2 different samples. HFFF2 cells were used as a positive control for α -SMA expression and HSC70 was used as a loading control [235]. Consistent with its utility as a marker of mesenchymal cells [260], α -SMA was not detected in either CLL sample analysed (Figure 4.1 and not shown). Thus, although it was not possible to completely remove CLL cells from HFFF2 cell co-cultures, contaminating CLL cells **can not contribute to apparent expression of α -SMA** in HFFF2 cells.

Thirteen CLL samples were analysed in the co-culture assays. Samples were selected to comprise both *IGHV* mutated and un-mutated CLL samples. The majority of samples chosen were surface IgM (sIgM) signallers as determined **by intracellular calcium flux; samples were classified as signallers when $\geq 5\%$ of cells responds to anti-IgM stimulation** [261]. 2×10^5 HFFF2 cells were co-cultured with CLL cells at a density of 5×10^6 /ml. Representative data for 4 separate CLL samples is shown in Figure 4.2 and quantitation for all samples is shown in Figure 4.3.

Overall, there was a statistically significant reduction in HFFF2 cell α -SMA expression following co-culture with CLL samples, indicating that CLL cell co-culture decreased spontaneous transdifferentiation of HFFF2 cells. As expected, treatment with TGF- β increased α -SMA expression in all

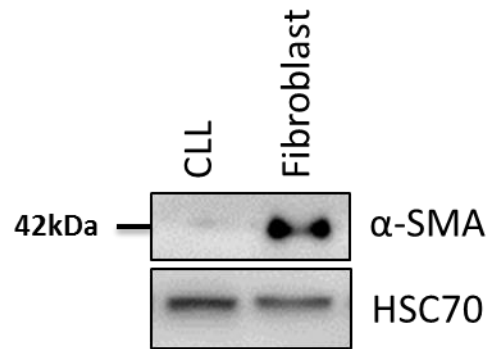


Figure 4.1: α -SMA expression in CLL cells.

Cells from CLL sample U602 were collected immediately after recovery from cryopreservation. Cells were analysed for α -SMA and HSC70 (loading control) expression by immunoblotting. HFFF2 fibroblasts cultured in complete DMEM media **were used as a positive control for α -SMA** expression. Blots are representative of results obtained with 2 separate CLL samples.

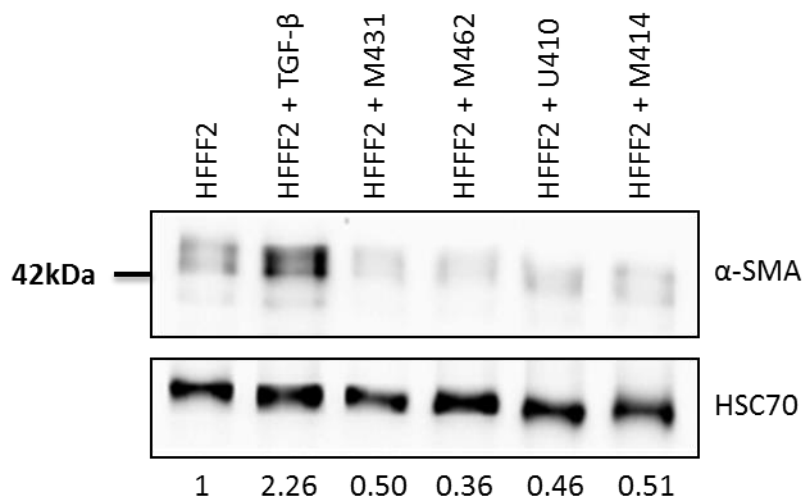


Figure 4.2: Effect of co-culture with CLL samples on α -SMA expression in HFFF2 cells.

HFFF2 cells were cultured in the presence or absence of CLL cells in DMEM media lacking FCS. After 48 hours CLL cells were removed and expression of α -SMA and HSC70 (loading control) in HFFF2 cells was analysed by immunoblotting. HFFF2 cells were also treated with TGF- β (2 ng/ml) without CLL cells as a positive control for transdifferentiation. Figure shows data for 4 different CLL samples, out of a total of 13 samples analysed. Results of quantitation are shown below the gels (α -SMA expression was normalised to HSC70 for each sample, with expression in control HFFF2 cells set to 1.0). (M, M-CLL; U, U-CLL).

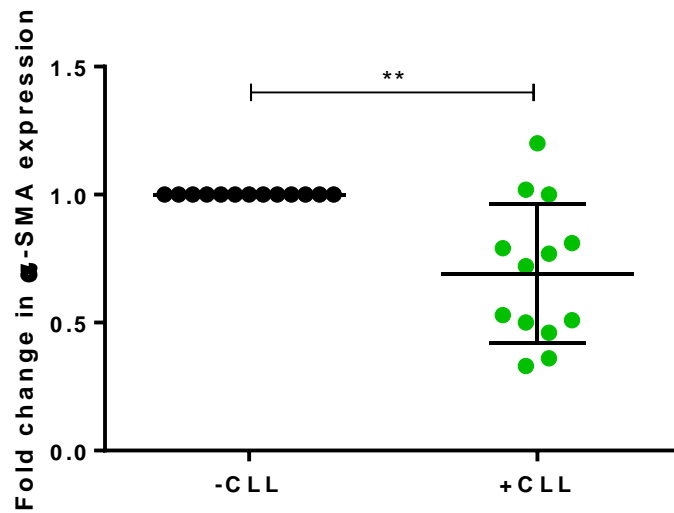


Figure 4.3: Effect of co-culture with CLL samples on HFFF2 α -SMA expression.

Graph shows the fold change in α -SMA expression in HFFF2 cells after co-culture with 13 separate CLL samples for 48 hours, for all samples analysed (n=13). For each sample, relative α -SMA expression in control HFFF2 cells cultured alone was set to 1.0. Each dot represents results for an individual CLL sample with mean \pm SD. The statistical significance of the difference was analysed using Wilcoxon's matched-pairs signed-rank test.

experiments (Figure 4.2 and not shown) confirming that cells were competent to undergo induced transdifferentiation. Although there was an overall **reduction in α -SMA** expression in HFFF2 cells following CLL sample co-culture, there was considerable variation in response between individual CLL samples. Of the 13 samples analysed, 6 reduced **α -SMA expression by $\geq 40\%$** , 4 reduced it by 15-39%, **1 sample had no effect on α -SMA** expression and 2 actually increased expression of this protein (Table 4.1).

I analysed the results to determine whether the variation in effects of CLL cells on α -SMA expression might correlate with the subset of disease defined by *IGHV* gene mutation status, or extent of anergy, defined by slgM signalling capacity [261]. Anergic CLL cells fail to respond to BCR stimuli and are generally suspended in a state of cellular lethargy. Additionally, anergy tends to present more in M-CLL or ZAP-70^{-ve} samples, i.e. less aggressive disease, therefore, anergy was considered as a parameter for subset analysis.

Six of the samples were M-CLL and seven were U-CLL. In subset analysis, there was a trend for stronger modulatory effects for M-CLL compared to U-CLL, and, compared to control cells; differences were only significant for M-CLL (Figure 4.4). However there was no statistical significant difference in effects of U-CLL and M-CLL.

For the eleven samples with available data, nine were classified as signallers and two were classified as non-signallers. All of the U-CLL samples were signallers whereas a proportion of the M-CLL samples were non-signallers (Table 4.1). Interestingly, both of the non-signaller samples showed reduced HFFF2 α -SMA expression; whereas effects were more varied amongst the signal competent samples (Figure 4.5). However, since there were only 2 non-signalling samples, statistical analysis of these differences was not performed.

Another potential variable which could impact α -SMA expression is ZAP-70. Samples were classed as ZAP-70 positive if greater than, or equal to, 20% of the tumour cells expressed ZAP-70 [262]. Unfortunately only two samples used for the co-culture assays (U432, U566) and one for the CM assays (U510) were ZAP-70 positive, thus statistical analysis could not be conducted. **However all three samples reduced HFFF2 α -SMA** expression by over 40%.

Overall, the results show that **co-culture with CLL samples decreases α -SMA** expression, consistent with a reduction in spontaneous transdifferentiation.

CLL sample	IgHV mutational status ^A	sIgM signalling capacity ^B (% Calcium)	α -SMA ^D (-/+, % of change)
431	Mutated	N/A ^C	-50
462	Mutated	11	-64
414	Mutated	0	-49
542	Mutated	2	-19
483	Mutated	5	-21
494	Mutated	6	-23
432	Un-mutated	N/A	-47
410	Un-mutated	25	-54
513	Un-mutated	62	-28
555	Un-mutated	28	0
566	Un-mutated	7	-67
505	Un-mutated	17	+20
508	Un-mutated	19	+2

Table 4.1: Summary of effect of CLL sample co-culture on HFFF2 α -SMA expression for 13 CLL samples analysed.

^AIndicates whether the sample expressed mutated or un-mutated *IGHV* genes.

^BsIgM signal capacity determined by intracellular calcium flux in response to anti-IgM stimulation; $\geq 5\%$ of responding cells indicate a signaller.

^CN/A, data not available.

^DShows whether HFFF2 α -SMA expression was reduced (-), increased (+) or unchanged (0) after 48 hours of co-culture with respective sample. The extent of the change is indicated (%).

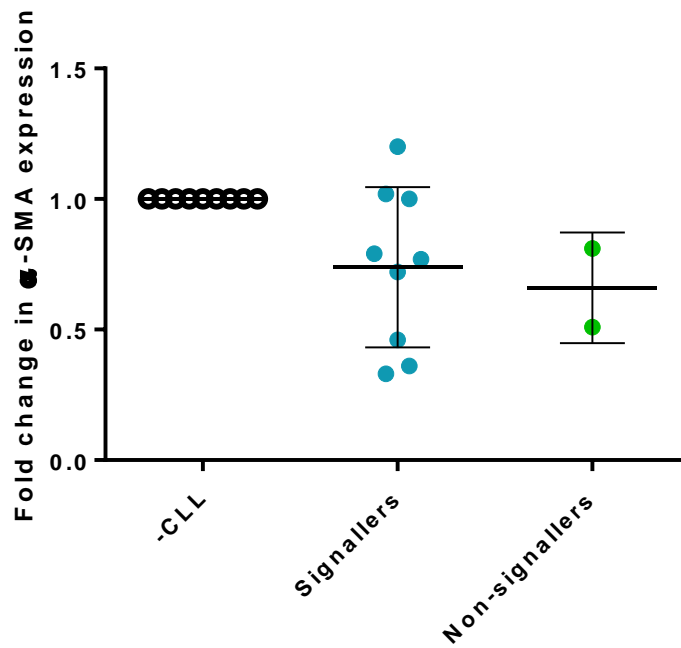


Figure 4.5: Comparison of effect of co-culture on sIgM signal responsive and non-responsive CLL samples **on HFFF2 α -SMA** expression.

Graph shows the effect of sIgM signallers (blue, n=9) and sIgM non-signallers (green, n=2) **on HFFF2 α -SMA** expression. For each sample α -SMA expression in control HFFF2 cells cultured alone has been set to 1.0. Each dot shows the results for an individual CLL sample with the mean \pm SD.

This is surprising, since in other systems, cancer cells appear to promote transdifferentiation [263]. Effects of CLL samples were not clearly distinct between M-CLL and U-CLL.

4.2.2 Determining the effect of CLL cell-derived soluble factors on HFFF2 fibroblasts

Following the co-culture studies I investigated whether the reduction in HFFF2 α -SMA expression is mediated by soluble factor(s) released by CLL cells or is dependent on direct cell-cell contact. HFFF2 cells were therefore treated with conditioned media (CM) derived from CLL samples and, as before, α -SMA expression was analysed by immunoblotting.

Before performing a larger scale study, I first optimised the conditions for production of CM. Variables selected for study were (i) the culture density of CLL samples and (ii) the length of time required to derive CM. All experiments described in this section were performed using DMEM media lacking serum to avoid the potential transdifferentiation of HFFF2 cells in response to serum factors. **Additionally all samples utilised comprised $\geq 80\%$ CLL cells to minimise effects of non-malignant cells.**

In the first optimisation experiments, I investigated the effect of varying the culture density of cells from CLL samples used to derive CM. One key aim was to minimise spontaneous CLL cell death in these experiments, since factors released from dead cells might alter HFFF2 transdifferentiation. Spontaneous CLL cell death can be reduced by culturing CLL PBMCs at high density [264] and CM was therefore prepared from sample U510 cultured at 5×10^6 /ml or 10×10^6 /ml for 72 hours. HFFF2 cells were then cultured in this CLL-derived CM or in serum-free DMEM media as a control. For these initial experiments, HFFF2 α -SMA expression was analysed at 72 hours post addition of CM (rather than the 48 hours studied in co-culture experiments), as it was speculated that the effect of the CM may be weaker than direct cell-to-cell contact and therefore may require more time to take effect.

Western blot analysis (Figure 4.6) revealed that, like co-culture (Figure 4.3), CLL-derived CM **also decreased HFFF2 α -SMA** expression (by $\sim 40\%$). As expected, treatment of HFFF2 cells with TGF- β **increased α -SMA** expression confirming that these cells were competent to undergo induced

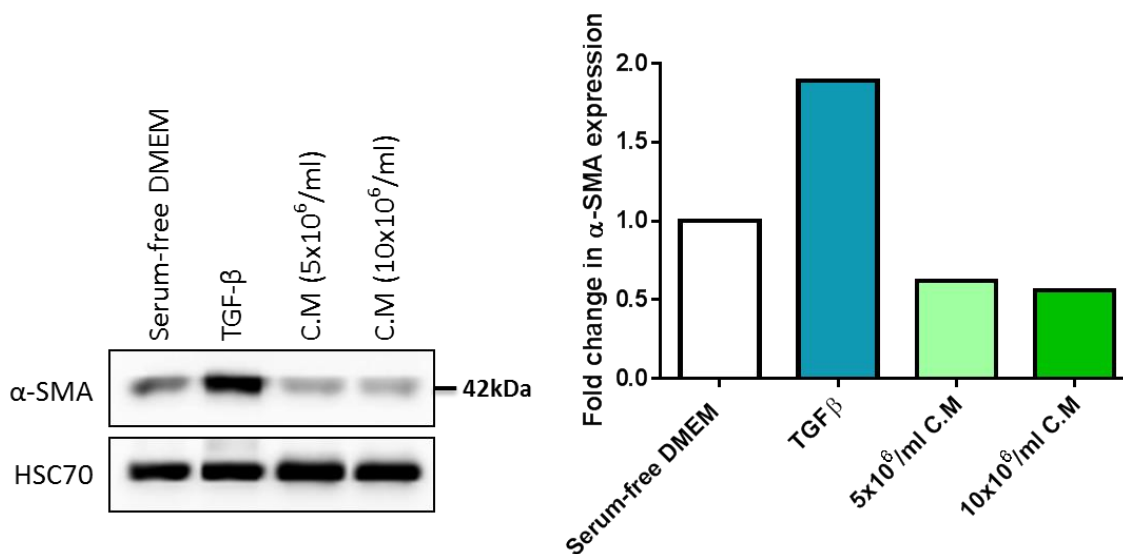


Figure 4.6: Effect conditioned media derived from a CLL sample at different cell densities on HFFF2 α -SMA expression.

HFFF2 cells were cultured in either serum-free DMEM as a control, or cultured in CLL cell-derived conditioned media (CM). CM was derived from CLL sample U510 at cell densities of 5×10^6 /ml or 10×10^6 /ml in serum-free DMEM, for 72 hours. HFFF2 cells were also treated with TGF- β (2 ng/ml) in serum-free DMEM as a positive control for myofibroblast transdifferentiation. **After 72 hours, α -SMA expression was analysed by immunoblotting (left panel). Right panel shows quantitation; α -SMA expression was normalised to HSC70 (loading control), with expression in control HFFF2 cells set to 1.0.**

transdifferentiation. Effects of CLL-derived CM were not clearly different between the two culture densities. Based on these data, CM was derived from CLL cells cultured at 5×10^6 /ml, unless otherwise stated.

The second variable I addressed was the duration of time required to produce the CM. The goal was to minimise the culture period, again to decrease potential confounding effects of cell death. Sample M518 was used and CM was collected following 24, 48 or 72 hours of culture. HFFF2 cell α -SMA expression was analysed at 72 hours, as in the experiment shown in Figure 4.6. CM derived from sample M518 decreased HFFF2 cell α -SMA expression (Figure 4.7). Treatment of HFFF2 cells with TGF- β up-regulated α -SMA expression as expected. Results were similar for all three CM preparations and 24 hours was selected for further studies.

Based on these pilot experiments, more detailed experiments were performed using CM derived from 6 further CLL samples cultured at 5×10^6 CLL cells/ml for 24 hours (Figure 4.8). α -SMA expression was significantly lower in HFFF2 cells cultured in CLL sample-derived CM compared to HFFF2 cells cultured in serum-free DMEM. Overall, the mean reduction in α -SMA expression was ~50%, similar to the effect of direct co-culture (Figure 4.3). There was also little variation in the size of the effect between samples. These data confirm that CLL cells reduce spontaneous HFFF2 cell transdifferentiation and show that this effect is at least partly mediated by soluble factor(s).

4.3 Investigating the effect of CLL cells on TGF- β directed myofibroblast transdifferentiation

To extend these analyses, I next investigated effects of CLL cells on TGF- β -induced transdifferentiation of HFFF2 cells. Since CLL-derived CM seems to recapitulate effects of direct co-culture, further experiments were restricted to CM. This design was selected to avoid potential confounding effects of TGF- β on CLL cells, and contamination of HFFF2 cells by tightly-bound CLL cells.

Experiments described to this point have used a relatively high concentration of TGF- β (**2 ng/ml**) to induce robust HFFF2 cell transdifferentiation. Therefore, before assessing effects of CLL-derived CM, I performed TGF- β **dose response** analysis to identify a lower concentration of TGF- β **that could be used in these** experiments. The goal was to identify a lower concentration of TGF- β **that still**

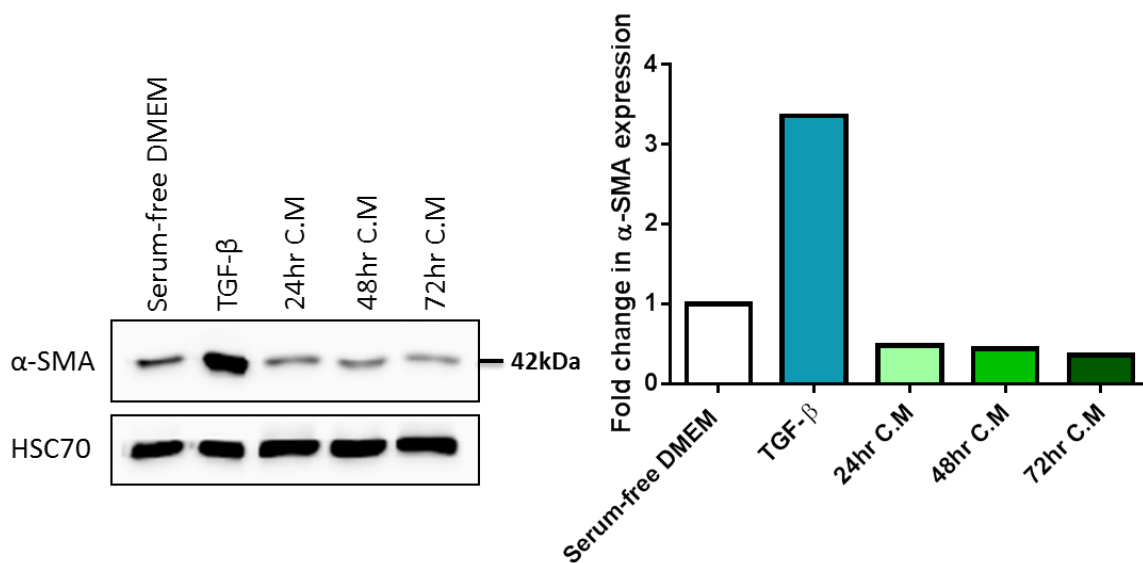


Figure 4.7: Effect of conditioned media derived from a CLL sample for different **times on HFFF2 α-SMA** expression.

HFFF2 cells were either cultured in serum-free DMEM as a control, or cultured in CLL cell-derived conditioned media (CM). CM was generated from CLL sample M518 cultured at 5×10^6 /ml for 24, 48 or 72 hours. HFFF2 cells were treated with TGF- β (2 ng/ml) in serum-free DMEM as a positive control for myofibroblast transdifferentiation. **After 72 hours, α-SMA** expression was analysed by immunoblotting (left panel). **Right panel shows quantitation; α-SMA** expression was normalised to HSC70 (loading control), with expression in control HFFF2 cells set to 1.0.

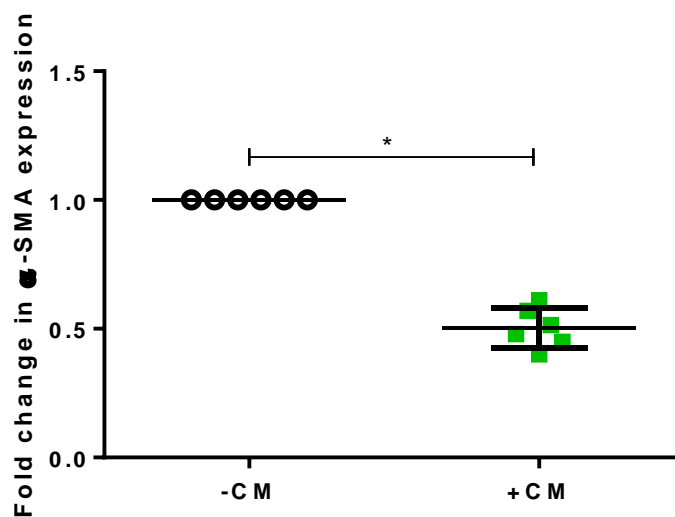


Figure 4.8: Effect of CLL sample-derived CM on HFFF2 α -SMA expression.

Graph shows the fold change in α -SMA expression between HFFF2 cells cultured in either serum-free DMEM media (control) or in CLL sample-derived CM (green) for 72 hours. CM was generated from 6 different CLL samples at 5×10^6 /ml for 24 hours. For each sample α -SMA expression in control HFFF2 cells cultured in serum free DMEM media was set to 1.0. Each dot represents the results for an individual CLL sample with mean \pm SD. The statistical significance of the difference was analysed using Wilcoxon's matched-pairs signed-rank test.

induced robust transdifferentiation, but perhaps provided a less strong drive that could be more effectively countered by CLL-derived CM.

HFFF2 cells were treated with lower concentrations of TGF- β (0.5, 1.0 and 1.5 ng/ml) for 72 hours and expression of α -SMA was analysed by Western blotting (Figure 4.9). α -SMA expression was increased in HFFF2 cells at all tested TGF- β concentrations, but was greater at 1.5 and 2.0 ng/ml TGF- β compared to 0.5 and 1.0 ng/ml. Based on this experiment, concentrations of 0.5 and 1.0 ng/ml TGF- β were selected for further analysis.

An initial experiment was performed using sample M518 (Figure 4.10). This sample was selected since it had been used previously to reduce α -SMA expression in HFFF2 cells in co-culture experiments (Figure 4.3). CM was prepared from this sample (as described in section 4.2.2) and used to treat HFFF2 cells in the presence or absence of TGF- β (0.5 ng/ml or 1.0 ng/ml). As controls, HFFF2 cells were cultured in CLL-derived CM without TGF- β , or with TGF- β alone. After 72 hours, α -SMA expression was analysed by immunoblotting.

HFFF2 cells treated with TGF- β showed a clear increase in α -SMA expression as expected. As shown previously (Figure 4.8), CLL-derived CM decreased α -SMA expression in the absence of TGF- β . In addition, CLL-derived CM also decreased TGF- β -induced α -SMA expression.

Similar experiments were performed using CM derived from a further 3 CLL samples. However, in these experiments, TGF- β was only used at 0.5ng/ml. Quantitative data for all 4 CLL samples are shown in Figure 4.11. Overall the pattern was similar to that described for sample M518 (Figure 4.10) and CLL-derived CM decreased α -SMA expression in the presence or absence of TGF- β . The effect of CLL-derived CM on α -SMA expression in the absence of TGF- β was not statistically significant in this smaller cohort of samples. However, CLL-derived CM did significantly decrease TGF- β -induced α -SMA expression compared to TGF- β treated control cells.

Therefore, in addition to effects on spontaneous transdifferentiation of HFFF2 cells, CLL sample-derived CM also decreases TGF- β -induced myofibroblast transdifferentiation.

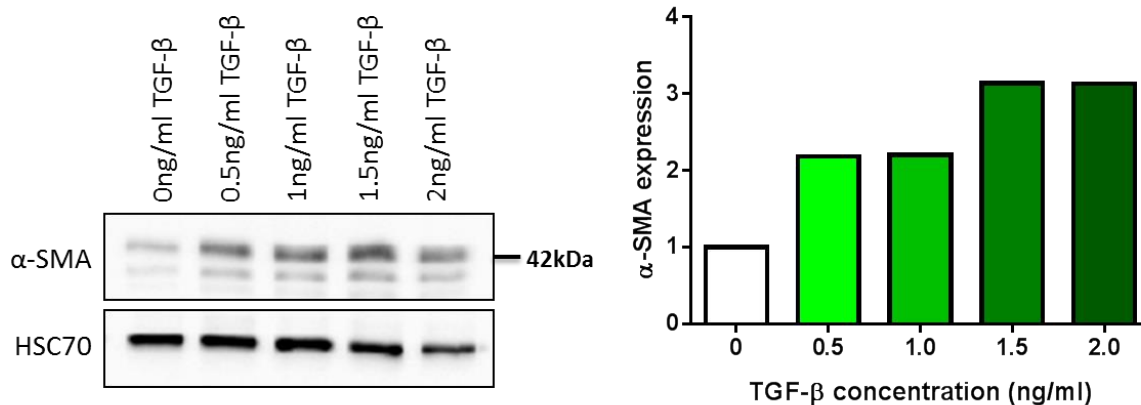


Figure 4.9: TGF- β titration on α -SMA expression of HFFF2 cells.

HFFF2 cells were treated with the indicated concentrations of TGF- β or were left untreated as a control. After 72 hours α -SMA expression was analysed by immunoblotting. Figure shows Western blot (left panel) and quantitation (right panel) with α -SMA expression normalised to the loading control HSC70. α -SMA expression in control HFFF2 cells was set to 1.0.

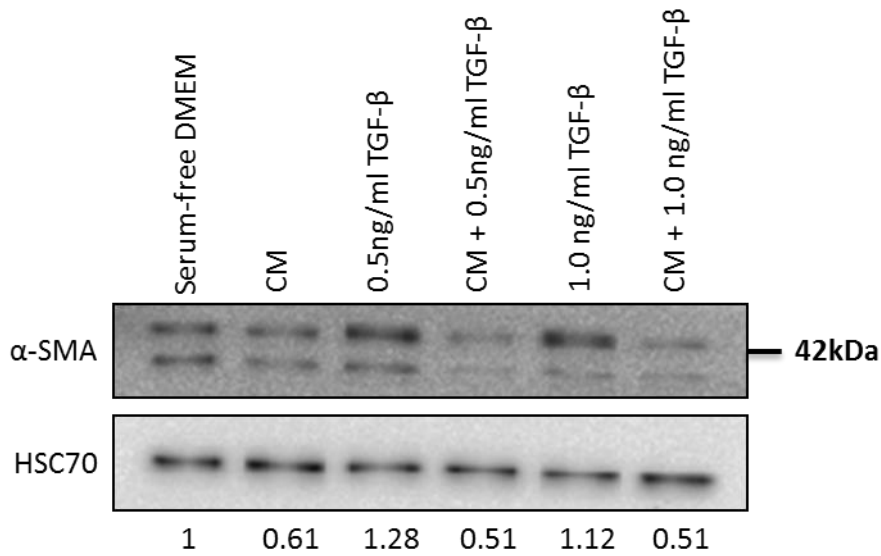


Figure 4.10: Effect of conditioned media derived from a CLL sample on TGF- β induced α -SMA expression in HFFF2 cells.

HFFF2 cells were cultured with CLL-derived conditioned media (CM) from sample M518 in the absence or presence of TGF- β as indicated. Cells were treated with TGF- β only as a control for α -SMA induction. After 72 hours, CLL cells were removed and α -SMA expression of HFFF2 cells was analysed by immunoblotting. Quantitation was performed and α -SMA expression was normalised to HSC70 (loading control); α -SMA expression of control HFFF2 cell was set to 1.0, values are displayed beneath respective bands.

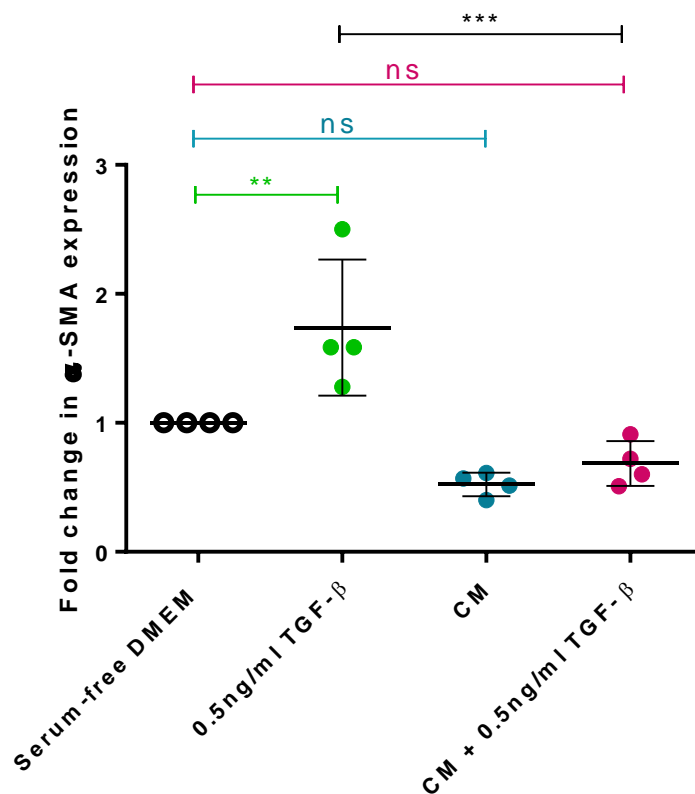


Figure 4.11: Effect of CLL-derived conditioned media on TGF- β induced α -SMA expression in HFFF2 cells.

Graph summarises results for 4 separate samples. Experimental details are as in the legend to Figure 4.10. α -SMA expression in control HFFF2 cells was set to 1.0. Each dot represents results from an individual CLL sample with mean \pm SD. The statistical significance of the differences was analysed by one-way ANOVA with Bonferroni correction (n=4).

4.4 Determining if CLL cells can activate TGF- β

The inhibitory effect of CLL cells and CLL-derived CM on HFFF2 cell transdifferentiation was surprising. For example, in many other systems cancer cells promote transdifferentiation, often via production of TGF- β [263]. Moreover, B-CLL cells have been shown to express TGF- β 1 mRNA as well as release low amounts of active TGF- β [201, 265]. Additionally, high levels of active TGF- β have been detected in plasma samples of patients with CLL [201]. Therefore it was not clear why CLL cells do not promote transdifferentiation. Regulation of TGF- β is complex; the cytokine is released in a latent form and requires activation in order to induce TGF- β signalling and have an effect [184, 185]. Therefore I investigated the ability of CLL cells to activate TGF- β 1 to better understand the potential expression of this cytokine by these cells.

The ability of CLL cells to activate TGF- β 1 was investigated using a reporter cell line. This is based on MLEC cells derived from mink lung epithelial cells and was a kind gift from Dr Veronika Jenei (Cancer Sciences Division, University of Southampton). MLEC cells were stably transfected with a reporter construct, p800neoLUC, which contains a truncated, TGF- β 1-responsive PAI-1 (plasminogen activator inhibitor-1) promoter fused to the firefly luciferase gene (Figure 4.12) [230]. Exposure to active TGF- β 1 induces downstream SMAD signalling which results in the activation of the PAI-1 reporter and expression of firefly luciferase. Luciferase activity can then be quantified in luciferin-based assays (luminescent substrate) and detected using a plate reader in 96-well plate format (Figure 4.13). The assay is well validated as a highly sensitive, specific and quantitative bioassay for the detection of active TGF- β 1 [85, 266].

For assessment of CLL cells, MLEC cells were co-cultured with CLL samples for 24 hours in serum-free RPMI media to minimise potential confounding effects of serum factors on PAI-1 promoter activity. 24 hours was chosen to allow sufficient time for CLL cells to activate TGF- β 1 and to minimise the degree of cell death. As controls, MLEC cells were cultured in serum-free RPMI media in the absence of CLL cells. In addition, a TGF- β dose response curve was performed for each experiment. This served to confirm comparable assay performance between individual experiments and was used to determine equivalent TGF- β concentrations in experiments with co-culture with CLL

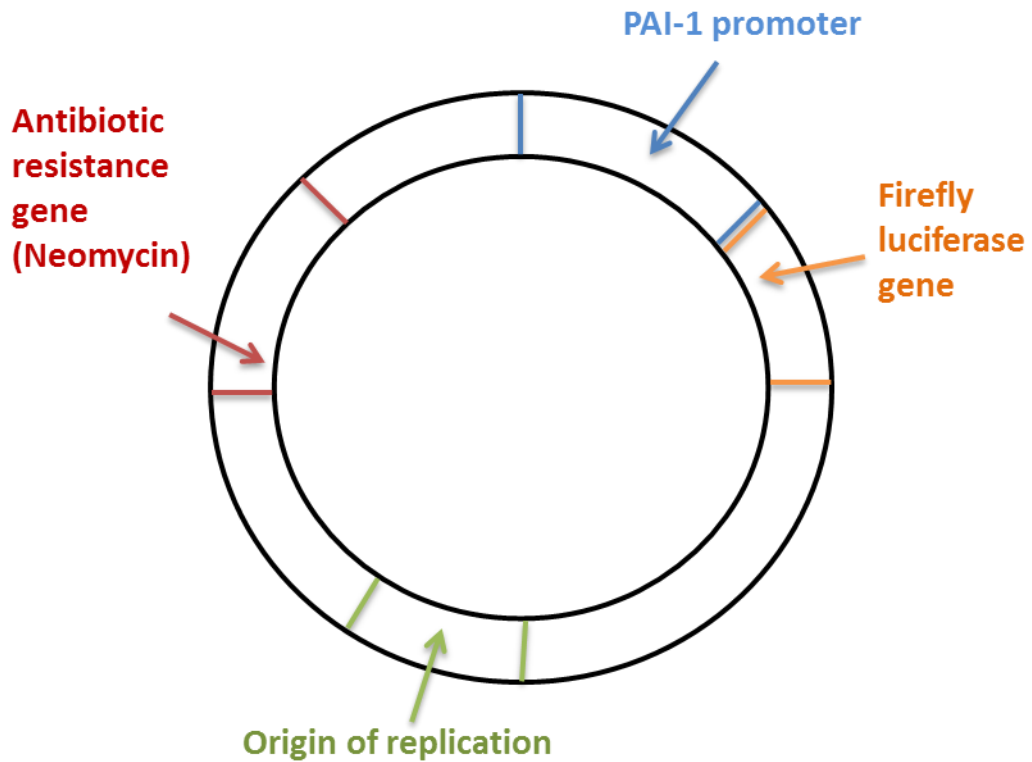


Figure 4.12: Schematic representation of TGF- β 1 responsive reporter construct.

The expression construct, p800neoLUC, comprises a truncated PAI-1 (plasminogen activator inhibitor 1) promoter (blue) which is fused upstream of the firefly luciferase gene (orange). The construct also contains an origin of replication element (green) and an antibiotic resistance gene for neomycin (red) [230].

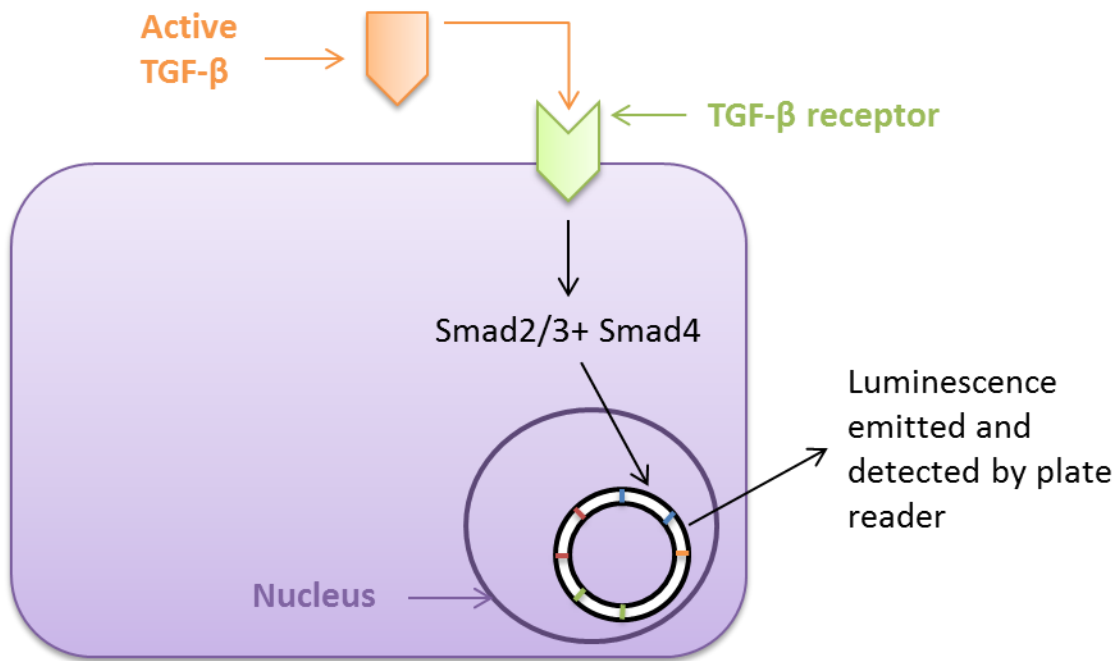


Figure 4.13: Diagram showing basis for quantitation of active TGF-**β1** using the MLEC reporter assay.

MLEC cells (purple) have been stably transfected with a TGF-**β1** responsive reporter construct which is linked to firefly luciferase. Exposure of MLEC cells to active TGF-**β1** induces signalling via the SMAD pathway downstream of the TGF-**β** receptor (green). Active SMAD complexes bind and activate the PAI-1 promoter and increases linked luciferase expression. Luciferase activity is detected in chemiluminescent assays using the luciferin substrate.

samples. A typical TGF- β 1 dose response curve and representative results of CLL sample co-culture are shown in Figures 4.14 and 4.15.

This assay was performed on 19 different CLL samples (Figure 4.16). Samples **comprised $\geq 80\%$ CLL cells to minimise effects** of contaminating cells and were selected to comprise both U-CLL and M-CLL. To allow comparison between experiments, the basal level of luciferase activity in MLEC cells without CLL cells or TGF- β was **set to 100 for each experiment. Of the 19 CLL samples** analysed, 11 significantly activated TGF- β 1.

There was substantial variation in the ability of CLL samples to activate TGF- β in the MLEC assay (Figure 4.16). However, there was no difference in the amount of luminescence generated from MLEC cells co-cultured with M-CLL samples and U-CLL samples (Figure 4.17) indicating that TGF- β 1 activation by CLL cells is independent of *IGHV* mutational status. Only one sample in this cohort was considered as a non-signaller, preventing meaningful analysis of whether TGF- β 1 activation differed between sIgM signal responsive and non-responsive samples.

4.5 **Correlating the effect of CLL cells on HFFF2 α -SMA expression with their ability to activate TGF- β 1**

The ability of CLL samples to activate TGF- β was **surprising, since CLL samples** actually decreased HFFF2 transdifferentiation. However, TGF- β activation was highly variable between individual CLL samples (although apparently unrelated to *IGHV* status) whereas the effects of CLL samples on transdifferentiation was rather consistent (Figures 4.3 and 4.8). This suggested that these phenomena may be unrelated and not mechanistically linked. Before probing further the functional significance of TGF- β activation by CLL cells, I **decided to more** formally investigate the relationship between these two responses.

Out of the 19 samples that were analysed in the MLEC assay, 10 had been used in earlier experiments investigating the effect of CLL cells (either direct co-culture or CM) on HFFF2 α -SMA expression (Table 4.1). Data for these 10 samples are summarised in Table 4.2.

Out of the ten samples listed in Table 4.2, nine reduced and one **increased α -SMA** expression in HFFF2 cells after co-culture with CLL samples

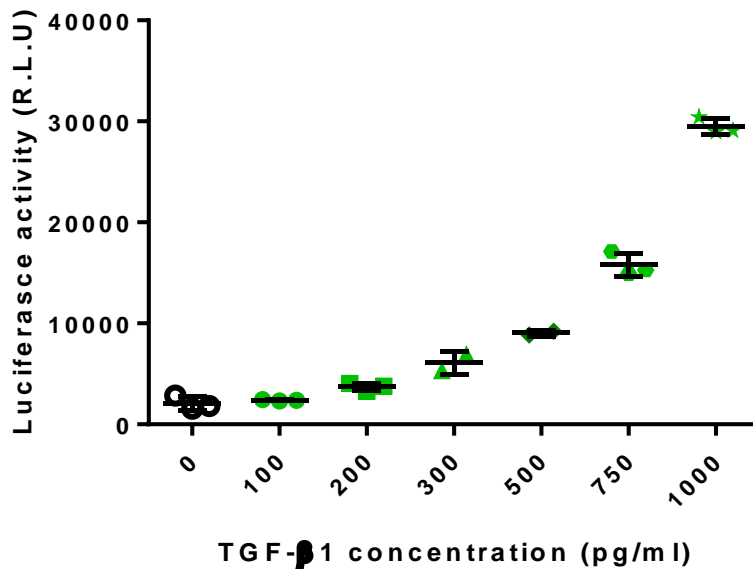


Figure 4.14: Typical TGF- β 1 dose-dependent curve generated from MLEC cells.

Graph shows MLEC cells that were incubated with the indicated TGF- β 1 concentrations for 24 hours before analysis of luciferase activity. Each TGF- β concentration was set up in triplicate; each dot represents the results from one triplicate. Graph shows the mean \pm SD.

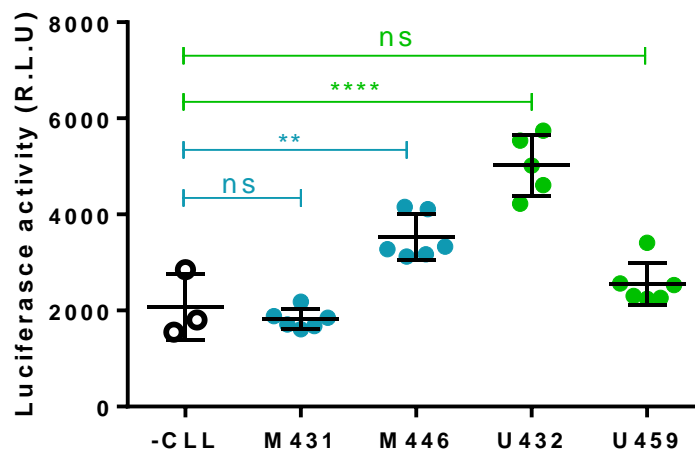


Figure 4.15: Typical results generated from a single TGF- β luciferase assay.

MLEC cells were co-cultured with 4 different CLL samples in serum-free RPMI media. MLEC cells were also cultured in serum-free RPMI media in the absence of CLL cells as a control. Luciferase activity was measured after 24 hours. Graph shows individual data points from 6 replicate determinations with mean \pm SD. The statistical significance of the differences was analysed by one-way ANOVA with Bonferroni correction (n=6).

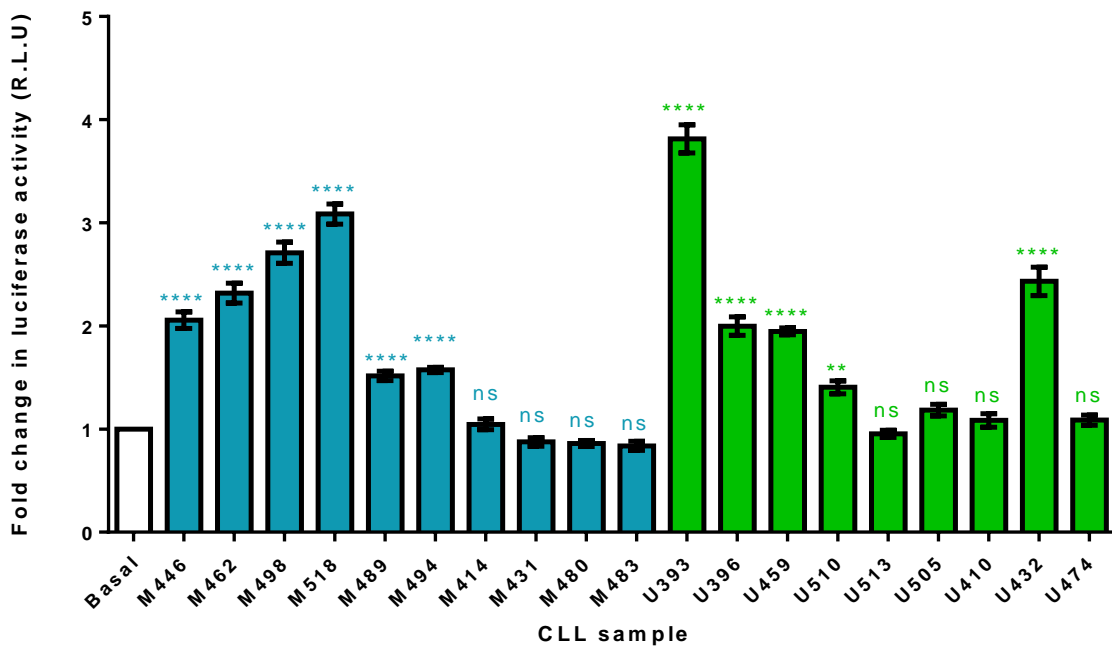


Figure 4.16: TGF-β1 activation by CLL samples.

Graph shows the fold change in luciferase activity of MLEC cells following co-culture with 19 different CLL samples for 24 hours. Experimental details are as described in Figure 4.15. Luciferase activity of control MLEC cells in the absence of CLL cells was set to 100 for each experiment. Bars show means ±SD derived from 6 replicates for each sample. The statistical significance of the differences was analysed by one-way ANOVA with Bonferroni correction.

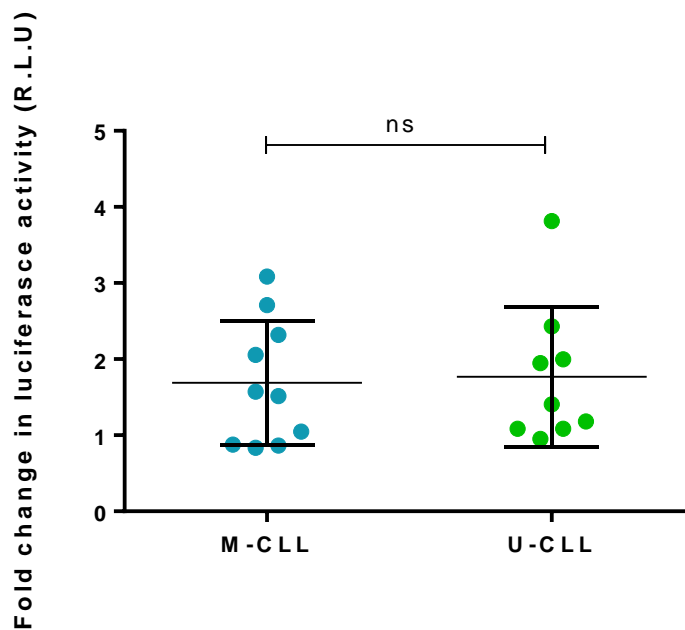


Figure 4.17: Effect of *IGHV* mutational status on TGF- β 1 activation.

Graph compares the effect of *IGHV* mutation status of CLL cells on TGF- β 1 activation for all 19 CLL samples analysed. Each dot shows results from one individual CLL sample; Graph shows the mean of all samples \pm SD. the mean of the 6 repeats per sample was calculated and has been plotted as one dot. For each sample the luciferase activity for MLEC cells cultured alone (basal luciferase activity) was set to 100 (not shown). The statistical significance of the differences was analysed by Mann-Whitney test.

or culture in CLL-derived CM. Of the nine samples which reduced HFFF2 α -SMA expression, four activated TGF- β 1 (44%), and five did not (56%). **Furthermore sample U505 increased α -SMA expression yet was unable to activate TGF- β 1. This indicates that the increase in HFFF2 α -SMA expression was not due to TGF- β 1 activation and release from this CLL sample.**

The effect of all ten CLL samples on HFFF2 α -SMA expression and TGF- β 1 activation has been correlated (Figure 4.18). For both variables the degree of change was normalised to 1.0. There was no significant correlation between these two variables for this cohort. Therefore these data indicate that the ability of CLL cells to activate TGF- β and reduce HFFF2 α -SMA expression is un-related. Therefore this was not pursued any further.

4.6 Preliminary analysis of effects of CLL cell-derived exosomes on myofibroblast transdifferentiation.

Since CLL sample-derived CM effectively recapitulated the ability of CLL cells to decrease HFFF2 transdifferentiation (Figure 4.8), this response appears to be mediated, at least in part, via soluble factors. One exciting new area of cell communication is exosomes. These are membrane bound vesicles of endosomal origin which are approximately 40-100 nm in size and contain various cytoplasmic proteins, mRNAs and microRNAs [267, 268]. Exosomes have been detected in various bodily fluids including blood [269] and saliva [270]. Formation of exosomes involves the inward budding of the endosomal membrane to form intraluminal vesicles (ILVs). The production of multiple ILVs within the endosome now denotes it a multivesicular endosome (MVE). The MVE either fuse with lysosomes if the proteins it carries are destined for degradation or fuse with the plasma membrane to release the exosomes into the extracellular environment. Once exosomes have reached their target cells they can be taken up by two different mechanisms. They can either be endocytosed by the cell or they can fuse to the plasma membrane and release their contents directly into the cell cytoplasm. Data has shown that mRNA and microRNAs transferred by exosomes can functionally bind with that of the target cell, resulting in altered mRNA and protein expression within the recipient cell [268].

CLL sample	<i>IGHV</i> mutational status ^A	Effect on α -SMA ^B (-/+, fold change)	Ability to activate TGF- β 1 ^D (-/+, fold change)
518	Mutated	-0.48* ^C	+3.10
431	Mutated	-0.50	-0.87
462	Mutated	-0.64	+2.31
414	Mutated	-0.49	-1.01
483	Mutated	-0.21	-0.84
510	Un-mutated	-0.45*	+1.41
432	Un-mutated	-0.47	+2.40
410	Un-mutated	-0.54	-1.08
513	Un-mutated	-0.28	-0.95
505	Un-mutated	+1.20	-1.18

Table 4.2: **Effect of CLL cells on HFFF2 α -SMA** expression correlated with their ability to activate TGF- β .

^AShows whether the CLL sample is M-CLL or U-CLL; the top six samples are M-CLL (Mutated) and the lower five are U-CLL (Un-mutated).

^BShows whether the CLL sample reduced (-) or increased (+) α -SMA expression in HFFF2 cells. The fold change is also displayed.

^C(*) highlights the samples from which CLL-derived CM was used, all other samples were directly co-cultured with HFFF2 cells.

^DShows whether the respective CLL sample activated TGF- β 1 (+) or not (-). The fold change is also displayed.

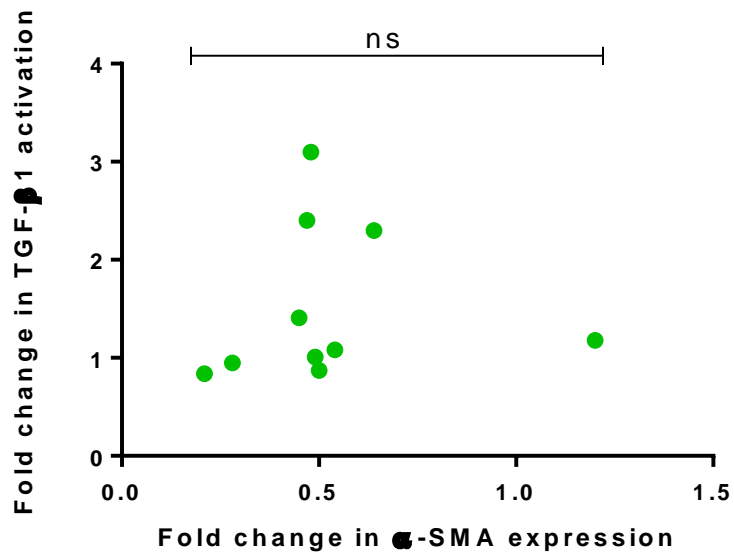


Figure 4.18: Correlation of CLL sample ability to activate TGF- β 1 and effect α -SMA expression.

The correlation of the ability for all 10 CLL samples to activate TGF- β 1 (Y axis) and reduce α -SMA expression (X axis) is shown. Each dot represents results of an individual CLL sample. For both variables the degree of change was normalised to 1.0. The statistical significance of the difference was analysed using Spearman's correlation test.

Several lines of evidence demonstrate that exosomes may promote cancer progression by targeting stromal cells. Chronic myeloid leukaemia (CML)-derived exosomes can promote angiogenesis in human umbilical endothelial cells (HUVECs), and induce IL-8 secretion in stromal cells resulting in the induction of multiple intracellular signalling pathways within the malignant cells [271, 272]. Furthermore, exosomes derived from acute myelogenous leukaemia (AML) cells alter the angiogenic, proliferative and migratory responses of stromal cells [273]. CLL cell-derived exosomes have not been extensively studied and therefore there is limited data about them in the literature. However **unpublished data generated from Dr Nagesh Kalakonda's** group (University of Liverpool) has shown that exosomes derived from CLL cells are enriched in miR-202 and can increase proliferation of human BM-derived stromal cells. Although transdifferentiation was not studied in these experiments, it is possible that this effect on mesenchymal cell proliferation is secondary to changes in differentiation. Therefore, I investigated whether CLL-derived exosomes altered transdifferentiation of HFFF2 cells.

CM was derived from CLL samples as described in section 4.2.2. Intact exosomes were isolated from a portion of the CM using Total Exosome Isolation Reagent. 0.5 volumes of the reagent was added to the CM and mixed thoroughly by pipetting to ensure a homogenous mixture had formed. The mixture was left overnight to allow the reagent to bind water molecules within the CM and force less soluble components (i.e. exosomes) out of solution upon centrifugation (section 2.10). The reagent does not bind to the exosome surface therefore only trace amounts are present in the exosome pellet after isolation. Isolated exosomes were re-suspended in the same volume of serum-free DMEM that they were originally isolated from. The exosome-depleted CM was also retained for analysis.

HFFF2 cells were cultured in (i) CLL-derived CM, (ii) CLL-derived exosomes or (iii) exosome-depleted CM, or were left untreated as a control. HFFF2 cells were also treated with TGF- β as a positive control. After 72 hours, HFFF2 cell α -SMA expression was analysed by immunoblotting. Unfortunately, HFFF2 cells cultured in exosome-depleted CM died during the 72 hour culture period, presumably due to direct effects of the Total Exosome Isolation Reagent on HFFF2 cells. However, viability of HFFF2 cells was not obviously affected by the other conditions, as assessed by microscopic visualisation. The experiment

was performed with CM derived from two CLL samples, M431 and M595B (Figure 4.19). **Both samples comprised $\geq 80\%$ CLL cells** to minimise deriving exosomes from contaminating cells.

Consistent with previous analysis (Figures 4.3 and 4.8) effects of CLL samples on α -SMA expression were variable. CM derived from sample M431 reduced α -SMA expression, whereas CM from sample M595B very modestly increased α -SMA expression. However, exosomes derived from either sample reduced α -SMA expression. Due to time constraints it was not possible to analyse further samples. Although preliminary, the results indicate that CLL-derived exosomes may contribute to the ability of CLL cells to decrease HFFF2 transdifferentiation.

4.7 Discussion

In solid cancers the presence of myofibroblasts correlates with enhanced disease progression and poor clinical outcome. This has been observed for multiple cancers including prostate, pancreatic, breast and colorectal cancer [171, 172, 174, 274]. Furthermore, malignant cells within solid tumours can promote myofibroblast transdifferentiation by releasing and activating TGF- β . A previous study showed that TGF- β signalling is hyper-activated within CAFs which were cultured in CM derived from epithelial cancer cells, thus leading to **an increase in α -SMA expression** [259]. Although the presence and clinical consequence of myofibroblasts have been extensively studied in solid cancers, it has not been investigated in CLL or any other type of B cell malignancy.

The data presented in chapter 3 demonstrate that α -SMA positive cells are present within CLL/SLL-affected LN tissue, thus indicating the presence of myofibroblasts within the CLL stroma. Therefore the main aim of the results obtained in this chapter was to determine if CLL cells effect myofibroblast transdifferentiation. This was investigated by initially co-culturing CLL samples **with HFFF2 cells for 48 hours and then analysing α -SMA expression** of the adherent cells. This was followed by culturing HFFF2 cells in CLL sample-derived CM, with or without the addition of TGF- β , **for 72 hours prior to analysis of HFFF2 α -SMA expression.** I then investigated the ability of CLL samples to activate the latent form of TGF- β 1. **Finally, the effect of CLL**

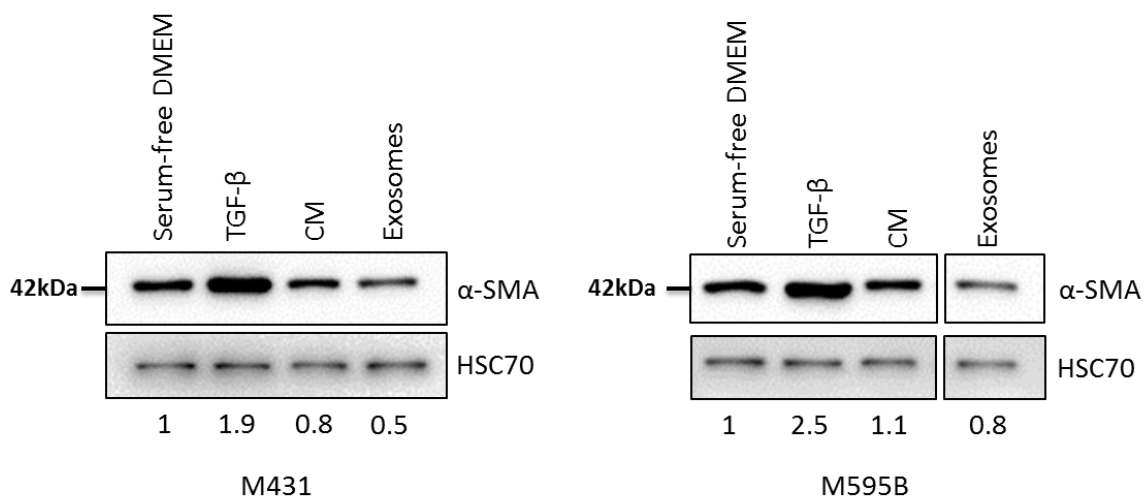


Figure 4.19: Effect of CLL cell-derived exosomes on HFFF2 cell α -SMA expression.

HFFF2 cells were cultured with TGF- β (2 ng/ml), CLL-derived CM, CLL-derived exosomes, or were cultured in serum-free DMEM as a control. CM was derived from CLL cells at a density of 5×10^6 /ml in serum-free DMEM for 24 hours. After 72 hours, expression of α -SMA was analysed using immunoblotting. Quantitation of α -SMA expression (normalised to the loading control HSC70) is displayed beneath the figures with expression in control HFFF2 cells cultured alone set at 1.0. Data shown for two CLL samples analysed.

Chapter 4

sample-derived exosomes on spontaneous myofibroblast transdifferentiation was analysed.

4.7.1 Effect of CLL cells on myofibroblast transdifferentiation

The main conclusion from the experiments described in this chapter, is that CLL cells decrease transdifferentiation of HFFF2 cells. Thus, co-culture with CLL samples overall significantly decreased HFFF2 cell α -SMA expression. Moreover, CLL-derived CM also significantly decreased HFFF2 cell α -SMA expression in both the absence and presence of TGF- β , **indicating that CLL cells can prevent both spontaneous and TGF- β induced myofibroblast transdifferentiation.** This is surprising as these data oppose observations in solid cancers, whereby cancer cells promote transdifferentiation, pointing to unusual behaviour of CLL.

Initial experiments involved examining myofibroblast transdifferentiation in response to direct co-culture of CLL samples and HFFF2 cells. However, drawback of this method was potential contamination of HFFF2 cells by CLL cells which could not be completely removed despite extensive washing. One potential consequence of this was that the apparent decrease in SMA **expression was a result of 'dilution'** of HFFF2 cell lysates with CLL-derived material. However, similar repression of HFFF2 transdifferentiation was also observed in experiments using CLL-derived CM, where this complication is avoided.

One drawback of these experiments is that all CLL samples comprise a heterogeneous population of peripheral blood mononuclear cells (PBMCs) with variable amounts of malignant and non-malignant cells. One option would have been to isolate the malignant cells prior to study, using, for example, negative selection and the MACS separator column. However, this process is fairly long and exposes CLL samples to non-optimal conditions (i.e. not 37°C/5% CO₂) **for an extended period of time. Since, it is possible that these manipulations would alter properties of CLL cells I instead chose to limit analysis to CLL samples with $\geq 80\%$ malignant (CD19+CD5+) cells** to minimise potential effects of non-malignant cells. However, it is not possible to exclude that residual non-malignant cells do not play a role in the apparent suppression of HFFF2 cells transdifferentiation. Although, there was no apparent relationship between the degree of HFFF2 α -SMA reduction with the

respective samples %CLL. For instance samples comprising a lower amount of CLL cells such as 432 (83%) and 462 (81%) reduced α -SMA expression by 47% and 64% respectively. This was similar to samples comprising a higher proportion of CLL cells such as 410 (95%) and 414 (95%) which reduced α -SMA by 54% and 49% respectively. Further parallel experiments could be performed using negatively selected CLL cells to define more precisely the relative contribution of malignant and non-malignant cells in CLL samples.

Myofibroblast transdifferentiation was only determined based on α -SMA expression by immunoblotting. Although α -SMA is a hallmark of myofibroblasts and a very reliable marker for their detection, characterisation could be expanded by utilising other methods. For instance other myofibroblast markers could be analysed by immunoblotting, such as the 85-90kDa isoform of palladin, which is specific for tumour associated fibroblasts [275]. Additionally **conducting immunofluorescence to analyse α -SMA** would allow the detection and visualisation of stress fibres, another key component of the myofibroblast phenotype. Moreover methods exist which analyse the key functional property of myofibroblasts, their contractility. Collagen gel contraction assays could be performed to compare the extent of gel contraction in response to HFFF2 cells cultured alone with those cultured in the presence of CLL cells or CLL CM.

Another drawback to these experiments is that only one cell line (HFFF2 cells) was utilised. As described in chapter 3 attempts were made to identify primary cells suitable for these studies. However, neither CLL-derived fibroblasts nor STRO-1 cells proved suitable. HFFF2 cells are derived from the skin and may therefore not be entirely relevant since CLL cells do not typically accumulate to high levels within dermal tissue. However, HFFF2 cells have proved to be a very robust model to probe transdifferentiation *in vitro* [235, 244] and these results are consistent with observations linking α -SMA expression to outcome in a wide range of cancer types.

CLL viability was not assessed in these assays. This is an important variable to take into account as CLL cells spontaneously undergo apoptosis over time. In the direct co-culture assays cells were cultured for 48 hours, over which time there could be substantial CLL cell death. This could impact the validity of the data by suggesting **that the reduction in HFFF2 α -SMA expression is caused by dead CLL cells**. However, multiple studies have shown that various types of

Chapter 4

stromal cells promote CLL cell survival. Furthermore the data described in the following chapters will demonstrate that HFFF2 fibroblasts can significantly protect CLL samples from apoptosis up to 72 hours. Additionally, for the CM assays, CM was derived from CLL cells for 24 hours to minimise the extent of generating CM from dead CLL cells. Therefore CLL viability should not impact the data.

However it is not known what effect CLL cells may have on HFFF2 cell viability. **This could potentially affect the data as the reduction in α -SMA expression** may correlate with HFFF2 cell death, opposed to a reduced rate of transdifferentiation. **Prior to analysis of α -SMA expression** HFFF2 cells were checked by eye to determine their viability. However, to avoid any bias in the data more accurate methods could be conducted to ensure there were no differences in cell viability between cells cultured alone and those cultured in the presence of CLL samples or CLL CM. An MTT assay could be performed which is a simple and sensitive assay by which the number of cells within a well can be determined through the detection of fluorescent or chromogenic signals by a plate reader. Additionally immunoblotting could be utilised to analyse caspase expression and levels of PARP cleavage between HFFF2 cells in the absence or presence of CLL samples.

4.7.2 Intrasmple variation

CLL is a highly heterogeneous disease and clinical course varies greatly between patients. However all patients fall into one of two disease subsets based on *IGHV* mutation status. This subset determines disease progression and clinical behaviour between the two is very different. Patients who acquire somatic mutations within their *IGHV* genes (M-CLL) suffer from a less severe form of the disease compared to patients who do not acquire these mutations (U-CLL). Additionally prognostic markers associated with poor disease outcome, such as ZAP-70 and Ki-67, have been shown to correlate with the more aggressive U-CLL subset of disease.

Given the variable *in vivo* behaviour of CLL, it was perhaps unsurprising that the ability of CLL samples to inhibit transdifferentiation of HFFF2 cells also varied between individual patients. Of the 13 CLL samples analysed, 10 reduced HFFF2 α -SMA expression, 2 increased it and 1 had no effect. Furthermore there was substantial variation in the degree of α -SMA reduction

between the 10 individual samples. 6 reduced α -SMA $\geq 40\%$ and 4 reduced α -SMA by 15-39%. This may in part explain why α -SMA expression in CLL/SLL LNs was shown to be so variable between individual patients (Chapter 3, Figure 3.2).

Of the 13 samples, 6 were M-CLL and 7 were U-CLL. All of the M-CLL samples **reduced** α -SMA expression; therefore the 3 CLL samples that did not reduce α -SMA expression were U-CLL samples. However there was no significant difference between the effect of M-CLL and U-CLL **samples on** α -SMA expression in HFFF2 cells therefore indicating the variation is not based on *IGHV* status.

It is currently unclear which factors affect the variable reduction in HFFF2 α -SMA expression. To elucidate this more samples need to be analysed. Although there was no significant difference between *IGHV* statuses for this cohort it should not be overlooked as a larger cohort may highlight a clearer trend. Another variable that may influence the degree **of HFFF2** α -SMA reduction could include whether or not the sample is a sIgM signaller. Unfortunately only two samples in the cohort were non-signallers and therefore statistical analysis could not be conducted, however both **samples decreased** α -SMA expression. **Data described in chapter 3 suggested an inverse correlation between** α -SMA and ZAP-70 expression within CLL/SLL LN tissue; the majority of samples **which expressed** α -SMA were negative for ZAP-70. Although this correlation was not statistically significant ZAP-70 could be a potential variable which **impacts** α -SMA expression. Unfortunately as only two samples used for the co-culture assays (U432, U566) and one for the CM assays (U510) were ZAP-70 positive statistical analysis could not be conducted. Other variables could include genetic variances, disease stage or even previous treatment. If α -SMA expression, and therefore myofibroblast presence, is linked with disease progression as it is in solid tumours then these could all be factors which modulate the effect of CLL cells **on** α -SMA expression.

4.7.3 Effect of soluble factors and exosomes on transdifferentiation

As CLL CM significantly decreased α -SMA expression in HFFF2 cells this suggests that soluble factors released by CLL cells impact myofibroblast transdifferentiation. As cells transdifferentiate their ability to proliferate typically declines. **Unpublished data from Dr Nagesh Kalakonda's lab**

Chapter 4

(University of Liverpool) has shown that exosomes derived from CLL cells can increase proliferation of BM-derived stromal cells. Thus, one possibility is that CLL-cell derived exosomes may mediate the inhibition of myofibroblast transdifferentiation (and thereby enhance differentiation). It was therefore speculated that exosomes generated from CLL cells may be a key factor within CLL CM responsible for preventing myofibroblast transdifferentiation which would be an extremely interesting mode of cell-to-cell communication.

Exosomes are membrane bound vesicles of endosomal origin which have been shown to play a role in intercellular communication. They contain cytoplasmic proteins, mRNAs and microRNAs. Exosomes transport their contents into other cells either by being endocytosed by the target cell or by fusing with its plasma membrane and releasing its contents directly into the cell. Data has shown that mRNA and microRNAs transferred by exosomes can functionally bind with that of the target cell, resulting in altered mRNA and protein expression within the recipient cell [268]. Several lines of evidence have demonstrated that exosomes and microRNAs modulate myofibroblast transdifferentiation. One study showed that exosomes derived from gastric cancer cells can induce myofibroblast transdifferentiation of human umbilical cord-derived MSCs [276]. Similarly breast cancer-derived exosomes have been shown to induce the myofibroblast phenotype in adipose tissue MSCs as indicated by increased α -SMA expression [277]. Furthermore studies have shown that microRNA expression is altered in fibroblasts which have undergone transdifferentiation [278, 279]. These data indicate that exosomes can modulate myofibroblast transdifferentiation possibly by altering microRNA expression. CLL-exosomes may adopt a similar method to prevent myofibroblast transdifferentiation and **unpublished data by Nagesh Kalakonda's groups has found that CLL-exosomes are enriched in miR-202.**

The data obtained in this chapter showed that culturing HFFF2 cells in media **containing only exosomes reduced α -SMA** expression. These data are very preliminary, however they do suggest that CLL-derived exosomes may prevent myofibroblast transdifferentiation. More samples need to be analysed to confirm this and to conduct statistical analysis. Furthermore, although HFFF2 cell viability was checked by eye prior to analysis and appeared fine, a more accurate method needs to be utilised, such as a MTT assay, to ensure there are

no variances in cell viability between conditions which would impact the results.

Although attempts have been made to determine if exosomes are responsible for the CLL-induced reduction of HFFF2 α -SMA expression, it is possible that soluble factors are also involved in this phenomenon. However this could include a vast range of different cytokines and chemokines. To narrow down which factors may be involved HFFF2 cells could be cultured in CLL CM separated into low and high molecular weight fractions. This would create a preliminary starting point from which various factors can be eliminated. Further to this neutralising antibodies could be utilised to deduce specifically which factor(s) are responsible. Previous work has shown that basic fibroblast growth factor (bFGF) effectively inhibits TGF- β induced myofibroblast transdifferentiation of valvular interstitial cells, **as seen by prevention of α -SMA induction** [280]. Additionally B-CLL cells have been shown to express elevated levels of bFGF, and thus could be a potential candidate involved in preventing myofibroblast transdifferentiation [281, 282].

4.7.4 CLL cells can activate TGF- β 1

One complicating area is the potential production of TGF- β by CLL cells themselves. Previous data has demonstrated that B-CLL cells express TGF- β 1 mRNA [201]. Furthermore CLL cells have been shown to secrete active TGF- β which acts in an autocrine fashion to reduce their proliferation [201, 265]. This is surprising considering that CLL samples reduce HFFF2 α -SMA expression, yet secrete the main cytokine responsible for its induction. To investigate this I used mink lung epithelial cells (MLEC cells) which stably express a TGF- β 1 responsive reporter construct. This assay allows detection and quantitation of active TGF- β 1.

Of the 19 CLL samples analysed 11 significantly activated TGF- β 1. Again, all samples utilised were PBMCs however samples were selected to comprise **$\geq 80\%$ CLL cells to minimise the** amount of non-B cells. However it is likely a degree of TGF- β 1 activation is due to contaminating cells. Additionally it is possible that a proportion TGF- β 1 activation may be a result of the MLEC cells themselves. There is no evidence of this in the literature, however for every assay conducted luciferase activity was detected in MLEC cells cultured in the absence of TGF- β and CLL samples (basal MLEC activity). As all cells are

Chapter 4

cultured in media lacking FCS we can eliminate the possibility that serum factors are responsible for this. Therefore this indicates that the reporter construct is detecting active TGF- β , **possibly released from MLEC cells**. However the basal level of MLEC luciferase activity is taken into account for every assay conducted.

There was great variability in these results. Of the 19 samples analysed 11 activated TGF- β 1 whereas 8 did not. I analysed the data to determine if this variability was due to *IGHV* mutation status. 10 of the samples were M-CLL and 9 were U-CLL. Out of the 11 samples that did activate TGF- β 1, 6 were M-CLL samples and 5 were U-CLL samples. There was no statistically significant difference between the two mutational subsets in their ability to activate TGF- β 1. Other variables could be analysed such as whether the sample is a sIgM signaller, unfortunately for this cohort only 1 sample was a non-signaller therefore meaningful analysis could not be performed.

Following this the data was analysed to determine if there is a link between the ability of CLL samples to activate TGF- β 1 and effect HFFF2 α -SMA expression. Of the 19 samples that were analysed for TGF- β 1 activation, 10 had previously been analysed to determine if they could affect myofibroblast transdifferentiation. Strangely, of the 9 samples which reduced α -SMA expression, 4 were able to activate TGF- β 1. For this cohort at least there was no significant correlation between CLL sample ability to activate TGF- β 1 and **effect HFFF2 α -SMA expression**, indicating they are not mechanistically linked therefore this was not pursued.

However this leaves the unanswered question of why TGF- β 1 activation fails to promote myofibroblast transdifferentiation of HFFF2 cells. One explanation is that although the CLL samples activated TGF- β 1 it does not necessarily mean they are secreting the cytokine. It is possible that the active form of TGF- β 1 remains bound to the CLL cell surface [283]. To confirm whether these samples secrete active TGF- β 1 MLEC cells could be cultured in CLL CM. Another explanation is that CLL samples are not activating the sufficient amount of TGF- β 1 required to induce transdifferentiation. A TGF- β dose response curve was set up for every assay conducted. Therefore, this curve could be used to extrapolate the concentration of TGF- β , from the luminescence detected from each CLL sample analysed. The optimal concentration of TGF- β 1 used to induce HFFF2 myofibroblast transdifferentiation *in vitro* is 2ng/ml. However, a

concentration as low as 0.5ng/ml, is sufficient for partial induction. Of the 19 samples analysed, sample U393 had the strongest ability to activate TGF- β 1, yet only 0.6ng/ml TGF- β 1 was detected. This sample may be able to induce myofibroblast transdifferentiation however this was not analysed. Moreover, no more than approximately 0.3ng/ml active TGF- β 1 was detected in the other samples. Furthermore it is possible that CLL samples release other factors which counteract the effect of TGF- β 1, such as bFGF [280, 282]. Similar to the interstitial cells, release of this growth factor from CLL cells may counteract myofibroblast transdifferentiation of HFFF2 cells.

Interestingly, sample U505 was not able to significantly activate TGF- β 1 **yet it was one of the few samples able to increase α -SMA expression**. Specifically this sample activated between 0-0.1ng/ml TGF- β 1. This suggests a number of possibilities. Firstly this sample may release the latent form of TGF- β 1 which is **subsequently activated by the HFFF2 fibroblasts leading to α -SMA up-regulation**. Secondly this sample may induce TGF- β 1 activation within HFFF2 cells resulting in it being released and acting on HFFF2 cells in an autocrine manner. This further supports that there is no mechanistic link between CLL sample ability to activate TGF- β 1 and affect HFFF2 α -SMA expression.

4.7.5 Summary

- CLL samples appear to block both spontaneous and TGF- β induced myofibroblast transdifferentiation, as direct co-culture with CLL samples and culture in CLL sample-derived CM, **resulted in lower levels of α -SMA expression** in HFFF2 cells, compared to controls. These data suggest soluble factor(s) released from CLL cells may be responsible for this.
- Preliminary data indicate CLL cell-derived exosomes may prevent myofibroblast transdifferentiation (Figure 4.20).

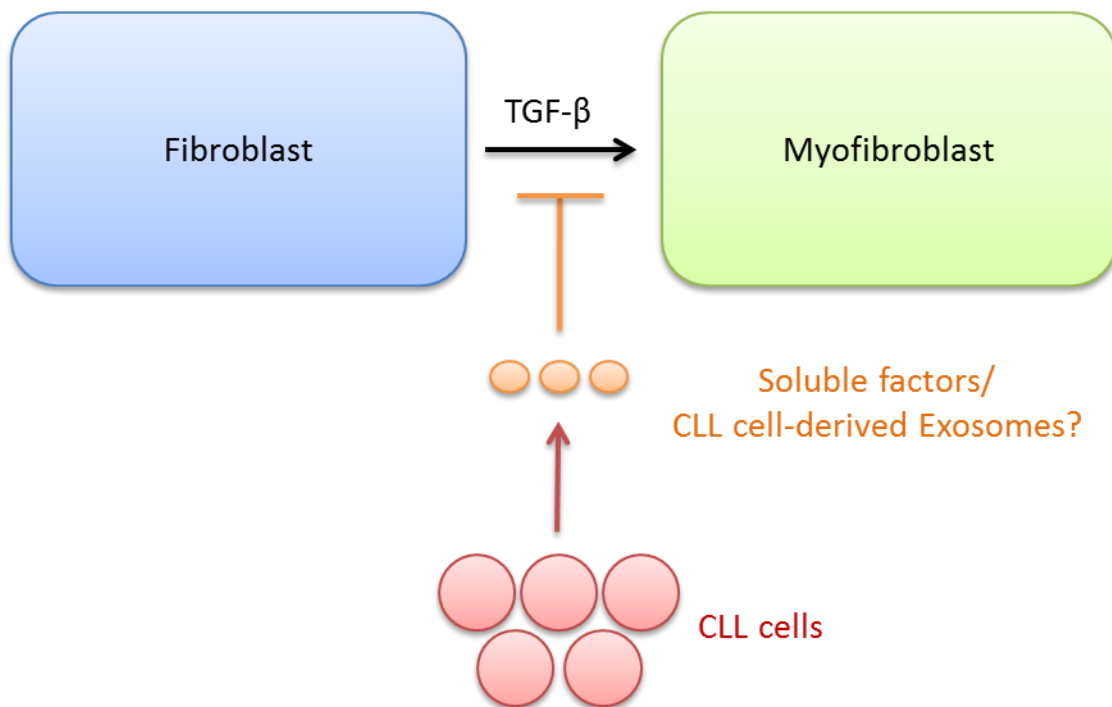


Figure 4.20: Diagram of key findings in Chapter 4.

HFFF2 fibroblasts (blue) can transdifferentiate into myofibroblasts (green), either spontaneously over time, or induced when treated with TGF- β . CLL cells (red) may block both spontaneous and TGF- β induced myofibroblast transdifferentiation, by direct cell-to-cell contact and/or through the release of soluble factor(s). Preliminary data suggest that CLL-derived exosomes (orange) may also be responsible for this.

Chapter 5:

Investigation of the impact
of stromal cells on CLL
viability and adhesion

5.1 Introduction

The main aim of the results described in this chapter was to investigate the effect of fibroblasts and myofibroblasts on CLL cells cultured *in vitro*. Although myofibroblasts differentiate from fibroblasts, these two cell types are phenotypically different. As previously discussed, fibroblasts express low levels of α -SMA and their main function is to produce components of the extracellular matrix, such as collagens and fibronectin, to maintain the microenvironment within which they reside. Myofibroblasts express high levels of α -SMA which is incorporated into stress fibres that are abundantly expressed within myofibroblasts, but not within fibroblasts [155]. Stress fibre formation is vital for myofibroblasts as they confer contractility to the cells allowing myofibroblasts to participate in wound healing. Therefore as fibroblasts and myofibroblasts are two distinct cell types it is possible that they may have different effects on CLL cell cells.

CLL cells readily accumulate within the BM and SLOs. However once they are removed from the body and cultured *in vitro* they rapidly undergo apoptosis. Multiple studies have shown that various non-malignant cell types within the microenvironment can protect CLL cells from apoptosis [127, 128]. However, direct comparison of the effects of fibroblasts and myofibroblasts has not been reported. Therefore, I initially directly compared the effects of fibroblasts and myofibroblasts (HFFF2 cells \pm TGF- β) on CLL cell survival. This was followed by investigating how apoptotic pathways within CLL cells are modulated by fibroblasts. I then compared CLL cell adhesion to fibroblasts and myofibroblasts. Finally I investigated how the expression of Bcl-2 family proteins, specifically the anti-apoptotic protein MCL-1 and the pro-apoptotic protein BIM_{EL}, were modulated by fibroblasts and myofibroblasts within CLL cells.

5.2 Comparing the protective effect of fibroblasts and myofibroblasts on CLL cells

The presence of α -SMA positive cells within the CLL LN stroma (Figures 3.2 and 3.4) indicated the presence of myofibroblasts within the CLL microenvironment. This led me to investigate whether there are any differences in CLL cell survival following co-culture with HFFF2 fibroblasts and HFFF2-

derived myofibroblasts. Apoptosis was initially analysed using annexin V assays after 24, 48 and 72 hours of co-culture. CLL cells were also analysed at the start of the experiment and at the same time-points in the absence of any supporting stromal cells. Annexin V assays were selected as they are a well validated, quantitative assay for analysis of apoptosis [284, 285]

The annexin V assay results were collected by FACS analysis; illustrative primary data is shown in Figure 5.1. Cells from CLL sample U505 that were cultured in the absence of fibroblasts or myofibroblasts at time-points 0 (left panel) and 72 hours (right panel) have been used as an example. The lymphocyte population was gated on their forward scatter (FSC)/side (SSC) scatter (dot plots, top (black line)) and this gate was applied to all samples at all time-points and conditions. After co-culture there may be some contamination of stromal cells within the CLL cell population, however gating the lymphocyte population (FSC/SSC) eliminates analysing HFFF2 cells. Within the figure, the population of cells encircled by the red line represents viable cells, whereas the green line displays the proportion of dead cells (top right graph). At 72 hours there is a clear increase in the amount of dead cells compared to at 0 hours. The gated (FSC/SSC) population was further divided into quadrants (bottom graphs). Viable cells are located in the bottom left quadrant (Annexin V FITC^{-ve}/Propidium iodide (PI)^{-ve}). Cells undergoing apoptosis fall into the bottom right quadrant (Annexin V FITC^{+ve}/PI^{-ve}), and dead cells fall into the top right quadrant (Annexin V FITC^{+ve}/PI^{+ve}).

At the 0 hour time-point there is a greater proportion of viable cells falling into the bottom left quadrant compared to at 72 hours. Conversely, at 72 hours there are a larger proportion of cells falling into the bottom right quadrant compared to at 0 hours. This indicates that, as expected, by 72 hours a greater proportion of CLL cells have undergone spontaneous apoptosis.

An example of the FACS plots comparing CLL cells cultured alone, co-cultured with fibroblasts or co-cultured with myofibroblasts is shown (Figure 5.2). The FACS plots show the two CLL populations consisting of viable cells and cells undergoing apoptosis. At 0 hours the majority of the lymphocyte population are viable (top left). After being cultured alone for 72 hours there is a clear increase in the proportion of cells undergoing apoptosis (top right). When CLL cells are co-cultured with fibroblasts (bottom left) or myofibroblasts (bottom right) there is a reduction in the proportion of cells undergoing apoptosis and

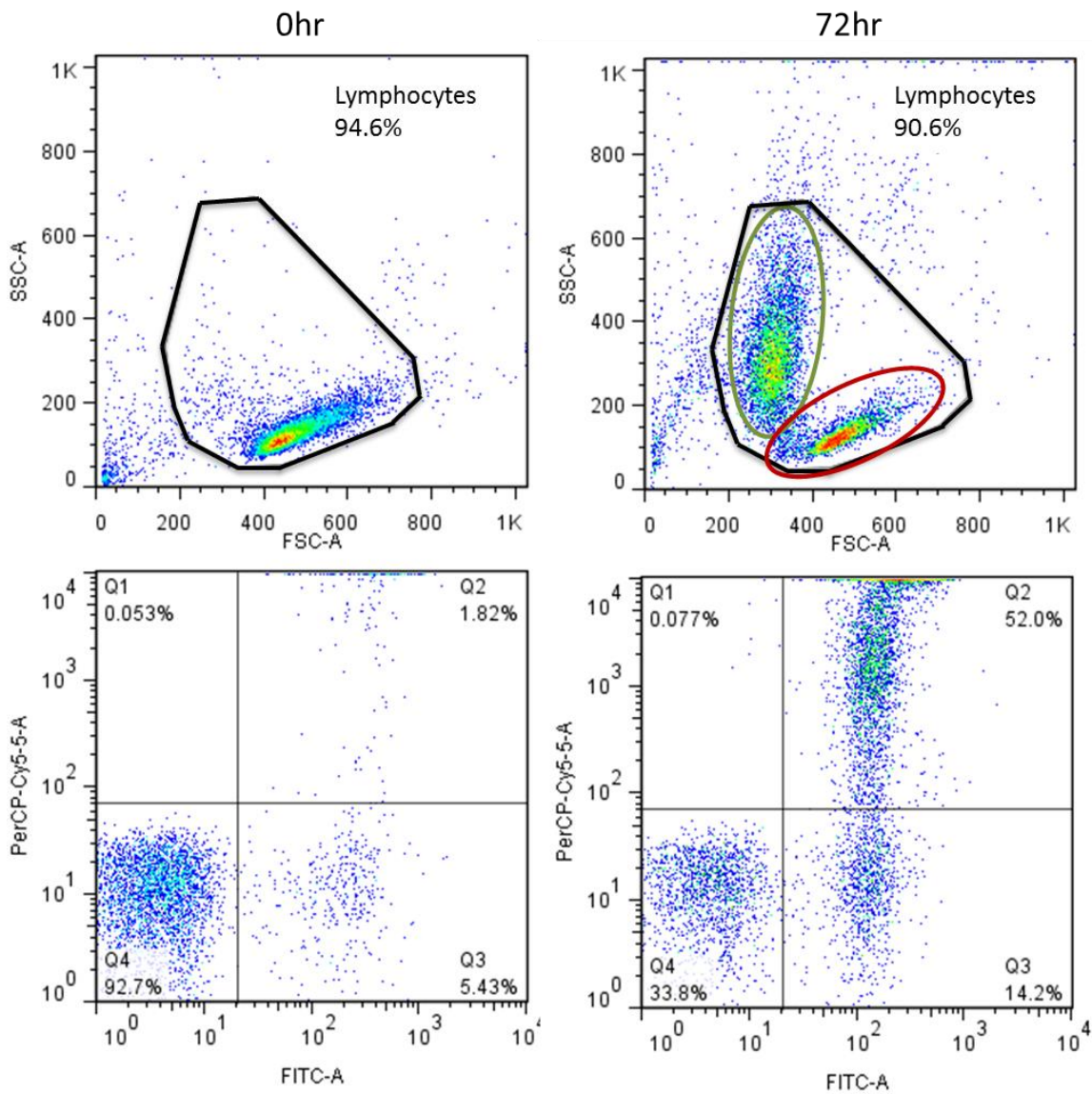


Figure 5.1: Analysis process of annexin V FACS data.

Figure shows primary FACS data of CLL sample U505. CLL sample cultured in complete RPMI-1640 media alone, at either 0 hours or 72 hours only is shown. Lymphocytes were gated (black line) on their forward scatter/side scatter (FSC/SSC) (top). The population of cells encircled by the green line, with increased SSC and reduced FSC, represents cells undergoing apoptosis. The population of cells encircled by the red line, with increased FSC and reduced SSC, represents viable cells (top right). The gated lymphocyte population (both viable and undergoing apoptosis) was then analysed for annexin V/PI staining (bottom). Viable cells fall into the bottom left quadrant. Cells undergoing apoptosis are in the bottom right quadrant. The top right quadrant comprises dead cells.

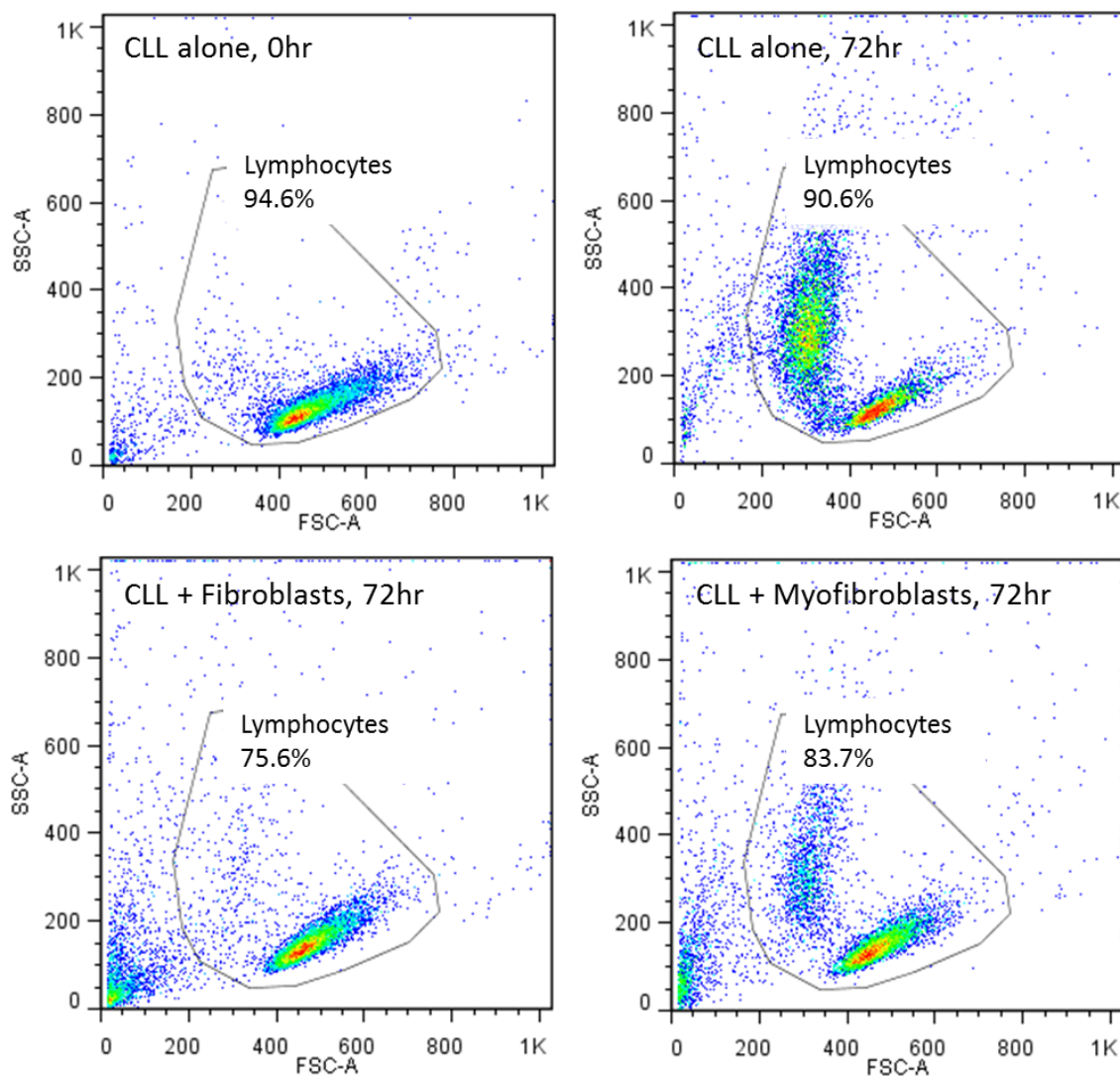


Figure 5.2: FACS plots comparing CLL viability when cultured in the absence or presence of fibroblasts and myofibroblasts.

Figure shows primary FACS data of CLL sample U505. The top left plot shows CLL cells cultured alone at 0 hours. The top right quadrant displays CLL cells cultured alone at 72 hours. The bottom quadrants shows CLL cells co-cultured with fibroblasts (left) or myofibroblasts (right) at 72 hours. Each population has been gated to include the lymphocyte population only (grey line).

Chapter 5

an increase in the proportion of viable cells, compared to CLL cells cultured in the absence of fibroblasts or myofibroblasts at 72 hours. Furthermore, when CLL cells are co-cultured with fibroblasts the proportion of cells undergoing apoptosis is lower compared to when CLL cells are co-cultured with myofibroblasts.

A total of 12 CLL samples were analysed (Figure 5.3, A-L). As CLL samples consist of PBMCs, samples were selected to comprise $\geq 80\%$ CLL cells to minimise analysing viability in contaminating cells. Samples were selected to comprise both M-CLL and U-CLL samples. The majority of samples chosen were surface IgM (sIgM) signallers as determined by intracellular calcium flux; **samples were classified as signallers when $\geq 5\%$ of cells respond to anti-IgM stimulation [261].**

Cell viability for all samples followed a similar trend in response to co-culture with fibroblasts or myofibroblasts (Figures 5.3 (A-F) and 5.4 (G-L)). As expected, CLL sample viability declined over time when cells were cultured alone. However in some samples CLL cell viability decreased but then increased with time (e.g. M494). This is due to the fact that the graphs display the percentage of viable CLL cells, not the exact number. Over the 72 hour period, as CLL cells undergo apoptosis the cells disintegrate and are eventually no longer detected, or are detected as debris; thus increasing the proportion of viable CLL cells.

Viability was consistently higher in CLL samples when cells were co-cultured with fibroblasts (green) or myofibroblasts (red) compared to cells cultured alone. Furthermore CLL viability was consistently higher in cells co-cultured with fibroblasts compared to cells that were co-cultured with myofibroblasts. Although there was an overall increase in CLL viability following co-culture with fibroblasts and myofibroblasts, there was considerable variation in response between individual CLL samples. Additionally there was great variation in CLL samples undergoing spontaneous apoptosis, i.e. a proportion of samples underwent apoptosis rapidly compared to others which were more resilient to this process. This is expected as CLL is a highly heterogeneous disorder. Therefore to avoid massive fluctuations in the data, the difference in cell viability between CLL cells co-cultured with fibroblasts or myofibroblasts, and CLL cells cultured alone was calculated and plotted (Figure 5.5); this shows the amount of protection conferred by fibroblasts and myofibroblasts to the

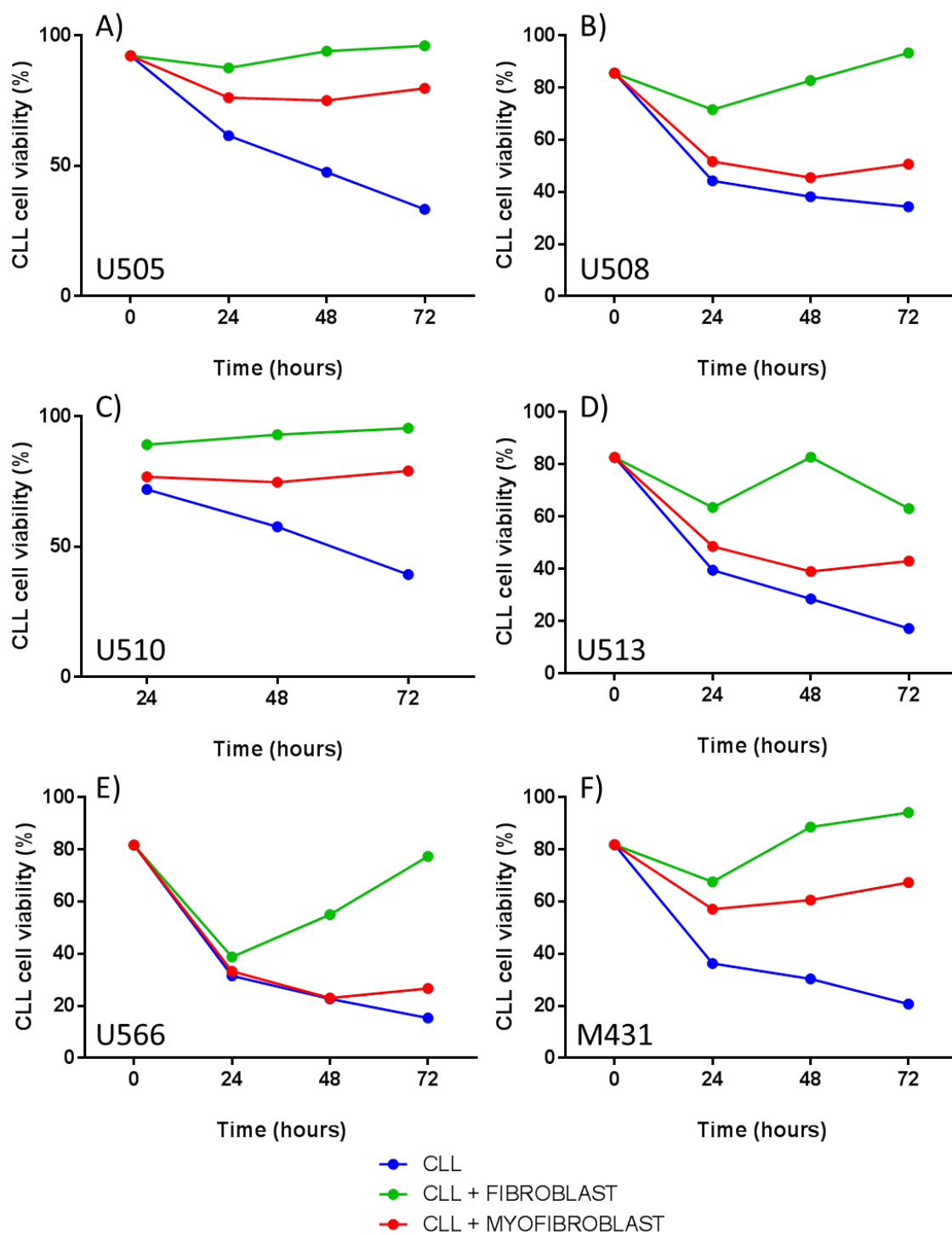


Figure 5.3: Graphs showing annexin V/PI staining data.

The graphs show the percentage of CLL viability for CLL samples cultured in complete RPMI-1640 media either alone as a control (blue), or co-cultured with fibroblasts (green) or myofibroblasts (red) at 24, 48 and 72 hours. CLL cells were also analysed at 0 hours. CLL cells were collected at the indicated time-points and cell viability was analysed by FACS. Each condition was carried out in triplicate. Figure shows 6 of the 12 different CLL samples that were analysed; A-E are U-CLL and F is an M-CLL sample.

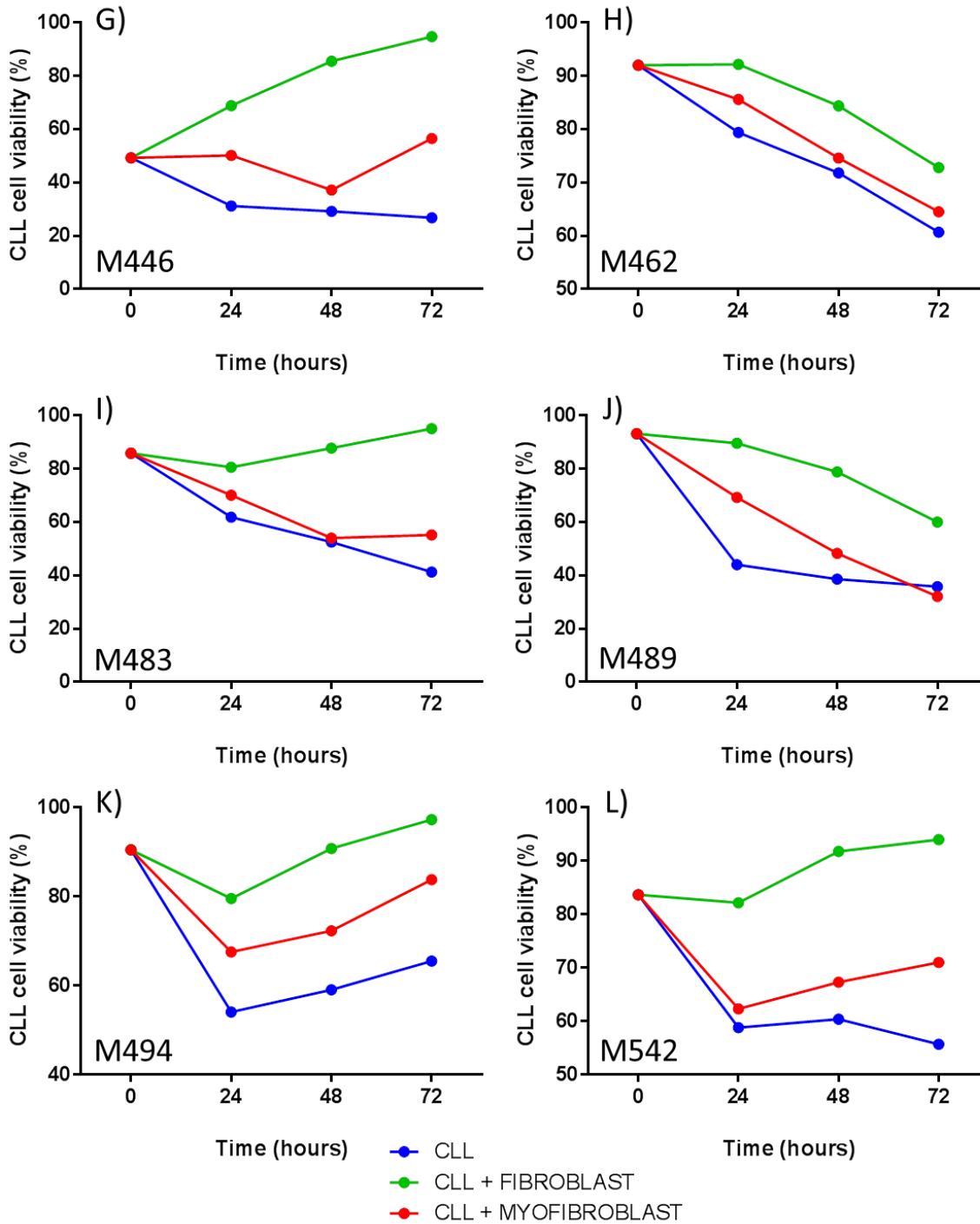


Figure 5.4: Graphs showing annexin V/PI staining data.

The graphs show the percentage of CLL viability for CLL samples cultured in complete RPMI-1640 media either alone as a control (blue), or co-cultured with fibroblasts (green) or myofibroblasts (red) at 24, 48 and 72 hours. CLL cells were also analysed at 0 hours. CLL cells were collected at the indicated time-points and cell viability was analysed by FACS. Each condition was carried out in triplicate. Figure shows 6 of the 12 different CLL samples that were analysed; G-L are an M-CLL samples.

CLL cells.

Overall, there was a statistically significant increase in CLL viability following co-culture with fibroblasts compared to cells cultured alone, at all time-points (Figure 5.5). Although CLL viability was higher at all time-points following co-culture with myofibroblasts, this increase was only statistically significant at 72 hours. Furthermore, CLL viability was significantly higher in cells co-cultured with fibroblasts compared to cells co-cultured with myofibroblasts at all time-points. The statistical analysis performed on the annexin V assay data from all 12 CLL samples is summarised in Table 5.1. Prior to analysis of CLL viability, fibroblasts and myofibroblasts were checked by eye to ensure that the differential protective effects conferred by the stromal cells were independent of confluency.

Following this I analysed the results to determine if *IGHV* mutational status has an impact on the protection inferred by fibroblasts and myofibroblasts (Figure 5.6). Only one sample was a slgM non-signaller therefore statistical analysis could not be performed on this subset.

Five of the samples were U-CLL and seven were M-CLL. Previous data has shown that U-CLL cells are more vulnerable to spontaneous apoptosis than M-CLL cells [286]. A trend towards this was observed within this small cohort and at 72 hours there was significantly more cells undergoing apoptosis within U-CLL samples compared to M-CLL. (Figure 5.6). Additionally there is no clear difference in fibroblast or myofibroblast-mediated protection between U-CLL and M-CLL (Figure 5.7). The protection conferred by myofibroblasts at 72 hours was only statistically significant for U-CLL samples; myofibroblasts did not have a statistically significant protective effect on the M-CLL samples at any of the time-points.

Overall these data show that both HFFF2 fibroblasts and HFFF2-derived myofibroblasts protect CLL cells from apoptosis but fibroblasts have a greater protective effect. Furthermore there was no differential protection between M-CLL and U-CLL samples.

To confirm that the differential protective effects conferred by fibroblasts and myofibroblasts was independent of confluency, confocal microscopy images were taken of both stromal cell types after co-culture with CLL cells for 72 hours. 72 hours was selected as this was the longest co-culture period used in

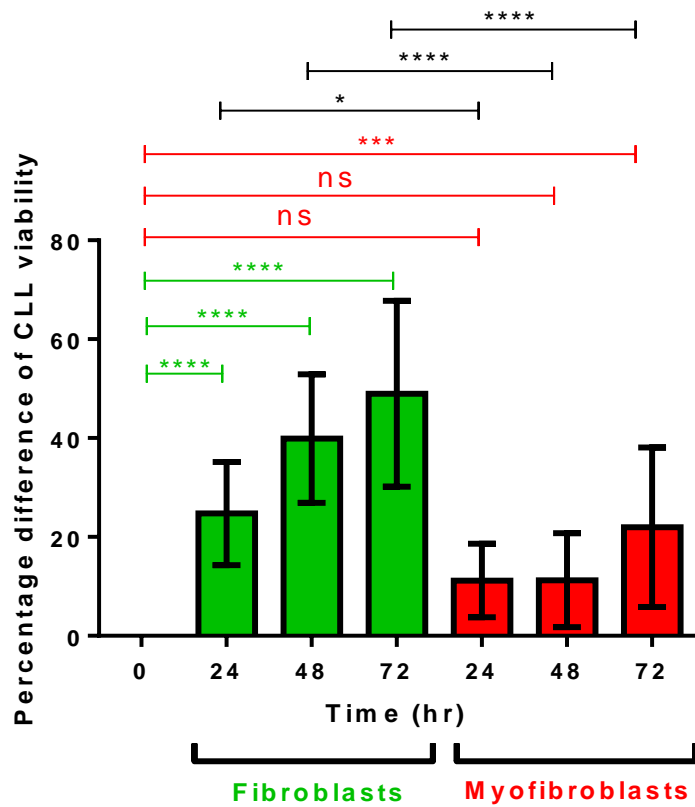


Figure 5.5: Graph summarising the effect of fibroblasts and myofibroblasts on CLL cell viability.

Graph shows the percentage increase in CLL viability of CLL samples cultured in complete RPMI-1640 media either alone or co-cultured with fibroblasts (green) or myofibroblasts (red). After 24, 48 and 72 hours CLL cells were collected and cell viability was analysed by FACS. Graph shows mean (\pm SD) for all 12 samples. The statistical significance of the differences was analysed using one-way ANOVA with Bonferroni correction set at a significance level of 0.05 (n=12).

CLL alone	CLL + Fibroblasts	CLL + Myofibroblasts	P value (significance level 0.05)
24hr	24hr	-	****
48hr	48hr	-	****
72hr	72hr	-	****
24hr	-	24hr	ns
48hr	-	48hr	ns
72hr	-	72hr	***
-	24hr	24hr	*
-	48hr	48hr	****
-	72hr	72hr	****

Table 5.1: Summary of statistical analysis performed on annexin V assay data.

CLL samples were cultured in complete RPMI-1640 media either alone or in the presence of fibroblasts or myofibroblasts. After 24, 48 and 72 hours CLL samples were collected and viability was analysed by FACS. CLL viability was compared between CLL samples cultured alone and cells co-cultured with fibroblasts at all time-points (top 3 rows). CLL viability was compared between CLL samples cultured alone and those co-cultured with myofibroblasts (middle 3 rows). CLL viability was compared between CLL samples co-cultured with fibroblasts and cells co-cultured with myofibroblasts (bottom 3 rows). The statistical significance of the differences was analysed using one-way ANOVA with Bonferroni correction (n=12).

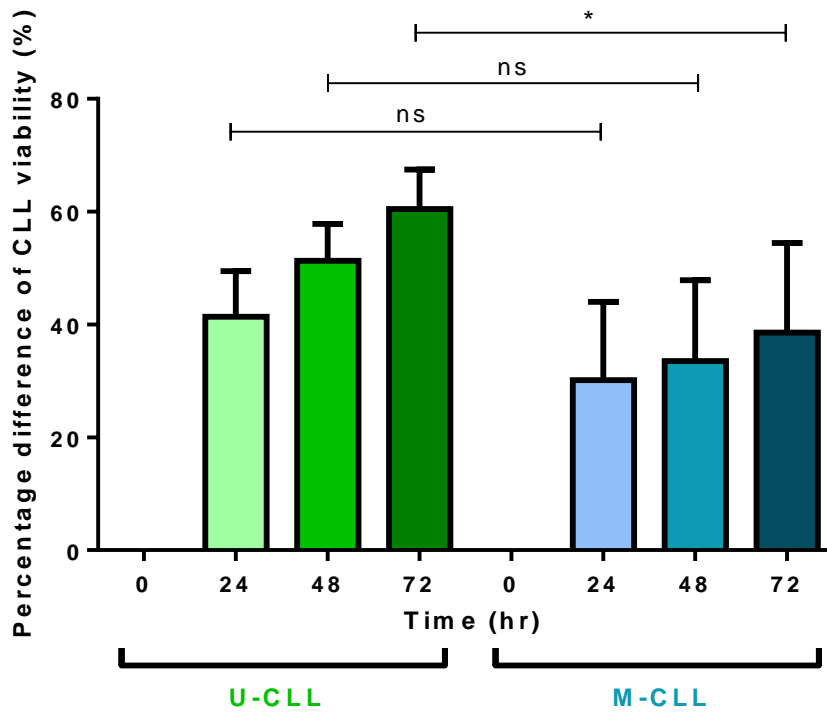


Figure 5.6: Comparison of spontaneous apoptosis in U-CLL and M-CLL samples.

Graph shows the percentage difference of CLL viability between CLL cells cultured alone at 0 hours and the indicated time-points. U-CLL samples are shown in green and M-CLL samples are shown in blue. The statistical significance of the differences was analysed using Mann-Whitney test.

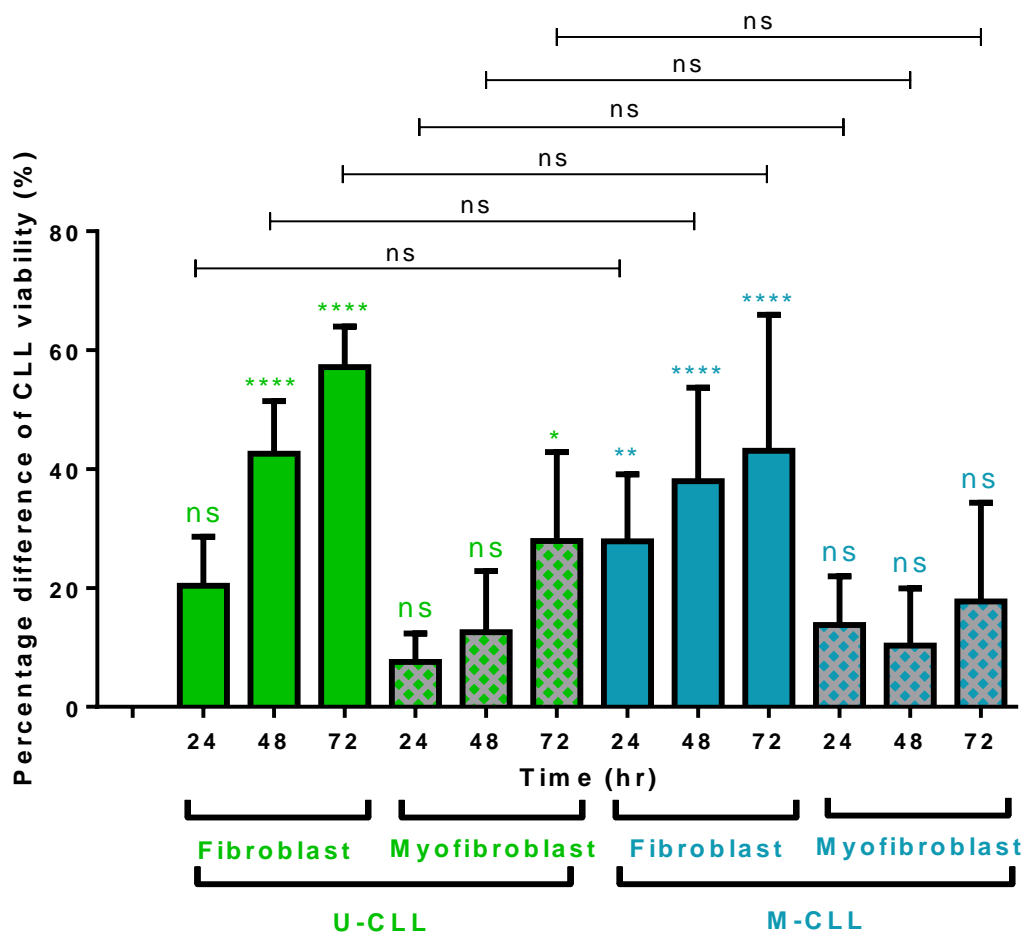


Figure 5.7: Comparison of the protective effect of stromal cells on U-CLL and M-CLL samples.

Graph shows the percentage difference in CLL cell viability between CLL cells cultured in complete RPMI-1640 media, either alone and CLL cells co-cultured with fibroblasts or myofibroblasts. After 24, 48 and 72 hours CLL cells were collected and cell viability was analysed by FACS. 12 different CLL samples were analysed; samples were divided based on *IGHV* mutational status; 5 were U-CLL (green) and 7 were M-CLL (blue). Graph shows mean (\pm SD) for all samples. The statistical significance of the differences between CLL cells cultured alone and cells co-cultured with stromal cells was analysed using one-way ANOVA with Bonferoni correction. The statistical significance of the differences between *IGHV* subsets was analysed using Mann Whitney test.

Chapter 5

the annexin V assays and it was speculated that any differences in confluency would be detected by this time-point.

The morphology between the two cell types differs (Figure 5.8). Fibroblasts appear thin and spindle shaped whereas the myofibroblasts are wider and less spindle shaped. Overall the confluency between the two stromal cell types was comparable and therefore this should not create any bias on the protection passed on to the CLL cells.

Similarly, the rate of apoptosis between fibroblasts and myofibroblasts appear to be comparable, as there was no clear difference in stromal cell viability, of either cell type, as determined by eye. Additionally, HFFF2-derived myofibroblasts were thoroughly washed with PBS, post-treatment with TGF- β ; therefore it is unlikely that this cytokine impacted cell viability. However, to confirm that the rate of apoptosis between both stromal cell types was similar, immunoblot analysis of PARP cleavage and caspase expression could be conducted.

5.3 Investigating the effect of fibroblasts on caspase activity

Following the annexin V assays I investigated the effects of HFFF2 fibroblasts on caspases within CLL cells. Only fibroblasts were investigated in these experiments as they had a greater protective effect on CLL cells than myofibroblasts. One potential difficulty in co-culture experiments is potential **contamination of CLL cells by detached/dying HFFF2 cells; “dilution” of CLL-derived cells** by contaminating non-CLL cells could reduce expression of apoptotic markers, thereby artefactually appearing as increased viability in co-cultures. To avoid this possibility, experiments to probe effects of HFFF2 fibroblasts on CLL cells were performed using HFFF2 cell-derived CM; parallel studies by Elizabeth Lemm (University of Southampton; Appendix A.2) confirmed that HFFF2 fibroblast cell-derived CM suppressed CLL cell apoptosis similar to direct co-culture.

CLL samples were cultured in CM derived from HFFF2 fibroblasts cultured in complete RPMI-1640 media for 72 hours. Un-cleaved (intact) caspase 3 and cleavage of the caspase 3 substrate PARP were analysed by immunoblotting after 8 or 24 hours. The 24 hour time point was selected to match the annexin

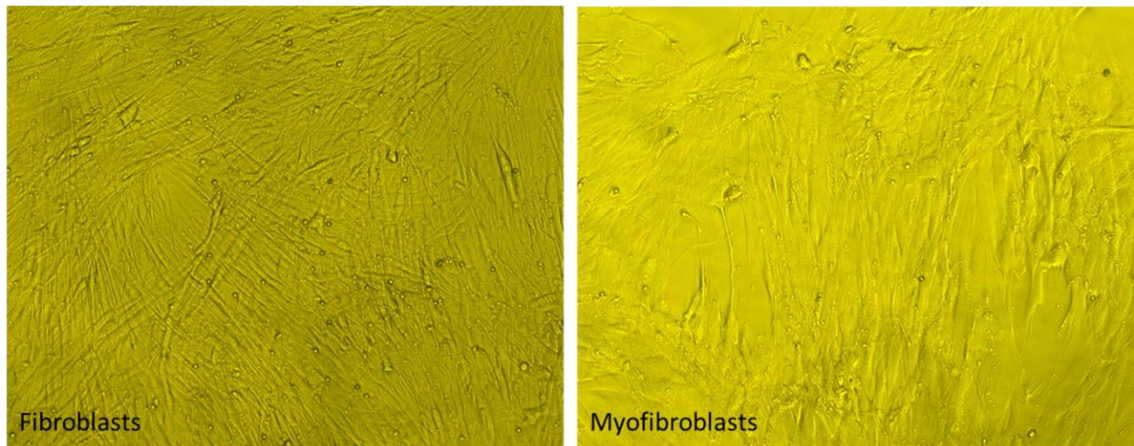


Figure 5.8: Comparison of fibroblast and myofibroblast confluency. HFFF2 Fibroblasts (left) and HFFF2-derived myofibroblasts (right) were co-cultured with CLL cells in complete RPMI-1640 media for 72 hours after which CLL cells were removed and confocal microscopy was utilised to acquire the above images. Original magnification was x10.

Chapter 5

V studies. However, since caspase activation precedes phosphatidylserine (PS) exposure, analysis was also performed at 8 hours. CLL samples were cultured in complete RPMI-1640 media as a control. I also analysed other caspases, including caspases 8 and 9. However, consistent data was obtained for un-cleaved caspase 3 and PARP only and other results are not shown.

A total of six different samples were analysed for caspase 3 expression and four were analysed for PARP cleavage. Samples were selected to comprise **≥80% CLL cells to minimise effects of contaminating non-malignant cells**. As this was not a large cohort samples were not selected based on *IGHV* status or sIgM signalling capacity. Overall, CLL cells cultured in HFFF2-derived CM expressed higher levels of un-cleaved caspase 3 at both time-points, but this was only statistically significant at 24 hours (Figures 5.9 and 5.10). Furthermore there was a clear reduction in PARP cleavage in CLL cells cultured in CM compared to control cells; however this reduction was not statistically significant at either time-point for this cohort (Figures 5.9 and 5.11).

The results suggest that HFFF2 fibroblasts release soluble factor(s) that prevent caspase 3, and possibly PARP, from being cleaved and therefore protect CLL cells from apoptosis.

5.4 Comparing CLL cell adhesion to fibroblasts and myofibroblasts

As fibroblasts and myofibroblasts are two distinct cell types that have differential effects on CLL cell viability I performed adhesion assays to investigate the extent of CLL cell binding to both cell types. CLL cells were co-cultured with either HFFF2 fibroblasts or HFFF2-derived myofibroblasts for 24 hours in serum-free RPMI-1640 media.

Cells were cultured in RPMI-1640 media lacking FCS to avoid serum factors affecting CLL cell adhesion. RPMI-1640 media was chosen over DMEM media as HFFF2 cells are far more resilient than CLL cells which readily undergo apoptosis. As both cell types have to be cultured in serum-free media for 24 hours it was decided to optimise conditions to suit CLL cells in an attempt to reduce CLL cell death over the course of the co-culture period. Furthermore, 24 hours was selected as it is long enough to allow sufficient time for CLL

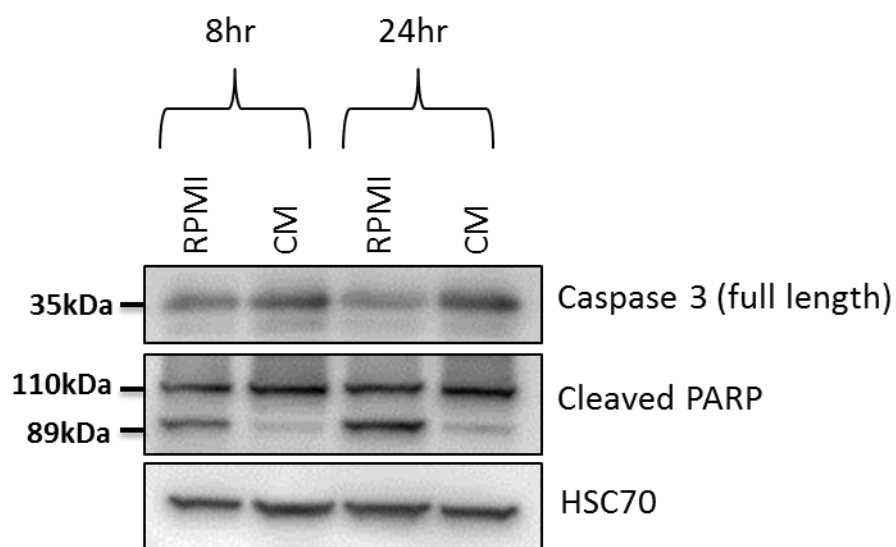


Figure 5.9: Effect of fibroblast CM on caspase 3 and PARP cleavage in CLL cells.

CLL samples were either cultured in complete RPMI-1640 media as a control, or cultured in fibroblast-derived CM, for 8 or 24 hours. CM was generated from HFFF2 fibroblasts cultured in complete RPMI-1640 media for 72 hours. CLL cells were then collected and analysed for protein expression by immunoblotting. HSC70 was used as the loading control. Western blot is representative of 6 different samples for caspase 3, and 4 different samples for PARP.

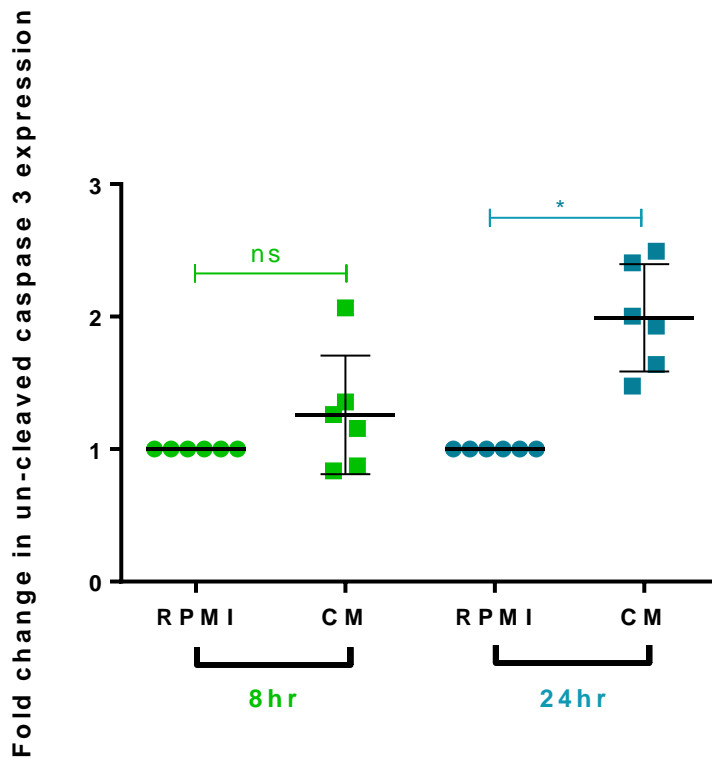


Figure 5.10: Effect of HFFF2 fibroblast-derived CM on un-cleaved caspase 3 expression.

Graph shows the fold change of un-cleaved caspase 3 expression in CLL cells when cultured in HFFF2 fibroblast-derived conditioned media for 8 hours (green) and 24 hours (blue). CM was generated from HFFF2 cells cultured in complete RPMI-1640 media for 72 hours. CLL cells were also cultured in complete RPMI-1640 media as a control. Expression of caspase 3 in CLL cells cultured in complete RPMI-1640 media has been set to 1.0. Each dot represents results for an individual CLL sample with mean (\pm SD). The statistical significance of the differences was analysed using Wilcoxon's matched-pairs signed-rank test (n=6).

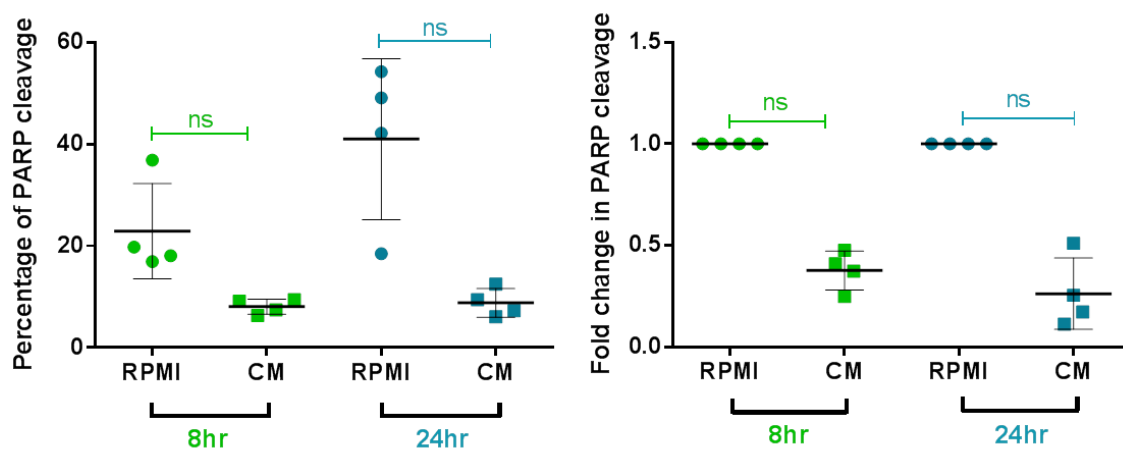


Figure 5.11: Effect of HFFF2 fibroblast-derived CM on PARP cleavage in CLL cells.

CLL cells were either cultured in complete RPMI-1640 media as a control, or cultured in fibroblast-derived CM for 8 hours (green) or 24 hours (blue). CM was generated from HFFF2 cells cultured in complete RPMI-1640 media for 72 hours. Cells were collected and analysed for protein expression by immunoblotting. The percentage of PARP cleavage is shown on the left. The fold change in PARP cleavage is shown on the right; Expression in CLL cells cultured in complete RPMI-1640 media has been set to 1.0. Each dot represents results from one individual sample with mean (\pm SD). The statistical significance of the differences was analysed using Wilcoxon's matched-pairs signed-rank test was used ($n=4$).

Chapter 5

samples to adhere to the stroma, yet short enough to avoid substantial CLL cell death.

CLL cells were pre-incubated with the fluorescent cell staining dye, CellTrace™ CFSE (Carboxyfluorescein succinimidyl ester), to allow easy detection of the malignant cells once bound to the stromal cells. CLL cells were then co-cultured with fibroblasts or myofibroblasts; each condition was set up in triplicate. After the 24 hour co-culture period unbound CLL cells were removed; all wells were washed once with PBS to remove unbound CLL cells and immunofluorescence images were taken of the remaining CLL cells and analysed using the automated cell counting tool on Image J. To use the automated cell counting tool however the image was first converted to a binary image (black and white) (Figure 5.12).

For each of the triplicate wells, fluorescent microscopy images were taken from 5 different areas of the well (Figure 5.13). The mean number of bound cells per triplicate well was calculated and plotted as an example in Figure 5.14. Generally there was little variation between the triplicate wells per condition. For each condition the mean of the triplicate values was calculated and represents the overall number of bound cells per condition (Figure 5.15).

A total of 7 different CLL samples were analysed; all comprised $\geq 80\%$ but were not selected based on *IGHV* status or sIgM signalling capacity. Overall, after 24 hours of co-culture a significantly higher number of CLL cells adhered to myofibroblasts than to fibroblasts (Figure 5.15).

Following this, I analysed CLL cell adhesion to fibroblasts and myofibroblasts at earlier time-points to gain a better understanding of CLL cell binding kinetics (Figure 5.16). The same method described above was used except for this assay CLL cells were removed after 1, 3 or 6 hours of co-culture.

A total of 6 different CLL samples were utilised, all comprise $\geq 80\%$ CLL cells. CLL adhesion varied greatly between individual samples. CLL sample adhesion to fibroblasts and myofibroblasts was comparable at 1, 3 and 6 hours. However there does appear to be a modest trend which favours adhesion to fibroblasts, although this was not statistically significant at any of the indicated time-points.

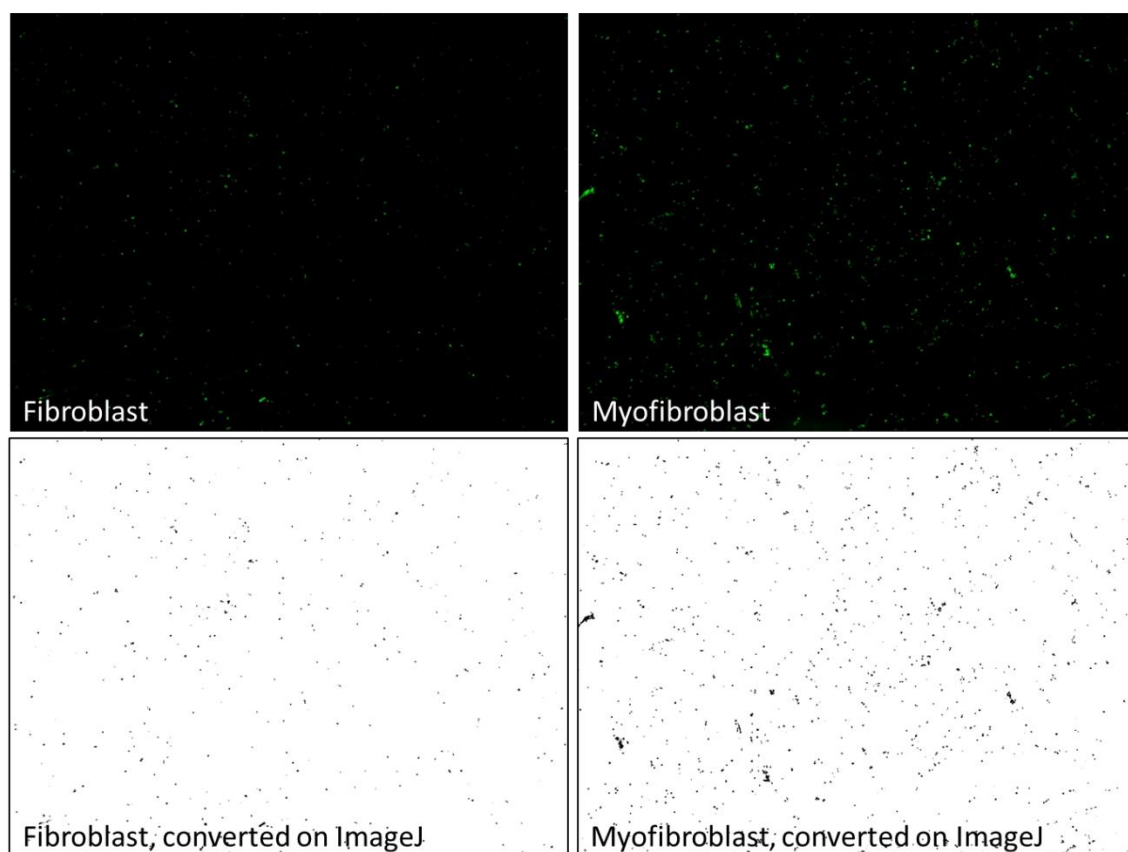


Figure 5.12: Converting fluorescent microscopy images into binary images.

CLL cells were pre-treated with $15\mu\text{M}$ CFSE in complete RPMI-1640 media for 15 minutes prior to co-culture with fibroblasts (left) or myofibroblasts (right) for 24 hours. Unbound CLL cells were then removed and immunofluorescent images were taken of the remaining bound CLL cells (top panel); green dots represent CLL cells. Image J was utilised to convert immunofluorescent images into binary form (bottom panel); each black dot represents a cell from the CLL sample and was counted by the Image J automated counting tool.

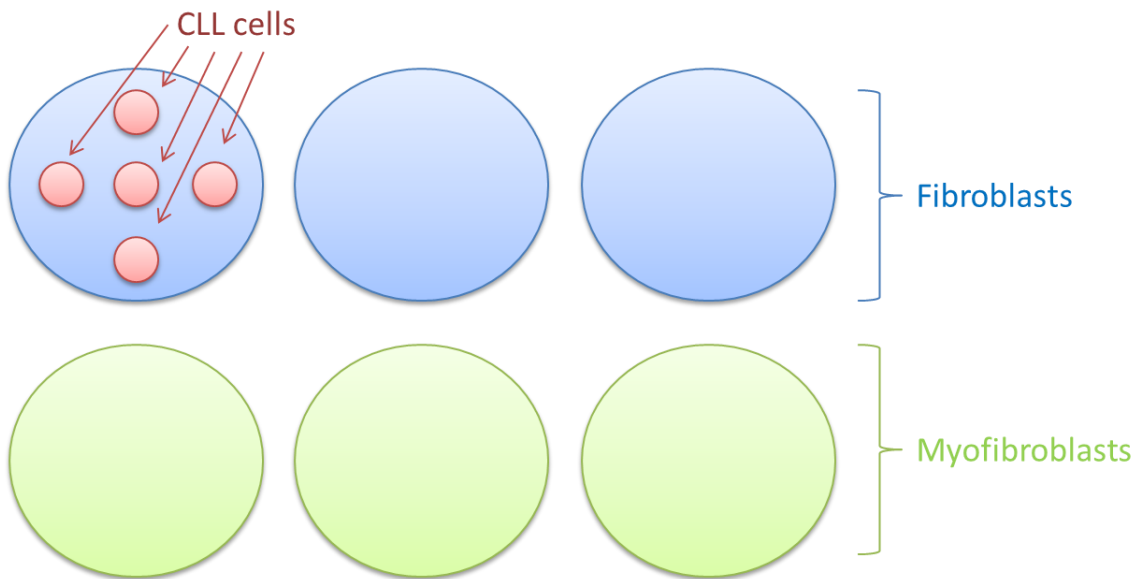


Figure 5.13: Method by which bound CLL cells were counted.

Diagram shows how bound CLL cells were counted. Each condition was set up in triplicate. CLL samples were pre-treated with 15 μ M CFSE in complete RPMI-1640 media for 15 minutes. CLL samples were then co-cultured with fibroblasts (blue) or myofibroblasts (green) for 24 hours after which unbound CLL cells were removed. The number of remaining bound CLL cells were counted by capturing fluorescent microscopy images from 5 different areas (red circles) within each of the triplicate wells. The images were converted to binary form and cells were counted using Image J. The mean was calculated for the number of bound CLL cells captured in the 5 images; this represents the number of bound CLL cells in that one well.

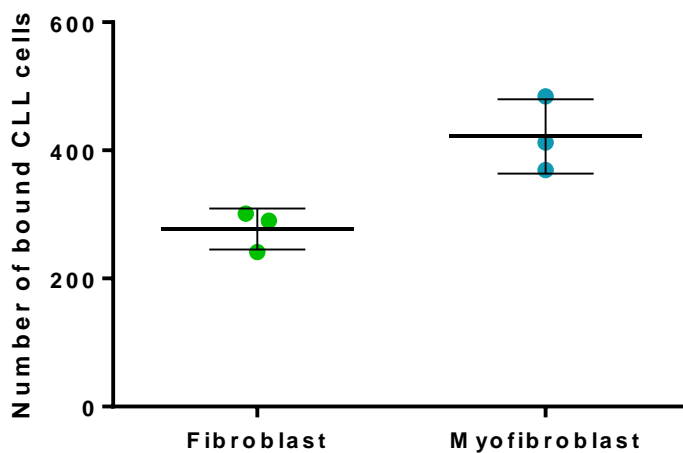


Figure 5.14: Variation of bound CLL cells per condition.

CLL sample M483 was used for this example. Graph shows the mean number of CLL cells bound to fibroblasts (green) or myofibroblasts (blue) after 24 hours of co-culture. Experimental details given in figure 5.13. Each condition was set up in triplicate. Fluorescent microscopy images were taken from 5 different areas within each triplicate well. All three dots represent one sample, and each dot represents the mean number of bound CLL cells per triplicate well. Graph shows the mean (\pm SD) for the triplicate values of one sample.

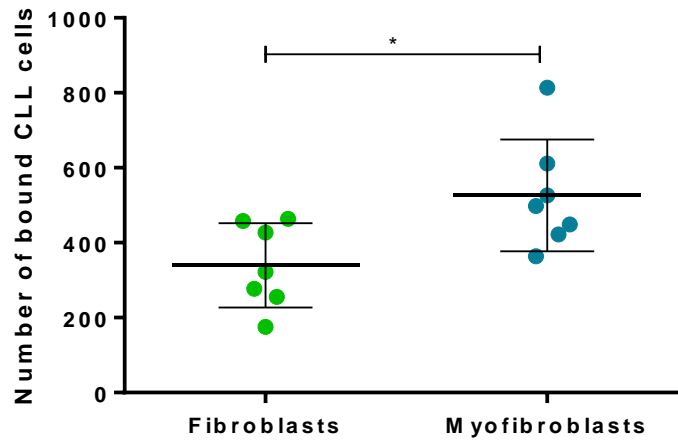


Figure 5.15: Summary graph of CLL cell adhesion to fibroblasts and myofibroblasts.

Graph shows the mean number of CLL cells bound to fibroblasts or myofibroblasts within the magnification field within which they were counted. CLL cells were pre-incubated with 15 μ M CFSE in complete RPMI-1640 media for 15 minutes. CLL cells were then co-cultured with fibroblasts or myofibroblasts in serum-free RPMI media for 24 hours after which unbound CLL cells were removed. Fluorescent microscopy images were taken of bound CLL cells which were counted using the automated counting tool on Image J. Each dot represents the results from an individual CLL sample with mean (\pm SD). The statistical significance of the difference was analysed using Wilcoxon's matched-pairs signed rank test ($n=7$).

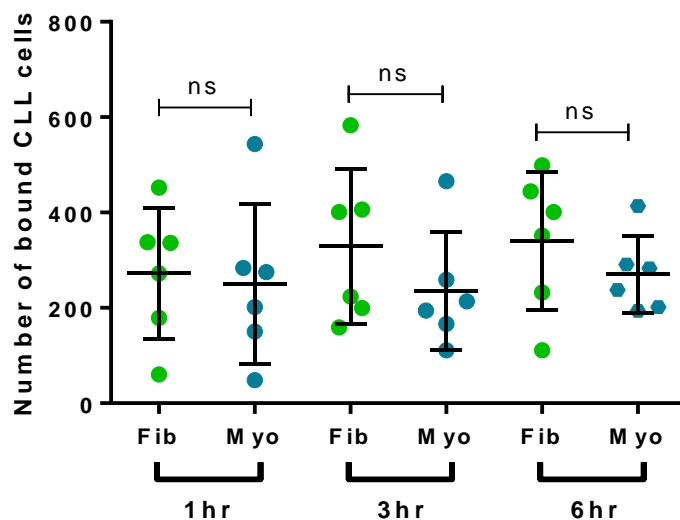


Figure 5.16: CLL sample adhesion to fibroblasts and myofibroblasts at earlier time points.

The graph shows the number of bound CLL cells to fibroblasts (green) or myofibroblasts (blue). CLL samples were pre-incubated with 15 μ M CFSE in complete RPMI-1640 media for 15 minutes. CLL samples were then co-cultured with fibroblasts or myofibroblasts in serum-free RPMI-1640 media for 1, 3 and 6 hours after which the unbound CLL cells were removed. Bound CLL cells were counted using the automated counting tool on image J. Each dot represents the results from an individual CLL sample with mean (\pm SD). The statistical significance of the differences was analysed using Wilcoxon's matched-pairs signed rank test (n=6).

5.5 Effect of HFFF2 fibroblasts on reactive oxygen species (ROS) signalling in CLL cells

One possibility was that HFFF2 cells reduced CLL apoptosis by countering accumulation of ROS. CLL cells contain higher levels of intracellular reactive oxygen species (ROS) compared to normal lymphocytes; this has a negative impact on their survival [287]. ROS comprise various reactive molecules and free radicals which are generated by reducing molecular oxygen to varying degrees. The antioxidant defence system in CLL cells is compromised as the

activity of major antioxidants such as superoxide dismutase (SOD) and catalase are reduced in CLL cells [288]. Additionally the antioxidant glutathione (GSH) protects CLL cells from intrinsic ROS stress; however levels of GSH cannot be maintained in CLL cells once removed from the stroma [289]. Furthermore, previous data has demonstrated that BM stromal cells can promote GSH synthesis within the malignant cells resulting in CLL cell survival and drug resistance [287]. Therefore high intrinsic levels of ROS could be one potential explanation for spontaneous apoptosis in CLL cells *in vitro*. The annexin V data showed that fibroblasts and myofibroblasts protect CLL cells from spontaneous apoptosis (Figure 5.4), it was therefore speculated that a possible mechanism by which these cells protect CLL cells is by reducing their intrinsic levels of ROS. Therefore I investigated whether HFFF2 fibroblasts can reduce levels intracellular ROS within CLL cells.

CLL samples were either cultured alone as a control, or co-cultured with HFFF2 fibroblasts in complete RPMI-1640 media for 24 and 48 hours. At each time-point the CLL samples were collected and treated with the fluorescent probe CM-H₂DCFDA for 1 hour after which their intrinsic ROS levels were analysed by FACS. CLL samples were also analysed at 0 hours. 24 and 48 hours were chosen as fibroblasts had a significant protective effect on CLL cells at these time-points (Figure 5.4). Only fibroblasts were analysed initially as they had a significantly better protective effect on CLL samples than myofibroblasts (Figure 5.4), so it was speculated they would therefore have a greater effect on intrinsic levels of ROS within CLL samples also.

Illustrative primary FACS data and how it was analysed is shown in Figure 5.17. CLL sample M561 at 0 hours is shown. The lymphocyte population is shown in

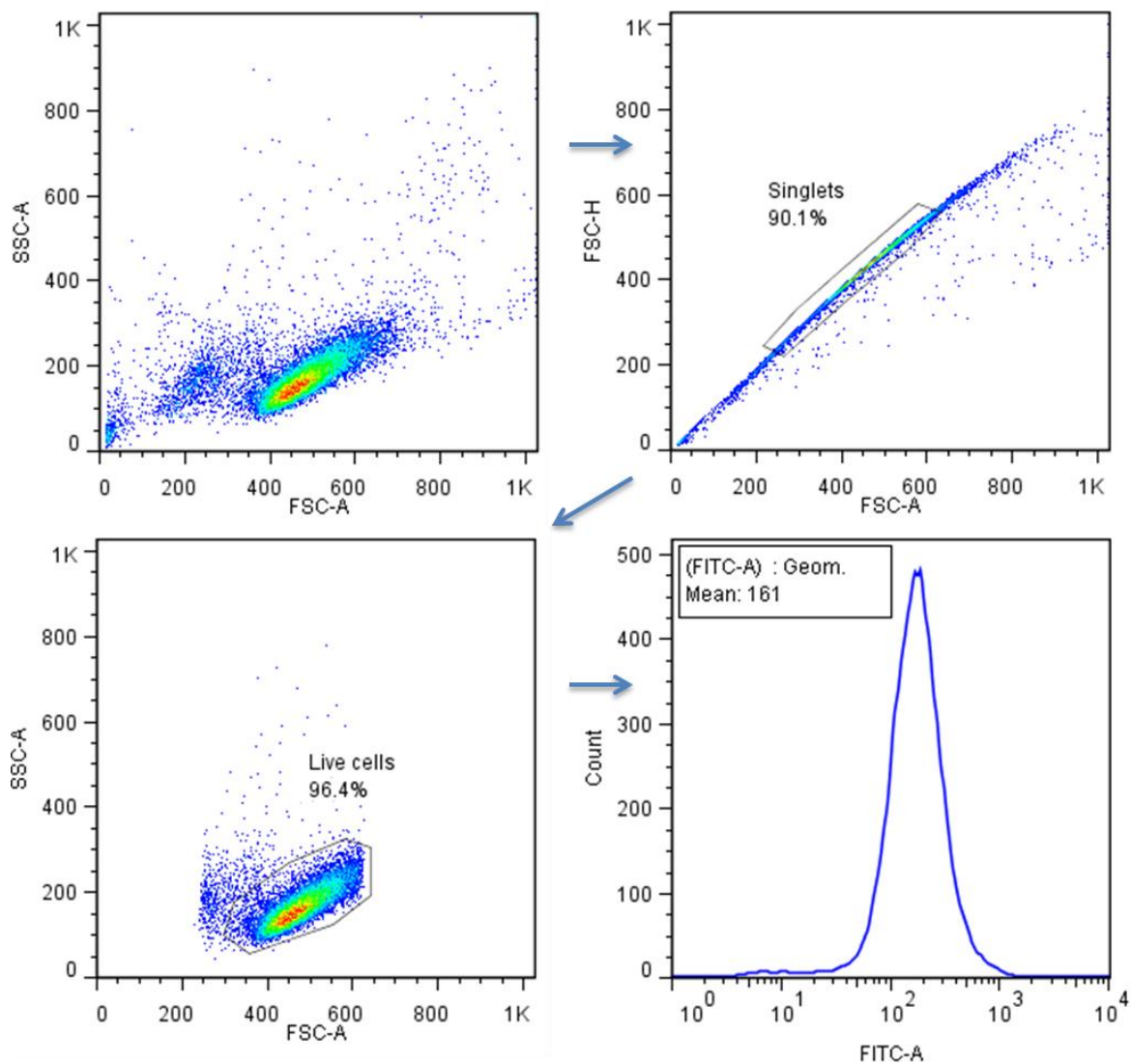


Figure 5.17: Analysis process of ROS data.

Example shows primary FACS data of CLL sample M561 at 0 hours treated with $1\mu\text{M}$ CM- H_2DCFDA for 1 hour in the dark. The lymphocyte population is displayed in the top left box. This population was gated to include singlets only (top right box). The singlet population was further gated to include viable cells only based on increased FSC and reduced SSC (bottom left box). This population was displayed as a histogram; the geometric mean is also shown which correlates with the amount of intrinsic ROS being detected (bottom right).

the top left box. Cells were initially gated to include singlets only to eliminate analysing clumps of cells which would skew the cell signal (top right box). The singlet population was further gated to contain viable cells only based on FSC and SSC (bottom left box). The data has been displayed as a histogram with the geometric mean included (bottom right box). The geometric mean correlates with the amount of intrinsic ROS being detected.

CLL cells at 0 hours which were either not incubated with CM-H₂DCFDA (red) or incubated with CM-H₂DCFDA (blue) are shown in Figure 5.18. The peak representing CM-H₂DCFDA-labelled cells is shifted to the right and has a higher geometric mean compared to un-labelled cells. This shows that higher levels of intrinsic ROS are detected in the cells which were incubated with the probe compared to cells which were not, confirming assay activity. This control was used in all experiments, at all time-points (not shown).

A total of four separate CLL samples were utilised, all were selected to **comprise ≥80% CLL cells and were previously shown to be protected by HFFF2 fibroblasts** in the annexin V assays. There was a clear shift in the histogram peak between CLL cells at 0 hours and CLL cells co-cultured with stromal cells (Figure 5.19). However there was no clear shift between the histogram peaks representing CLL cells cultured alone or co-cultured with fibroblasts at 24 and 48 hours. Additionally, for all assays there was a clear shift between peaks representing CM-H₂DCFDA **labelled and un-labelled** CLL samples as expected, indicating consistent assay function.

Yet, closer analysis indicates there is a trend favouring higher levels of intrinsic ROS within CLL cells co-cultured with fibroblasts compared with control cells; however this was not statistically significant at either time-point (Figure 5.20).

Overall these results suggest that HFFF2 fibroblasts have no effect on intracellular levels of ROS within CLL cells; therefore fibroblasts do not protect the malignant cells through modulation of intrinsic ROS.

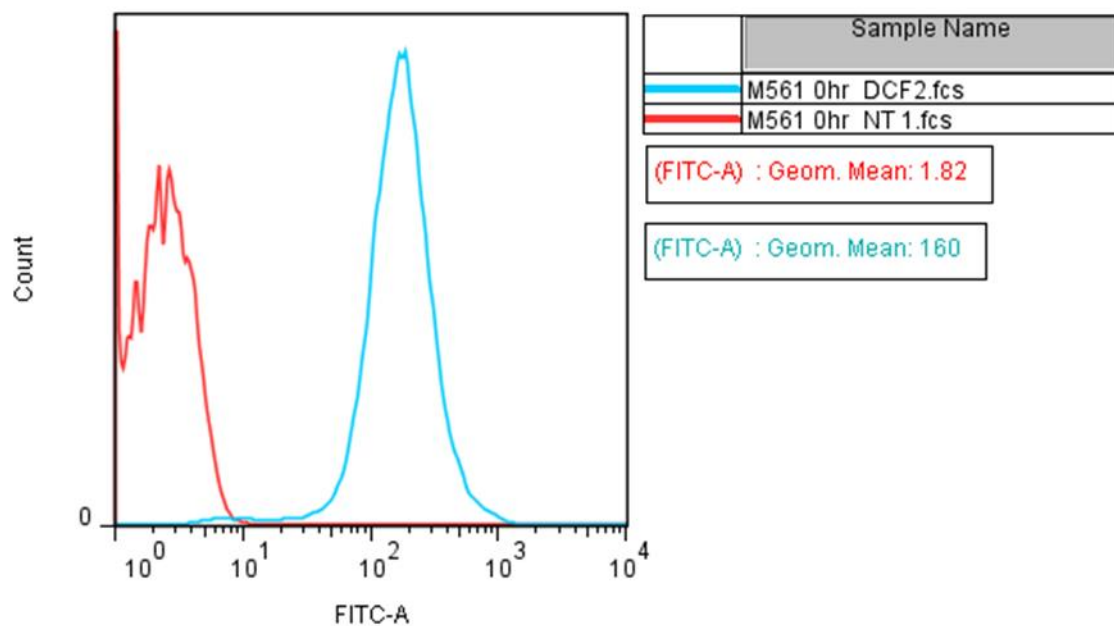


Figure 5.18: Comparison of CM-H₂DCFDA labelled and un-labelled samples.

Example shows CLL sample M561 at 0 hours. Histogram shows primary FACS data of CLL cells that were labelled with 1 μ M CM-H₂DCFDA for 1 hour in the dark (blue). CLL cells were also not labelled with CM-H₂DCFDA (red) as a negative control for ROS detection. The geometric mean which correlates with the amount of intrinsic ROS being detected is shown.

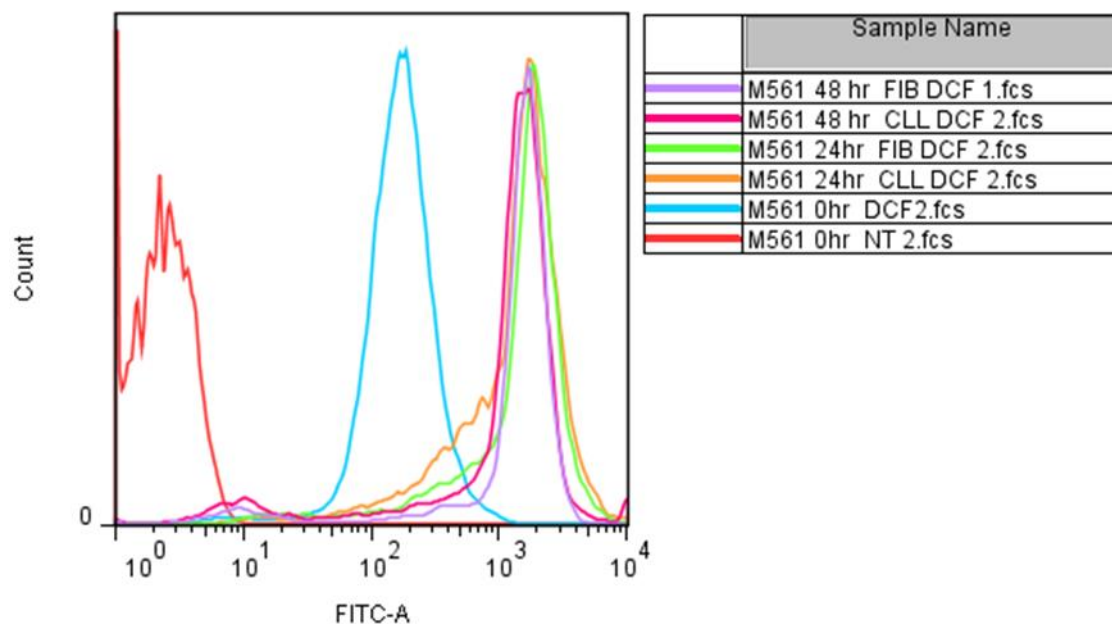


Figure 5.19: Intracellular ROS levels in CLL cells cultured alone and co-cultured with fibroblasts.

CLL samples were either cultured alone as a control, or in the presence of fibroblasts in complete RPMI-1640 media. After 24 or 48 hours CLL cells were collected and labelled with $1\mu\text{M}$ CM-H₂DCFDA for 1 hour in the dark prior to analysis of intrinsic ROS levels by FACS. CLL samples were also analysed at 0 hours; a portion of these cells were not labelled with CM-H₂DCFDA as a **negative control for intrinsic ROS detection (red)**. CLL cells at 0 hours which were treated with CM-H₂DCFDA are **shown in blue**. CLL cells cultured alone or co-cultured with fibroblasts for 24 hours are shown in orange and green respectively. CLL cells cultured alone or co-cultured with fibroblasts for 48 hours are shown in pink and lilac respectively. All cells at 24 and 48 hours were treated with CM-H₂DCFDA prior to FACS analysis.

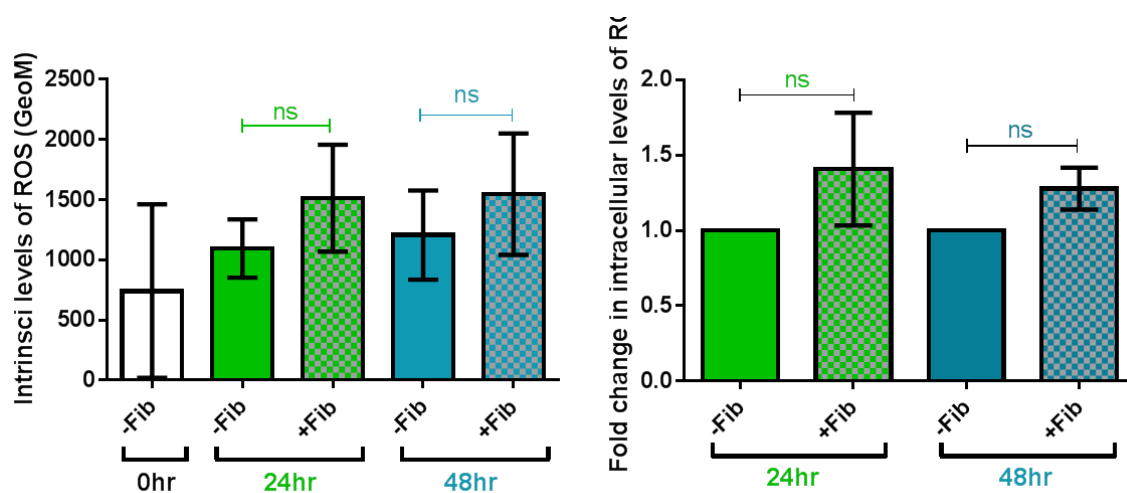


Figure 5.20: Comparison of intrinsic ROS levels in CLL samples cultured alone or co-cultured with fibroblasts.

CLL samples were either cultured alone as a control or co-cultured with HFFF2 fibroblasts in complete RPMI-1640 media. After 24 (green) or 48 hours (blue) CLL samples were collected and labelled with $1\mu\text{M}$ CM- H_2DCFDA for 1 hour in the dark prior to analysis of intrinsic levels of ROS by FACS. CLL cells were also analysed at 0 hours; a portion of these cells were CM- H_2DCFDA un-labelled as a negative control for intrinsic ROS detection (not shown). Geometric mean has been plotted with mean (\pm SD) for all 4 samples (left). The fold change in ROS levels is shown (right); expression of ROS levels in CLL cells cultured alone has been set to 1.0. Graph shows the mean (\pm SD) for all 4 samples analysed. The statistical significance of the differences was analysed using Wilcoxon's **matched**-pairs signed-rank test ($n=4$).

5.6 Investigating the effects of HFFF2 fibroblasts on Bcl-2 family proteins in CLL cells

5.6.1 Analysis of MCL-1 and BIM_{EL} expression in CLL cells

The Bcl-2 family proteins comprise both anti-apoptotic and pro-apoptotic proteins [290]. Following the results which demonstrated that fibroblasts protect CLL cells from apoptosis I investigated whether the protection conferred by fibroblasts was mediated by Bcl-2 family proteins. Regulation of the anti-apoptotic protein MCL-1 and the pro-apoptotic protein BIM have been shown to be crucial in CLL cell survival [214, 291]; therefore I initially investigated expression of these two proteins. There are several isoforms of BIM: BIM_S (short), BIM_L (long) and BIM_{EL} (extra-long). BIM_S and BIM_L failed to be detected but BIM_{EL} was consistently and reliably detected, as well as MCL-1.

CLL samples were cultured in complete RPMI-1640 media as a control, or in CM derived from HFFF2 fibroblasts. As before, CM was used opposed to direct co-culture to avoid contamination of the CLL population with HFFF2 cells. Initially, only the effect of fibroblasts was investigated as they had a greater protective effect on CLL samples than myofibroblasts (Figure 5.4). After 16 and 24 hours CLL samples were collected and analysed. These time-points were selected as fibroblasts conferred significant protection to CLL samples at 24 hours (Figure 5.4), therefore it was speculated that Bcl-2 family proteins would be modulated prior to, or by 24 hours. CLL samples were initially analysed for expression of MCL-1 and BIM_{EL}.

Following this various other Bcl-2 proteins were analysed however a number of them failed to be detected. These include the pro-apoptotic proteins BAX and BAD as well as the anti-apoptotic protein bcl-xL [207, 292, 293]. Expression of the pro-apoptotic protein BIM was also analysed. The anti-apoptotic protein Bcl-2 was also analysed and reliably detected however expression of this protein remained unaltered between CLL cells cultured in complete RPMI-1640 media and those cultured in HFFF2-derived CM therefore was not pursued (Figure 5.21); only two samples were analysed therefore statistical analysis was not conducted.

MCL-1 expression was higher in CLL samples cultured in HFFF2 CM compared to control cells cultured in complete RPMI-1640 media, at both 16 and 24

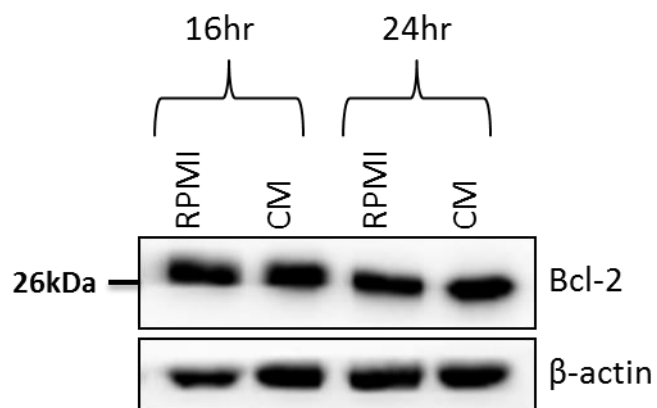


Figure 5.21: Effect of fibroblast conditioned media on Bcl-2 expression.

CLL samples were cultured in either complete RPMI-1640 media as a control, or cultured in fibroblast-derived CM for 16 or 24 hours. CM was generated from HFFF2 fibroblasts cultured in complete RPMI-1640 media for 72 hours. CLL samples were then collected and analysed for Bcl-2 expression (left) and β -actin (loading control). Data is representative of 2 different CLL samples.

Chapter 5

hours (Figure 5.22). Conversely BIM_{EL} expression was lower in CLL cells cultured in HFFF2-derived CM compared to control counterparts, at both time-points. This was repeated with a total of 7 different samples for MCL-1 and 5 separate samples for BIM_{EL}. **Samples selected comprised $\geq 80\%$ CLL cells to minimise the extent of analysing protein expression in contaminating cells.**

As MCL-1 is an anti-apoptotic protein its expression was expected to decline over time in CLL cells cultured in complete RPMI-1640 media. However for this cohort MCL-1 expression remains constant over the 24 hour time-period; there is no significant difference in MCL-1 expression between CLL cells cultured in complete RPMI-1640 media at any of these time-points. However, MCL-1 expression was significantly higher in CLL samples cultured in fibroblast-derived CM compared to CLL samples cultured in complete RPMI-1640 media at both 16 and 24 hours (Figure 5.23).

As BIM_{EL} is a pro-apoptotic protein its expression increases over time in CLL samples cultured in complete RPMI-1640 media, as expected; however this increase is not statistically significant (Figure 5.24, left graph). CLL samples cultured in HFFF2-derived CM express lower levels of BIM_{EL} compared to control cells cultured in complete RPMI-1640 media, at both time-points; however this trend just failed to reach significance ($p=0.06$) (Figure 5.24; left and right graphs).

The balance between the pro-apoptotic and anti-apoptotic members of the Bcl-2 family determine whether or not apoptosis will occur. Higher levels of pro-apoptotic proteins result in the induction of apoptosis whereas higher levels of the anti-apoptotic proteins prevent it; this is generally referred to as the apoptotic switch. Therefore the ratio between pro-apoptotic and anti-apoptotic proteins determine whether or not apoptosis is induced. In cells which are not undergoing apoptosis MCL-1 sequesters BIM (all isoforms) [294]. MCL-1 can be degraded by caspase 8 or caspase 3 resulting in MCL-1-free BIM which goes onto mediate apoptosis [294]. Therefore the BIM_{EL}/MCL-1 ratio was calculated for CLL cells cultured in complete RPMI-1640 media and CLL cells cultured in fibroblast-derived CM.

For CLL samples cultured in complete RPMI-1640 media, at both 16 and 24 hours, the BIM_{EL}/MCL-1 ratio is approximately 2:1. When CLL samples were cultured in fibroblast-derived CM at 16 and 24 hours the ratio is

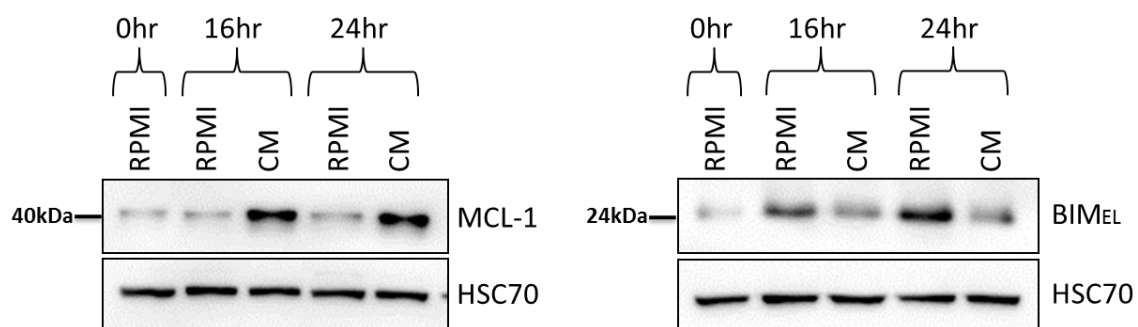


Figure 5.22: Effect of fibroblast conditioned media on MCL-1 and BIM_{EL} expression.

CLL samples were cultured in either complete RPMI-1640 media as a control, or cultured in fibroblast-derived CM for 16 or 24 hours. CM was generated from HFFF2 fibroblasts cultured in complete RPMI-1640 media for 72 hours. CLL samples were then collected and analysed for MCL-1 expression (left) or BIM_{EL} expression (right). CLL samples were also analysed at 0 hours. HSC70 was used as the loading control. Data is representative of 7 different CLL samples for MCL-1 and 5 different CLL samples for BIM_{EL}.

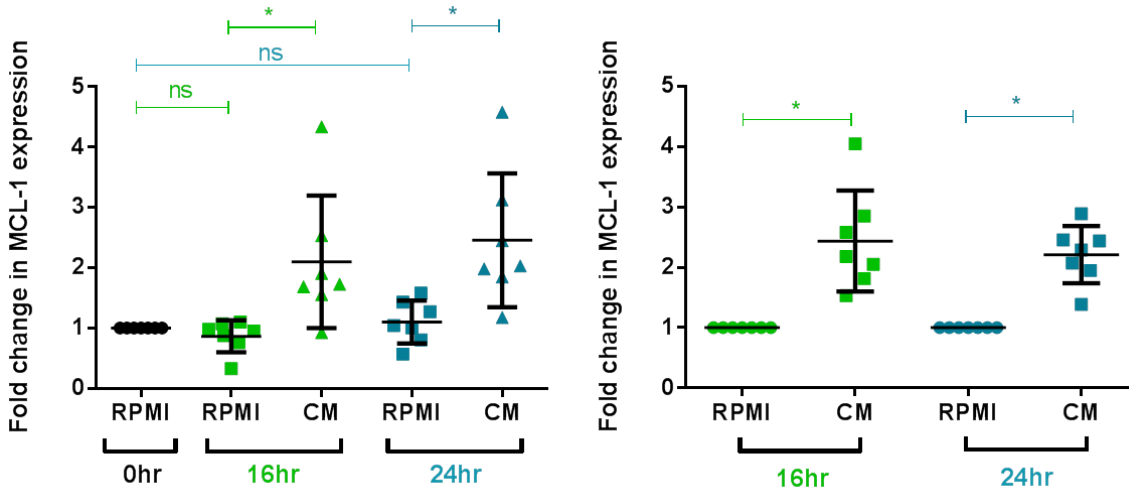


Figure 5.23: Effect of fibroblast CM on MCL-1 expression in CLL samples.

CLL samples were either cultured in complete RPMI-1640 media as a control, or cultured in fibroblast-derived CM for 16 (green) or 24 (blue) hours. CM was generated from HFFF2 cells cultured in complete RPMI-1640 media for 72 hours. CLL samples were also analysed at 0 hours. Graphs show fold change in MCL-1 expression in CLL samples analysed at 0 hours set to 1.0 (left), or MCL-1 expression in CLL samples cultured in complete RPMI-1640 media set to 1.0 (right). Each dot represents results from an individual CLL sample with mean (\pm SD). The statistical significance of the differences was analysed using Wilcoxon's matched-pairs signed rank test ($n=7$).

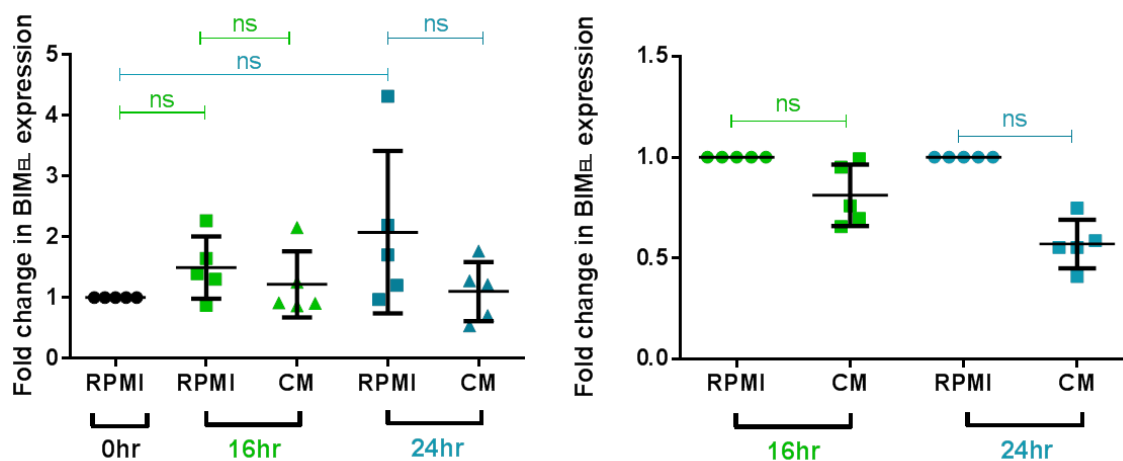


Figure 5.24: Effect of fibroblast conditioned media on BIM_{EL} expression in CLL cells.

CLL cells were either cultured in complete RPMI-1640 media as a control, or cultured in fibroblast-derived CM for 16 (green) or 24 (blue) hours; CM was generated from HFFF2 cells cultured in complete RPMI-1640 media for 72 hours. CLL cells were then collected and analysed for BIM_{EL} expression by immunoblotting. Graphs show the fold change in BIM_{EL} expression in CLL cells analysed at 0 hour set to 1.0 (left), or BIM_{EL} expression in CLL cells cultured in complete RPMI-1640 media set to 1.0 (right). Each dot represents the results from an individual CLL sample with mean (\pm SD). The **statistical significance of the differences was analysed using Wilcoxon's matched-pairs signed rank test** (n=5).

Chapter 5

approximately 1:2. However these differences just failed to reach statistical significance ($p=0.6$) (Figure 5.25).

5.6.2 Analysis of MCL-1 expression at earlier time-points

Following this I investigated the kinetics of this fibroblast-induced up-regulation of MCL-1. As fibroblast CM had no significant effect on BIM_{EL} expression at 24 hours it was decided not to analyse its expression at earlier time-points. The same method described above was performed, however CLL samples were collected at 6, 8 and 24 hour time-points and analysed for MCL-1 expression by immunoblotting. CLL samples were also analysed at 0 hours.

Similar to earlier results (Figure 5.22) MCL-1 expression was higher in CLL samples cultured in fibroblast CM compared to control cells cultured in complete RPMI-1640 media, at 24 hours. Similarly, at 6 and 8 hours, MCL-1 expression is higher in CLL cells cultured in fibroblast CM compared to control cells; the increase in MCL-1 expression is greater at 8 hours than at 6 hours (Figure 5.26). This was performed on a total of 5 different CLL samples, all **comprising $\geq 80\%$ CLL cells (Figure 5.27)**

For this cohort, MCL-1 expression in CLL samples cultured in complete RPMI-1640 media declines over time (Figure 5.27, left). This is expected as MCL-1 is a short-lived protein which is induced by signalling *in vivo* and declines *in vitro* in the absence of stimulation. However this reduction was not statistically significant. In CLL samples cultured in fibroblast-derived CM, MCL-1 expression remains constant over time; this suggests that the fibroblast CM is maintaining MCL-1 expression opposed to increasing it. MCL-1 expression was higher in CLL samples cultured in fibroblast CM compared to control cells at all time-points; however for this cohort this difference was not statistically significant (Figure 5.27, both graphs). This trend just failed to reach statistical significance at 8 and 24 hours ($p=0.06$).

5.6.3 Comparing the effect of fibroblasts and myofibroblasts on MCL-1 expression

As fibroblast CM was able to increase, or maintain, MCL-1 expression in CLL cells, I then investigated the effect of myofibroblasts on MCL-1 expression in CLL cells. CLL samples were cultured in complete RPMI-1640 media as a

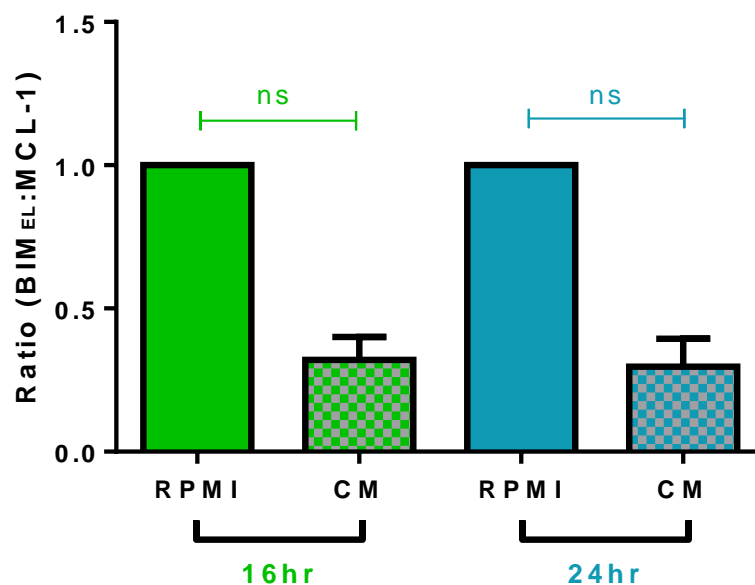


Figure 5.25: Graphical representation of the BIM_{EL}/MCL-1 ratio.

Graph shows the BIM_{EL}:MCL-1 ratio for CLL cells cultured in either complete RPMI-1640 media (plain bars) or cultured in HFFF2-derived CM (patterned bars) for 16 hours (green) or 24 hours (blue). CM was generated from HFFF2 cells cultured in complete RPMI-1640 media for 72 hours. CLL cells were analysed for MCL-1 and BIM_{EL} protein expression by immunoblotting. For cells cultured in complete RPMI media the ratio has been set at 1.0. Graph shows mean (\pm SD). The statistical significance of the differences was analysed using Wilcoxon's matched-pairs signed-rank test (n=5)

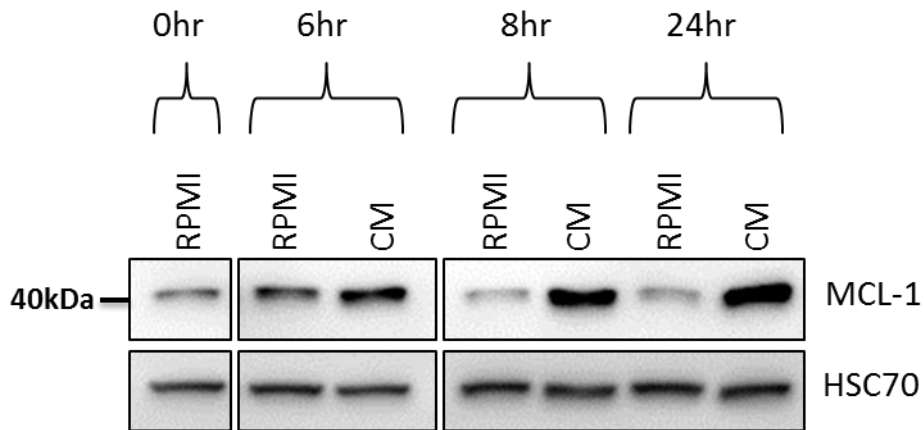


Figure 5.26: Effect of fibroblast conditioned media on MCL-1 expression in CLL samples at earlier time-points.

Western blot shows MCL-1 expression in CLL samples cultured in either complete RPMI-1640 media as a control, or cultured in HFFF2-derived CM for 6, 8 and 24 hours. CM was generated from HFFF2 fibroblasts cultured in complete RPMI-1640 media for 72 hours. CLL samples were then collected and analysed for MCL-1 expression by immunoblotting. CLL samples were also analysed at 0 hours. HSC70 was used as the loading control. Data is representative of 5 separate CLL samples.

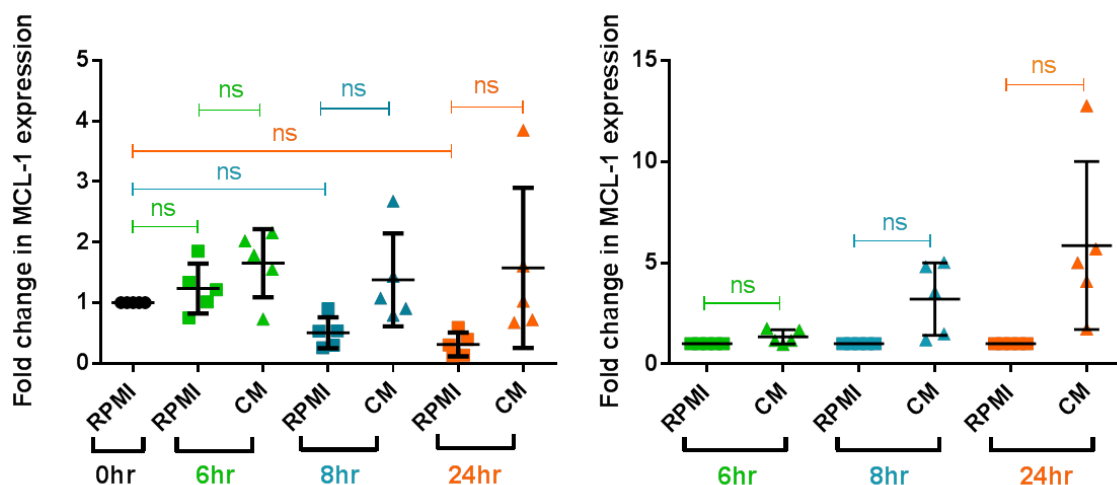


Figure 5.27: Effect of fibroblast conditioned media on MCL-1 expression at earlier time-points.

CLL samples were cultured in fibroblast-derived CM for 6 (green), 8 (blue) or 24 (orange) hours; CM was generated from HFFF2 cells cultured in complete RPMI-1640 media for 72 hours. CLL samples were also cultured in complete RPMI-1640 media as a control. CLL samples were then collected and analysed for MCL-1 expression by immunoblotting. Graphs show the fold change in MCL-1 expression in CLL cells analysed at 0 hours set at 1.0 (left graph), or MCL-1 expression in CLL cells cultured in complete RPMI-1640 media set to 1.0 (right graph). Each dot represents results from an individual CLL sample with mean (\pm SD). The significance of the differences was analysed using Wilcoxon's matched-pairs signed-rank test ($n=5$).

Chapter 5

control, or in HFFF2 fibroblast CM or HFFF2 myofibroblast CM. After 6 and 8 hours CLL cells were collected and analysed for MCL-1 expression by immunoblotting. These time-points were selected as they were identified as the earliest times required to allow differential MCL-1 expression between control CLL samples those cultured in CM; it was speculated that differential MCL-1 expression modulated by fibroblasts and myofibroblasts would be clearer at earlier time-points.

Four different CLL samples were analysed and **all comprised $\geq 80\%$ CLL cells**. For this cohort MCL-1 expression remained constant up until 8 hours in CLL cells cultured in complete RPMI-1640 media (Figure 5.29, left). MCL-1 expression was higher in CLL samples cultured in fibroblast CM compared to control cells at both 6 and 8 hours (Figure 5.28); this was statistically significant at both time-points (Figure 5.29, right). Additionally CLL samples cultured in myofibroblast CM expressed higher levels of MCL-1 compared to control cells; however MCL-1 expression was increased to a lesser extent compared to cells cultured in fibroblast CM. Furthermore this was only statistically significant at 8 hours. Additionally there is no significant difference between the effect of fibroblast CM and myofibroblast CM on MCL-1 expression in CLL cells at either time-point.

Overall these data suggest that soluble factor(s) released by fibroblasts and myofibroblasts up-regulate MCL-1 expression and down-regulate BIM_{EL} expression in CLL cells. Fibroblast-derived soluble factors increase MCL-1 expression in CLL cells as early as 6 hours. Additionally, soluble factors released by fibroblasts and myofibroblasts up-regulate MCL-1 expression in CLL cells by 8 hours; however myofibroblasts have a less prominent effect. Therefore inducing MCL-1 expression may be one potential mechanism by which fibroblasts and myofibroblasts protect CLL cells from apoptosis.

5.7 Discussion

The presence of myofibroblasts within the stroma of solid tumours correlates with aggressive disease behaviour and poor clinical outcome in multiple types of cancer [171, 172, 174]. However the clinical significance of myofibroblasts within CLL has not been previously investigated. The data described in chapter **3 suggest that myofibroblasts are present within the CLL stroma. Since α -SMA**

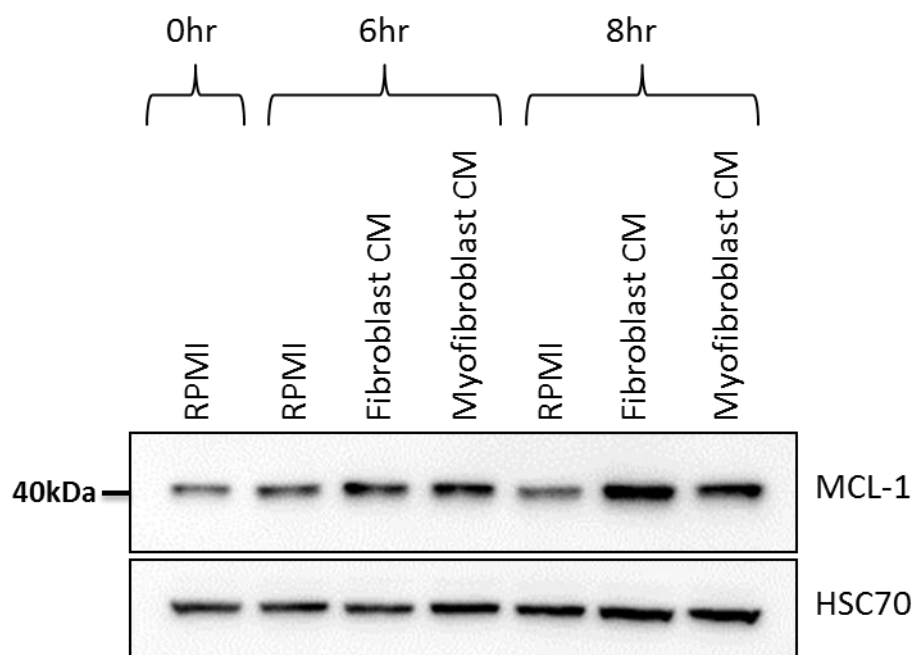


Figure 5.28: Comparison of fibroblast and myofibroblast conditioned media on MCL-1 expression in CLL samples.

HFFF2 cells were either untreated (fibroblasts) or treated (myofibroblasts) with TGF- β (2ng/ml) in complete DMEM media for 72 hours to allow transdifferentiation into myofibroblasts. HFFF2 fibroblasts and HFFF2-derived myofibroblasts were then washed twice with PBS to remove all traces of TGF- β ; **cells were subsequently cultured** in complete RPMI-1640 media for 72 hours to generate CM. CLL samples were cultured in HFFF2 fibroblast CM or HFFF2 myofibroblast CM for 6 and 8 hours. CLL samples were then collected and analysed for MCL-1 expression by immunoblotting. CLL samples were also cultured in complete RPMI-1640 media as a control. CLL samples were also analysed at 0 hours. HSC70 was used as the loading control. Data is representative of 4 separate CLL samples.

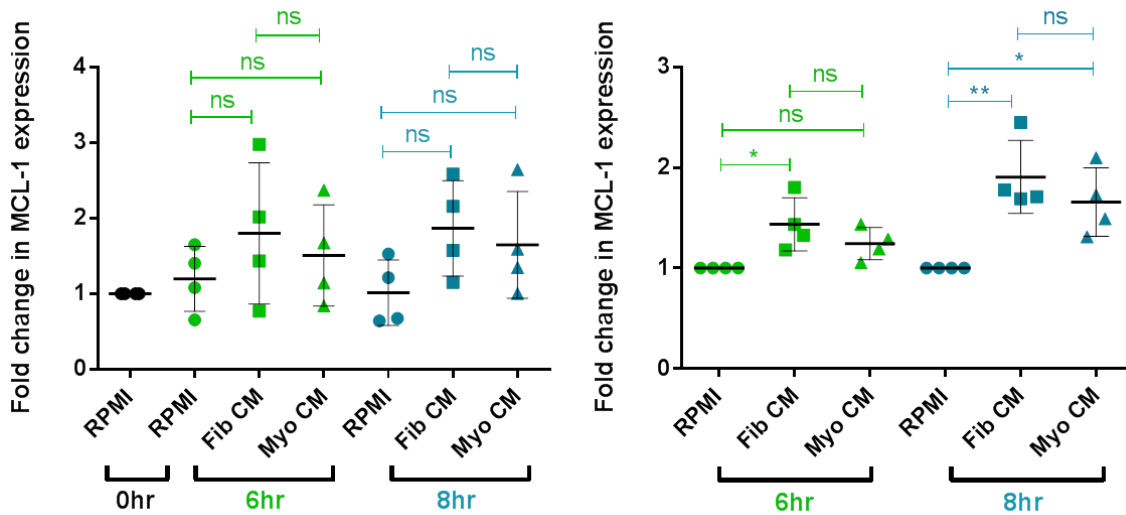


Figure 5.29: Effect of fibroblast and myofibroblast conditioned media on MCL-1 expression in CLL samples

HFFF2 cells were cultured in complete DMEM media in the absence (fibroblasts) or presence (myofibroblasts) of TGF- β (2ng/ml) for 72 hours to allow transdifferentiation into myofibroblasts. Wells were subsequently washed twice with PBS to remove all traces of TGF- β . HFFF2 fibroblasts and HFFF2 myofibroblasts when then cultured in complete RPMI-1640 media for 72 hours to generate CM. CLL cells were cultured in fibroblast CM, myofibroblast CM or complete RPMI-1640 media as a control for 6 hours (green) or 8 hours (blue). CLL cells were then collected and analysed for MCL-1 expression by immunoblotting. CLL cells were also analysed at 0 hours. Graphs show the fold change in MCL-1 expression in CLL cells analysed at 0 hours set to 1.0 (left), or MCL-1 expression in CLL cells cultured in complete RPMI-1640 media set to 1.0 (right). Each dot represents results from an individual CLL sample with mean (\pm SD). The statistical significance of the differences was analysed using one-way ANOVA with Bonferroni correction; significance level was set at 0.05 (n=4).

expression may be inversely correlated with ZAP-70, it is possible that myofibroblasts are associated with a more indolent disease in CLL. Furthermore the data described in chapter 4 indicate that CLL cells may actually decrease myofibroblast transdifferentiation.

The main aim of the experiments described in this chapter was to determine how fibroblasts and myofibroblasts alter CLL cell survival. This was investigated by co-culturing CLL cells with HFFF2 fibroblasts and HFFF2-derived myofibroblasts and comparing their effect on CLL viability. Following this the apoptotic pathways involved in fibroblast mediated protection of CLL cells was investigated by culturing CLL samples in CM derived from HFFF2 fibroblasts. Subsequently I compared the degree of CLL cell adhesion to fibroblasts and myofibroblasts. Next the effect of fibroblasts on intracellular levels of ROS within CLL cells was investigated. Finally I studied what effect fibroblasts have on Bcl-2 family proteins within CLL cells cultured in HFFF2 fibroblast-derived CM; the anti-apoptotic protein MCL-1 and the pro-apoptotic protein BIM_{EL} were analysed.

5.7.1 Fibroblasts have a greater protective effect on CLL cells than myofibroblasts

The main conclusion of the results described in this chapter is that fibroblasts and myofibroblasts protect CLL cells from apoptosis; however fibroblasts have a greater protective effect. This was demonstrated as CLL viability was higher in cells co-cultured with fibroblasts compared to those co-cultured with myofibroblasts. Additionally, culturing CLL samples in fibroblast CM reduced caspase 3 and PARP cleavage indicating that HFFF2 fibroblasts blocked these apoptotic pathways.

The finding that fibroblasts have a greater protective effect than myofibroblasts was surprising as the presence of myofibroblasts within various solid tumours, including prostate, breast, pancreatic and colon cancer, are associated with aggressive disease progression [171, 172, 174]; the ability of myofibroblasts to protect malignant cells as well as increase their invasive capacity has been well documented, within solid tumours [295]. This suggests unusual behaviour of CLL cells indicating that within B-cell malignancies, or at least within CLL, fibroblasts may be a greater driving force of disease

Chapter 5

progression than myofibroblasts as they more effectively sustain CLL cell survival, thus protecting them better from spontaneous apoptosis.

The differential effects of fibroblast and myofibroblasts do not appear to be confluency driven as this was evaluated by eye. However a potential drawback of this assay could include variation in cell viability between fibroblasts and myofibroblasts which would impact the degree of protection passed on to the CLL cells, therefore skewing the data. To determine if cell viability was comparable between fibroblasts and myofibroblasts post-culture, immunoblotting could be utilised to analyse caspase activity and PARP cleavage within the stromal cells.

Further evidence demonstrating the protective effect of HFFF2 fibroblasts on CLL samples was shown through analysis of apoptotic pathways. The un-cleaved form of caspase 3 was significantly higher in CLL samples cultured in fibroblast CM compared to control cells at 24 hours. Additionally there was a clear reduction in PARP cleavage in CLL cells cultured in fibroblast CM compared to control cells; however this was not statistically significant. This is possibly due to such a small cohort being analysed and more samples may reveal statistical significance.

Caspase 3 is an effector caspase which induces apoptosis leading to the destruction of the cell upon being cleaved itself. One downstream target of caspase 3 is PARP (poly (ADP-ribose) polymerase); consequently PARP cleavage serves as a reliable indicator that apoptosis is being executed [296, 297]. The reduction in cleaved caspase 3 and PARP within CLL cells cultured in fibroblast CM may be mechanistically linked, indicating that fibroblasts prevent PARP cleavage by inhibiting activation of its upstream effector caspase 3. Although, caspase 3 and PARP are not exclusively linked; other caspases can induce PARP cleavage such as caspase 7 [297]. To expand on this other caspases could be analysed such as caspases 8 and 9 which act downstream of caspase 3 and would highlight whether apoptosis is being implemented through the extrinsic or intrinsic pathways, respectively. To determine whether there is a link between fibroblast-mediated CLL cell survival and cleavage of caspase 3 and PARP, CLL cells could be treated with caspase inhibitors prior to culture in fibroblast CM.

Furthermore if there was sufficient time I would have compared the effect of fibroblasts and myofibroblasts on caspase 3 and PARP cleavage. If their expression follows the same trend as CLL viability and MCL-1 expression this would be more indicative of their role in fibroblast and myofibroblast-mediated CLL cell protection.

5.7.2 HFFF2 fibroblasts do not protect CLL cells by reducing intrinsic ROS

Moreover these data suggest that HFFF2 fibroblasts do not protect CLL cells from apoptosis by reducing the intracellular levels of ROS. CLL cells contain higher levels of intrinsic ROS compared to normal lymphocytes, which is detrimental to their survival [287]. Previous work has shown that stromal cells can promote CLL cell survival by aiding in the uptake of the antioxidant glutathione (GSH) [287]. However, although it was not statistically significant, there was a trend supporting higher intracellular levels of ROS within CLL cells co-cultured with fibroblasts compared to control cells that were cultured alone. This is unusual as it suggests a harmful role of fibroblasts on CLL cell survival. However, as this increase in ROS was subtle, fibroblasts may compensate by inducing stronger protective mechanisms to override the detrimental effects of ROS. Furthermore, if fibroblasts partially increase ROS within CLL cells, myofibroblasts may further enhance ROS induction as they have a less protective effect on the malignant cells. This could provide further evidence that myofibroblasts correlate with a more indolent disease course in CLL.

5.7.3 Fibroblasts and myofibroblasts alter Bcl-2 family proteins in CLL cells

MCL-1 and BIM_{EL} expression were increased and reduced, respectively, in CLL cells cultured in fibroblast CM, suggesting HFFF2 fibroblasts protect CLL cells by modulating levels of these anti- and pro-apoptotic proteins. Moreover, MCL-1 expression was increased in CLL cells cultured in myofibroblast CM, but to a lesser extent than cells cultured in fibroblast CM. This suggests a principle role for MCL-1 in HFFF2-mediated protection of CLL cells as the extent of MCL-1 induction appears to translate to a similar degree of CLL protection.

Chapter 5

Several studies have shown that various types of stromal cells including FDCs, NLCs and BM stromal cells can protect CLL cells from apoptosis through the induction of MCL-1 [214, 298, 299]. Furthermore MCL-1 expression in CLL cells is associated with poor clinical outcome, again indicating fibroblasts encourage a more aggressive disease progression than myofibroblasts [300]. To determine whether MCL-1 is indeed a principle mediator of fibroblast and myofibroblast-induced CLL cell survival, methods could be adopted to block MCL-1 expression within CLL cells prior to co-culture with stromal cells. Utilising AT-101 which targets Bcl-2 family anti-apoptotic proteins by binding to their BH3 domains has been shown to suppress stromal cell protection of CLL cells by down-regulating MCL-1 expression [301]. Additionally it has been demonstrated that MCL-1 antisense oligonucleotides can block protection conferred by FDCs through reducing MCL-1 expression in CLL cells [214]. More recently, down-regulating MCL-1 utilising siRNA has been found to induce rapid and potent apoptosis of CLL cells [302].

BIM_{EL} expression was reduced in CLL cells cultured in fibroblast CM compared to control cells, however this was not statistically significant. As BIM is a pro-apoptotic protein, its expression is expected to increase in CLL cells cultured alone, over time. BIM_{EL} expression has been shown to increase with spontaneous apoptosis, both here (Figure 5.21, right) and in previous published data [303]. Therefore the effect of fibroblast CM on CLL cell BIM_{EL} expression may be greater at later time-points, such as 48 and 72 hours, when CLL cells would have likely undergone substantial cell death.

If there was sufficient time I would have compared the effect of fibroblast and myofibroblast CM on BIM_{EL} expression. BIM is a favoured dimerization partner of MCL-1 and the former stabilises the latter against degradation [304]. Furthermore BIM-MCL-1 interactions have been shown to modulate apoptosis in CLL cells. Previous work has demonstrated that fludarabine treatment of CLL cells results in MCL-1 degradation thus releasing BIM and inducing CLL cell death [305]. Therefore further studies could investigate the effect of fibroblasts and myofibroblasts on drug-induced Bcl-2 family protein expression in CLL cells. As fibroblast and myofibroblast CM effect MCL-1 expression to varying degrees it would be interesting to investigate their effect on BIM to determine if expression of this protein follows a similar, but inverse trend as MCL-1.

To probe how fibroblasts and myofibroblasts regulate MCL-1 and BIM expression, methods could be utilised to target the mechanisms responsible for MCL-1 induction and BIM down-regulation. Initial studies revealed that MCL-1 induction is dependent on transcriptional up-regulation by multiple growth factors [306, 307]. Furthermore MCL-1 transcription is mediated by various transcription factors, most notably the STAT family. In macrophages STAT3 activation appears to be essential for MCL-1 induction [308]. Similarly in CLL it has been demonstrated that phosphorylation of STAT3 by c-Abl induces MCL-1 expression [309]. Inhibitors could be utilised to block STAT3 and c-Abl within CLL cells prior to culture with fibroblasts to determine whether these mechanisms regulate fibroblast-mediated MCL-1 induction. FDCs have been shown to down-regulate BIM expression in NHL cells as a result of microRNA-181a up-regulation which posttranscriptionally regulates BIM [310]; however expression of this microRNA is low in CLL yet other microRNAs may be involved in stromal cell-mediated BIM down-regulation. Furthermore phosphorylation of BIM_{EL} at serine 69 via ERK1/2 leads to its proteasomal degradation [311]. CLL cells could be treated with proteasome inhibitors prior to culture in fibroblast CM to determine if HFFF2 fibroblasts down-regulate BIM_{EL} expression by targeting it for degradation by the proteasome.

As BIM and MCL-1 are closely related and possibly involved in fibroblast and myofibroblast-mediated protection of CLL cells, I calculated the ratio between BIM_{EL} and MCL-1 (BIM_{EL}:MCL-1) expression. The ratio for control cells cultured in complete RPMI-1640 media was 2:1. Conversely it was 1:2 for CLL cells cultured in fibroblast CM. However this correlation was not statistically significant. Although there were clear changes in MCL-1 expression, alterations in BIM_{EL} expression were less compelling. The other isoforms of BIM may need to be detected to identify a correlation. Additionally the cohort analysed was relatively small and more samples should be analysed. Overall this indicates that HFFF2 fibroblast CM alters expression of both anti-apoptotic proteins (MCL-1) and pro-apoptotic proteins (BIM_{EL}) in order to promote survival in the CLL cells.

Furthermore, studies could be conducted to analyse expression of caspases, MCL-1 and BIM in CLL cells after direct co-culture with HFFF2 cells. To avoid HFFF2 contamination of the CLL population cells could be analysed by flow

Chapter 5

cytometry and therefore gated on their FSC/SSC to ensure exclusive analysis of the lymphocyte population. Therefore expression of these proteins could be analysed in response to direct-contact as well as soluble factor(s).

Collectively these data indicate that fibroblast CM increases MCL-1 and reduces BIM_{EL} expression, possibly resulting in the prevention of both caspase 3 and PARP cleavage, thus leading to CLL cell survival. This is supported by data in the literature as several studies have shown that co-culture of CLL cells with FDCs, BM stromal cells and endothelial cells can induce CLL cell survival through MCL-1 induction and reduced PARP cleavage [214, 301, 312]. Additionally CLL cell co-culture with BM stromal cells down-regulates active caspase 3, although this was not linked with MCL-1 or BIM expression [149]. However other data has demonstrated that inducing apoptosis in CLL cells using agents such as all-trans retinoic acid (ATRA) and Honokiol can reduce MCL-1 expression as well as induce caspase 3 activity, indicating a link between these pathways [313, 314].

5.7.4 Effect of soluble factors on CLL viability

Other than the annexin V assays and ROS experiments, the majority of the aforementioned assays involved culturing CLL cells in HFFF2 fibroblast or myofibroblast-derived CM. This was mainly to ensure there was no HFFF2 contamination within the CLL samples after culture, thus all protein expression detected is CLL cell specific. Additionally these data indicate that all changes occurring in protein expression is a result of soluble factors released from the stromal cells. As CLL, MCL-1 expression, varied between the two stromal subsets, this indicates that fibroblasts and myofibroblasts release different amounts of the same soluble factor(s), or release an array of different factors altogether. Additionally, these data indicate that fibroblasts release soluble factors which reduce BIM_{EL} expression, and reduce caspase 3 and PARP cleavage.

Previous studies have demonstrated that SDF-1 secreted by NLCs can protect CLL cells from apoptosis [128]. Additionally CLL cells express the receptors BR3, BCMA and TACI, which bind the TNF family member BAFF, and the latter receptor also binds the proliferation inducing ligand APRIL [315]. NLCs release these factors which consequently protect CLL cells from apoptosis [298]. Moreover it was demonstrated that BAFF and APRIL induce MCL-1 expression

within CLL cells [298]. These could be potential soluble factors implicated in fibroblast and myofibroblast mediated protection of CLL cells. To test this CLL cells could be cultured in fibroblast or myofibroblast CM supplemented with neutralising antibodies against these factors prior to analysis of CLL viability or protein expression for MCL-1, BIM, caspase 3 and PARP.

To further confirm the effect of stromal cell-derived soluble factors on CLL cell viability, transwell assays could also be utilised. This technique allows physical separation of both cell types, whilst still exposing each cell type to the soluble factors released by the other. Thus, this assay also allows for the investigation of the non-contact bi-directional interplay between both cell types.

5.7.5 Variation in CLL viability

Although all samples followed a similar trend in viability when co-cultured with fibroblasts and myofibroblasts, there was a substantial amount of variation in the degree of apoptosis between individual samples. For instance some samples would undergo rapid spontaneous apoptosis such as sample U566 whose viability was at 30% at 24 hours and further declined to 15% by 72 hours, compared to other samples which were more resilient such as sample M462 whose viability was 80% at 24 hours and only reached 60% by 72 hours. Furthermore there was a great deal of variation in the degree of protection conferred by the stromal cells between individual samples. Using the same samples as examples, for sample U566 fibroblasts and myofibroblasts protected the cells by 62% and 11%, respectively, by 72 hours. However for sample M462 fibroblasts and myofibroblasts protected the cells by 12% and 4%, respectively, at 72 hours. The variation in protection is partly due to the differences in spontaneous apoptosis between these two samples. Cell viability for sample M462 remained high by 72 hours and therefore there was only a limited amount of protection which the stromal cells could confer. Conversely by 72 hours the majority of cells within sample U566 had undergone apoptosis therefore the stromal cells could have a greater protective effect.

This variation in CLL viability in response to fibroblasts and myofibroblasts indicate that some samples are more dependent on stromal cells compared to others, i.e. those which undergo rapid spontaneous apoptosis are likely to be more dependent compared to more apoptosis-resilient samples. This could correlate with disease prognosis as a previous study demonstrated that U-CLL

samples are more prone to spontaneous apoptosis than M-CLL samples [286]. This could indicate that U-CLL samples are potentially more dependent on stromal cells for survival, and therefore targeting interactions between CLL cells and stromal cells may be more beneficial for U-CLL patients compared to M-CLL patients. For this cohort, by 72 hours the degree of spontaneous apoptosis was significantly greater in U-CLL samples than M-CLL, yet there was no statistically significant difference in the degree of fibroblast and myofibroblast-mediated protection between *IGHV* mutation subsets. However this was a small cohort and analysing more samples may reveal clearer differences.

Furthermore other factors may influence the dependency of CLL cells on fibroblasts and myofibroblasts. One variable could be whether or not the sample is a sIgM signaller, unfortunately only one sample in this cohort was a non-signaller and therefore this factor could not be examined. Another variable could include prognostic factors such as ZAP-70, Ki-67 and CD38, all of which correlate with a more aggressive disease progression, and thus positive expression may correlate with a greater degree of stromal cell dependency. Also factors such as genetic variances, disease stage and previous treatment may influence stromal cell protection of CLL cells.

5.7.6 CLL cells preferentially bind to fibroblasts than to myofibroblasts

As fibroblasts and myofibroblasts are two phenotypically different cell types with differential effects on CLL cell survival, I compared CLL cell binding to both cell types. CLL cells preferentially bound to myofibroblasts than to fibroblasts when co-cultured for 24 hours. This was unexpected as fibroblasts have a superior protective effect on CLL cells than myofibroblasts, thus it was expected that CLL cells would preferentially bind to the stromal cell type that enhanced their survival. One possible explanation could be due to interactions between CLL cells and fibronectin. Myofibroblasts express higher levels of fibronectin than fibroblasts; during the transdifferentiation process TGF- β up-regulates the expression of the EDA splice variant of fibronectin [316]. Additionally CLL cells express the integrin receptor $\alpha 4\beta 1$ (VLA-4) which binds fibronectin [317], therefore CLL cells may preferentially bind to myofibroblasts due to this interaction. Secondly, similar to the annexin V assays a potential drawback of this assay is variation between fibroblast and myofibroblast

viability, after co-culture. This was checked by eye and although stromal cell viability appeared comparable between the two subtypes a more accurate method would be to analyse expression of cleaved caspases and PARP by immunoblotting. Overall this indicates that adhesion does not mediate the survival effect of HFFF2 fibroblasts and myofibroblasts on CLL cells. This is consistent with the CM data which suggests that survival is mediated by soluble factors.

It would be interesting to determine which receptor-ligand interactions are involved in CLL cell adhesion to the stromal cells. To investigate this CLL cells could be co-cultured with fibroblasts and myofibroblasts in the presence of neutralising antibodies against specific receptors such as VLA-4. Using this method it was previously demonstrated that CLL cells bind stromal cells through ICAM-1 and VCAM-1 which bind the CLL integrins LFA-1 and VLA-4, respectively [318].

5.7.7 Summary

- Soluble factor(s) released from HFFF2 fibroblasts may up-regulate expression of MCL-1, and down-regulate expression of Bim^{EL}, leading to increased CLL cell resistance to apoptosis.
- Soluble factor(s) released from HFFF2 fibroblasts prevent caspase 3 cleavage, and subsequently PARP cleavage within CLL cells.
- Soluble factors released from fibroblasts appear to up-regulate MCL-1 expression, to a greater extent, than soluble factors released from myofibroblasts; this may in turn be partially responsible for why myofibroblasts are less effective at protecting CLL cells from apoptosis compared to fibroblasts.
- Fibroblasts do not appear to protect CLL cells by lowering intrinsic levels of ROS within the malignant cells.
- CLL cells preferentially bind to myofibroblasts than to fibroblasts.

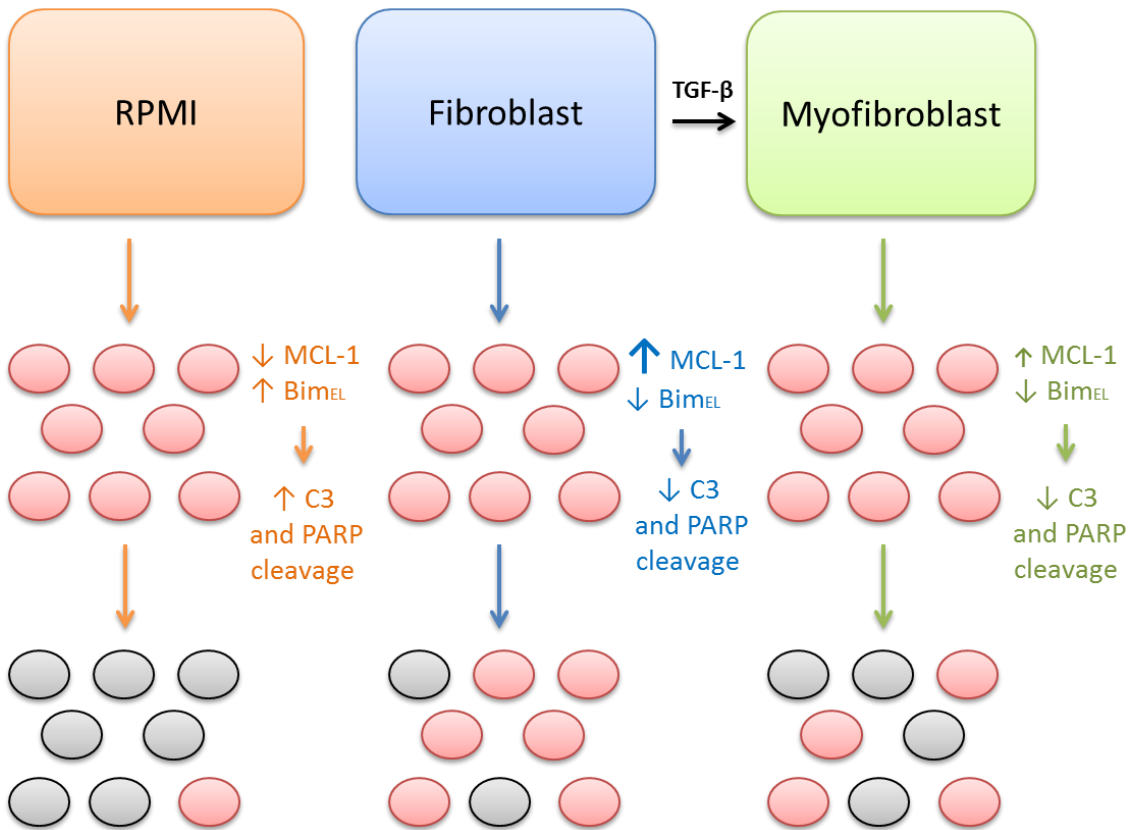


Figure 5.30: Summary of survival data.

CLL cells (red circles; viable CLL cells) cultured in complete RPMI-1640 media (orange) express low levels of MCL-1 and high levels of Bim_{EL} expression. This leads to increased caspase 3 (C3) and PARP cleavage; consequently CLL cells undergo apoptosis (black circles; CLL cells undergoing apoptosis). In response to soluble factors released from fibroblasts (blue) and myofibroblasts (green) Bim_{EL} expression remains low and MCL-1 expression increases. MCL-1 expression is higher within CLL cells in the presence of fibroblasts compared to myofibroblasts (depicted by larger and smaller arrows respectively). This leads to lower levels of caspase 3 and PARP cleavage. Consequently less CLL cells undergoing apoptosis; soluble factors released from fibroblasts induce less CLL cell apoptosis compared to soluble factors released from myofibroblasts.

Chapter 6:

Investigation of the
effect of fibroblasts on
intracellular signalling
pathways in CLL

6.1 Introduction

CLL remains an incurable disease despite major advances in treatment strategies. This is generally due to patients relapsing as a result of minimal residual disease (MRD) [319]. Growing evidence suggests that MRD is due to CLL cells infiltrating specific tissue microenvironments within which they are protected from both spontaneous and drug-induced cell death, by stromal cells [127, 318]. The data presented in chapter 5 demonstrate that HFFF2 fibroblasts protect CLL cells from apoptosis, possibly by up-regulating or maintaining the anti-apoptotic protein MCL-1 (Figures 5.4 and 5.21). Blocking the signal transduction pathways which induce these protective mechanisms may lead to potential novel treatment strategies, which make the leukemic cells insensitive to stromal cell protection. Therefore the main aim of the results described in this chapter was to determine which protective signalling pathways are activated within CLL cells in response to co-culture with fibroblasts.

Initial investigations were made to characterise activation of various intracellular signalling pathways are activated within CLL cells in response to fibroblasts. This was followed by determining which signalling pathways are involved in fibroblast-mediated protection of CLL cells by utilising small molecule inhibitors to target various signal transduction pathways. Finally I investigated which intracellular signalling pathways are specifically responsible for fibroblast-mediated induction of MCL-1 expression in CLL cells.

6.2 Determining which intracellular signal transduction pathways are activated within CLL cells by HFFF2 fibroblasts

To investigate which intracellular signalling pathways are activated within CLL cells in response to fibroblast co-culture, an initial experiment was performed using sample M462. It was decided to only investigate the effect of fibroblasts as they had a significantly greater protective effect compared to myofibroblasts (Table 5.1). I directly co-cultured the CLL sample with HFFF2 fibroblasts in complete RPMI-1640 media for 24 hours. This time-point was selected as fibroblasts significantly protected CLL samples from apoptosis at this time (Figure 5.4). The CLL cells were then collected and analysed for phospho ERK

(pERK) expression by immunoblotting. CLL cells were also cultured in complete RPMI-1640 media in the absence of HFFF2 fibroblasts, and analysed after 24 hours of culture as a control, but also at 0 hours. β -actin was used for the loading control as it is stably expressed in CLL cells and has been previously used as a loading control in other studies [320].

At 0 hours pERK expression in CLL sample M462 was high which is likely due to antigen stimulation *in vivo*, indicating CLL cell anergy. However when cultured alone *in vitro* pERK expression declines over time and was clearly reduced by 24 hours. This is typical of CLL cells and has been previously documented [261]. CLL cells that were co-cultured with fibroblasts expressed higher levels of pERK compared to control cells cultured alone (Figure 6.1, left). This was repeated with one other sample and a similar trend was observed.

As discussed earlier, one potential complication of co-culture experiments is contamination of the CLL cell sample by non-adherent/dying HFFF2 cells. Thus, one possibility was that HFFF2-derived pERK was responsible for the apparent increase in expression in co-cultured CLL cells. Indeed, immunoblot analysis revealed that HFFF2 cells express extremely high levels of basal pERK (Figure 6.1, right).

To further probe potential contamination of CLL samples by HFFF2 cells, I performed an additional experiment where CLL cells were co-cultured with HFFF2 fibroblasts **for 24 hours and expression of pERK and α -SMA** were analysed by Western blotting (Figure 6.2). As shown previously (Figure 4.1), CLL cells do not express α -SMA and α -SMA was therefore used as a measure of HFFF2 cell contamination of CLL samples. In this experiment, Bcl-2 was used as the loading control as it is stably expressed in CLL cells and has been used in previous studies as a loading control for these cells [321]. Additionally I found that Bcl-2 expression is not altered by HFFF2 fibroblasts (Figure 5.20).

Despite the absence of α -SMA in CLL cells, α -SMA was detected (with increased pERK expression) in CLL cells following co-culture indicating that there is a low, but significant level of cross-contamination in these experiments (Figure 6.2).

To avoid HFFF2 contamination, further experiments were performed using HFFF2 fibroblast-derived CM. As before (chapter 5) CM was generated from

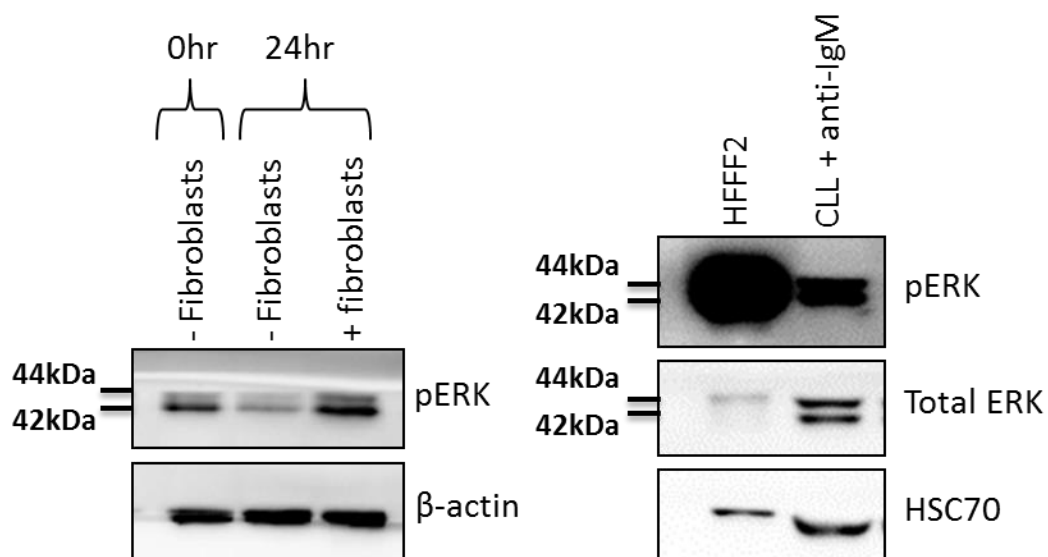


Figure 6.1: Effect of HFFF2 fibroblasts on pERK expression in CLL cells and analysis of pERK expression in HFFF2 fibroblasts.

Left - Western blot showing pERK expression in CLL cells either cultured alone as a control or co-cultured with HFFF2 fibroblasts in complete RPMI-1640 media for 24 hours. CLL cells were also analysed at 0 hours. CLL cells were then collected and analysed by immunoblotting for pERK and β -actin (loading control). CLL sample M462 is shown; this figure is representative of 2 samples. Right-Western blot shows basal levels of pERK expression in HFFF2 fibroblasts. CLL cells treated with soluble anti-IgM for 15 minutes were used as a positive control. HSC70 was used as the loading control.

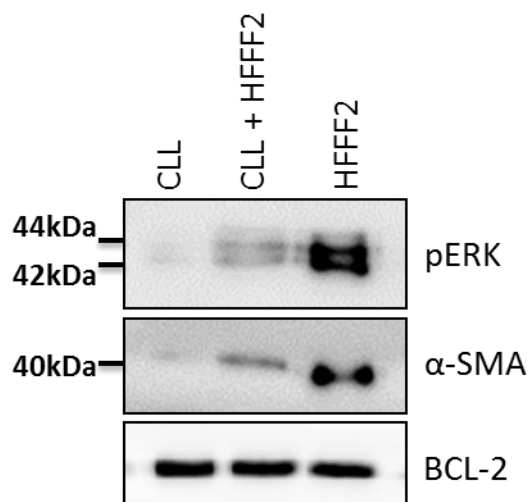


Figure 6.2: α -SMA expression in CLL cells after co-culture with HFFF2 fibroblasts.

CLL cells were co-cultured with HFFF2 fibroblasts in complete RPMI-1640 media for 24 hours. CLL cells were then collected and **analysed for pERK, α -SMA and Bcl-2** (loading control) by immunoblotting. CLL cells were also cultured in the absence of HFFF2 cells in complete RPMI-1640 media as a control for basal pERK expression and **as a negative control for α -SMA**. HFFF2 Fibroblasts were also analysed as a positive control for α -SMA expression. This was performed once.

Chapter 6

HFFF2 fibroblasts cultured in complete RPMI-1640 media for 72 hours. CLL samples were either cultured in complete RPMI-1640 media as a control or in HFFF2-derived CM for 8 or 24 hours. These time-points were selected as HFFF2 fibroblasts were shown to significantly protect CLL cells from apoptosis by 24 hours. Additionally HFFF2 fibroblasts significantly increased MCL-1 expression in CLL samples by 16 hours. Therefore the signalling pathways responsible should be activated prior to 16 hours, and may be maintained by 24 hours. CLL cells were then collected and analysed for pERK and phospho AKT-473 (pAKT⁴⁷³) expression by immunoblotting (Figure 6.3).

Nine different samples were analysed for pERK expression and five different samples were analysed for pAKT⁴⁷³ expression. Samples selected comprised **≥80% CLL cells to minimise the extent of analysing protein expression in contaminating cells.**

Unlike the earlier sample pERK expression here was low at 0 hours and pAKT⁴⁷³ is undetectable (Figure 6.3). Furthermore expression remains low in CLL samples cultured in complete RPMI-1640 media at 8 and 24 hours (Figures 6.3 and 6.4). However, when CLL samples were cultured in fibroblast CM expression of pERK was significantly increased compared to control cells, at both time-points. Additionally pAKT⁴⁷³ expression was higher in CLL samples cultured in fibroblast CM compared to control cells but was not statistically significant at either time-point; this trend just failed to reach significance at 24 hours ($p=0.06$) (Figure 6.5).

Following analysis of pERK and pAKT⁴⁷³, I next analysed phosphorylation of SYK at tyrosine 352 (pSYK³⁵²) in CLL cells cultured in HFFF2 fibroblast CM or directly co-cultured with HFFF2 fibroblasts. HFFF2 cells were also analysed for pSYK³⁵² expression. Due to issues with the antibody and time constraints this was only performed on two separate samples, therefore statistical analysis could not be performed.

In contrast to pERK, HFFF2 cells do not express pSYK³⁵² (Figure 6.6). pSYK³⁵² expression was higher in CLL cells cultured in fibroblast CM compared to control cells at 24 hours. pSYK³⁵² expression was also higher in CLL samples which were directly co-cultured with fibroblasts compared to control cells, however this increase was lower compared to in CLL samples cultured in CM. This may be due to HFFF2 contamination of the CLL population therefore

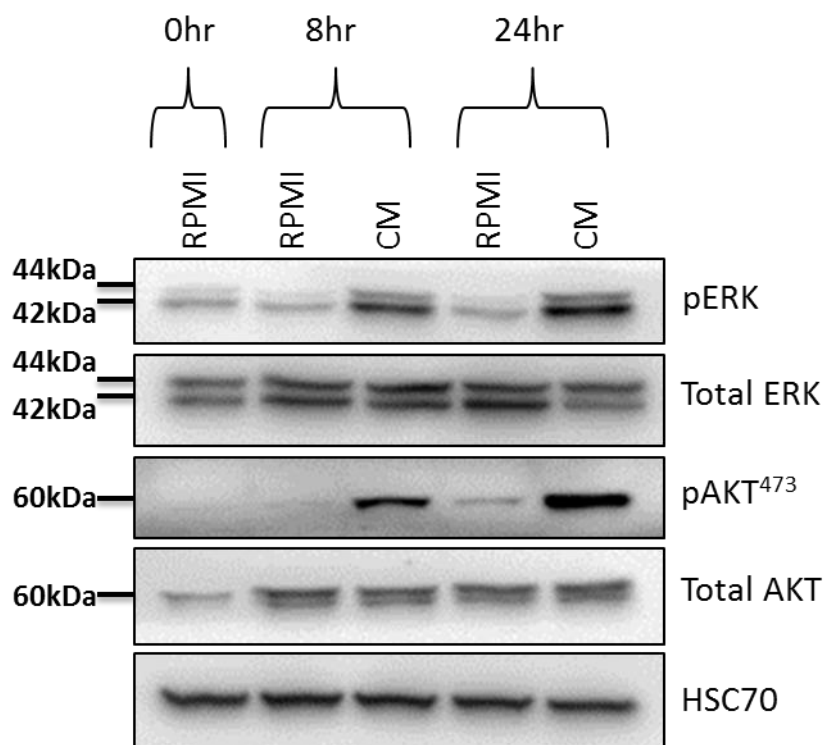


Figure 6.3: pERK and pAKT⁴⁷³ expression in CLL cells in response to HFFF2-derived conditioned media:

CLL cells were either cultured in complete RPMI-1640 media as a control, or cultured in HFFF2 fibroblast-derived CM for 8 hours and 24 hours. CM was generated from HFFF2 cells cultured in complete RPMI-1640 media for 72 hours. CLL cells were then collected and analysed for pERK and pAKT⁴⁷³ expression by immunoblotting. CLL cells were also analysed at 0 hours. Total ERK and total AKT expression was also analysed as loading controls for their respective phospho-proteins; HSC70 was used as the overall loading control. This figure is representative of 9 separate samples for pERK expression and 5 separate samples for pAKT⁴⁷³ expression. CLL sample M643A is shown.

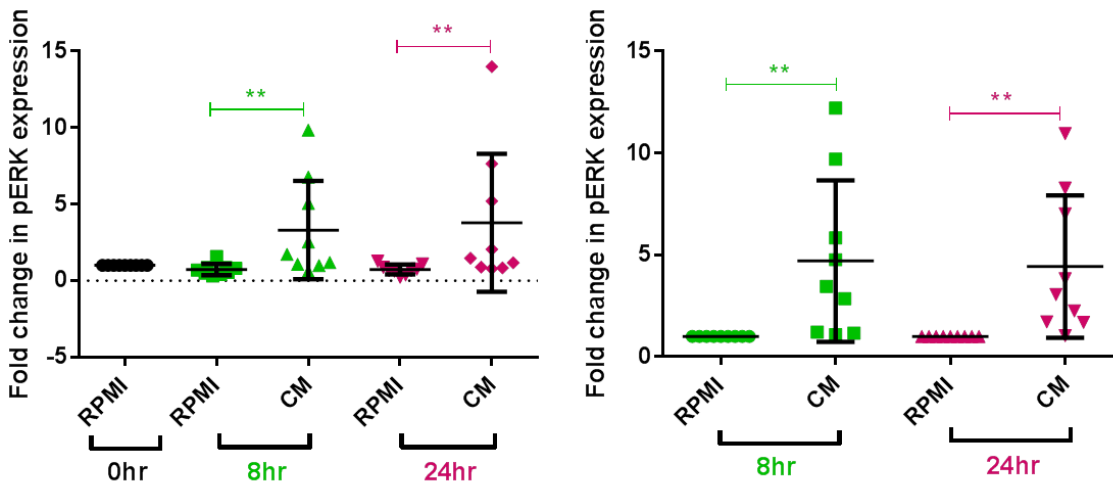


Figure 6.4: Effect of HFFF2-derived conditioned media on pERK expression.

CLL samples were either cultured in complete RPMI-1640 media as a control, or cultured in HFFF2-derived CM for 8 hours (green) or 24 hours (pink). CM was derived from HFFF2 cells cultured in complete RPMI-1640 media for 72 hours. CLL samples were then collected and analysed for pERK expression by immunoblotting. CLL samples were also analysed at 0 hours. Graphs show fold change in pERK expression in CLL cells at 0 hours set to 1.0 (left); or pERK expression in CLL cells cultured in complete RPMI-1640 media set to 1.0 (right). Each dot represents results for an individual CLL sample with the mean (\pm SD). The statistical significance of differences was analysed by Wilcoxon's matched-pairs signed-rank test ($n=9$).

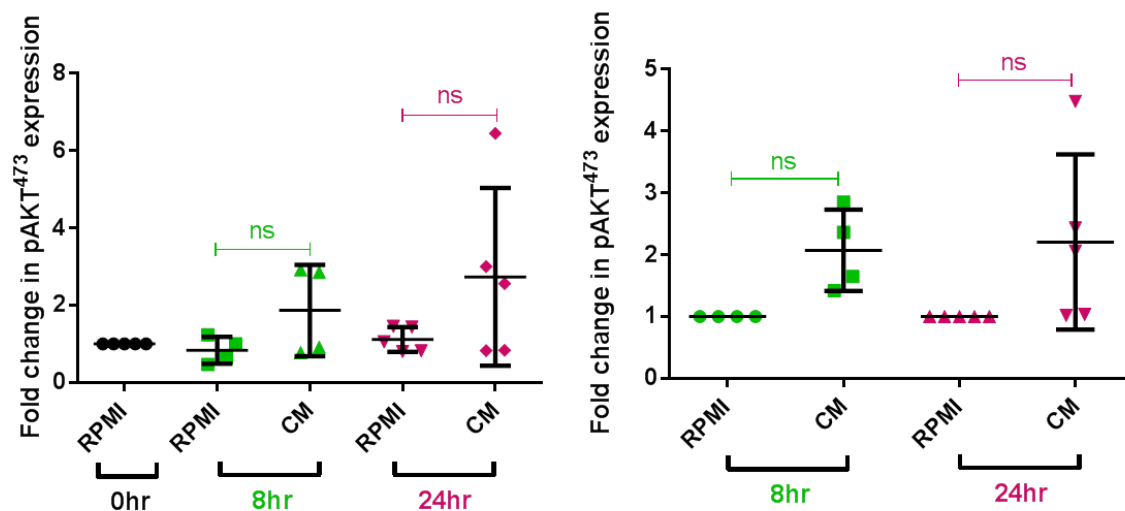


Figure 6.5: Effect of HFFF2-derived conditioned media on pAKT⁴⁷³ expression.

CLL cells were cultured in either complete RPMI-1640 media or cultured in fibroblast CM for 8 hours (green) or 24 hours (pink). CM was derived from HFFF2 cells cultured in complete RPMI-1640 media for 72 hours. CLL samples were collected and analysed for pAKT⁴⁷³ expression by immunoblotting. CLL samples were also analysed at 0 hours. Graphs show the fold change in pAKT⁴⁷³ expression in CLL cells at 0 hours set to 1.0 (left), or pAKT⁴⁷³ expression in CLL cells cultured in complete RPMI-1640 media set to 1.0 (right). Each dot represents results from an individual sample with mean (\pm SD). The statistical significance of the differences was analysed using Wilcoxon's matched-pairs signed-rank test (8hr n=4), (24hr n=5).

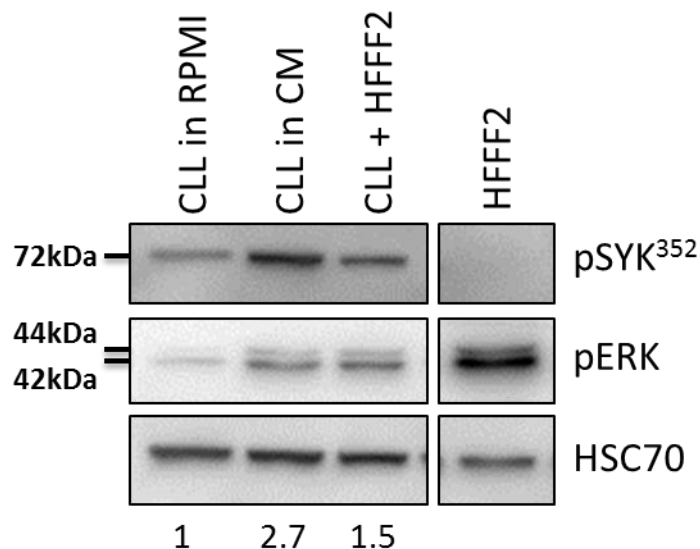


Figure 6.6: Effect of HFFF2 fibroblast CM and HFFF2 direct contact on pSYK³⁵² expression in CLL cells.

Representative western blot shows the effect of HFFF2 fibroblasts on pSYK³⁵² expression in CLL cells. CM was generated from HFFF2 fibroblasts in complete RPMI-1640 for 72 hours. CLL cells were either cultured in HFFF2-derived CM or directly co-cultured with HFFF2 cells for 24 hours. CLL cells were also cultured in complete RPMI-1640 media as a control. CLL samples were then collected and analysed for pSYK³⁵² and pERK expression by immunoblotting. HFFF2 cells were also analysed. Quantitation of pSYK³⁵² is displayed beneath respective bands; pSYK³⁵² expression was normalised to HSC70 (loading control) and expression in CLL cells cultured in complete RPMI-1640 media was set to 1.0. Western blot is representative of 2 separate CLL samples.

diluting pSYK³⁵² expression as HFFF2 cells do not express this phospho-protein. A similar trend was observed in the other sample analysed.

Overall these data show that soluble factors released by HFFF2 fibroblasts can up-regulate expression of pERK, pAKT⁴⁷³ and pSYK³⁵² in CLL cells. This indicates that HFFF2 fibroblasts release soluble factor(s) that induce the MAPK signalling pathway, PI3K/AKT signalling pathway and signal transduction pathways activated downstream of pSYK.

6.3 Investigating the effect of small molecule inhibitors on fibroblast-induced protection of CLL cells

Following this I investigated which intracellular signalling pathways are involved in fibroblast-mediated protection of CLL cells. CLL samples were treated with a range of different small molecule inhibitors which target specific proteins within various intracellular signalling pathways. The signalling pathways that were targeted included the MAPK pathway, PI3K/AKT pathway, NFκB pathway and JAK/STAT pathway. The inhibitor AZD6244 (AZD) was used to block the MAPK pathway by inhibiting MEK1/2 [322]. The inhibitors CAL-101 (CAL) and LY294002 (LY) were used to block the PI3K pathway by inhibiting PI3K [323, 324]. The inhibitor BAY-11-7082 (BAY) was used to block the NFκB pathway by inhibiting IKK [325]. The inhibitor CP-690550 (CP, Tofacitinib) was utilised to inhibit the JAK/STAT pathway by inhibiting JAK [326]. Additionally Ibrutinib (iBTK) [327] and R406 (iSYK) [215], a BTK and SYK inhibitor respectively, were also used determine if signalling downstream of these proteins is activated. The concentrations used have been previously tested and confirmed to work by other members of the lab as well as in published work [328, 329].

As fibroblast CM significantly up-regulated pERK expression in CLL samples (Figure 6.4) I initially investigated the effect of blocking the MAPK pathway on fibroblast-mediated protection of CLL cells. CLL samples were pre-treated with AZD for one hour and then washed with PBS prior to co-culture with fibroblasts. As HFFF2 cells express high levels of pERK this step was required to fully remove all traces of AZD that may reduce HFFF2 pERK expression and thus potentially affect their protective ability on CLL samples. CLL samples were either cultured alone as a control, or co-cultured with HFFF2 fibroblasts

Chapter 6

for 24 and 48 hours after which CLL cells were collected and their viability was analysed by FACS as described in section 5.2. Cells were co-cultured with HFFF2 cells in order to assess the effect of both HFFF2 direct contact and soluble factors on intracellular signalling pathways linked to CLL cell viability. Additionally, at the start of the experiment CLL cell viability was analysed at time-point 0.

Over time viability of CLL samples cultured alone declines as expected (Figure 6.7; blue line). As shown previously, co-culture with fibroblasts protected CLL cells from apoptosis (green line). Viability of CLL samples that were pre-treated with AZD and cultured alone is slightly lower than un-treated counterparts (black line), indicating that the inhibitor has a slight negative effect on CLL cell viability. Additionally CLL viability was lower in samples pre-treated with the inhibitor and co-cultured with fibroblasts compared to their un-treated counterparts (red line). However, this may be a result of the inhibitor inducing CLL cell death (as we see this effect from the black line), opposed to AZD blocking the protective effect of the fibroblasts. To correct for this, the difference in cell viability between CLL samples cultured alone (blue) and CLL samples pre-treated with AZD then cultured alone (black) was added onto the viability of CLL cells treated with AZD and co-cultured with fibroblasts (red) (i.e. red + (blue-black)). This is shown as the normalised graph in figure 6.7 (left).

This was performed with a total of 5 separate CLL samples (figure 6.8). **Samples were selected to comprise $\geq 80\%$ CLL cells to minimise analysing viability in contaminating cells.** As previously shown fibroblasts protect CLL samples from apoptosis at both 24 and 48 hours; this was significant at both time-points. Additionally, fibroblasts significantly protect CLL samples pre-treated with AZD, at both time-points. AZD partially blocks fibroblast-mediated protection on CLL cells however this reduction is not statistically significant at either time-point.

Washing cells with PBS after AZD treatment may partially wash out the inhibitor from the CLL cells, therefore rendering it less effective. Therefore I compared **the effect of 'washing out' the inhibitor with adding the inhibitor directly to the cells and leaving it in culture.** CLL samples were analysed for pERK expression after 48 hours of culture, by immunoblotting, to determine the efficacy of the

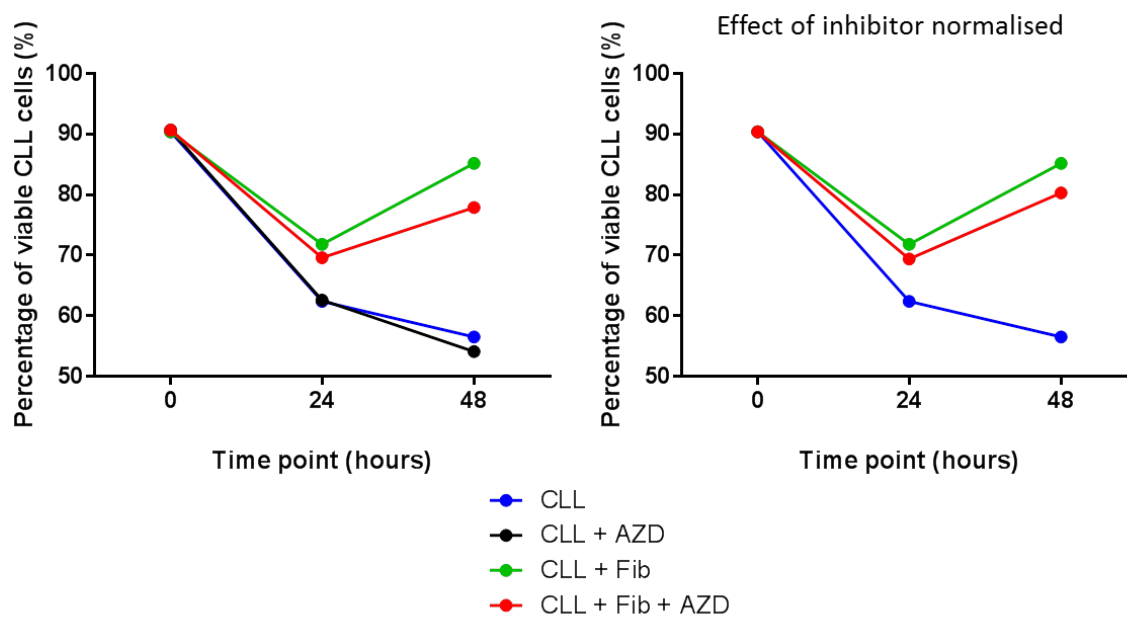


Figure 6.7: Correcting for inhibitor-induced apoptosis.

Graphs show the percentage of viable CLL cells when samples were cultured in complete RPMI-1640 media either alone as a control (blue), alone with AZD pre-treatment (black), co-cultured with fibroblasts (green) or co-cultured with fibroblasts with AZD pre-treatment (red), for 24 and 48 hours. CLL cells were cultured in complete RPMI-1640 media with or without AZD (10 μ M) for 1 hour at 37°C. Cells were then washed with PBS to remove excess AZD and cultured in respective conditions. CLL samples were also analysed at time-point 0. CLL viability after correction for inhibitor treatment is shown (right); this is the difference in CLL viability between CLL samples cultured alone and CLL samples pre-treated with AZD and cultured alone, added onto the CLL viability of samples pre-treated with AZD and co-cultured with HFFF2 cells, to allow for CLL cell death caused by AZD, (red + (blue-black)).

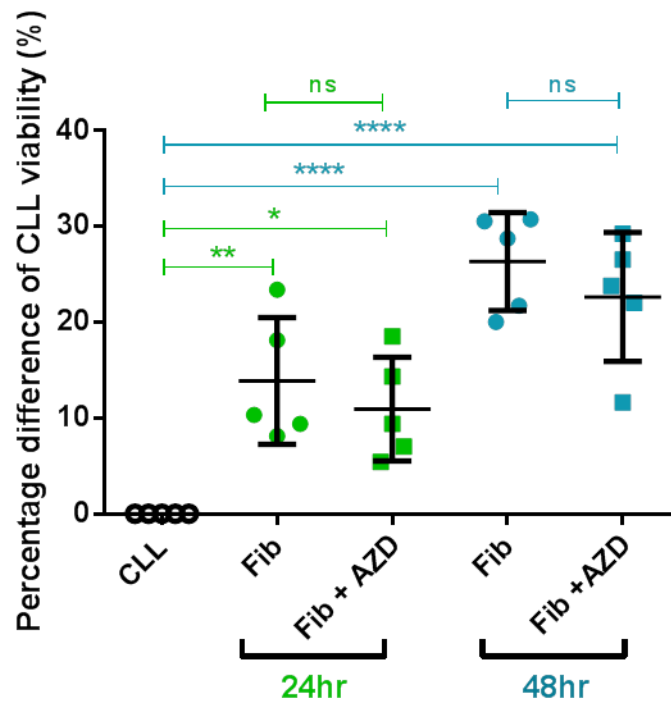


Figure 6.8: Effect of AZD on HFFF2 fibroblast-mediated protection of CLL cells.

Graph shows the percentage difference in CLL viability between CLL samples cultured alone (white circles) and CLL samples co-cultured with fibroblasts with or without inhibitor treatment. CLL samples were either cultured in complete RPMI-1640 media alone with or without AZD pre-treatment or co-cultured with fibroblasts with or without AZD pre-treatment, for 24 or 48 hours, prior to analysis of cell viability by FACS. CLL samples were cultured in complete RPMI-1640 media with or without AZD (10 μ M) for 1 hour at 37°C; cells were then washed once with PBS to remove excess AZD. The percentage of viable CLL cells shown has been corrected to exclude the effect of AZD on cell death. Each dot represents results from an individual CLL sample with mean (\pm SD). The statistical significance of the differences was analysed using one-way ANOVA with Bonferonni correction (n=5).

inhibitor (Figure 6.9, left). Additionally CLL viability was analysed by FACS analysis after 24 and 48 hours of culture (Figure 6.9, right).

Expression of pERK was low, or undetectable in CLL samples cultured alone, however after co-culture with fibroblasts pERK is up-regulated (Figure 6.9, left). As discussed above, it is difficult to know whether this is due to increased pERK in CLL cells or contamination by HFFF2 cells. When CLL samples were washed with PBS after AZD pre-treatment pERK expression is partially reduced. This reduction is much greater when AZD is left in culture as pERK expression is barely detectable, but again, it was not clear whether this was due to effects of AZD in CLL cells, in HFFF2 cells or in both.

As previously shown, CLL viability is higher in samples co-cultured with fibroblasts (green) compared to control cells cultured alone (blue) (Figure 6.9, right). Both AZD pre-treatment (red) and continuous treatment (black) partially blocked fibroblast-mediated CLL protection, however continuous treatment had a greater effect. This could be mediated by effects of AZD in HFFF2 cells, CLL cells, or both. Fibroblast viability was checked by eye prior to analysis for both pERK expression and CLL viability and cells appeared equally confluent and viable between conditions.

Based on these results, I decided to evaluate all the compounds in co-culture experiments, with continuous exposure. Although interpretation of effects were more complex (potentially acting on HFFF2 cells and/or CLL cells), this experimental set-up most clearly demonstrated the potential effects of chemical inhibition. Moreover, the decision to directly co-culture samples, with the addition of inhibitors, opposed to culture CLL cells in stromal cell-derived CM supplemented with inhibitors, was made as we wanted to keep the conditions in these assays as similar to the initial annexin V assays conducted in chapter 5. Also, it was believed that direct contact would have a greater effect on CLL cell viability, than soluble factors only, and therefore effects of the compounds used would be clearer. Moreover, this experimental set-up would not only highlight which signalling pathways are required to be induced within the CLL cells for their survival, but would also indicate which signalling pathways need to be active within the stromal cells, in order for them to protect the malignant cells from apoptosis. Thus, direct effects of inhibitors on stromal cells could also be important from a therapeutic point of view.

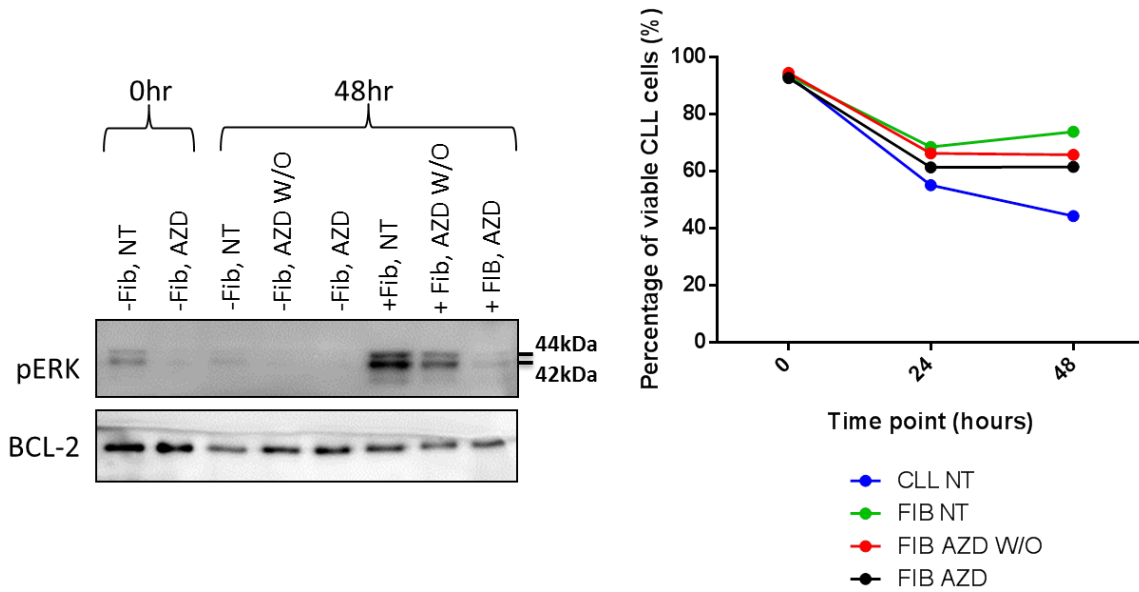


Figure 6.9: Comparison of the effect of AZD pre-treatment with continuous AZD treatment on CLL samples.

Left- The western blot shows pERK expression in CLL samples that were either pre-treated with AZD (10 μ M) for 1 hour then washed with PBS before being re-suspended in complete RPMI-1640 media (AZD W/O), or AZD was added to CLL samples and left in culture (AZD). CLL samples were then cultured in complete RPMI-1640 media either alone or in the presence of fibroblasts for 48 hours. Un-treated CLL samples were also analysed as a control. CLL cells were then collected and analysed for pERK and Bcl-2 (loading control) expression by immunoblotting. Right-The graph shows the percentage of viable CLL cells that were either not treated with AZD, pre-treated with AZD (10 μ M) for 1 hour then washed with PBS (AZD W/O; red line), or continuously treated with AZD (AZD; black line). CLL samples were then cultured in complete RPMI-1640 media either alone or in the presence of fibroblasts for 24 and 48 hours. CLL samples were then collected and cell viability was analysed by FACS. The percentage of viable cells plotted in the graph has been corrected to exclude the effect of AZD on cell death.

These assays were performed with five separate CLL samples using R406, four different samples using ibrutinib and CAL-101, and three different samples **using LY and AZD. Samples selected comprised $\geq 80\%$ CLL cells to minimise** analysing viability of contaminating cells. CLL samples were either cultured alone or co-cultured with fibroblasts with or without continuous inhibitor treatment. Prior to collection and analysis of CLL samples, fibroblasts were checked by eye for confluency and viability.

The inhibitors had no apparent effect on fibroblast confluency or viability (Figures 6.10-6.14, left). All inhibitors reduced CLL sample viability when cultured alone (not shown), to varying degrees; this has been corrected for in all graphs (Figures 6.10-6.15). Different samples were used for different inhibitors. Fibroblasts significantly protected CLL cells at both time-points but for some cohorts (LY and AZD treated) this was only significant at 48 hours. Additionally CLL viability was significantly reduced in cells co-cultured with fibroblasts which were continuously treated with R406, ibrutinib and CAL-101 at 48 hours only (Figure 6.10-6.12). CLL viability was also reduced in cells co-cultured with fibroblasts and continuously treated with LY or AZD compared to untreated control cells, however this was not statistically significant at either time-point (Figure 6.13 and 6.14), therefore the effect of these inhibitors were not pursued to the same extent and fewer samples were analysed.

The data indicate that blocking SYK and the PI3K/AKT pathway within CLL cells and HFFF2 cells significantly blocks fibroblast-mediated protection of CLL samples. To determine if this effect is a result of pathway inhibition exclusive to CLL cells I investigated whether HFFF2 cells express SYK and AKT.

HFFF2 cells were analysed for expression of total SYK, pSYK^{Y525/526} (left), total AKT and pAKT⁴⁷³ (right) expression by immunoblotting. I decided to analyse a different SYK phosphorylation site as earlier it was shown that HFFF2 cells do not express pSYK³⁵² (Figure 6.6). Therefore pSYK^{Y525/526} was analysed for further confirmation that SYK is not activated within HFFF2 cells. Additionally I wanted to eliminate the possibility that CLL cells induce SYK expression within fibroblasts so I also co-cultured HFFF2 cells with varying densities of CLL cells. CLL samples treated with soluble anti-IgM for 15 minutes were used as a positive control (Figure 6.16). This was performed once as I only wanted to check if HFFF2 cells express these proteins.

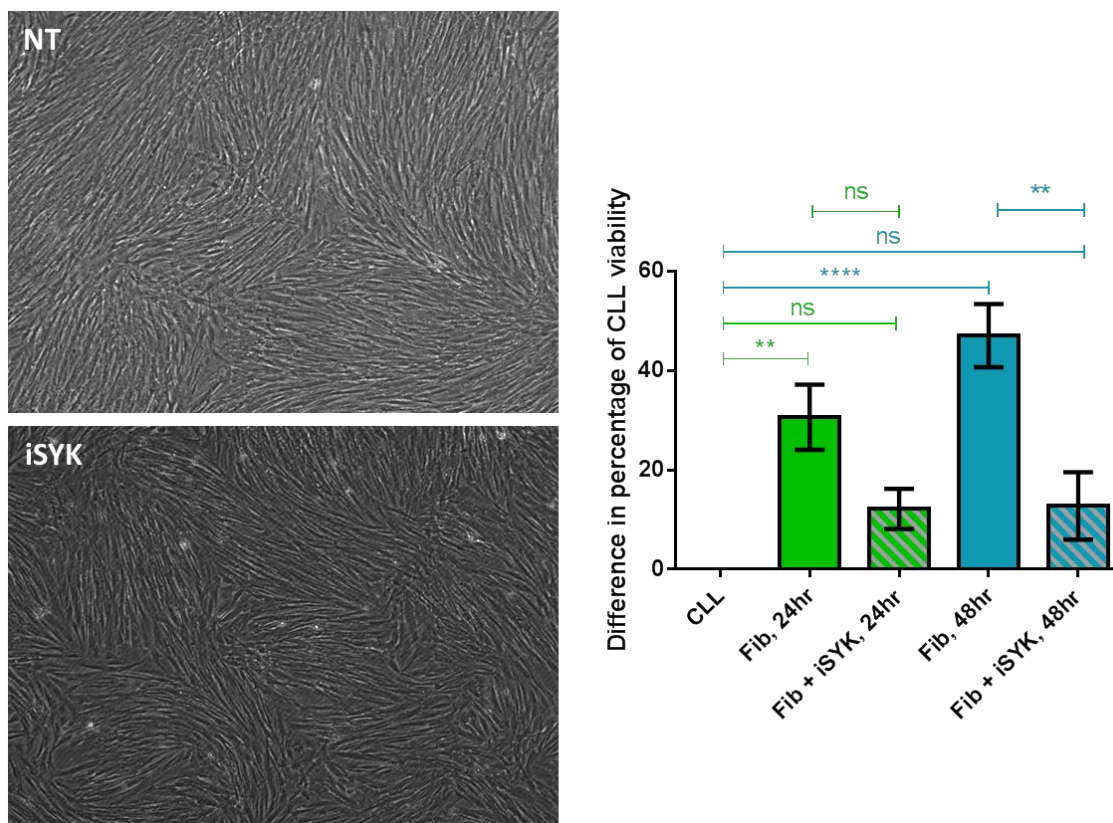


Figure 6.10: Effect of R406 on HFFF2 fibroblast-mediated protection of CLL cells.

Left- Images show HFFF2 fibroblasts that were co-cultured with CLL samples and either not treated with any inhibitors (top, NT) or continuously treated with 10 μ M R406 (bottom, iSYK) in complete RPMI-1640 media for 48 hours. CLL cells were removed prior to images being taken. Right- Graph shows the percentage difference in CLL viability between CLL samples cultured alone and CLL samples co-cultured with fibroblasts with or without R406 treatment. CLL samples were cultured in complete RPMI-1640 media and treated with 10 μ M R406 (iSYK). CLL samples were then either cultured alone as a control or in the presence of fibroblasts for 24 hours (green) or 48 hours (blue). CLL cells were collected and cell viability was analysed by FACS. The inhibitors were left in culture for the duration of this assay. Graph shows the mean (\pm SD) for all samples. The statistical significance of the differences was analysed using one-way ANOVA with Bonferroni correction (n=5). The image for NT control is the same as for iBTK (Figure 6.11) and AZD (Figure 6.14), as these treatments were conducted in the same assay.

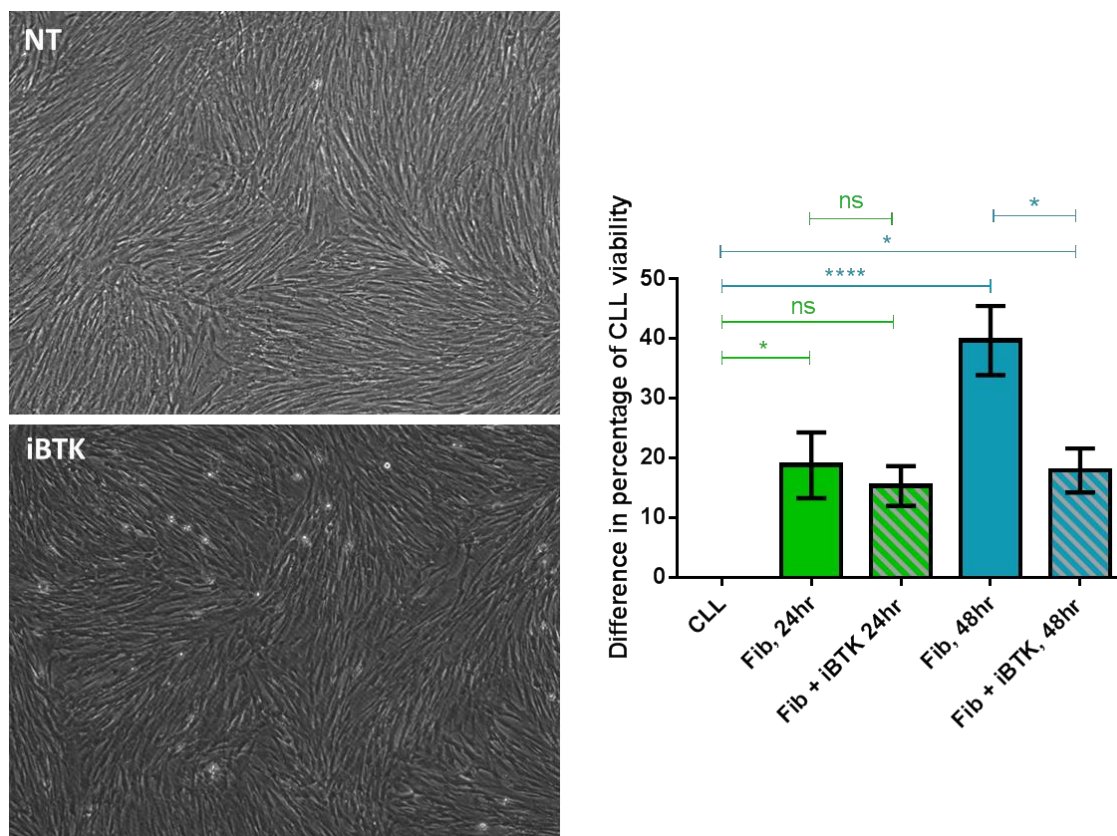


Figure 6.11: Effect of ibrutinib on HFFF2 fibroblast-mediated protection of CLL cells.

Left- Images show HFFF2 fibroblasts that were co-cultured with CLL samples and either not treated with any inhibitors (top, NT) or continuously treated with 10 μ M ibrutinib (bottom, iBTK) in complete RPMI-1640 media for 48 hours. CLL cells were removed prior to images being taken. Right- Graph shows the percentage difference in CLL viability between CLL samples cultured alone and CLL samples co-cultured with fibroblasts with or without ibrutinib treatment. CLL samples were cultured in complete RPMI-1640 media and treated with 10 μ M ibrutinib (iBTK). CLL samples were then either cultured alone as a control or in the presence of fibroblasts for 24 hours (green) or 48 hours (blue). CLL cells were collected and cell viability was analysed by FACS. The inhibitors were left in culture for the duration of this assay. Graph shows the mean (\pm SD) for all samples. The statistical significance of the differences was analysed using one-way ANOVA with Bonferroni correction ($n=4$). The image for NT control is the same as for iSYK (Figure 6.10) and AZD (Figure 6.14), as these treatments were conducted in the same assay.

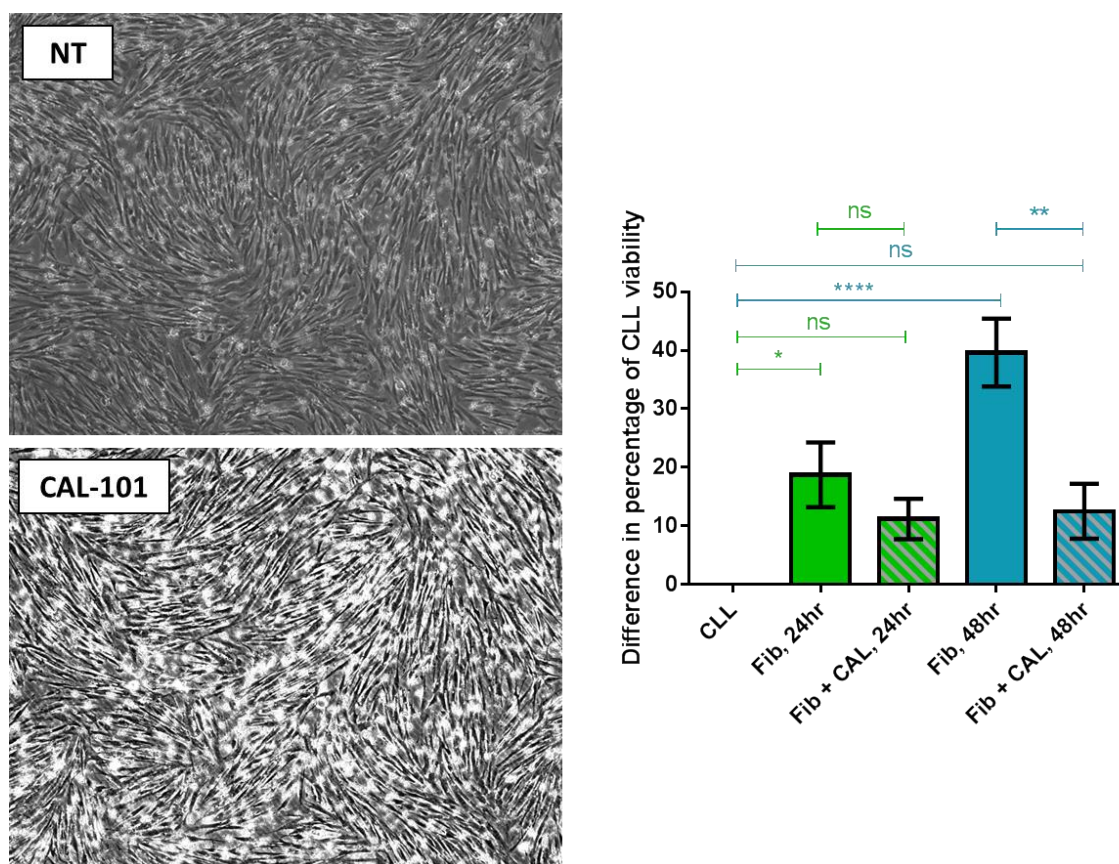


Figure 6.12: Effect of CAL-101 on HFFF2 fibroblast-mediated protection of CLL cells.

Left- Images show HFFF2 fibroblasts that were co-cultured with CLL samples and either not treated with any inhibitors (top, NT) or continuously treated with 10 μ M CAL-101 (bottom) in complete RPMI-1640 media for 48 hours. Images were taken prior to CLL sample removal. Right- Graph shows the percentage difference in CLL viability between CLL samples cultured alone and CLL samples co-cultured with fibroblasts with or without CAL-101 treatment. CLL samples were cultured in complete RPMI-1640 media and treated with 10 μ M CAL-101 (CAL). CLL samples were then either cultured alone as a control or in the presence of fibroblasts for 24 hours (green) or 48 hours (blue). CLL cells were collected and cell viability was analysed by FACS. The inhibitors were left in culture for the duration of this assay. Graph shows the mean (\pm SD) for all samples. The statistical significance of the differences was analysed using one-way ANOVA with Bonferroni correction (n=4)

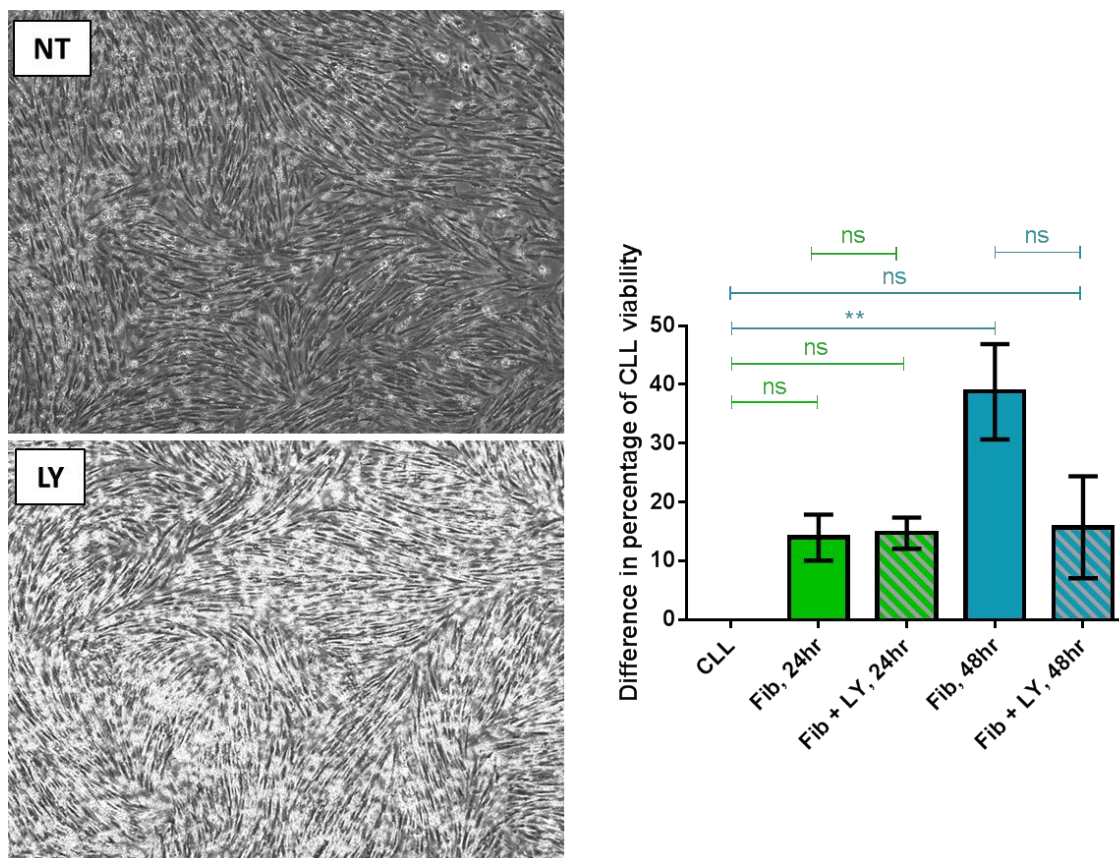


Figure 6.13: Effect of LY294002 on HFFF2 fibroblast-mediated protection of CLL cells.

Left- Images show HFFF2 fibroblasts that were co-cultured with CLL samples and either not treated with any inhibitors (top, NT) or continuously treated with 10 μ M LY294002 (bottom, LY) in complete RPMI-1640 media for 48 hours. Images were taken prior to CLL sample removal. Right- Graph shows the percentage difference in CLL viability between CLL samples cultured alone and CLL samples co-cultured with fibroblasts with or without LY treatment. CLL samples were cultured in complete RPMI-1640 media and treated with 10 μ M LY294002 (LY). CLL samples were then either cultured alone as a control or in the presence of fibroblasts for 24 hours (green) or 48 hours (blue). CLL cells were collected and cell viability was analysed by FACS. The inhibitors were left in culture for the duration of this assay. Graph shows the mean (\pm SD) for all samples. The statistical significance of the differences was analysed using one-way ANOVA with Bonferroni correction ($n=3$)

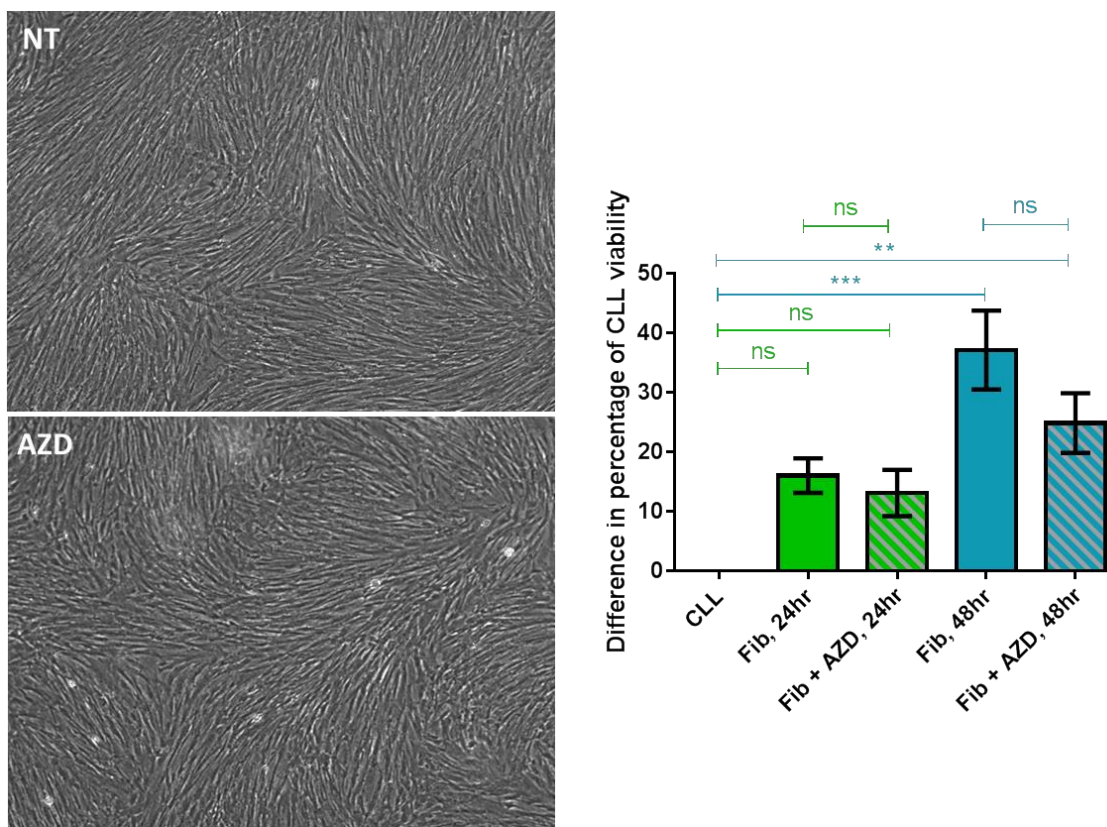


Figure 6.14: Effect of AZD6244 on HFFF2 fibroblast-mediated protection of CLL cells.

Left- Images show HFFF2 fibroblasts that were co-cultured with CLL samples and either not treated with any inhibitors (top, NT) or continuously treated with 10 μ M AZD6244 (bottom, AZD) in complete RPMI-1640 media for 48 hours. CLL cells were removed prior to images being taken. Right- Graph shows the percentage difference in CLL viability between CLL samples cultured alone and CLL samples co-cultured with fibroblasts with or without AZD6244 treatment. CLL samples were cultured in complete RPMI-1640 media and treated with 10 μ M AZD6244 (AZD). CLL samples were then either cultured alone as a control or in the presence of fibroblasts for 24 hours (green) or 48 hours (blue). CLL cells were collected and cell viability was analysed by FACS. The inhibitors were left in culture for the duration of this assay. Graph shows the mean (\pm SD) for all samples. The statistical significance of the differences was analysed using one-way ANOVA with Bonferroni correction ($n=3$). The image for NT control is the same as for iSYK (Figure 6.10) and iBTK (Figure 6.11), as these treatments were conducted in the same assay.

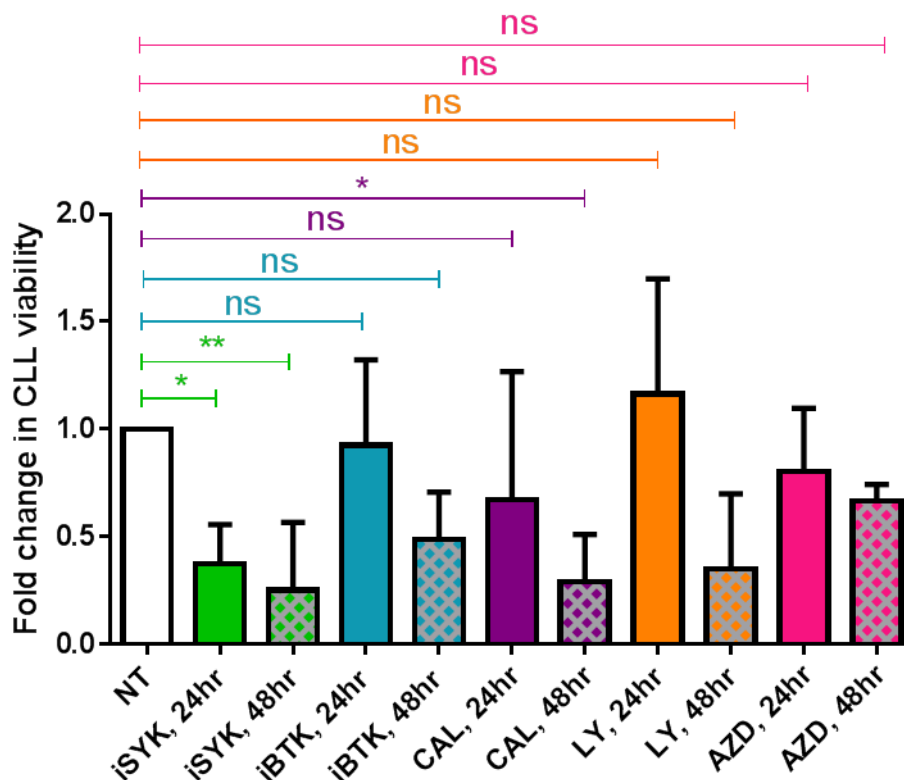


Figure 6.15: Effect of small molecule inhibitors on HFFF2 fibroblast mediated protection of CLL samples at 24 and 48 hours.

Graph shows the fold change in CLL viability between CLL samples co-cultured with fibroblasts (white) with or without inhibitor treatment. CLL samples were cultured in complete RPMI-1640 media with either 10 μ M R406 (iSYK (n=5), green), 10 μ M ibrutinib (iBTK (n=4), blue), 10 μ M CAL-101 (CAL (n=4), purple), 10 μ M LY294002 (LY (n=3), orange) or 10 μ M AZD6244 (AZD (n=3), pink). CLL samples were then cultured alone or co-cultured with fibroblasts for 24 and 48 hours. CLL cells were collected and cell viability was analysed by FACS. For each sample CLL viability in cells co-cultured with fibroblasts without inhibitor treatment has been set to 1.0. Graph shows mean (\pm SD) for all samples. The statistical significance of the differences was analysed by one-way ANOVA with Bonferroni correction.

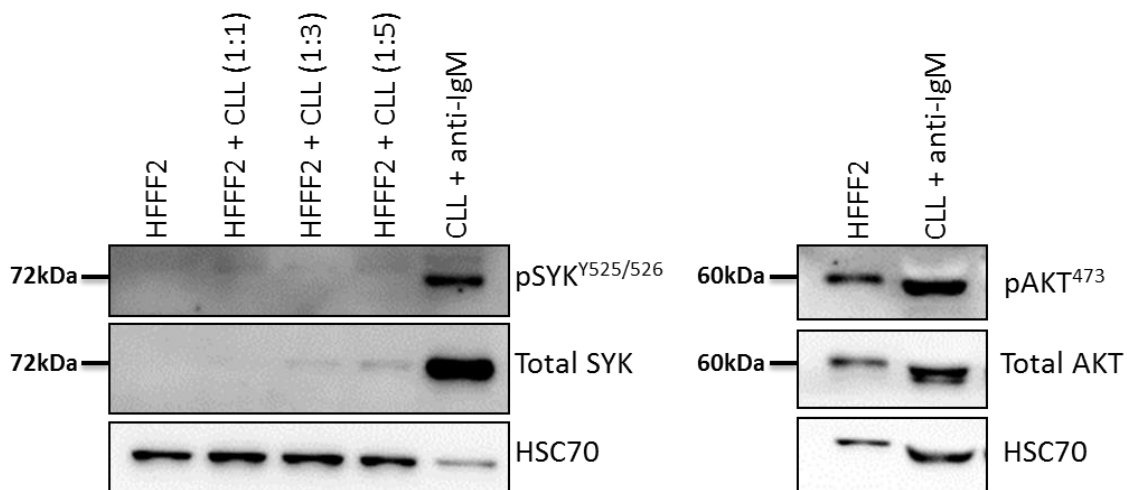


Figure 6.16: Expression of SYK and AKT in HFFF2 cells.

HFFF2 fibroblasts were cultured in complete RPMI-1640 media in the absence or presence of CLL cells at the indicated ratios (HFFF2:CLL) for 48 hours. CLL cells were removed by washing cells with PBS three times to ensure optimal removal. HFFF2 cells were then analysed for expression of total SYK and pSYK^{Y525/526} (left) or total AKT and pAKT⁴⁷³ (right) by immunoblotting. CLL cells were treated with soluble anti-IgM in complete RPMI-1640 media for 15 minutes as a positive control for both pSYK^{Y525/526} and pAKT⁴⁷³. HSC70 was used as the loading control. This was performed once.

HFFF2 cells do not express total SYK or pSYK^{Y525/526} even after co-culture with CLL cells (Figure 6.16, left), indicating that R406 should not have an effect on signalling pathways within these cells. However HFFF2 cells do express both total AKT and pAKT⁴⁷³ (Figure 6.16, right), therefore it is possible both CAL-101 and LY block PI3K/AKT signalling within HFFF2 cells.

The NFκB and JAK/STAT signal transduction pathways were also investigated using the same method described earlier. Fibroblast confluency and viability were checked by eye prior to analysis of CLL samples (not shown).

Fibroblast confluency remained comparable between conditions and viability did not appear to be affected by either CP or BAY. CP had no effect, but BAY had a partially negative effect on CLL viability when cells were cultured alone; this was corrected for when analysing the data (Figure 6.17). Blocking the JAK/STAT pathway with CP (green) had no effect on fibroblast protection of CLL cells (Figure 6.17). However, blocking the NFκB pathway using BAY (blue) enhanced the protective effect of fibroblasts at both time points, thus leading to increased CLL viability. However as it was clear that neither pathway was involved in fibroblast-induced protection of CLL cells only two CLL samples were analysed for each pathway and statistical analysis was not conducted (Figure 6.17).

Overall these results indicate that HFFF2 fibroblasts may induce intracellular signal transduction pathways downstream of SYK within CLL cells leading to their survival. Additionally the PI3K/AKT pathway may be involved in fibroblast-mediated protection of CLL cells, either through activation within CLL cells, HFFF2 cells, or both.

6.4 Investigating the effect of small molecule inhibitors on MCL-1 expression

Following this I investigated which intracellular signalling pathways mediate fibroblast induced up-regulation of MCL-1 in CLL cells. I focused on SYK, BTK and the PI3K/AKT pathway as R406, ibrutinib, CAL-101 and LY294002 had the greatest effects on blocking fibroblast-mediated protection of CLL cells (Figures 6.10-6.12).

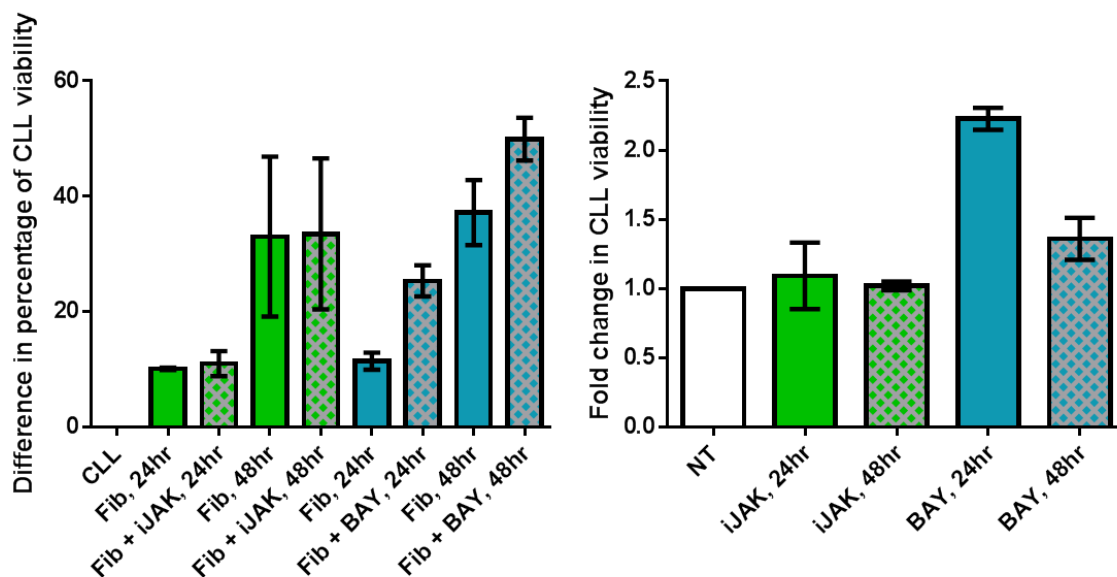


Figure 6.17: Effect of blocking the NFκB and JAK/STAT signalling pathways on HFFF2 fibroblast-mediated protection of CLL cells.

CLL cells were cultured alone or co-cultured with fibroblasts, with or without addition of 50 nM BAY-11-7082 (BAY, green) and 10 μM CP-690550 (CP, blue) to inhibit the NFκB and JAK/STAT signalling pathways respectively, for 24 and 48 hours. The percentage difference in CLL viability between CLL samples cultured alone and cells co-cultured with fibroblasts with or without inhibitor treatment are shown (left). The fold change in CLL viability between CLL samples co-cultured with fibroblasts with or without inhibitor treatment are also shown (right). Graphs show mean (±SD) for both samples (n=2).

CLL cells were cultured in fibroblast-derived CM, with or without continuous treatment of small molecule inhibitors. As before, the experiments were based on CM, rather than direct co-culture, to avoid potential contamination of CLL cells by HFFF2 cells. CM was derived from HFFF2 cells cultured in complete RPMI-1640 media for 72 hours. After 24 hours of culture CLL samples were collected and analysed for MCL-1 expression by immunoblotting. This time-point was selected as MCL-1 expression is significantly higher in CLL samples cultured in fibroblast CM compared to control cells, by 24 hours. CLL samples were also cultured in complete RPMI-1640 media for 24 hours as a control, as well as analysed at 0 hours.

Four separate CLL samples were utilised for analysis of R406 and LY294002, and five separate samples were analysed for ibrutinib and CAL-101. Samples **selected comprised $\geq 80\%$ CLL samples to minimise analysing viability in** contaminating cells. MCL-1 expression in CLL samples is high at 0 hours but there is a clear reduction by 24 hours in control cells cultured in complete RPMI-1640 media (Figure 6.18). As shown before MCL-1 expression is higher in CLL samples cultured in fibroblast CM compared to control cells, at 24 hours, however this increase was only statistically significant for cohorts treated with R406 and CAL-101 (Figures 6.18 and 6.19). Additionally all 4 inhibitors significantly reduced MCL-1 expression in CLL samples cultured in CM compared to control cells (Figure 6.20).

Overall these results indicate that soluble factor(s) released by HFFF2 fibroblasts induce MCL-1 expression in CLL cells by activating SYK, BTK and the PI3K/AKT pathway within the malignant cells, thus encouraging their survival.

Due to time constraints the blocking activity of all the inhibitors utilised was not confirmed. As R406 had the greatest effect on blocking the protective effect of fibroblasts I prioritised checking the activity of this inhibitor. CLL samples were cultured in complete RPMI-1640 media with or without R406 continuous treatment for 24 hours. Cells were then collected and analysed for pERK as it is downstream of SYK. As earlier data showed that HFFF2 fibroblasts increase pSYK expression in CLL samples (Figure 6.6) I also analysed the effect of R406 on CLL samples in the presence of fibroblasts. Therefore samples were additionally cultured in fibroblast CM and directly co-cultured with fibroblasts. This was performed on 2 separate CLL samples.

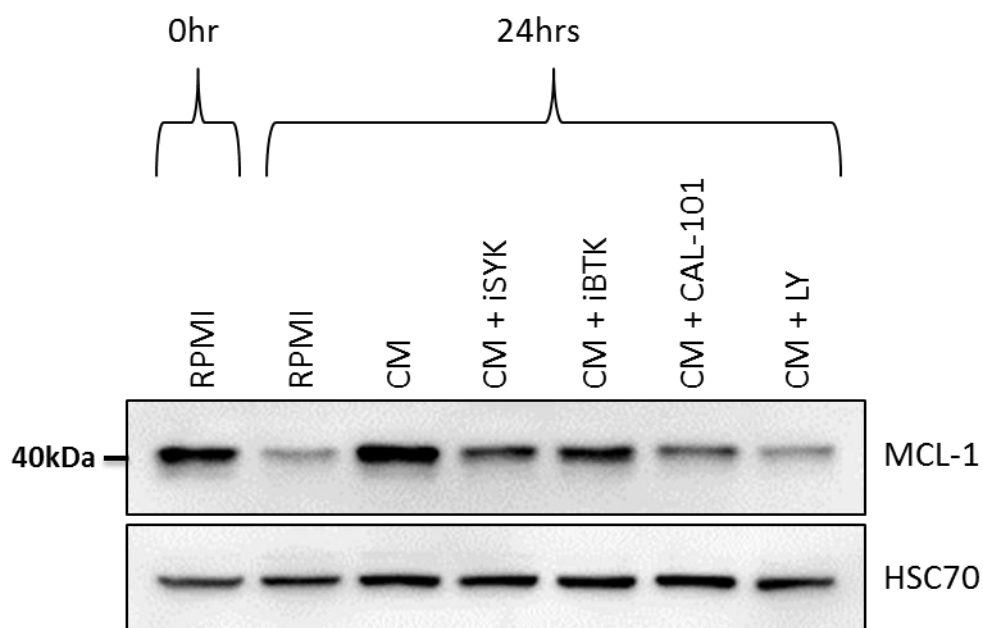


Figure 6.18: Effect of small molecule inhibitors on MCL-1 expression in CLL cells.

CLL samples were cultured in either complete RPMI-1640 media as a control or cultured in fibroblast-derived CM in the absence or presence of various small molecule inhibitors. CM was derived from HFFF2 cells cultured in complete RPMI-1640 media for 72 hours. CLL cells were cultured in fibroblast-derived CM supplemented with R406 (iSYK, 10 μ M), ibrutinib (iBTK, 10 μ M), CAL-101 (10 μ M) and LY24900 (LY, 10 μ M) for 24 hours. Inhibitors were left in culture for the full 24 hour period. CLL samples were then collected and analysed for MCL-1 and HSC70 (loading control) by immunoblotting. CLL samples were also analysed at 0 hours. Data is representative of 4 separate CLL samples for R406 and LY treatment, and 5 separate CLL samples for ibrutinib and CAL-101 treatment.

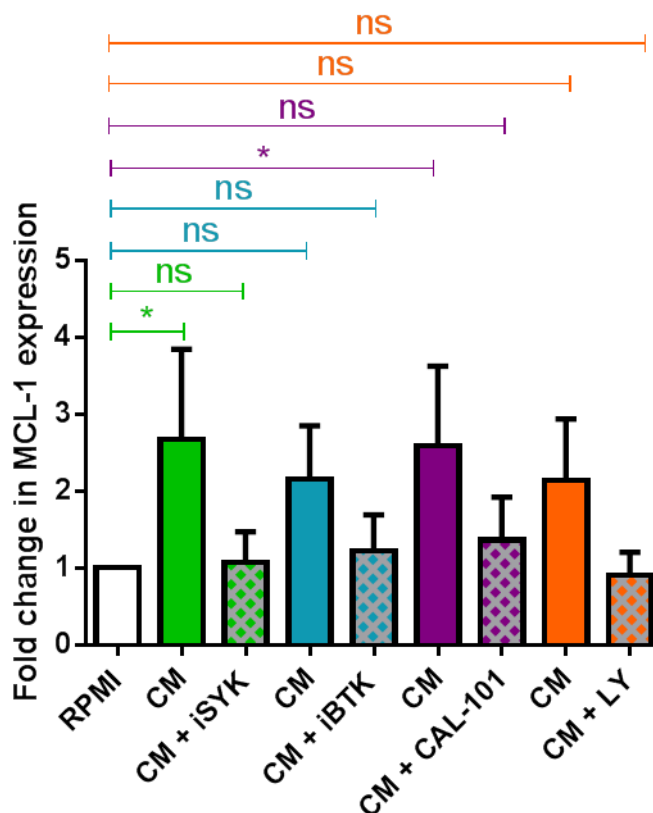


Figure 6.19: Effect of inhibitors on MCL-1 expression in CLL samples.

Graph shows the fold change in MCL-1 expression between CLL samples cultured in complete RPMI-1640 media and CLL samples cultured in fibroblast-derived CM with or without inhibitor treatment. Fibroblast CM was derived from HFFF2 cells in complete RPMI-1640 media for 72 hours. CLL cells were cultured in fibroblast CM with or without 10 μ M R406 (iSYK (n=4), green), 10 μ M ibrutinib (IBTK (n=5), blue), 10 μ M CAL-101 (n=5, purple) and 10 μ M LY24900 (LY (n=4), orange). CLL samples were also cultured in complete RPMI-1640 media as a control (white bar). After 24 hours CLL cells were collected and analysed for MCL-1 expression by immunoblotting. For all samples, MCL-1 expression in cells cultured in complete RPMI-1640 media was set to 1.0. Graph shows mean (\pm SD) for all samples. The statistical significance of the differences was analysed using one-way ANOVA with Bonferroni correction.

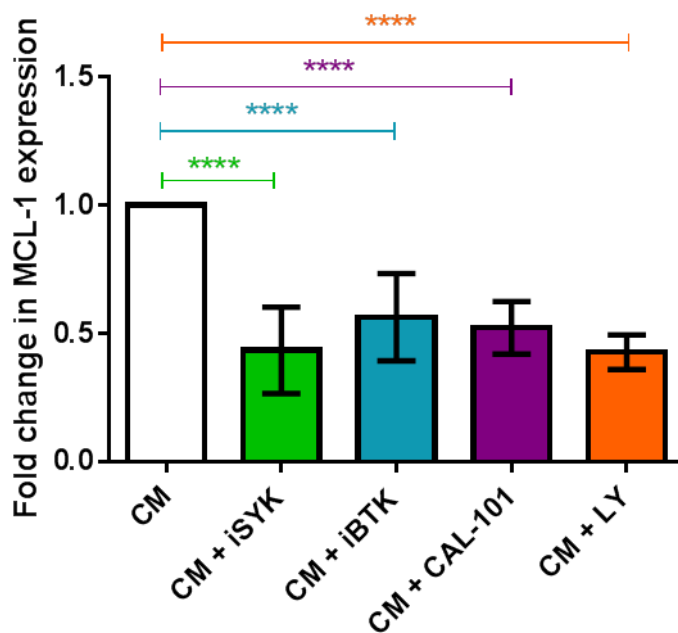


Figure 6.20: Comparison of the effect of inhibitors on MCL-1 expression in CLL samples.

Graph shows the fold change in MCL-1 expression between CLL samples cultured in fibroblast CM with or without inhibitor treatment. Fibroblast CM was derived from HFFF2 cells in complete RPMI-1640 media for 72 hours. CLL cells were cultured in fibroblast CM with or without R406 (iSYK 10 μ M (n=4), green), ibrutinib (iBTK 10 μ M (n=5), blue), CAL-101 (10 μ M (n=5), purple) and LY294002 (LY 10 μ M (n=4), orange) for 24 hours. CLL cells were collected and analysed for MCL-1 expression by immunoblotting. For each sample MCL-1 expression of cells cultured in fibroblast CM was set to 1.0. Graph shows mean (\pm SD) for all samples. The statistical significance of the differences was analysed using one-way ANOVA with Bonferroni correction.

As previously shown (Figures 6.1 and 6.4), pERK expression was higher in CLL cells cultured in fibroblast CM or co-cultured with fibroblasts compared to control cells cultured in complete RPMI-1640 media. Treatment with R406 however reduced pERK expression in all conditions indicating that R406 is effectively inhibiting SYK expression (Figure 6.21). This trend was observed in the other CLL sample analysed.

6.5 Discussion

Multiple studies have shown that various types of stromal cells protect CLL cells from apoptosis including BM-derived stromal cells, FDCs and NLCs [128, 214, 318]. Additionally, increasing evidence suggests that CLL cells avoid both spontaneous and treatment induced apoptosis *in vivo* by infiltrating specific microenvironments within which they are protected by stromal cells, such as the ones listed above. This allows CLL cells to acquire resistance to treatments, consequently leading to minimal residual disease (MRD) which ultimately resulting in patient relapse [127]. Therefore targeting the intracellular signal transduction pathways responsible for the mechanisms behind stromal cell-induced protection of CLL cells could lead to novel therapeutic strategies which aim to make CLL cells insensitive to stromal cell protection. Data described in chapter 5 suggest that fibroblasts and myofibroblasts protect CLL cells from apoptosis, but fibroblasts have a superior protective effect. Therefore the main aim of the results obtained in this chapter was to determine which intracellular signalling pathways are involved in fibroblast-mediated protection of CLL cells.

This was investigated by culturing CLL cells in HFFF2 fibroblast CM to determine which intracellular signalling pathways are activated within CLL cells by analysing expression of various phospho-proteins. Following this I investigated which signal transduction pathways are involved in fibroblast mediated protection of CLL cells by co-culturing CLL cells with fibroblasts in conjunction with treatment of various small molecule inhibitors known to target specific intracellular signalling pathways. Finally I investigated which intracellular signalling pathways are involved in fibroblast-mediated induction, or maintenance, of MCL-1 in CLL cells by culturing the malignant cells in fibroblast CM.

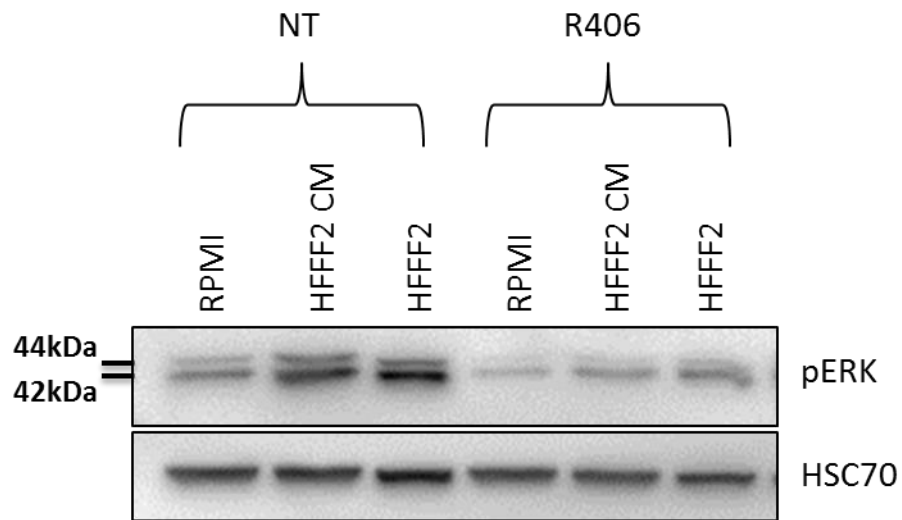


Figure 6.21: Effect of R406 on pERK expression in CLL cells.

Western blot shows pERK and HSC70 (loading) expression in CLL cells that were cultured in complete RPMI-1640 media as a control, HFFF2 fibroblast CM or co-cultured with HFFF2 fibroblasts in complete RPMI-1640 media, with or without addition of R406 (10 μ M) for 24 hours. CM was derived from HFFF2 cells in complete RPMI-1640 media for 72 hours. CLL cells were collected and analysed for pERK expression by immunoblotting. Data is representative of 2 separate CLL samples.

6.5.1 Determining which signalling pathways effect fibroblast-induced CLL survival

The main conclusion from the data obtained in this chapter is that SYK and the PI3K/AKT pathway are implicated in HFFF2 fibroblast-mediated protection of CLL cells. Inhibiting SYK and PI3K in CLL-HFFF2 fibroblast co-cultures utilising the small molecule inhibitors R406 and CAL-101, respectively, effectively blocked fibroblast-induced protection of CLL cells as shown by reduced levels of CLL viability. Additionally culturing CLL cells in fibroblast CM supplemented with inhibitors against SYK, BTK and PI3K significantly blocked fibroblast induced up-regulation of the anti-apoptotic protein MCL-1 within CLL cells. Collectively these data suggest that fibroblasts activate various signalling pathways downstream of SYK, one of which could be PI3K/AKT, resulting in the prevention of MCL-1 up-regulation, thus inducing CLL cell death.

Expression of pAKT⁴⁷³ was higher in CLL cells cultured in HFFF2 fibroblast CM compared to control cells; however this was not statistically significant. As this was a small cohort analysing more samples may be required to reach statistical significance. Thus it is unsurprising that blocking PI3K, using CAL-101, significantly blocked fibroblast-mediated protection and MCL-1 up-regulation, in CLL cells. However, blocking PI3K utilising LY did not have a significant effect on fibroblast-mediated protection, but did significantly prevent MCL-1 up-regulation.

The PI3Ks are a family of kinases which fall into 4 different classes ranging from class I-IV. Class I PI3K have been the most extensively studied and can be further divided into class 1A and 1B, the former of which consist of PI3Ks composed of a regulatory (p85) and a catalytic (p110) subunit. p110 exists in 3 isoforms, α , β and δ . **CAL-101 specifically targets the p110 δ subunit of PI3K**, which is primarily expressed in haematopoietic lineages including B lymphocytes [221, 323, 330]. CAL-101 is effective across a broad range of B-cell malignancies including CLL, acute B lymphoblastic leukaemia (B-ALL), acute myeloid leukaemia (AML) and multiple myeloma (MM) [323, 331]. On the other hand, although LY294002 specifically blocks PI3K, it has a broad inhibitory effect across the PI3K classes and typically targets all class I PI3Ks [332]. This difference in inhibitor specificity between CAL-101 and LY may account for the variable degree in their ability to block fibroblast-induced protection of CLL cells. Although, as LY is broader acting than CAL-101 it

could be assumed that the former would have a greater blocking effect, however this was not the case. This could partly be due to LY interfering with a wider range of signalling pathways downstream of PI3K. A previous study showed that LY is implicated in inhibiting NF κ B transcription factors [333]. **Interestingly blocking the NF κ B pathway** appeared to enhance fibroblast-mediated protection of CLL cells (Figure 6.16), thus possibly counteracting the effect of LY in preventing fibroblast protection.

Additionally, as the inhibitors were added directly to CLL-HFFF2 co-cultures, it is unclear to what extent the inhibitors affected the stromal cells. AKT is expressed in HFFF2 cells therefore it is likely signalling within the stromal cells was affected by these inhibitors. However, due to the differences in inhibitor specificity, the extent at which they affected PI3K/AKT signalling within the stromal cells may have also differed. As mentioned above, **PI3K δ** is primarily expressed within haematopoietic cells. As CAL-101 specifically acts on this isoform, compared to LY which is broader acting, it is possible that CAL-101 affected the HFFF2 cells to a lesser extent than LY. This could be investigated by culturing HFFF2 cells in the presence of these inhibitors and comparing their impact on pAKT expression by immunoblotting. However the cohort analysed was small therefore more samples could be investigated to clarify whether these two PI3K inhibitors effect fibroblast-induced protection of CLL cells to different degrees. Interestingly, both inhibitors blocked fibroblast mediated MCL-1 up-regulation to similar degrees. For these assays CLL cells were cultured in fibroblast CM, therefore the inhibitors only affected signalling within the malignant cells. As LY significantly blocked MCL-1 in these CM assays, yet was less effective in the co-culture assays, this further suggests that LY and CAL-101 affected HFFF2 cells to different extents.

The PI3K/AKT pathway is implicated in BCR signalling. Previous data has suggested that utilising CAL-101 to block PI3K signalling downstream of the BCR can block CLL protection conferred by NLCs [334]. Additionally PI3K/AKT signalling can be induced in response to activation of CD44, a type 1 transmembrane glycoprotein receptor which is expressed by CLL cells [154]. Previous data has shown that signalling through this receptor via the PI3K/AKT pathway protects CLL cells from both spontaneous and drug-induced apoptosis by increasing MCL-1 expression [154]. Furthermore, utilising siRNA to delete CD44 in E μ -TCL1 transgenic mice reduced MCL-1 expression and

increased cell death [335]. The main ligand for CD44 is hyaluronic acid, however it also binds various extracellular ligands such as fibronectin and collagen which are both expressed by fibroblasts and myofibroblasts [151, 316, 336]. This suggests that fibroblasts may protect CLL cells by activating intracellular signalling pathways downstream of the BCR and CD44. This could be investigated by treating CLL cells with inhibitory antibodies against these receptors prior to co-culture with fibroblasts, such as the anti-CD44 antibodies, IM7 and A3D8, which have been shown to reduce CLL viability in cells co-cultured with stromal cells through MCL-1 reduction [335].

SYK has multiple phosphorylation sites [337]. When the B-cell receptor (BCR) is activated SYK is initially phosphorylated at its tyrosine-352 site (pSYK³⁵²) by src-family kinases which leads to trans-autophosphorylation at its 525/526 sites (pSYK^{525/526}) [337]. Multiple attempts were made to examine the expression of pSYK^{525/526}, with no success as the protein was difficult to detect, at which point pSYK³⁵² was analysed and shown to be up-regulated within CLL cells cultured in fibroblast CM compared to control cells. Unfortunately only two samples were analysed due to time constraints and thus statistical analysis was not conducted. More samples should be analysed to confirm the effect of HFFF2 fibroblasts on CLL pSYK³⁵² expression. However, as R406 significantly blocked fibroblast mediated protection and MCL-1 expression within CLL cells this indicates a principle role for SYK within these protective mechanisms. This is consistent with previous data which has demonstrated that R406 treatment blocks CLL protection conferred by anti-IgM stimulation and NLC co-culture [215]. Additional data has shown that other highly selective SYK inhibitors, PRT318 and P505-15, also block NLC-induced and BCR-induced protection of CLL cells [334]. These data suggest that HFFF2 fibroblast-induced SYK activation within CLL cells could potentially be due to BCR activation. However, although SYK is a key mediator of BCR signalling in CLL cells it also acts independent of the BCR to promote CLL cell migration and adhesion [215, 334]; therefore we cannot eliminate the possibility of other receptor involvement. Furthermore as SYK expression was not detected within HFFF2 cells it is unlikely R406 affected signalling within these cells.

Blocking BTK using ibrutinib partially blocked fibroblast mediated protection of CLL cells and significantly blocked MCL-1 up-regulation. Ibrutinib has had promising activity in early CLL clinical trials and is now a licenced drug both

here in the UK and in the USA. It is able to block CLL proliferation both *in vivo* and *in vitro* [338]. BTK acts downstream of the BCR, toll like receptors and in response to CD40 ligation [339, 340]. Ibrutinib has been shown to block BTK phosphorylation in BCR and CD40 stimulated cells, resulting in the inhibition **of various signalling pathways including the MAPK, PI3K/AKT and NFκB** pathways [328, 338]. This suggests that signalling through the BCR and TLRs could potentially be responsible for HFFF2 fibroblast-mediated activation of BTK, resulting in the induction of various signalling pathways including the PI3K/AKT pathway, which is involved in fibroblast-induced CLL viability and MCL-1 up-regulation (Figures 6.15 and 6.20). However, expression of BTK was not analysed within HFFF2 cells therefore it is uncertain whether ibrutinib affected signalling downstream of BTK in CLL cells exclusively. To determine this BTK expression should be analysed within HFFF2 cells by immunoblotting. However, similar to LY, ibrutinib had a greater effect on blocking MCL-1 expression than CLL viability, indicating that this inhibitor may have affected signalling within HFFF2 cells.

Previous data have shown that blocking BTK and PI3K signalling, using ibrutinib and CAL-101 respectively, promotes CLL cell egress from the tissue, into the blood. The data shown here indicates that ibrutinib and CAL-101 can partially block fibroblast-induced protection, *in vitro*. Thus, the ability of both these inhibitors to mediate stromal cell protection may be limited, *in vivo*, as the malignant cells may not be in direct contact with the fibroblasts, due to their induced redistribution into the blood.

Expression of pERK was significantly higher in CLL cells cultured in fibroblast CM. This supports previous data which has demonstrated that SDF-1 secreted by NLCs can induce activation of the p44/42 MAPK signalling pathway within CLL cells [128]. Moreover pERK expression was up-regulated to a greater extent than pAKT⁴⁷³. However when MAPK signalling was inhibited within CLL-HFFF2 cultures utilising AZD, there was only a partial reduction in CLL cell survival. Additionally, HFFF2 cells express extremely high levels of pERK; therefore it is likely AZD inhibited MAPK signalling within the stromal cells, as well as within CLL cells. This suggests that MAPK signalling is not principle in protecting CLL cells. Previous work has demonstrated that the protective effect of BM stromal cells was significantly reduced when the MAPK p38 was inhibited within CLL cells [341]. This is a separate branch of the MAPK pathway to pERK,

therefore indicating the MEK/ERK branch may not have a principle role in fibroblast-mediated protection but other pathways within this cascade do. To test this, CLL-HFFF2 co-cultures could be treated with different small molecule inhibitors which specifically target proteins within the other MAPK branches.

Inhibition of the JAK/STAT signalling pathway using CP-690550 did not alter CLL viability after HFFF2 co-culture thus indicating that this pathway has no effect on fibroblast mediated protection of CLL cells. The JAK/STAT pathway appears to have differential effects on CLL cells. A previous study demonstrated that treating CLL cells with IL-15 induced phosphorylation of STAT5 which led to CLL cell proliferation [342]. Conversely treatment with IL-21 induced phosphorylation of STAT1 and STAT3 which promoted apoptosis [342]. However there does not appear to be any clear evidence in the literature that stromal cells protect CLL cells through activating the JAK/STAT pathway. Interestingly, inhibiting the NFκB pathway using BAY-11-7082 appeared to enhance the protection conferred by HFFF2 fibroblasts, indicating that the NFκB pathway inhibits the protective effect of fibroblasts on CLL cells. This is surprising as the **NFκB pathway generally has a pro-survival effect** in CLL [343]. Also this is not consistent with earlier data which has shown that the induction of the NFκB pathway within BM stromal cells is vital for CLL cell survival [344]. Additionally co-culture with murine fibroblasts has been shown to maintain basal levels of NFκB within CLL cells thus supporting their survival [345]. Overall this is not definitive evidence for either the JAK/STAT or NFκB pathways as only two samples were analysed and statistical analysis cannot be conducted, thus more samples need to be analysed.

It is also important to note that these compounds may have potential off-target effects. For instance one study observed highly toxic effects of BAY on both primary MM cells and an MM cell line which were found to occur **independent of NFκB pathway activation** [233]. Off-target effects would impact the degree of protection conferred by stromal cells, as it could affect the ability of the stromal cells to protect the malignant cells or it could cause the CLL cells to become more resistant/sensitive to stromal cell protection.

Data described in chapter 5 showed that HFFF2 myofibroblasts also protect CLL cells from apoptosis and up-regulate their expression of MCL-1, but to a lesser extent than HFFF2 fibroblasts. The signalling pathways activated within CLL cells were only analysed in response to fibroblasts but it would be

Chapter 6

interesting to determine if myofibroblasts can activate the same pathways, but to a lesser extent, thus following the same trend seen in CLL viability and MCL-1 expression. This would provide additional support for which signalling pathways are implicated in these protective mechanisms.

A drawback to the annexin V co-culture assays is the uncertainty of whether the inhibitors are affecting signalling within CLL cells, HFFF2 cells or both. To avoid this, the annexin V assays could be conducted utilising fibroblast and myofibroblast-derived CM, opposed to direct co-culture. Unpublished data by Elizabeth Lemm has demonstrated that HFFF2 fibroblast-CM protects CLL cells from apoptosis to levels comparable with direct co-culture (Appendix, A.2). The data in appendix A.2 differs from my data as CLL cells were cultured in CM derived from HFFF2 fibroblasts, in the absence of fibroblasts, and therefore only shows the extent of fibroblast induced protection of CLL cells, as determined by the soluble factors released by the stromal cells. There is no direct contact between the CLL cells and the HFFF2 cells, whereas my assays probe the effect of both soluble factors and direct cell-to-cell contact, between the malignant cells and stromal cells.

Another drawback to these assays was that due to time constraints only the efficacy of AZD and R406 were confirmed. Both inhibited pERK expression indicating they were working effectively. Although the remaining inhibitors were not checked, the same concentrations were used that are routinely utilised by other members within the lab and cited in published work [328, 329]. Additionally all the inhibitors had a negative impact on CLL viability in cells cultured alone, indicating the detrimental effect of blocking these pathways, which again has been documented [231, 346].

Potential variation in stromal cell viability between treated and un-treated conditions is another drawback to these assays. This would impact the data as variances would affect the degree of protection passed onto CLL cells and therefore alter mediation of intracellular signalling pathways. Fibroblasts were checked by eye at all time-points after co-culture and the inhibitors had no apparent effect on HFFF2 viability, as determined by normal fibroblast morphology and cell attachment. However to confirm this, more accurate methods could be conducted. Immunoblotting could be utilised to determine if expression of caspases and PARP cleavage was comparable between fibroblasts and myofibroblasts, post-culture.

6.5.2 Summary

- Soluble factors released by fibroblasts activate intracellular signalling pathways downstream of SYK, including the PI3K/AKT and MAPK signalling pathways; this was demonstrated by increased expression of pSYK³⁵², pAKT⁴⁷³ and pERK within CLL cells cultured in fibroblast-derived CM, respectively (Figure 6.22).
- Fibroblast-induced up-regulation of MCL-1 expression and CLL survival appear to be counteracted when SYK, the PI3K/AKT pathway, and possibly BTK were inhibited. This suggests that induction of these signalling pathways may up-regulate expression of the anti-apoptotic protein MCL-1 resulting in protection of CLL cells from apoptosis. Therefore, targeting these intracellular signalling pathways may result in CLL cell resistance to fibroblast protection.

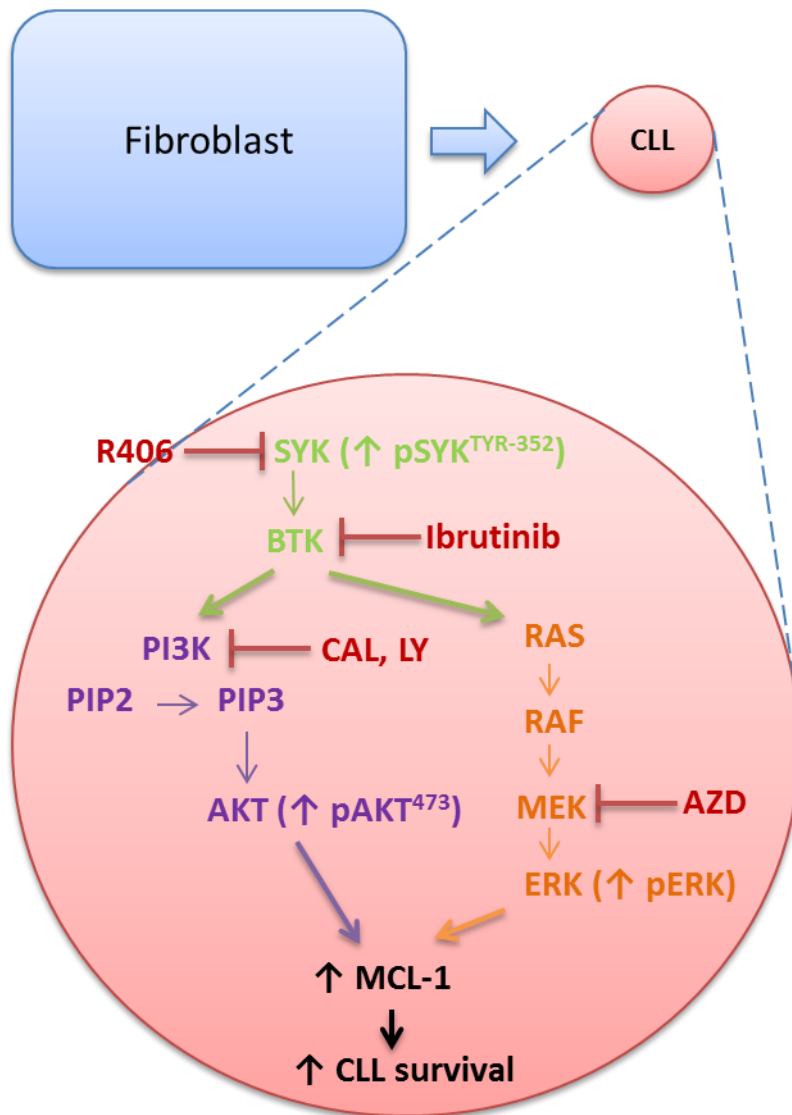


Figure 6.22: Effect of HFFF2 fibroblasts on intracellular signalling within CLL cells.

Diagram shows the effect of HFFF2 fibroblasts on intracellular signalling pathways, MCL-1 expression and survival within CLL cells. In response to HFFF2 fibroblasts (blue), expression of pSYK³⁵², pERK and pAKT⁴⁷³ are up-regulated in CLL cells (red circle). This leads to an increase in MCL-1 expression resulting in increased CLL cell survival. Small molecule inhibitors are shown in red; R406 inhibits SYK, ibrutinib inhibits BTK, CAL-101 (CAL) and LY294002 block PI3K, and AZD6244 (AZD) blocks MEK. The PI3K/AKT signalling pathway (purple) and the MAPK signalling pathway (orange) are shown.

Chapter 7:

Final Discussion

7.1 Basis of project

The main aim of this project was to investigate the interactions between CLL cells, and fibroblasts and myofibroblasts. Multiple studies have shown that various types of stromal cells protect CLL cells from both spontaneous and drug-induced apoptosis, including NLCs and FDCs [133, 214]. However the effect of myofibroblasts on CLL cell survival has not been previously examined, and thus the clinical consequence of these cells in CLL has not yet been evaluated. In solid tumours the presence of myofibroblasts correlates with aggressive disease progression and poor clinical outcome as has been observed for multiple types of cancer [171, 172, 174]. Thus the bi-directional communication between CLL cells, and fibroblasts and myofibroblasts was investigated.

7.2 Summary of key findings

- Chapter 3: The main aim of the immunohistochemical studies in this chapter was to determine whether myofibroblasts are present within the CLL tissue microenvironment.
 - α -SMA positive and palladin positive cells are present within CLL/SLL LN tissue, indicating the presence of myofibroblasts within the CLL stroma.
 - There appeared to be trend towards an inverse relationship between α -SMA and the prognostic marker ZAP-70, suggesting that α -SMA positive cells may correlate with a more indolent disease progression.
 - HFFF2 cells were selected as a suitable experimental model as they transdifferentiated into myofibroblasts when induced using TGF- β **and maintained their fibroblast phenotype in the absence** of stimuli.
- Chapter 4: The main aim of the experiments in this chapter was to investigate what effect CLL cells have on myofibroblast transdifferentiation.
 - α -SMA expression was lower in HFFF2 cells, compared to controls, after co-culture with CLL cells or culture in CLL-derived CM, in the absence or presence of TGF- β . These data indicate

Chapter 6

that CLL cells may prevent spontaneous and TGF- β -induced myofibroblast transdifferentiation.

- Very preliminary data suggest that CLL-derived exosomes may prevent myofibroblast transdifferentiation.
- Some CLL samples were able to activate TGF- β 1; however this was not shown to be mechanistically linked with the ability of CLL cells **to reduce HFFF2 α -SMA** expression.
- Chapter 5: The main aim of the experiments conducted in this chapter was to investigate what effect fibroblasts and myofibroblasts have on CLL cell survival.
 - The key findings were that both fibroblasts and myofibroblasts protect CLL cells from spontaneous apoptosis; however fibroblasts have a superior protective effect.
 - Soluble factors released by fibroblasts prevented cleavage of caspase 3 and PARP, induced expression of the anti-apoptotic protein MCL-1 and reduced expression of the pro-apoptotic protein BIM_{EL}.
 - Soluble factors released by myofibroblasts also induced MCL-1 expression within CLL cells, but to a lesser extent than fibroblast CM.
- Chapter 6: The aim of the assays performed in this chapter was to determine which intracellular signalling pathways are involved in fibroblast-mediated protection of CLL cells.
 - SYK, PI3K signalling and possibly BTK are involved in fibroblast-mediated protection of CLL cells and induction of MCL-1 expression.
 - Fibroblasts induce MAPK signalling within CLL cells as seen by an increase in pERK expression, however this does not have an apparent role in CLL cell survival.

Taken together, these data show that CLL cells prevent up-regulation of HFFF2 α -SMA expression, and that CLL cell viability is significantly higher after co-culture with fibroblasts than with myofibroblasts. Overall these data are consistent with the initial hypothesis that CLL cells alter fibroblast to myofibroblast transdifferentiation. In particular, CLL cells appear to suppress transdifferentiation, which, in turn, may create an optimal protective niche

through modulation of BIM_{EL} and MCL-1 Bcl-2-family proteins and suppression of apoptosis (Figure 7.1).

7.3 Overview of key findings

The presence of myofibroblasts within the stroma of various solid tumours, including pancreatic, prostate, breast and colon cancer, is associated with an aggressive disease progression and poor patient outcome [171, 172, 174]. CLL is generally an indolent disease associated with a prolonged clinical course yet the majority of samples analysed contained α -SMA positive cells. As α -SMA is a hallmark of myofibroblasts this indicates the presence of these cells within the CLL stroma. Although α -SMA positive cells were present in the majority of cases the degree of expression varied greatly between individual patients. As CLL is a highly heterogeneous disorder and clinical behaviour varies greatly between patients, this was unsurprising. In fact it suggests a potential relationship between α -SMA (i.e. potential myofibroblasts) and disease progression. Interestingly, the majority of samples from both the CLL/SLL and **Richter's groups were positive for α -SMA** and negative for ZAP-70. Although there was no significant correlation between these two markers for the CLL/SLL cohort, **there was for the Richter's samples thus suggesting an inverse correlation between α -SMA and ZAP-70**. As ZAP-70 is a CLL prognostic marker associated with poor patient outcome it indicates that the presence of α -SMA positive cells may correlate with a less aggressive disease progression within B-cell malignancies, or at least within CLL. This contrasts with current data on the impact of myofibroblasts within solid tumours. Yamashita et al observed that patients diagnosed with invasive breast cancer, who had high α -SMA expression within their tissue stroma, had a significantly poorer survival rate compared with patients with low α -SMA expression, indicating that α -SMA positive cells promote tumour progression [171]. However the data shown here is consistent with the limited previous work examining α -SMA expression within B-cell malignancies. Ruan et al analysed α -SMA expression within various types of NHLs, both aggressive and indolent subsets. Interestingly this study found that indolent NHLs such as CLL/SLL contained a diffuse pattern of α -SMA positive cells, compared to more aggressive subtypes such as BL and DLBCL which contained a scant perivascular pattern [252].

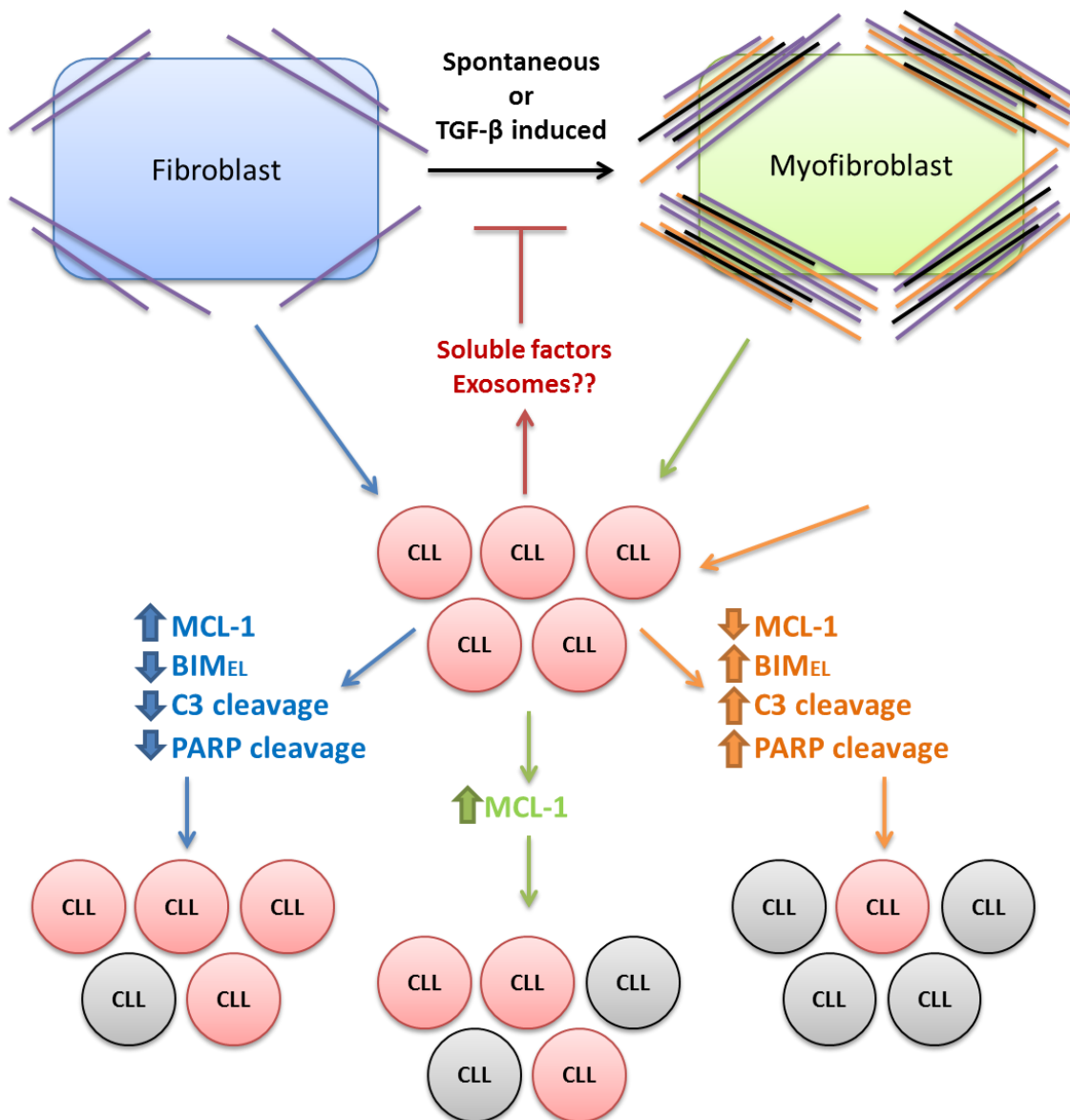


Figure 7.1: Diagram summarising key findings.

Soluble factors released by CLL cells prevent spontaneous and TGF- β induced myofibroblast transdifferentiation, thus maintaining fibroblasts in their undifferentiated form. In turn this creates an optimal protective niche which promotes CLL cell survival. Fibroblasts up-regulate MCL-1 expression, reduce BIM_{EL} expression and reduce cleavage of caspase 3 and PARP, within CLL cells, therefore promoting CLL cell survival. Myofibroblasts up-regulate MCL-1 expression in CLL cells, but to a lesser extent than fibroblasts, resulting in more CLL cells undergoing spontaneous apoptosis (black). CLL cells cultured alone express reduced levels of MCL-1, increased BIM_{EL} expression and increased cleavage of caspase 3 and PARP, resulting in CLL cells undergoing spontaneous apoptosis.

The idea that myofibroblasts may associate with a more indolent disease course is supported by the annexin V data which demonstrated that myofibroblasts support CLL cell survival to a lesser extent than fibroblasts. Furthermore myofibroblasts induced MCL-1 expression to a lesser degree than fibroblasts. MCL-1 expression in CLL cells isolated from the peripheral blood has previously been shown to correlate with poor prognostic markers in CLL such as the un-mutated *IGHV* subset (U-CLL), ZAP-70 and CD38, again indicating that fibroblasts may promote disease severity [300]. This is unusual behaviour of tumour biology as myofibroblasts within solid tumours promote disease progression. Studies conducted by Hwang et al and Olumi et al have demonstrated that myofibroblasts can stimulate growth of pancreatic stellate cells and initiated human prostatic epithelial cells, respectively [172, 174].

Although unusual the notion that myofibroblasts associate with indolent disease in CLL is further supported by the data which indicates that CLL cells prevent spontaneous and TGF- β induced myofibroblast transdifferentiation, thus suggesting that the malignant cells are attempting to maintain the stromal cell type which optimally promotes their survival. Again, this contrasts with current data examining the impact of malignant cells within solid tumours on myofibroblast transdifferentiation. Hawinkels et al demonstrated that culturing CAFs in CM derived from epithelial colorectal cancer cells, induced hyperactivation of TGF- β signalling and increased α -SMA expression of the stromal cells [259].

Interestingly, during the course of my studies, another study published by Lutzny et al demonstrated that co-culture of primary CLL cells with the murine cell line EL08-1D2 actually led to an increase in α -SMA expression and stress fibre formation of the stromal cells [344]. One possible reason for this is the use of stromal cells of mouse origin, whereas I utilised stromal cells derived from human skin. To determine which outcome is true, the effect of CLL cells on various other, preferably more physiologically relevant, stromal cell types should be examined. Additionally the degree of protection conferred to CLL cells by fibroblasts and myofibroblasts varied greatly between individual samples. It is possible this variation is related to *IGHV* mutation status. Previous studies have shown that U-CLL cells are more sensitive to spontaneous apoptosis than M-CLL cells [286]. Therefore U-CLL samples may be more dependent on stromal cell protection. If so, U-CLL cells may prevent

Chapter 6

myofibroblast transdifferentiation to a greater extent than M-CLL samples. However this was not observed for this small cohort and more samples need to be analysed to determine this.

It is likely that soluble factors released by fibroblasts and myofibroblasts are predominantly responsible for CLL cell survival opposed to direct cell-to-cell contact. This is supported by the data showing that fibroblast CM was sufficient to prevent induction of apoptotic pathways as seen by reduced caspase 3 and PARP cleavage compared to control cells. Additionally fibroblast CM induced MCL-1 and reduced BIM_{EL} expression. Furthermore data by Elizabeth Lemm (Appendix, A.2) has shown that HFFF2 fibroblast CM can protect CLL cells from spontaneous apoptosis to a similar extent as direct co-culture; however the effect of myofibroblast CM has not been analysed. Moreover, CLL cells preferentially bound to myofibroblasts than to fibroblasts. This uncoupling between adhesion and survival suggests that these processes are independent.

When co-culturing CLL cells and HFFF2 cells, consideration had to go into which type of media to use, and what percentage of atmospheric CO₂ to culture the cells in. This is due to the fact that CLL cells preferentially grow in 10% RPMI, in 5% CO₂, whereas HFFF2 cells are traditionally grown in 10% DMEM, in 10% CO₂. Therefore the decision to culture the cells in RPMI/DMEM, 5%/10% atmospheric CO₂, depended on which cells were being analysed. For instance, in chapter 4, the co-cultured cells were cultured in DMEM in 10% CO₂, as the aim of these assays was to analyse α -SMA expression in the HFFF2 cells. Conversely, in the annexin V assays, in chapters 5 and 6, cells were cultured in 10% RPMI at 5% CO₂, as the aim of these assays were to analyse CLL cell viability, and therefore conditions were optimised for the CLL cells.

7.4 Further work to extend current data

7.4.1 Chapter 3

Although α -SMA positive cells which potentially co-express palladin were detected within CLL/SLL LNs further work is still required to confirm the presence of myofibroblasts within the CLL stroma. Initially dual immunofluorescence staining could be conducted to confirm cells co-express

α -SMA and palladin. Furthermore other markers, such as the EDA splice variant of fibronectin, which is incorporated within myofibroblast stress fibres, and negative myofibroblast markers such as smoothelin and caldesmon should be analysed [180, 254]. Further studies could be conducted to confirm whether there is an inverse relationship between α -SMA and ZAP-70, as this could reveal a potential **prognostic attribute to α -SMA**; thus a larger cohort needs to be studied, preferably including disease stage and patient survival.

7.4.2 Chapter 4

CLL cells were shown to release soluble factors which prevent spontaneous and TGF- β induced myofibroblast transdifferentiation, however these factors remain unidentified. Very preliminary data indicate that CLL cell-derived exosomes may, at least partly, be responsible for this phenomenon. More samples should be analysed to confirm this. Additionally attempts could be made to determine whether soluble factors are also involved. CLL CM could be separated into high and low molecular weight fractions prior to treatment with HFFF2 cells. This would serve as a preliminary starting point to narrow down the responsible factors based on weight. Subsequently, neutralising antibodies could be utilised to specifically target potential candidates, such as bFGF which has previously been shown to prevent myofibroblast transdifferentiation and is secreted by CLL cells [280, 281]. Furthermore, it would be interesting to determine which intracellular signalling pathways are induced, or blocked, within fibroblasts in response to CLL cells to prevent myofibroblast transdifferentiation. This could be investigated by analysing phospho-proteins (pERK, pAKT, pSYK) within HFFF2 cells after culture with CLL cells or CLL CM by **immunoblotting**; HFFF2 α -SMA expression would be analysed in parallel to ensure myofibroblast transdifferentiation was prevented. For the TGF- β luciferase assays, renilla luciferase control reporter vectors could be utilised to generate an internal control value, against which the value of experimental firefly luciferase could be normalised. Additionally, as a negative control, MLEC reported plasmids with mutated SMAD binding sites could be utilised to confirm that the luminescence generated is solely due to TGF- β binding.

Chapter 6

7.4.3 Chapter 5

Investigations could be made to ensure that the differential degree of protection conferred by fibroblasts and myofibroblasts was not due to variation of cell viability between the two stromal subtypes. Immunoblotting could be utilised to analyse caspase activity and PARP cleavage within the stromal cells after co-culture with CLL cells. The degree of protection conferred by fibroblasts and myofibroblasts onto CLL cells varied greatly between patients. To determine which factors may be responsible, such as *IGHV* mutation status, a larger cohort could be analysed. Additionally assays could be conducted to investigate the effect of myofibroblast-derived CM on caspase activity, PARP cleavage and BIM_{EL} expression, to determine if these proteins are affected to a lesser extent compared to cells cultured in fibroblast CM. Further analysis of apoptotic pathways could be conducted to determine if fibroblasts and myofibroblasts block the extrinsic or intrinsic pathways by analysing cleavage of caspases 8 and 9, respectively, by immunoblotting. Additionally assays could be performed to confirm whether MCL-1 and BIM_{EL} are involved in fibroblast and myofibroblast mediated protection of CLL cells. Prior to culture in stromal cell CM, CLL cells could be transfected with MCL-1-specific siRNA to 'knock-down' MCL-1 expression. To determine if BIM is involved in fibroblast and myofibroblast-mediated protection, CLL cells could be treated with proteasome inhibitors to block degradation of BIM, prior to culture in stromal cell CM. Additionally experiments could be performed to determine the effect of direct cell-to-cell contact of CLL cells and HFFF2 cells on caspase activity and Bcl-2 family protein expression. However to avoid HFFF2 contamination of the CLL population, cells could be analysed by flow cytometry to ensure exclusive analysis of the lymphocyte population.

7.4.4 Chapter 6

Initial experiments should be conducted to confirm the efficacy of all the small molecule inhibitors utilised. Additionally to avoid the uncertainty of whether the inhibitors are acting on the CLL cells, HFFF2 cells or both, further assays could be conducted where CLL cells are cultured in fibroblast CM. Alternately, it could be possible to use siRNA to knock-down specific kinases (such as SYK) in CLL cells prior to co-culture. Furthermore the effects of these inhibitors could be analysed in response to myofibroblast CM. Also, the effect of these

inhibitors on caspase activity, PARP cleavage and BIM expression, within CLL cells after culture in stromal cell CM could also be analysed by immunoblotting.

Additionally, as HFFF2 cells are derived from the skin, a location within which CLL cells do not predominantly infiltrate, the aforementioned assays could be repeated utilising other, preferably more physiologically relevant, fibroblast cell lines. This would determine whether the results obtained in this project are replicable with other type of fibroblasts and myofibroblasts, and thus strengthen the possibility that these mechanisms occur within CLL-specific sites (i.e. BM and SLOs).

7.5 Future work

Conducting the aforementioned assays would primarily support the data already presented. This section highlights future studies which would take this work further.

7.5.1 Gene expression profiling (GEP) study

GEP analysis would be one approach to gain a more global view of the effects of HFFF2 cell co-culture on CLL cells. I designed an experiment to address this, based on the Illumina platform. This utilises BeadArray technology, which involves using gene-specific probes attached to beads assembled into arrays. Samples would be analysed on the Human-HT-12 expression BeadChip which analyses over 47,000 transcripts and splice variants using probes generated from the National Centre for Biotechnology reference Sequence (NCBI) RefSeq. Although I devised the experimental design and performed initial processing of samples, I was unable to complete this experiment due to lack of time. However, the project is being taken forward in the host laboratory by Elizabeth Lemm. In particular, the experiment was designed not just to probe responses to HFFF2 co-culture, but to also investigate how HFFF2 cells may modulate the transcriptional responses to anti-IgM.

The experimental design was to culture CLL samples alone \pm anti-IgM, co-culture CLL samples with HFFF2 fibroblasts \pm anti-IgM, and culture CLL samples in HFFF2 fibroblast CM. CLL cells would be collected after 8 hours and RNA prepared. This time-point was chosen as it was sufficient for fibroblast

Chapter 6

CM to activate intracellular signalling pathways, as observed by up-regulation of pERK and pAKT⁴⁷³ expression (Figure 6.3), as well as induce alterations in Bcl-2 family proteins (Figure 5.26) within CLL cells. Analysis would be performed in triplicate to allow for biological variation, and a total of 3 different CLL samples were to be analysed. All samples selected should **comprise \geq 80% CLL cells and** will have been previously analysed in the annexin V assays to determine a high degree of protection conferred by fibroblasts. The results from this assay will determine which genes are altered within CLL cells in response to direct contact with HFFF2 cells and in response to soluble factors released by HFFF2 fibroblast. Controls were set in place for potential contamination of HFFF2 cells within the CLL population after direct co-culture. These include culturing CLL cells in fibroblast CM, and setting up an additional condition comprising HFFF2 cells only. This experiment will highlight which genes are activated within CLL cells in response to both direct contact with fibroblasts as well as exposure to fibroblast-derived soluble factors, thus indicating which mechanisms are involved in fibroblast-mediated protection of CLL cells. Underpinning these mechanisms will allow us to develop strategies to block them, thus producing potential novel targets for future therapies.

7.5.2 In vivo studies

The TCL-1 mouse is a well characterised transgenic mouse model for the study of CLL. These mice develop a chronic CD5+ B-cell leukaemia and are sensitive to therapies utilised for the treatment of human CLL patients (i.e. fludarabine) [347]. Additionally the murine lymphocytes express relevant therapeutic targets in CLL, such as Bcl-2 and MCL-1 [347]. One possible approach to directly investigate the requirement for stromal support in CLL development *in vivo* would be to create a new mouse strain that would allow conditional deletion of certain mesenchymal cells in the context of the E μ -TCL1 transgene. Conditional deletion of cells expressing fibroblast activation protein (FAP), expressed by tumour-associated fibroblasts, has been shown to induce regression of both lung and pancreatic cancer in mouse models [348, 349]. It would be attractive to cross these FAP-targeting strains to the E μ -TCL1 mouse and then to monitor the effects of deletion of FAP-positive cells on leukaemic cell numbers in both the blood and tissues. Although attractive, it would be

important to first characterise the presence of FAP positive cells and their relationship with potential fibroblasts/myofibroblasts.

7.5.3 Drug-induced apoptosis

The protective effect of fibroblasts and myofibroblasts was only examined in relation to spontaneous CLL cell death. Further studies could investigate the effect of these stromal cells on drug-induced CLL cell death to determine if they can overcome the detrimental impact of therapy. Multiple studies have previously shown that stromal cells can overcome drug-induced apoptosis of CLL cells [127, 214]. The ability of fibroblasts and myofibroblasts to prevent drug-induced apoptosis for individual patients could be correlated to prognostic markers and clinical responses (i.e. relapse). This would aid in determining if certain markers affect the ability of either stromal cell type to overcome treatment, and thus protect CLL cells. Additionally α -SMA expression could be analysed in tissue samples for individual patients at time of presentation and at relapse to determine if there is an association between myofibroblasts and disease stage.

Appendices

Appendix A

A.1 CLL samples

CLL sample	IGHV mutational status ^A	% CLL ^B	ZAP-70 (%) ^C	CD38 (%) ^D	IgM (GeoM) ^E	IgM (%Ca) ^F
348A	M	93	0	0	66	4
393	U	92	96	59	60	41
396	U	90	29	3	58	65
409	U/M	77	77	56	56	15
410	U	95	8	56	114	25
414	M	95	0	1	19	0
421	U	75	94	86	39	48
431	M	87	6	6	119	N/A
432	U	83	41	10	39	N/A
440	-	92	52	64	39	29
446	M	88	N/A ^G	0	33	N/A
459	U	90	6	44	105	43
462	M	81	8	3	56	11
474	U	83	86	50	117	7
480	M	92	2	1	49	33
481	M	86	0	0	1877	75
483	M	90	3	0	48	5
489	M	91	2	1	25	5
494	M	95	19	1	29	6
498	M	88	2	0	15	N/A

Appendix A

CLL sample	IGHV mutational status ^A	% CLL ^B	ZAP-70 (%) ^C	CD38 (%) ^D	IgM (GeoM) ^E	IgM (%Ca) ^F
505	U	96	14	14	44	17
508	U	93	13	13	46	19
508B	U	95	3	13	25	60
510	U	87	83	84	48	33
513	U	99	2	1	79	62
518	M	89	1	0	17	16
533B	N/A	87	51	93	38	7
542	M	93	0	1	21	2
543A	M	84	5	12	6	3
555	U	99	2	27	37	28
561	M	94	24	2	39	50
564B	M	92	7	0	1665	82
566	U	96	57	9	67	7
588	M	87	10	9	30	5
595B	M	95	3	75	38	20
602	U	96	0	33	19	25
604A	M	92	2	0	90	42
607	U	80	23	89	40	72
619	U	96	4	88	8	1
629	U	89	3	10	17	16
632A	N/A	95	52	76	73	61
635	U	87	12	1	66	82

CLL sample	IGHV mutational status ^A	% CLL ^B	ZAP-70 (%) ^C	CD38 (%) ^D	IgM (GeoM) ^E	IgM (%Ca) ^F
643A	M	92	0	0	14	21
651	M	99	2	0	22	8
654	M	84	0	0	22	36

Table A.1: CLL samples.

^AIndicates whether the sample expressed mutated (M) or un-mutated (U) *IGHV* genes.

^BDisplays the percentage of B-CLL cells within the sample.

^CDisplays the percentage of cells within the sample which are positive for ZAP-70.

^DDisplays the percentage of cells within the sample which are positive for CD38.

^EDisplays the amount of surface IgM (sIgM) expression by CLL cells.

^FsIgM signal capacity determined by intracellular calcium flux in response to anti-IgM stimulation.

^GN/A, data not available.

A.2 Effect of HFFF2 fibroblast CM on CLL cell viability

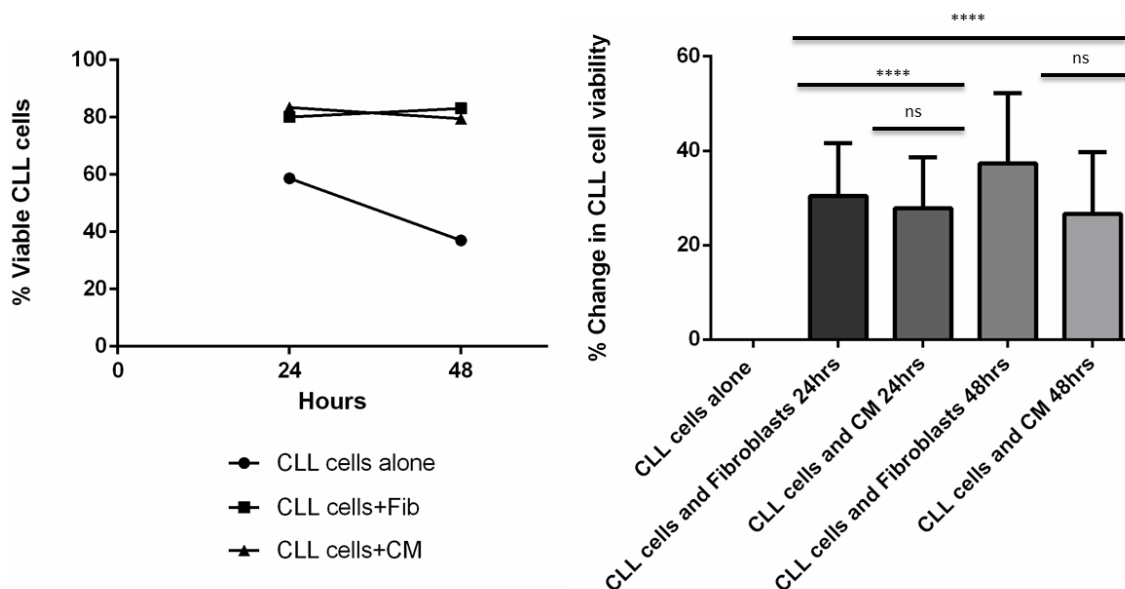


Figure A.2: Effect of HFFF2 fibroblast CM on CLL cell viability.

Data by Elizabeth Lemm. CLL cells were cultured in complete RPMI-1640 media either alone as a control (circles), co-cultured with fibroblasts (squares) or cultured in fibroblast CM (triangles). CM was derived from HFFF2 fibroblasts cultured in complete RPMI-1640 media for 72 hours. After 24 and 48 hours of culture CLL cells were collected and cell viability was analysed by FACS. Left- Graphs shows the percentage of viable CLL cells for one sample. Right- Graph shows percentage change in CLL cell viability between CLL cells co-cultured with fibroblasts/cultured in CM and cells cultured alone. Graph shows the mean (\pm SD) for all samples. The statistical significance of the differences was analysed using one-way ANOVA with Bonferroni correction ($n=12$).

List of References

1. Durrieu, F., et al., *Normal levels of peripheral CD19(+) CD5(+) CLL-like cells: toward a defined threshold for CLL follow-up -- a GEIL-GOELAMS study*. *Cytometry B Clin Cytom*, 2011. 80(6): p. 346-53.
2. Natoni, A., M. O'Dwyer, and C. Santocanale, *A cell culture system that mimics chronic lymphocytic leukemia cells microenvironment for drug screening and characterization*. *Methods Mol Biol*, 2013. 986: p. 217-26.
3. Messmer, B.T., et al., *In vivo measurements document the dynamic cellular kinetics of chronic lymphocytic leukemia B cells*. *Journal of Clinical Investigation*, 2005. 115(3): p. 755-764.
4. Damle, R.N., et al., *Telomere length and telomerase activity delineate distinctive replicative features of the B-CLL subgroups defined by immunoglobulin V gene mutations*. *Blood*, 2004. 103(2): p. 375-382.
5. Grabowski, P., et al., *Telomere length as a prognostic parameter in chronic lymphocytic leukemia with special reference to V-H gene mutation status*. *Blood*, 2005. 105(12): p. 4807-4812.
6. Soma, L.A., F.E. Craig, and S.H. Swerdlow, *The proliferation center microenvironment and prognostic markers in chronic lymphocytic leukemia/small lymphocytic lymphoma*. *Hum Pathol*, 2006. 37(2): p. 152-9.
7. Herishanu, Y., et al., *The lymph node microenvironment promotes B-cell receptor signaling, NF-kappaB activation, and tumor proliferation in chronic lymphocytic leukemia*. *Blood*, 2011. 117(2): p. 563-74.
8. Stevenson, F.K. and F. Caligaris-Cappio, *Chronic lymphocytic leukemia: revelations from the B-cell receptor*. *Blood*, 2004. 103(12): p. 4389-95.
9. Burton, G.F., et al., *Follicular dendritic cells and B cell costimulation*. *J Immunol*, 1993. 150(1): p. 31-8.
10. Hamblin, T.J., et al., *Unmutated Ig V(H) genes are associated with a more aggressive form of chronic lymphocytic leukemia*. *Blood*, 1999. 94(6): p. 1848-54.
11. Hamblin, T.J., et al., *Unmutated Ig VH genes are associated with a more aggressive form of chronic lymphocytic leukemia*. *Blood*, 1999. 94: p. 1848-1854.
12. Deaglio, S., et al., *CD38 is a signaling molecule in B-cell chronic lymphocytic leukemia cells*. *Blood*, 2003. 102(6): p. 2146-55.
13. Orchard, J.A., et al., *ZAP-70 expression and prognosis in chronic lymphocytic leukaemia*. *Lancet*, 2004. 363(9403): p. 105-11.
14. Del Principe, M.I., et al., *Clinical significance of ZAP-70 protein expression in B-cell chronic lymphocytic leukemia*. *Blood*, 2006. 108(3): p. 853-61.
15. Panovska, A., et al., *Chronic lymphocytic leukemia and focusing on epidemiology and management in everyday hematologic practice: recent data from the Czech Leukemia Study Group for Life (CELL)*. *Clin Lymphoma Myeloma Leuk*, 2010. 10(4): p. 297-300.
16. Zent, C.S., et al., *Chronic lymphocytic leukemia incidence is substantially higher than estimated from tumor registry data*. *Cancer*, 2001. 92(5): p. 1325-30.
17. Redaelli, A., et al., *The clinical and epidemiological burden of chronic lymphocytic leukaemia*. *Eur J Cancer Care (Engl)*, 2004. 13(3): p. 279-87.

List of References

18. Cuttner, J., *Increased incidence of hematologic malignancies in first-degree relatives of patients with chronic lymphocytic leukemia*. *Cancer Invest*, 1992. 10(2): p. 103-9.
19. Horwitz, M., E.L. Goode, and G.P. Jarvik, *Anticipation in familial leukemia*. *Am J Hum Genet*, 1996. 59(5): p. 990-8.
20. Shanafelt, T.D., et al., *MBL or CLL: which classification best categorizes the clinical course of patients with an absolute lymphocyte count $\geq 5 \times 10^9$ L(-1) but a B-cell lymphocyte count $< 5 \times 10^9$ L(-1)?* *Leuk Res*, 2008. 32(9): p. 1458-61.
21. Nieto, W.G., *Increased frequency (12%) of circulating chronic lymphocytic leukemia-like B-cell clones in healthy subjects using a highly sensitive multicolor flow cytometry approach*. *Blood*, 2009. 114: p. 33-37.
22. Randen, U., et al., *Bone marrow histology in monoclonal B-cell lymphocytosis shows various B-cell infiltration patterns*. *Am J Clin Pathol*, 2013. 139(3): p. 390-5.
23. Malone, K.E., et al., *Chronic lymphocytic leukemia in relation to chemical exposures*. *Am J Epidemiol*, 1989. 130(6): p. 1152-8.
24. Arp, E.W., Jr., P.H. Wolf, and H. Checkoway, *Lymphocytic leukemia and exposures to benzene and other solvents in the rubber industry*. *J Occup Med*, 1983. 25(8): p. 598-602.
25. Dohner, H., *Genomic aberrations and survival in chronic lymphocytic leukemia*. *N. Engl. J. Med.*, 2000. 343: p. 1910-1916.
26. Ripolles, L., et al., *Genetic abnormalities and clinical outcome in chronic lymphocytic leukemia*. *Cancer Genet Cytogenet*, 2006. 171(1): p. 57-64.
27. Liu, Y., et al., *Chronic lymphocytic leukemia cells with allelic deletions at 13q14 commonly have one intact RB1 gene: evidence for a role of an adjacent locus*. *Proc Natl Acad Sci U S A*, 1993. 90(18): p. 8697-701.
28. Juliusson, G., et al., *Prognostic subgroups in B-cell chronic lymphocytic leukemia defined by specific chromosomal abnormalities*. *N Engl J Med*, 1990. 323(11): p. 720-4.
29. Ouilllette, P., et al., *The prognostic significance of various 13q14 deletions in chronic lymphocytic leukemia*. *Clin Cancer Res*, 2011. 17(21): p. 6778-90.
30. Lin, K., et al., *Loss of MIR15A and MIR16-1 at 13q14 is associated with increased TP53 mRNA, de-repression of BCL2 and adverse outcome in chronic lymphocytic leukaemia*. *Br J Haematol*, 2014. 167(3): p. 346-55.
31. Neilson, J.R., et al., *Deletions at 11q identify a subset of patients with typical CLL who show consistent disease progression and reduced survival*. *Leukemia*, 1997. 11(11): p. 1929-32.
32. Dohner, H., *11q deletions identify a new subset of B-cell chronic lymphocytic leukemia characterized by extensive nodal involvement and inferior prognosis*. *Blood*, 1997. 89: p. 2516-2522.
33. Austen, B., *Mutations in the ATM gene lead to impaired overall and treatment-free survival that is independent of IGVH mutation status in patients with B-CLL*. *Blood*, 2005. 106: p. 3175-3182.
34. Wang, L., et al., *SF3B1 and other novel cancer genes in chronic lymphocytic leukemia*. *N Engl J Med*, 2011. 365(26): p. 2497-506.
35. Rose-Zerilli, M.J., et al., *ATM mutation rather than BIRC3 deletion and/or mutation predicts reduced survival in 11q-deleted chronic lymphocytic leukemia: data from the UK LRF CLL4 trial*. *Haematologica*, 2014. 99(4): p. 736-42.

36. Starostik, P., et al., *Deficiency of the ATM protein expression defines an aggressive subgroup of B-cell chronic lymphocytic leukemia*. Cancer Research, 1998. 58(20): p. 4552-7.
37. Schaffner, C., et al., *Somatic ATM mutations indicate a pathogenic role of ATM in B-cell chronic lymphocytic leukemia*. Blood, 1999. 94: p. 748-753.
38. Robert, K.H., et al., *Extra chromosome 12 and prognosis in chronic lymphocytic leukaemia*. Scand J Haematol, 1982. 28(2): p. 163-8.
39. Juliusson, G., et al., *Prognostic information from cytogenetic analysis in chronic B-lymphocytic leukemia and leukemic immunocytoma*. Blood, 1985. 65(1): p. 134-41.
40. Pittman, S. and D. Catovsky, *Prognostic significance of chromosome abnormalities in chronic lymphocytic leukaemia*. Br J Haematol, 1984. 58(4): p. 649-60.
41. Del Giudice, I., et al., *NOTCH1 mutations in +12 chronic lymphocytic leukemia (CLL) confer an unfavorable prognosis, induce a distinctive transcriptional profiling and refine the intermediate prognosis of +12 CLL*. Haematologica, 2012. 97(3): p. 437-41.
42. Zenz, T., *Monoallelic TP53 inactivation is associated with poor prognosis in chronic lymphocytic leukemia: results from a detailed genetic characterization with long-term follow-up*. Blood, 2008. 112: p. 3322-3329.
43. el Rouby, S., *p53 gene mutation in B-cell chronic lymphocytic leukemia is associated with drug resistance and is independent of MDR1/MDR3 gene expression*. Blood, 1993. 82: p. 3452-3459.
44. Dohner, H., *p53 gene deletion predicts for poor survival and non-response to therapy with purine analogs in chronic B-cell leukemias*. Blood, 1995. 85: p. 1580-1589.
45. Thornton, P.D., et al., *Characterisation of TP53 abnormalities in chronic lymphocytic leukaemia*. Hematol J, 2004. 5(1): p. 47-54.
46. Zenz, T., et al., *TP53 mutation and survival in chronic lymphocytic leukemia*. J Clin Oncol, 2010. 28(29): p. 4473-9.
47. Rosati, E., et al., *Constitutively activated Notch signaling is involved in survival and apoptosis resistance of B-CLL cells*. Blood, 2009. 113(4): p. 856-65.
48. Willander, K., et al., *NOTCH1 mutations influence survival in chronic lymphocytic leukemia patients*. BMC Cancer, 2013. 13: p. 274.
49. Rossi, D., et al., *Mutations of the SF3B1 splicing factor in chronic lymphocytic leukemia: association with progression and fludarabine-refractoriness*. Blood, 2011. 118(26): p. 6904-8.
50. Rossi, D., et al., *Disruption of BIRC3 associates with fludarabine chemorefractoriness in TP53 wild-type chronic lymphocytic leukemia*. Blood, 2012. 119(12): p. 2854-62.
51. Kim, S.J. and J. Letterio, *Transforming growth factor-beta signaling in normal and malignant hematopoiesis*. Leukemia, 2003. 17(9): p. 1731-7.
52. Knaus, P.I., et al., *A dominant inhibitory mutant of the type II transforming growth factor beta receptor in the malignant progression of a cutaneous T-cell lymphoma*. Mol Cell Biol, 1996. 16(7): p. 3480-9.
53. Schiemann, W.P., et al., *A deletion in the gene for transforming growth factor beta type I receptor abolishes growth regulation by transforming growth factor beta in a cutaneous T-cell lymphoma*. Blood, 1999. 94(8): p. 2854-61.

List of References

54. Imai, Y., et al., *Mutations of the Smad4 gene in acute myelogenous leukemia and their functional implications in leukemogenesis*. Oncogene, 2001. 20(1): p. 88-96.
55. Schiemann, W.P., et al., *Transforming growth factor-beta (TGF-beta)-resistant B cells from chronic lymphocytic leukemia patients contain recurrent mutations in the signal sequence of the type I TGF-beta receptor*. Cancer Detect Prev, 2004. 28(1): p. 57-64.
56. Calin, G.A., et al., *MicroRNA profiling reveals distinct signatures in B cell chronic lymphocytic leukemias*. Proc Natl Acad Sci U S A, 2004. 101(32): p. 11755-60.
57. Calin, G.A., et al., *A MicroRNA signature associated with prognosis and progression in chronic lymphocytic leukemia*. N Engl J Med, 2005. 353(17): p. 1793-801.
58. Mraz, M., et al., *miR-150 influences B-cell receptor signaling in chronic lymphocytic leukemia by regulating expression of GAB1 and FOXP1*. Blood, 2014. 124(1): p. 84-95.
59. Stamatopoulos, B., et al., *microRNA-29c and microRNA-223 down-regulation has in vivo significance in chronic lymphocytic leukemia and improves disease risk stratification*. Blood, 2009. 113(21): p. 5237-45.
60. Sthoeger, Z.M., et al., *Mechanism of autoimmune hemolytic anemia in chronic lymphocytic leukemia*. Am J Hematol, 1993. 43(4): p. 259-64.
61. Campo, E., et al., *The 2008 WHO classification of lymphoid neoplasms and beyond: evolving concepts and practical applications*. Blood, 2011. 117(19): p. 5019-32.
62. Cheson, B.D., et al., *National Cancer Institute-sponsored Working Group guidelines for chronic lymphocytic leukemia: revised guidelines for diagnosis and treatment*. Blood, 1996. 87(12): p. 4990-7.
63. Stilgenbauer, S. and T. Zenz, *Understanding and managing ultra high-risk chronic lymphocytic leukemia*. Hematology Am Soc Hematol Educ Program, 2010. 2010: p. 481-8.
64. Rai, K.R., et al., *Fludarabine compared with chlorambucil as primary therapy for chronic lymphocytic leukemia*. N Engl J Med, 2000. 343(24): p. 1750-7.
65. Leporrier, M., et al., *Randomized comparison of fludarabine, CAP, and ChOP in 938 previously untreated stage B and C chronic lymphocytic leukemia patients*. Blood, 2001. 98(8): p. 2319-25.
66. O'Brien, S.M., et al., *Results of the fludarabine and cyclophosphamide combination regimen in chronic lymphocytic leukemia*. J Clin Oncol, 2001. 19(5): p. 1414-20.
67. Nguyen, D.T., et al., *IDEC-C2B8 anti-CD20 (rituximab) immunotherapy in patients with low-grade non-Hodgkin's lymphoma and lymphoproliferative disorders: evaluation of response on 48 patients*. Eur J Haematol, 1999. 62(2): p. 76-82.
68. Almasri, N.M., et al., *Reduced expression of CD20 antigen as a characteristic marker for chronic lymphocytic leukemia*. Am J Hematol, 1992. 40(4): p. 259-63.
69. Woyach, J.A., et al., *Chemoimmunotherapy with fludarabine and rituximab produces extended overall survival and progression-free survival in chronic lymphocytic leukemia: long-term follow-up of CALGB study 9712*. J Clin Oncol, 2011. 29(10): p. 1349-55.
70. Tam, C.S., et al., *Long-term results of the fludarabine, cyclophosphamide, and rituximab regimen as initial therapy of chronic lymphocytic leukemia*. Blood, 2008. 112(4): p. 975-80.

71. Kay, N.E., et al., *Combination chemoimmunotherapy with pentostatin, cyclophosphamide, and rituximab shows significant clinical activity with low accompanying toxicity in previously untreated B chronic lymphocytic leukemia*. *Blood*, 2007. 109(2): p. 405-11.
72. Jilani, I., et al., *Transient down-modulation of CD20 by rituximab in patients with chronic lymphocytic leukemia*. *Blood*, 2003. 102(10): p. 3514-20.
73. Lim, S.H., et al., *Fc gamma receptor IIb on target B cells promotes rituximab internalization and reduces clinical efficacy*. *Blood*, 2011. 118(9): p. 2530-40.
74. Osterborg, A., et al., *Phase II multicenter study of human CD52 antibody in previously treated chronic lymphocytic leukemia. European Study Group of CAMPATH-1H Treatment in Chronic Lymphocytic Leukemia*. *J Clin Oncol*, 1997. 15(4): p. 1567-74.
75. Keating, M.J., et al., *Therapeutic role of alemtuzumab (Campath-1H) in patients who have failed fludarabine: results of a large international study*. *Blood*, 2002. 99(10): p. 3554-61.
76. Fraser, G., et al., *Alemtuzumab in chronic lymphocytic leukemia*. *Curr Oncol*, 2007. 14(3): p. 96-109.
77. Sutton, L., et al., *Autologous hematopoietic stem cell transplantation as salvage treatment for advanced B cell chronic lymphocytic leukemia*. *Leukemia*, 1998. 12(11): p. 1699-707.
78. Pavletic, Z.S., et al., *High incidence of relapse after autologous stem-cell transplantation for B-cell chronic lymphocytic leukemia or small lymphocytic lymphoma*. *Annals of Oncology*, 1998. 9(9): p. 1023-6.
79. Hoellenriegel, J., et al., *The phosphoinositide 3'-kinase delta inhibitor, CAL-101, inhibits B-cell receptor signaling and chemokine networks in chronic lymphocytic leukemia*. *Blood*, 2011. 118(13): p. 3603-12.
80. Byrd, J.C., et al., *Targeting BTK with ibrutinib in relapsed chronic lymphocytic leukemia*. *N Engl J Med*, 2013. 369(1): p. 32-42.
81. Furman, R.R., et al., *Idelalisib and rituximab in relapsed chronic lymphocytic leukemia*. *N Engl J Med*, 2014. 370(11): p. 997-1007.
82. Byrd, J.C., et al., *Ibrutinib versus ofatumumab in previously treated chronic lymphoid leukemia*. *N Engl J Med*, 2014. 371(3): p. 213-23.
83. Wu, J.Y., et al., *Osteoblastic regulation of B lymphopoiesis is mediated by Gs{alpha}-dependent signaling pathways*. *Proc Natl Acad Sci U S A*, 2008. 105(44): p. 16976-81.
84. Zhu, J., et al., *Osteoblasts support B-lymphocyte commitment and differentiation from hematopoietic stem cells*. *Blood*, 2007. 109(9): p. 3706-12.
85. Dong, C., et al., *Upregulation of PAI-1 is mediated through TGF-beta/Smad pathway in transplant arteriopathy*. *J Heart Lung Transplant*, 2002. 21(9): p. 999-1008.
86. LeBien, T.W. and T.F. Tedder, *B lymphocytes: how they develop and function*. *Blood*, 2008. 112(5): p. 1570-1580.
87. Islam, A., C. Glomski, and E.S. Henderson, *Bone lining (endosteal) cells and hematopoiesis: a light microscopic study of normal and pathologic human bone marrow in plastic-embedded sections*. *Anat Rec*, 1990. 227(3): p. 300-6.
88. Guezguez, B., et al., *Regional localization within the bone marrow influences the functional capacity of human HSCs*. *Cell Stem Cell*, 2013. 13(2): p. 175-89.

List of References

89. Manz, M.G., et al., ***Prospective isolation of human clonogenic common myeloid progenitors***. Proc Natl Acad Sci U S A, 2002. 99(18): p. 11872-7.
90. Kondo, M., I.L. Weissman, and K. Akashi, ***Identification of clonogenic common lymphoid progenitors in mouse bone marrow***. Cell, 1997. 91(5): p. 661-72.
91. Chasis, J.A., ***Erythroblastic islands: specialized microenvironmental niches for erythropoiesis***. Curr Opin Hematol, 2006. 13(3): p. 137-41.
92. Friedenstein, A.J., R.K. Chailakhjan, and K.S. Lalykina, ***The development of fibroblast colonies in monolayer cultures of guinea-pig bone marrow and spleen cells***. Cell Tissue Kinet, 1970. 3(4): p. 393-403.
93. Majumdar, M.K., et al., ***Phenotypic and functional comparison of cultures of marrow-derived mesenchymal stem cells (MSCs) and stromal cells***. Journal of Cellular Physiology, 1998. 176(1): p. 57-66.
94. Conget, P.A. and J.J. Minguell, ***Phenotypical and functional properties of human bone marrow mesenchymal progenitor cells***. Journal of Cellular Physiology, 1999. 181(1): p. 67-73.
95. Lagneaux, L., et al., ***Chronic lymphocytic leukemic B cells but not normal B cells are rescued from apoptosis by contact with normal bone marrow stromal cells***. Blood, 1998. 91: p. 2387-2396.
96. Mueller, S.N. and R.N. Germain, ***Stromal cell contributions to the homeostasis and functionality of the immune system***. Nature Reviews Immunology, 2009. 9(9): p. 618-629.
97. Drinker, C.K., M.E. Field, and H.K. Ward, ***The Filtering Capacity of Lymph Nodes***. Journal of Experimental Medicine, 1934. 59(4): p. 393-405.
98. Szakal, A.K., K.L. Holmes, and J.G. Tew, ***Transport of immune complexes from the subcapsular sinus to lymph node follicles on the surface of nonphagocytic cells, including cells with dendritic morphology***. J Immunol, 1983. 131(4): p. 1714-27.
99. Anderson, A.O. and N.D. Anderson, ***Studies on the structure and permeability of the microvasculature in normal rat lymph nodes***. American Journal of Pathology, 1975. 80(3): p. 387-418.
100. Katakai, T., et al., ***Organizer-like reticular stromal cell layer common to adult secondary lymphoid organs***. J Immunol, 2008. 181(9): p. 6189-200.
101. Chyou, S., et al., ***Fibroblast-type reticular stromal cells regulate the lymph node vasculature***. J Immunol, 2008. 181(6): p. 3887-96.
102. Steiniger, B., P. Barth, and A. Hellinger, ***The perifollicular and marginal zones of the human splenic white pulp : do fibroblasts guide lymphocyte immigration?*** American Journal of Pathology, 2001. 159(2): p. 501-12.
103. Aznavoorian, S., et al., ***Signal transduction for chemotaxis and haptotaxis by matrix molecules in tumor cells***. J Cell Biol, 1990. 110(4): p. 1427-38.
104. Bredin, C.G., et al., ***Integrin dependent migration of lung cancer cells to extracellular matrix components***. Eur Respir J, 1998. 11(2): p. 400-7.
105. Netti, P.A., et al., ***Role of extracellular matrix assembly in interstitial transport in solid tumors***. Cancer Research, 2000. 60(9): p. 2497-503.
106. Brekken, C., O.S. Bruland, and C. de Lange Davies, ***Interstitial fluid pressure in human osteosarcoma xenografts: significance of implantation site and the response to intratumoral injection of hyaluronidase***. Anticancer Res, 2000. 20(5B): p. 3503-12.
107. Koong, A.C., et al., ***Pancreatic tumors show high levels of hypoxia***. Int J Radiat Oncol Biol Phys, 2000. 48(4): p. 919-22.

108. Vaupel, P., et al., *Oxygenation of human tumors: evaluation of tissue oxygen distribution in breast cancers by computerized O₂ tension measurements*. *Cancer Research*, 1991. 51(12): p. 3316-22.
109. Tannock, I.F., *The relation between cell proliferation and the vascular system in a transplanted mouse mammary tumour*. *Br J Cancer*, 1968. 22(2): p. 258-73.
110. Muthukkaruppan, V.R., L. Kubai, and R. Auerbach, *Tumor-induced neovascularization in the mouse eye*. *J Natl Cancer Inst*, 1982. 69(3): p. 699-708.
111. Hashizume, H., et al., *Openings between defective endothelial cells explain tumor vessel leakiness*. *American Journal of Pathology*, 2000. 156(4): p. 1363-80.
112. Stewart, P.A., et al., *Quantitative study of microvessel ultrastructure in human peritumoral brain tissue. Evidence for a blood-brain barrier defect*. *J Neurosurg*, 1987. 67(5): p. 697-705.
113. Spaeth, E.L., et al., *Mesenchymal stem cell transition to tumor-associated fibroblasts contributes to fibrovascular network expansion and tumor progression*. *Plos One*, 2009. 4(4): p. e4992.
114. Erikson, J., et al., *Transcriptional activation of the translocated c-myc oncogene in burkitt lymphoma*. *Proc Natl Acad Sci U S A*, 1983. 80(3): p. 820-4.
115. Garrido, S.M., et al., *Acute myeloid leukemia cells are protected from spontaneous and drug-induced apoptosis by direct contact with a human bone marrow stromal cell line (HS-5)*. *Experimental Hematology*, 2001. 29(4): p. 448-57.
116. Manabe, A., et al., *Bone marrow-derived stromal cells prevent apoptotic cell death in B-lineage acute lymphoblastic leukemia*. *Blood*, 1992. 79(9): p. 2370-7.
117. Wang, L., J.E. Fortney, and L.F. Gibson, *Stromal cell protection of B-lineage acute lymphoblastic leukemic cells during chemotherapy requires active Akt*. *Leuk Res*, 2004. 28(7): p. 733-42.
118. Vianello, F., et al., *Bone marrow mesenchymal stromal cells non-selectively protect chronic myeloid leukemia cells from imatinib-induced apoptosis via the CXCR4/CXCL12 axis*. *Haematologica*, 2010. 95(7): p. 1081-9.
119. Gupta, D., et al., *Small lymphocytic lymphoma with perifollicular, marginal zone, or interfollicular distribution*. *Mod Pathol*, 2000. 13(11): p. 1161-6.
120. Gine, E., et al., *Expanded and highly active proliferation centers identify a histological subtype of chronic lymphocytic leukemia ("accelerated" chronic lymphocytic leukemia) with aggressive clinical behavior*. *Haematologica*, 2010. 95(9): p. 1526-33.
121. Schmid, C. and P.G. Isaacson, *Proliferation centres in B-cell malignant lymphoma, lymphocytic (B-CLL): an immunophenotypic study*. *Histopathology*, 1994. 24(5): p. 445-51.
122. Chen, L.L., J.C. Adams, and R.M. Steinman, *Anatomy of germinal centers in mouse spleen, with special reference to "follicular dendritic cells"*. *J Cell Biol*, 1978. 77(1): p. 148-64.
123. Shi, Y.F. and X.H. Li, *[Immunohistochemical patterns of follicular dendritic cell meshwork and Ki-67 in small B-cell lymphomas]*. *Zhonghua Bing Li Xue Za Zhi*, 2013. 42(4): p. 222-6.
124. Rozman, C., et al., *Bone marrow histologic pattern--the best single prognostic parameter in chronic lymphocytic leukemia: a multivariate survival analysis of 329 cases*. *Blood*, 1984. 64(3): p. 642-8.

List of References

125. Kim, Y.S., et al., *B-cell chronic lymphocytic leukemia/small lymphocytic lymphoma involving bone marrow with an interfollicular pattern*. Am J Clin Pathol, 2000. 114(1): p. 41-6.
126. Gray, J.L., A. Jacobs, and M. Block, *Bone marrow and peripheral blood lymphocytosis in the prognosis of chronic lymphocytic leukemia*. Cancer, 1974. 33(4): p. 1169-78.
127. Kurtova, A.V., et al., *Diverse marrow stromal cells protect CLL cells from spontaneous and drug-induced apoptosis: development of a reliable and reproducible system to assess stromal cell adhesion-mediated drug resistance*. Blood, 2009. 114(20): p. 4441-4450.
128. Burger, J.A., et al., *Blood-derived nurse-like cells protect chronic lymphocytic leukemia B cells from spontaneous apoptosis through stromal cell-derived factor-1*. Blood, 2000. 96(8): p. 2655-2663.
129. D'Apuzzo, M., et al., *The chemokine SDF-1, stromal cell-derived factor 1, attracts early stage B cell precursors via the chemokine receptor CXCR4*. Eur J Immunol, 1997. 27(7): p. 1788-93.
130. Burger, J.A., M. Burger, and T.J. Kipps, *Chronic lymphocytic leukemia B cells express functional CXCR4 chemokine receptors that mediate spontaneous migration beneath bone marrow stromal cells*. Blood, 1999. 94(11): p. 3658-3667.
131. Burkle, A., et al., *Overexpression of the CXCR5 chemokine receptor, and its ligand, CXCL13 in B-cell chronic lymphocytic leukemia*. Blood, 2007. 110(9): p. 3316-25.
132. Bleul, C.C., et al., *A highly efficacious lymphocyte chemoattractant, stromal cell-derived factor 1 (SDF-1)*. Journal of Experimental Medicine, 1996. 184(3): p. 1101-9.
133. Burger, J.A., *Blood-derived nurse-like cells protect chronic lymphocytic leukemia B cells from spontaneous apoptosis through stromal cell-derived factor-1*. Blood, 2000. 96: p. 2655-2663.
134. Tsukada, N., et al., *Distinctive features of [ldquo]nurselike[rdquo] cells that differentiate in the context of chronic lymphocytic leukemia*. Blood, 2002. 99: p. 1030-1037.
135. Carlsen, H.S., et al., *Monocyte-like and mature macrophages produce CXCL13 (B cell-attracting chemokine 1) in inflammatory lesions with lymphoid neogenesis*. Blood, 2004. 104(10): p. 3021-7.
136. Allen, C.D., et al., *Germinal center dark and light zone organization is mediated by CXCR4 and CXCR5*. Nat Immunol, 2004. 5(9): p. 943-52.
137. Giannoni, P., et al., *Chronic lymphocytic leukemia nurse-like cells express hepatocyte growth factor receptor (c-MET) and indoleamine 2,3-dioxygenase and display features of immunosuppressive type 2 skewed macrophages*. Haematologica, 2014. 99(6): p. 1078-87.
138. Reynes, M., et al., *Human follicular dendritic cells express CR1, CR2, and CR3 complement receptor antigens*. J Immunol, 1985. 135(4): p. 2687-94.
139. Allen, C.D. and J.G. Cyster, *Follicular dendritic cell networks of primary follicles and germinal centers: phenotype and function*. Semin Immunol, 2008. 20(1): p. 14-25.
140. Pauly, S., et al., *CD137 is expressed by follicular dendritic cells and costimulates B lymphocyte activation in germinal centers*. J Leukoc Biol, 2002. 72(1): p. 35-42.
141. Javazon, E.H., K.J. Beggs, and A.W. Flake, *Mesenchymal stem cells: Paradoxes of passaging*. Experimental Hematology, 2004. 32(5): p. 414-425.

142. Jones, E. and D. McGonagle, *Human bone marrow mesenchymal stem cells in vivo*. *Rheumatology*, 2008. 47(2): p. 126-131.
143. Murray, P.J. and T.A. Wynn, *Protective and pathogenic functions of macrophage subsets*. *Nature Reviews Immunology*, 2011. 11(11): p. 723-37.
144. Zamani, F., et al., *Induction of CD14 Expression and Differentiation to Monocytes or Mature Macrophages in Promyelocytic Cell Lines: New Approach*. *Adv Pharm Bull*, 2013. 3(2): p. 329-32.
145. Mach, F., et al., *Functional CD40 ligand is expressed on human vascular endothelial cells, smooth muscle cells, and macrophages: implications for CD40-CD40 ligand signaling in atherosclerosis*. *Proc Natl Acad Sci U S A*, 1997. 94(5): p. 1931-6.
146. Burger, J.A., *High-level expression of the T-cell chemokines CCL3 and CCL4 by chronic lymphocytic leukemia B cells in nurselike cell cocultures and after BCR stimulation*. *Blood*, 2009. 113: p. 3050-3058.
147. Pedersen, I.M., *Protection of CLL B cells by a follicular dendritic cell line is dependent on induction of Mcl-1*. *Blood*, 2002. 100: p. 1795-1801.
148. Dancescu, M., et al., *Interleukin 4 protects chronic lymphocytic leukemic B cells from death by apoptosis and upregulates Bcl-2 expression*. *Journal of Experimental Medicine*, 1992. 176(5): p. 1319-26.
149. Nwabo Kamdje, A.H., et al., *Role of stromal cell-mediated Notch signaling in CLL resistance to chemotherapy*. *Blood Cancer J*, 2012. 2(5): p. e73.
150. Hegde, G.V., et al., *Hedgehog-induced survival of B-cell chronic lymphocytic leukemia cells in a stromal cell microenvironment: a potential new therapeutic target*. *Mol Cancer Res*, 2008. 6(12): p. 1928-36.
151. Zhang, S., et al., *Targeting chronic lymphocytic leukemia cells with a humanized monoclonal antibody specific for CD44*. *Proc Natl Acad Sci U S A*, 2013. 110(15): p. 6127-32.
152. Aruffo, A., et al., *CD44 is the principal cell surface receptor for hyaluronate*. *Cell*, 1990. 61(7): p. 1303-13.
153. Clark, R.A., et al., *Fibroblast invasive migration into fibronectin/fibrin gels requires a previously uncharacterized dermatan sulfate-CD44 proteoglycan*. *J Invest Dermatol*, 2004. 122(2): p. 266-77.
154. Herishanu, Y., et al., *Activation of CD44, a receptor for extracellular matrix components, protects chronic lymphocytic leukemia cells from spontaneous and drug induced apoptosis through MCL-1*. *Leuk Lymphoma*, 2011. 52(9): p. 1758-69.
155. Hinz, B., et al., *Alpha-smooth muscle actin expression upregulates fibroblast contractile activity*. *Mol Biol Cell*, 2001. 12(9): p. 2730-41.
156. Chang, H.Y., et al., *Diversity, topographic differentiation, and positional memory in human fibroblasts*. *Proc Natl Acad Sci U S A*, 2002. 99(20): p. 12877-82.
157. Goodpaster, T., et al., *An immunohistochemical method for identifying fibroblasts in formalin-fixed, paraffin-embedded tissue*. *J Histochem Cytochem*, 2008. 56(4): p. 347-58.
158. Bandopadhyay, R., et al., *Contractile proteins in pericytes at the blood-brain and blood-retinal barriers*. *J Neurocytol*, 2001. 30(1): p. 35-44.
159. Wang, R., Q. Li, and D.D. Tang, *Role of vimentin in smooth muscle force development*. *Am J Physiol Cell Physiol*, 2006. 291(3): p. C483-9.
160. Touhami, A., et al., *Characterisation of myofibroblasts in fibrovascular tissues of primary and recurrent pterygia*. *Br J Ophthalmol*, 2005. 89(3): p. 269-74.

List of References

161. Skalli, O., et al., *Alpha-smooth muscle actin, a differentiation marker of smooth muscle cells, is present in microfilamentous bundles of pericytes.* J Histochem Cytochem, 1989. 37(3): p. 315-21.
162. Ronty, M.J., et al., *Isoform-specific regulation of the actin-organizing protein palladin during TGF-beta1-induced myofibroblast differentiation.* J Invest Dermatol, 2006. 126(11): p. 2387-96.
163. Grillo, H.C., *Origin of fibroblasts in wound healing. An autoradiographic study of inhibition of cellular proliferation by local x-irradiation.* Ann Surg, 1963. 157: p. 453-67.
164. Stewart, R.J., et al., *The wound fibroblast and macrophage. II: Their origin studied in a human after bone marrow transplantation.* Br J Surg, 1981. 68(2): p. 129-31.
165. Jahoda, C.A. and A.J. Reynolds, *Hair follicle dermal sheath cells: unsung participants in wound healing.* Lancet, 2001. 358(9291): p. 1445-8.
166. Abe, R., et al., *Peripheral blood fibrocytes: differentiation pathway and migration to wound sites.* J Immunol, 2001. 166(12): p. 7556-62.
167. Yang, J. and Y. Liu, *Dissection of key events in tubular epithelial to myofibroblast transition and its implications in renal interstitial fibrosis.* American Journal of Pathology, 2001. 159(4): p. 1465-75.
168. Kim, K.K., et al., *Alveolar epithelial cell mesenchymal transition develops in vivo during pulmonary fibrosis and is regulated by the extracellular matrix.* Proc Natl Acad Sci U S A, 2006. 103(35): p. 13180-5.
169. Rajkumar, V.S., et al., *Shared expression of phenotypic markers in systemic sclerosis indicates a convergence of pericytes and fibroblasts to a myofibroblast lineage in fibrosis.* Arthritis Res Ther, 2005. 7(5): p. R1113-23.
170. Hao, H., et al., *Phenotypic modulation of intima and media smooth muscle cells in fatal cases of coronary artery lesion.* Arterioscler Thromb Vasc Biol, 2006. 26(2): p. 326-32.
171. Yamashita, M., et al., *Role of stromal myofibroblasts in invasive breast cancer: stromal expression of alpha-smooth muscle actin correlates with worse clinical outcome.* Breast Cancer, 2012. 19(2): p. 170-6.
172. Hwang, R.F., et al., *Cancer-associated stromal fibroblasts promote pancreatic tumor progression.* Cancer Research, 2008. 68(3): p. 918-26.
173. Fujita, H., et al., *alpha-Smooth Muscle Actin Expressing Stroma Promotes an Aggressive Tumor Biology in Pancreatic Ductal Adenocarcinoma.* Pancreas, 2010.
174. Olumi, A.F., et al., *Carcinoma-associated fibroblasts direct tumor progression of initiated human prostatic epithelium.* Cancer Research, 1999. 59(19): p. 5002-11.
175. Lee, H.W., et al., *Alpha-smooth muscle actin (ACTA2) is required for metastatic potential of human lung adenocarcinoma.* Clin Cancer Res, 2013. 19(21): p. 5879-89.
176. Gabbiani, G., et al., *Granulation tissue as a contractile organ. A study of structure and function.* Journal of Experimental Medicine, 1972. 135(4): p. 719-34.
177. Darby, I., O. Skalli, and G. Gabbiani, *Alpha-smooth muscle actin is transiently expressed by myofibroblasts during experimental wound healing.* Lab Invest, 1990. 63(1): p. 21-9.
178. Desmouliere, A., et al., *Transforming growth factor-beta 1 induces alpha-smooth muscle actin expression in granulation tissue myofibroblasts and in quiescent and growing cultured fibroblasts.* J Cell Biol, 1993. 122(1): p. 103-11.

179. Hinz, B., et al., ***Mechanical tension controls granulation tissue contractile activity and myofibroblast differentiation.*** American Journal of Pathology, 2001. 159(3): p. 1009-20.
180. Serini, G., et al., ***The fibronectin domain ED-A is crucial for myofibroblastic phenotype induction by transforming growth factor-beta1.*** J Cell Biol, 1998. 142(3): p. 873-81.
181. Vaughan, M.B., E.W. Howard, and J.J. Tomasek, ***Transforming growth factor-beta1 promotes the morphological and functional differentiation of the myofibroblast.*** Exp Cell Res, 2000. 257(1): p. 180-9.
182. Ronnov-Jessen, L. and O.W. Petersen, ***Induction of alpha-smooth muscle actin by transforming growth factor-beta 1 in quiescent human breast gland fibroblasts. Implications for myofibroblast generation in breast neoplasia.*** Lab Invest, 1993. 68(6): p. 696-707.
183. Shen, C.N., Z.D. Burke, and D. Tosh, ***Transdifferentiation, metaplasia and tissue regeneration.*** Organogenesis, 2004. 1(2): p. 36-44.
184. Lawrence, D.A., R. Pircher, and P. Jullien, ***Conversion of a high molecular weight latent beta-TGF from chicken embryo fibroblasts into a low molecular weight active beta-TGF under acidic conditions.*** Biochem Biophys Res Commun, 1985. 133(3): p. 1026-34.
185. Pircher, R., P. Jullien, and D.A. Lawrence, ***Beta-transforming growth factor is stored in human blood platelets as a latent high molecular weight complex.*** Biochem Biophys Res Commun, 1986. 136(1): p. 30-7.
186. Dubois, C.M., et al., ***Processing of transforming growth factor beta 1 precursor by human furin convertase.*** J Biol Chem, 1995. 270(18): p. 10618-24.
187. Unsold, C., et al., ***Latent TGF-beta binding protein LTBP-1 contains three potential extracellular matrix interacting domains.*** J Cell Sci, 2001. 114(Pt 1): p. 187-197.
188. Franzen, P., C.H. Heldin, and K. Miyazono, ***The GS domain of the transforming growth factor-beta type I receptor is important in signal transduction.*** Biochem Biophys Res Commun, 1995. 207(2): p. 682-9.
189. Sekelsky, J.J., et al., ***Genetic characterization and cloning of mothers against dpp, a gene required for decapentaplegic function in Drosophila melanogaster.*** Genetics, 1995. 139(3): p. 1347-58.
190. Savage, C., et al., ***Caenorhabditis elegans genes sma-2, sma-3, and sma-4 define a conserved family of transforming growth factor beta pathway components.*** Proc Natl Acad Sci U S A, 1996. 93(2): p. 790-4.
191. Goumans, M.J., et al., ***TGF-beta1 induces efficient differentiation of human cardiomyocyte progenitor cells into functional cardiomyocytes in vitro.*** Stem Cell Res, 2007. 1(2): p. 138-49.
192. Zhou, S., ***TGF-beta regulates beta-catenin signaling and osteoblast differentiation in human mesenchymal stem cells.*** Journal of Cellular Biochemistry, 2011. 112(6): p. 1651-60.
193. McKinnon, R.D., et al., ***A role for TGF-beta in oligodendrocyte differentiation.*** J Cell Biol, 1993. 121(6): p. 1397-407.
194. Munger, K., et al., ***Transforming growth factor beta 1 regulation of c-myc expression, pRB phosphorylation, and cell cycle progression in keratinocytes.*** Cell Growth Differ, 1992. 3(5): p. 291-8.
195. Serra, R., R.W. Pelton, and H.L. Moses, ***TGF beta 1 inhibits branching morphogenesis and N-myc expression in lung bud organ cultures.*** Development, 1994. 120(8): p. 2153-61.
196. Sun, L., et al., ***Expression of transforming growth factor beta type II receptor leads to reduced malignancy in human breast cancer MCF-7 cells.*** J Biol Chem, 1994. 269(42): p. 26449-55.

List of References

197. Hoosein, N.M., et al., *Differential sensitivity of subclasses of human colon carcinoma cell lines to the growth inhibitory effects of transforming growth factor-beta 1*. Exp Cell Res, 1989. 181(2): p. 442-53.
198. Sing, G.K., et al., *Growth inhibition of a human lymphoma cell line: induction of a transforming growth factor-beta-mediated autocrine negative loop by phorbol myristate acetate*. Cell Growth Differ, 1990. 1(11): p. 549-57.
199. Markowitz, S., et al., *Inactivation of the type II TGF-beta receptor in colon cancer cells with microsatellite instability*. Science, 1995. 268(5215): p. 1336-8.
200. Moses, H.L., et al., *TGF beta regulation of cell proliferation*. Princess Takamatsu Symp, 1994. 24: p. 250-63.
201. Lotz, M., E. Ranheim, and T.J. Kipps, *Transforming growth factor beta as endogenous growth inhibitor of chronic lymphocytic leukemia B cells*. Journal of Experimental Medicine, 1994. 179(3): p. 999-1004.
202. Israels, L.G., et al., *Role of transforming growth factor-beta in chronic lymphocytic leukemia*. Leuk Res, 1993. 17(1): p. 81-7.
203. DeCoteau, J.F., et al., *Loss of functional cell surface transforming growth factor beta (TGF-beta) type 1 receptor correlates with insensitivity to TGF-beta in chronic lymphocytic leukemia*. Proc Natl Acad Sci U S A, 1997. 94(11): p. 5877-81.
204. Oberhammer, F.A., et al., *Chromatin condensation during apoptosis is accompanied by degradation of lamin A+B, without enhanced activation of cdc2 kinase*. J Cell Biol, 1994. 126(4): p. 827-37.
205. Tone, S., et al., *Three distinct stages of apoptotic nuclear condensation revealed by time-lapse imaging, biochemical and electron microscopy analysis of cell-free apoptosis*. Exp Cell Res, 2007. 313(16): p. 3635-44.
206. Placzek, W.J., et al., *A survey of the anti-apoptotic Bcl-2 subfamily expression in cancer types provides a platform to predict the efficacy of Bcl-2 antagonists in cancer therapy*. Cell Death Dis, 2010. 1: p. e40.
207. Kitada, S., et al., *Expression and location of pro-apoptotic Bcl-2 family protein BAD in normal human tissues and tumor cell lines*. American Journal of Pathology, 1998. 152(1): p. 51-61.
208. Griffiths, G.J., et al., *Cell damage-induced conformational changes of the pro-apoptotic protein Bak in vivo precede the onset of apoptosis*. J Cell Biol, 1999. 144(5): p. 903-14.
209. Hanada, M., et al., *Bcl-2 Gene Hypomethylation and High-Level Expression in B-Cell Chronic Lymphocytic-Leukemia*. Blood, 1993. 82(6): p. 1820-1828.
210. Campas, C., et al., *Bcl-2 inhibitors induce apoptosis in chronic lymphocytic leukemia cells*. Experimental Hematology, 2006. 34(12): p. 1663-1669.
211. Kitada, S., et al., *Expression of apoptosis-regulating proteins in chronic lymphocytic leukemia: Correlations with in vitro and in vivo chemoresponses*. Blood, 1998. 91(9): p. 3379-3389.
212. Sanz, L., et al., *Bcl-2 family gene modulation during spontaneous apoptosis of B-chronic lymphocytic leukemia cells*. Biochem Biophys Res Commun, 2004. 315(3): p. 562-7.
213. Morales, A.A., et al., *High expression of bfl-1 contributes to the apoptosis resistant phenotype in B-cell chronic lymphocytic leukemia*. Int J Cancer, 2005. 113(5): p. 730-7.

214. Pedersen, I.M., et al., *Protection of CLL B cells by a follicular dendritic cell line is dependent on induction of Mcl-1*. *Blood*, 2002. 100(5): p. 1795-801.
215. Quiroga, M.P., et al., *B-cell antigen receptor signaling enhances chronic lymphocytic leukemia cell migration and survival: specific targeting with a novel spleen tyrosine kinase inhibitor, R406*. *Blood*, 2009. 114(5): p. 1029-37.
216. Schamel, W.W. and M. Reth, *Monomeric and oligomeric complexes of the B cell antigen receptor*. *Immunity*, 2000. 13(1): p. 5-14.
217. Flaswinkel, H. and M. Reth, *Dual role of the tyrosine activation motif of the Ig-alpha protein during signal transduction via the B cell antigen receptor*. *EMBO J*, 1994. 13(1): p. 83-9.
218. Kraus, M., et al., *Interference with immunoglobulin (Ig)alpha immunoreceptor tyrosine-based activation motif (ITAM) phosphorylation modulates or blocks B cell development, depending on the availability of an Igbeta cytoplasmic tail*. *Journal of Experimental Medicine*, 2001. 194(4): p. 455-69.
219. Brdicka, T., et al., *Intramolecular regulatory switch in ZAP-70: analogy with receptor tyrosine kinases*. *Mol Cell Biol*, 2005. 25(12): p. 4924-33.
220. Chen, L., et al., *SYK inhibition modulates distinct PI3K/AKT- dependent survival pathways and cholesterol biosynthesis in diffuse large B cell lymphomas*. *Cancer Cell*, 2013. 23(6): p. 826-38.
221. Chantry, D., et al., *p110delta, a novel phosphatidylinositol 3-kinase catalytic subunit that associates with p85 and is expressed predominantly in leukocytes*. *J Biol Chem*, 1997. 272(31): p. 19236-41.
222. Persad, S., et al., *Regulation of protein kinase B/Akt-serine 473 phosphorylation by integrin-linked kinase: critical roles for kinase activity and amino acids arginine 211 and serine 343*. *J Biol Chem*, 2001. 276(29): p. 27462-9.
223. Kane, L.P., et al., *Induction of NF-kappaB by the Akt/PKB kinase*. *Curr Biol*, 1999. 9(11): p. 601-4.
224. Muzio, M., *Constitutive activation of distinct BCR-signaling pathways in a subset of CLL patients: a molecular signature of anergy*. *Blood*, 2008. 112: p. 188-195.
225. Kawachi, K., T. Ogasawara, and M. Yasuyama, *Activation of extracellular signal-regulated kinase through B-cell antigen receptor in B-cell chronic lymphocytic leukemia*. *Int J Hematol*, 2002. 75(5): p. 508-13.
226. Petlickovski, A., et al., *Sustained signaling through the B-cell receptor induces Mcl-1 and promotes survival of chronic lymphocytic leukemia B cells*. *Blood*, 2005. 105(12): p. 4820-7.
227. D'Ambrosio, D., K.L. Hippen, and J.C. Cambier, *Distinct mechanisms mediate SHC association with the activated and resting B cell antigen receptor*. *Eur J Immunol*, 1996. 26(8): p. 1960-5.
228. Pede, V., et al., *Expression of ZAP70 in chronic lymphocytic leukaemia activates NF-kappaB signalling*. *Br J Haematol*, 2013. 163(5): p. 621-30.
229. Tare, R.S., et al., *Isolation, differentiation, and characterisation of skeletal stem cells from human bone marrow in vitro and in vivo*. *Methods Mol Biol*, 2012. 816: p. 83-99.
230. Abe, M., et al., *An assay for transforming growth factor-beta using cells transfected with a plasminogen activator inhibitor-1 promoter-luciferase construct*. *Anal Biochem*, 1994. 216(2): p. 276-84.

List of References

231. Plate, J.M., *PI3-kinase regulates survival of chronic lymphocytic leukemia B-cells by preventing caspase 8 activation*. *Leuk Lymphoma*, 2004. 45(8): p. 1519-29.
232. Davies, B.R., et al., *AZD6244 (ARRY-142886), a potent inhibitor of mitogen-activated protein kinase/extracellular signal-regulated kinase kinase 1/2 kinases: mechanism of action in vivo, pharmacokinetic/pharmacodynamic relationship, and potential for combination in preclinical models*. *Molecular Cancer Therapeutics*, 2007. 6(8): p. 2209-19.
233. Rauert-Wunderlich, H., et al., *The IKK inhibitor Bay 11-7082 induces cell death independent from inhibition of activation of NFkappaB transcription factors*. *Plos One*, 2013. 8(3): p. e59292.
234. Kudlacz, E., et al., *The novel JAK-3 inhibitor CP-690550 is a potent immunosuppressive agent in various murine models*. *Am J Transplant*, 2004. 4(1): p. 51-7.
235. Moutasim, K.A., et al., *Betel-derived alkaloid up-regulates keratinocyte alphavbeta6 integrin expression and promotes oral submucous fibrosis*. *J Pathol*, 2011. 223(3): p. 366-77.
236. Gibson, S.E., et al., *Reassessment of small lymphocytic lymphoma in the era of monoclonal B-cell lymphocytosis*. *Haematologica*, 2011. 96(8): p. 1144-52.
237. Goffin, J.M., et al., *Focal adhesion size controls tension-dependent recruitment of alpha-smooth muscle actin to stress fibers*. *J Cell Biol*, 2006. 172(2): p. 259-68.
238. Fakan, F., L. Boudova, and A. Skalova, *[Immunohistochemical detection of follicular dendritic cells in the diagnosis of small B-cell lymphomas]*. *Cesk Patol*, 2003. 39(3): p. 96-101.
239. Skalli, O., et al., *Myofibroblasts from diverse pathologic settings are heterogeneous in their content of actin isoforms and intermediate filament proteins*. *Lab Invest*, 1989. 60(2): p. 275-85.
240. Brentnall, T.A., et al., *Arousal of cancer-associated stroma: overexpression of palladin activates fibroblasts to promote tumor invasion*. *Plos One*, 2012. 7(1): p. e30219.
241. Hus, I., et al., *The clinical significance of ZAP-70 and CD38 expression in B-cell chronic lymphocytic leukaemia*. *Annals of Oncology*, 2006. 17(4): p. 683-90.
242. Wang, M., et al., *miRNA analysis in B-cell chronic lymphocytic leukaemia: proliferation centres characterized by low miR-150 and high BIC/miR-155 expression*. *J Pathol*, 2008. 215(1): p. 13-20.
243. Tsimberidou, A.M., et al., *Clinical outcomes and prognostic factors in patients with Richter's syndrome treated with chemotherapy or chemoimmunotherapy with or without stem-cell transplantation*. *J Clin Oncol*, 2006. 24(15): p. 2343-51.
244. Marsh, D., et al., *alpha vbeta 6 Integrin promotes the invasion of morphoeic basal cell carcinoma through stromal modulation*. *Cancer Research*, 2008. 68(9): p. 3295-303.
245. Lin, G., et al., *Tissue distribution of mesenchymal stem cell marker Stro-1*. *Stem Cells Dev*, 2011. 20(10): p. 1747-52.
246. Simmons, P.J. and B. Torok-Storb, *Identification of stromal cell precursors in human bone marrow by a novel monoclonal antibody, STRO-1*. *Blood*, 1991. 78(1): p. 55-62.
247. Stewart, K., et al., *Further characterization of cells expressing STRO-1 in cultures of adult human bone marrow stromal cells*. *Journal of Bone and Mineral Research*, 1999. 14(8): p. 1345-56.

248. Gronthos, S., et al., *The STRO-1+ fraction of adult human bone marrow contains the osteogenic precursors*. Blood, 1994. 84(12): p. 4164-73.
249. Zhang, Y., et al., *Germinal center B cells govern their own fate via antibody feedback*. Journal of Experimental Medicine, 2013. 210(3): p. 457-64.
250. Toccanier-Pelte, M.F., et al., *Characterization of stromal cells with myoid features in lymph nodes and spleen in normal and pathologic conditions*. American Journal of Pathology, 1987. 129(1): p. 109-18.
251. Togoo, K., Y. Takahama, and K. Takada, *Alpha-smooth muscle actin expression identifies subpopulations of mouse lymph node non-hematopoietic cells*. Biochem Biophys Res Commun, 2014. 449(2): p. 241-7.
252. Ruan, J., et al., *Magnitude of stromal hemangiogenesis correlates with histologic subtype of non-Hodgkin's lymphoma*. Clin Cancer Res, 2006. 12(19): p. 5622-31.
253. Papadopoulos, N., et al., *Differential expression of alpha-smooth muscle actin molecule in a subset of bone marrow stromal cells, in b-cell chronic lymphocytic leukemia, autoimmune disorders and normal fetuses*. Eur J Gynaecol Oncol, 2001. 22(6): p. 447-50.
254. Roberts, J.A., et al., *Smoothelin and caldesmon are reliable markers for distinguishing muscularis propria from desmoplasia: a critical distinction for accurate staging colorectal adenocarcinoma*. Int J Clin Exp Pathol, 2014. 7(2): p. 792-6.
255. Golbar, H.M., et al., *Immunohistochemical characterization of macrophages and myofibroblasts in alpha-Naphthylisothiocyanate (ANIT)--induced bile duct injury and subsequent fibrogenesis in rats*. Toxicologic Pathology, 2011. 39(5): p. 795-808.
256. Park, S.R., R.O. Oreffo, and J.T. Triffitt, *Interconversion potential of cloned human marrow adipocytes in vitro*. Bone, 1999. 24(6): p. 549-54.
257. Mostafa, N.Z., et al., *Osteogenic differentiation of human mesenchymal stem cells cultured with dexamethasone, vitamin D3, basic fibroblast growth factor, and bone morphogenetic protein-2*. Connect Tissue Res, 2012. 53(2): p. 117-31.
258. Lewis, M.P., et al., *Tumour-derived TGF-beta1 modulates myofibroblast differentiation and promotes HGF/SF-dependent invasion of squamous carcinoma cells*. Br J Cancer, 2004. 90(4): p. 822-32.
259. Hawinkels, L.J., et al., *Interaction with colon cancer cells hyperactivates TGF-beta signaling in cancer-associated fibroblasts*. Oncogene, 2014. 33(1): p. 97-107.
260. Hung, S.C., et al., *Alpha-smooth muscle actin expression and structure integrity in chondrogenesis of human mesenchymal stem cells*. Cell Tissue Res, 2006. 324(3): p. 457-66.
261. Apollonio, B., et al., *Targeting B-cell anergy in chronic lymphocytic leukemia*. Blood, 2013. 121(19): p. 3879-88, S1-8.
262. Krysov, S., et al., *Surface IgM stimulation induces MEK1/2-dependent MYC expression in chronic lymphocytic leukemia cells*. Blood, 2012. 119(1): p. 170-179.
263. Kellermann, M.G., et al., *Mutual paracrine effects of oral squamous cell carcinoma cells and normal oral fibroblasts: induction of fibroblast to myofibroblast transdifferentiation and modulation of tumor cell proliferation*. Oral Oncol, 2008. 44(5): p. 509-17.

List of References

264. Burgess, M., et al., *CCL2 and CXCL2 enhance survival of primary chronic lymphocytic leukemia cells in vitro*. *Leuk Lymphoma*, 2012. 53(10): p. 1988-98.
265. Kremer, J.P., et al., *B-cell chronic lymphocytic leukaemia cells express and release transforming growth factor-beta*. *Br J Haematol*, 1992. 80(4): p. 480-7.
266. Kutz, S.M., et al., *TGF-beta1-induced PAI-1 gene expression requires MEK activity and cell-to-substrate adhesion*. *J Cell Sci*, 2001. 114(Pt 21): p. 3905-14.
267. Pan, B.T., et al., *Electron microscopic evidence for externalization of the transferrin receptor in vesicular form in sheep reticulocytes*. *J Cell Biol*, 1985. 101(3): p. 942-8.
268. Valadi, H., et al., *Exosome-mediated transfer of mRNAs and microRNAs is a novel mechanism of genetic exchange between cells*. *Nat Cell Biol*, 2007. 9(6): p. 654-9.
269. Caby, M.P., et al., *Exosomal-like vesicles are present in human blood plasma*. *Int Immunol*, 2005. 17(7): p. 879-87.
270. Ogawa, Y., et al., *Proteomic analysis of two types of exosomes in human whole saliva*. *Biol Pharm Bull*, 2011. 34(1): p. 13-23.
271. Mineo, M., et al., *Exosomes released by K562 chronic myeloid leukemia cells promote angiogenesis in a Src-dependent fashion*. *Angiogenesis*, 2012. 15(1): p. 33-45.
272. Corrado, C., et al., *Exosome-mediated crosstalk between chronic myelogenous leukemia cells and human bone marrow stromal cells triggers an interleukin 8-dependent survival of leukemia cells*. *Cancer Lett*, 2014. 348(1-2): p. 71-6.
273. Huan, J., et al., *RNA trafficking by acute myelogenous leukemia exosomes*. *Cancer Research*, 2013. 73(2): p. 918-29.
274. Tsujino, T., et al., *Stromal myofibroblasts predict disease recurrence for colorectal cancer*. *Clin Cancer Res*, 2007. 13(7): p. 2082-90.
275. Goicoechea, S.M., et al., *Isoform-specific upregulation of palladin in human and murine pancreas tumors*. *Plos One*, 2010. 5(4): p. e10347.
276. Gu, J., et al., *Gastric cancer exosomes trigger differentiation of umbilical cord derived mesenchymal stem cells to carcinoma-associated fibroblasts through TGF-beta/Smad pathway*. *Plos One*, 2012. 7(12): p. e52465.
277. Cho, J.A., et al., *Exosomes from breast cancer cells can convert adipose tissue-derived mesenchymal stem cells into myofibroblast-like cells*. *Int J Oncol*, 2012. 40(1): p. 130-8.
278. Liu, Z., et al., *MicroRNA-146a modulates TGF-beta1-induced phenotypic differentiation in human dermal fibroblasts by targeting SMAD4*. *Arch Dermatol Res*, 2012. 304(3): p. 195-202.
279. Yao, Q., et al., *Micro-RNA-21 regulates TGF-beta-induced myofibroblast differentiation by targeting PDCD4 in tumor-stroma interaction*. *Int J Cancer*, 2011. 128(8): p. 1783-92.
280. Cushing, M.C., et al., *Fibroblast growth factor represses Smad-mediated myofibroblast activation in aortic valvular interstitial cells*. *FASEB J*, 2008. 22(6): p. 1769-77.
281. Kay, N.E., et al., *B-CLL cells are capable of synthesis and secretion of both pro- and anti-angiogenic molecules*. *Leukemia*, 2002. 16(5): p. 911-9.
282. Krejci, P., et al., *FGF-2 abnormalities in B cell chronic lymphocytic and chronic myeloid leukemias*. *Leukemia*, 2001. 15(2): p. 228-37.

283. Yang, Z.Z., et al., *Soluble and membrane-bound TGF-beta-mediated regulation of intratumoral T cell differentiation and function in B-cell non-Hodgkin lymphoma*. Plos One, 2013. 8(3): p. e59456.
284. Aubry, J.P., et al., *Annexin V used for measuring apoptosis in the early events of cellular cytotoxicity*. Cytometry, 1999. 37(3): p. 197-204.
285. Fischer, K., R. Andreesen, and A. Mackensen, *An improved flow cytometric assay for the determination of cytotoxic T lymphocyte activity*. J Immunol Methods, 2002. 259(1-2): p. 159-69.
286. Coscia, M., et al., *IGHV unmutated CLL B cells are more prone to spontaneous apoptosis and subject to environmental prosurvival signals than mutated CLL B cells*. Leukemia, 2011. 25(5): p. 828-37.
287. Zhang, W., et al., *Stromal control of cystine metabolism promotes cancer cell survival in chronic lymphocytic leukaemia*. Nat Cell Biol, 2012. 14(3): p. 276-86.
288. Oltra, A.M., et al., *Antioxidant enzyme activities and the production of MDA and 8-oxo-dG in chronic lymphocytic leukemia*. Free Radic Biol Med, 2001. 30(11): p. 1286-92.
289. Silber, R., et al., *Glutathione depletion in chronic lymphocytic leukemia B lymphocytes*. Blood, 1992. 80(8): p. 2038-43.
290. Al-Harbi, S., et al., *An antiapoptotic BCL-2 family expression index predicts the response of chronic lymphocytic leukemia to ABT-737*. Blood, 2011. 118(13): p. 3579-90.
291. Paterson, A., et al., *Mechanisms and clinical significance of BIM phosphorylation in chronic lymphocytic leukemia*. Blood, 2012. 119(7): p. 1726-36.
292. Janumyan, Y.M., et al., *Bcl-xL/Bcl-2 coordinately regulates apoptosis, cell cycle arrest and cell cycle entry*. EMBO J, 2003. 22(20): p. 5459-70.
293. Wei, M.C., et al., *Proapoptotic BAX and BAK: a requisite gateway to mitochondrial dysfunction and death*. Science, 2001. 292(5517): p. 727-30.
294. Han, J., et al., *Interrelated roles for Mcl-1 and BIM in regulation of TRAIL-mediated mitochondrial apoptosis*. J Biol Chem, 2006. 281(15): p. 10153-63.
295. Kharaziha, P., et al., *Targeting of distinct signaling cascades and cancer-associated fibroblasts define the efficacy of Sorafenib against prostate cancer cells*. Cell Death Dis, 2012. 3: p. e262.
296. Los, M., et al., *Activation and caspase-mediated inhibition of PARP: a molecular switch between fibroblast necrosis and apoptosis in death receptor signaling*. Mol Biol Cell, 2002. 13(3): p. 978-88.
297. Fernandes-Alnemri, T., et al., *Mch3, a novel human apoptotic cysteine protease highly related to CPP32*. Cancer Research, 1995. 55(24): p. 6045-52.
298. Nishio, M., et al., *Nurselike cells express BAFF and APRIL, which can promote survival of chronic lymphocytic leukemia cells via a paracrine pathway distinct from that of SDF-1 alpha*. Blood, 2005. 106(3): p. 1012-20.
299. Chen, R., et al., *Homoharringtonine reduced Mcl-1 expression and induced apoptosis in chronic lymphocytic leukemia*. Blood, 2011. 117(1): p. 156-64.
300. Pepper, C., et al., *Mcl-1 expression has in vitro and in vivo significance in chronic lymphocytic leukemia and is associated with other poor prognostic markers*. Blood, 2008. 112(9): p. 3807-17.

List of References

301. Balakrishnan, K., et al., *AT-101 induces apoptosis in CLL B cells and overcomes stromal cell-mediated Mcl-1 induction and drug resistance*. Blood, 2009. 113(1): p. 149-53.
302. Longo, P.G., et al., *The Akt/Mcl-1 pathway plays a prominent role in mediating antiapoptotic signals downstream of the B-cell receptor in chronic lymphocytic leukemia B cells*. Blood, 2008. 111(2): p. 846-55.
303. Iglesias-Serret, D., et al., *Regulation of the proapoptotic BH3-only protein BIM by glucocorticoids, survival signals and proteasome in chronic lymphocytic leukemia cells*. Leukemia, 2007. 21(2): p. 281-7.
304. Czabotar, P.E., et al., *Structural insights into the degradation of Mcl-1 induced by BH3 domains*. Proc Natl Acad Sci U S A, 2007. 104(15): p. 6217-22.
305. Sharma, A., et al., *BECN1 and BIM interactions with MCL-1 determine fludarabine resistance in leukemic B cells*. Cell Death Dis, 2013. 4: p. e628.
306. Huang, H.M., C.J. Huang, and J.J. Yen, *Mcl-1 is a common target of stem cell factor and interleukin-5 for apoptosis prevention activity via MEK/MAPK and PI-3K/Akt pathways*. Blood, 2000. 96(5): p. 1764-71.
307. Le Gouill, S., et al., *VEGF induces Mcl-1 up-regulation and protects multiple myeloma cells against apoptosis*. Blood, 2004. 104(9): p. 2886-92.
308. Liu, H., et al., *Serine phosphorylation of STAT3 is essential for Mcl-1 expression and macrophage survival*. Blood, 2003. 102(1): p. 344-52.
309. Allen, J.C., et al., *c-Abl regulates Mcl-1 gene expression in chronic lymphocytic leukemia cells*. Blood, 2011. 117(8): p. 2414-22.
310. Lwin, T., et al., *Follicular dendritic cell-dependent drug resistance of non-Hodgkin lymphoma involves cell adhesion-mediated Bim down-regulation through induction of microRNA-181a*. Blood, 2010. 116(24): p. 5228-36.
311. Luciano, F., et al., *Phosphorylation of Bim-EL by Erk1/2 on serine 69 promotes its degradation via the proteasome pathway and regulates its proapoptotic function*. Oncogene, 2003. 22(43): p. 6785-93.
312. Buggins, A.G., et al., *Interaction with vascular endothelium enhances survival in primary chronic lymphocytic leukemia cells via NF-kappaB activation and de novo gene transcription*. Cancer Research, 2010. 70(19): p. 7523-33.
313. Pepper, C., et al., *Retinoid-induced apoptosis in B-cell chronic lymphocytic leukaemia cells is mediated through caspase-3 activation and is independent of p53, the retinoic acid receptor, and differentiation*. Eur J Haematol, 2002. 69(4): p. 227-35.
314. Battle, T.E., J. Arbiser, and D.A. Frank, *The natural product honokiol induces caspase-dependent apoptosis in B-cell chronic lymphocytic leukemia (B-CLL) cells*. Blood, 2005. 106(2): p. 690-7.
315. Endo, T., et al., *BAFF and APRIL support chronic lymphocytic leukemia B-cell survival through activation of the canonical NF-kappaB pathway*. Blood, 2007. 109(2): p. 703-10.
316. Tomasek, J.J., et al., *Myofibroblasts and mechano-regulation of connective tissue remodelling*. Nat Rev Mol Cell Biol, 2002. 3(5): p. 349-63.
317. de la Fuente, M.T., et al., *Fibronectin interaction with alpha4beta1 integrin prevents apoptosis in B cell chronic lymphocytic leukemia: correlation with Bcl-2 and Bax*. Leukemia, 1999. 13(2): p. 266-74.

318. Lagneaux, L., et al., *Chronic lymphocytic leukemic B cells but not normal B cells are rescued from apoptosis by contact with normal bone marrow stromal cells*. *Blood*, 1998. 91(7): p. 2387-96.
319. Rawstron, A.C., et al., *Quantitation of minimal disease levels in chronic lymphocytic leukemia using a sensitive flow cytometric assay improves the prediction of outcome and can be used to optimize therapy*. *Blood*, 2001. 98(1): p. 29-35.
320. Boysen, J., et al., *The tumor suppressor axis p53/miR-34a regulates Axl expression in B-cell chronic lymphocytic leukemia: implications for therapy in p53-defective CLL patients*. *Leukemia*, 2014. 28(2): p. 451-5.
321. Gobessi, S., et al., *Inhibition of constitutive and BCR-induced Syk activation downregulates Mcl-1 and induces apoptosis in chronic lymphocytic leukemia B cells*. *Leukemia*, 2009. 23(4): p. 686-97.
322. Bhalla, S., et al., *The novel anti-MEK small molecule AZD6244 induces BIM-dependent and AKT-independent apoptosis in diffuse large B-cell lymphoma*. *Blood*, 2011. 118(4): p. 1052-61.
323. Lannutti, B.J., et al., *CAL-101, a p110delta selective phosphatidylinositol-3-kinase inhibitor for the treatment of B-cell malignancies, inhibits PI3K signaling and cellular viability*. *Blood*, 2011. 117(2): p. 591-4.
324. Damle, R.N., et al., *T-cell independent, B-cell receptor-mediated induction of telomerase activity differs among IGHV mutation-based subgroups of chronic lymphocytic leukemia patients*. *Blood*, 2012. 120(12): p. 2438-49.
325. Bauerle, K.T., R.E. Schweppe, and B.R. Haugen, *Inhibition of nuclear factor-kappa B differentially affects thyroid cancer cell growth, apoptosis, and invasion*. *Mol Cancer*, 2010. 9: p. 117.
326. Ghoreschi, K., et al., *Modulation of innate and adaptive immune responses by tofacitinib (CP-690,550)*. *J Immunol*, 2011. 186(7): p. 4234-43.
327. Honigberg, L.A., et al., *The Bruton tyrosine kinase inhibitor PCI-32765 blocks B-cell activation and is efficacious in models of autoimmune disease and B-cell malignancy*. *Proc Natl Acad Sci U S A*, 2010. 107(29): p. 13075-80.
328. Herman, S.E., et al., *Bruton tyrosine kinase represents a promising therapeutic target for treatment of chronic lymphocytic leukemia and is effectively targeted by PCI-32765*. *Blood*, 2011. 117(23): p. 6287-96.
329. Ringshausen, I., et al., *Constitutively activated phosphatidylinositol-3 kinase (PI-3K) is involved in the defect of apoptosis in B-CLL: association with protein kinase Cdelta*. *Blood*, 2002. 100(10): p. 3741-8.
330. Clayton, E., et al., *A crucial role for the p110delta subunit of phosphatidylinositol 3-kinase in B cell development and activation*. *Journal of Experimental Medicine*, 2002. 196(6): p. 753-63.
331. Ikeda, H., et al., *PI3K/p110delta is a novel therapeutic target in multiple myeloma*. *Blood*, 2010. 116(9): p. 1460-8.
332. Vlahos, C.J., et al., *A specific inhibitor of phosphatidylinositol 3-kinase, 2-(4-morpholinyl)-8-phenyl-4H-1-benzopyran-4-one (LY294002)*. *J Biol Chem*, 1994. 269(7): p. 5241-8.
333. Kim, Y.H., et al., *LY294002 inhibits LPS-induced NO production through a inhibition of NF-kappaB activation: independent mechanism of phosphatidylinositol 3-kinase*. *Immunol Lett*, 2005. 99(1): p. 45-50.
334. Hoellenriegel, J., et al., *Selective, novel spleen tyrosine kinase (Syk) inhibitors suppress chronic lymphocytic leukemia B-cell activation and migration*. *Leukemia*, 2012. 26(7): p. 1576-83.

List of References

335. Fedorchenko, O., et al., *CD44 regulates the apoptotic response and promotes disease development in chronic lymphocytic leukemia*. *Blood*, 2013. 121(20): p. 4126-36.
336. Jalkanen, S. and M. Jalkanen, *Lymphocyte CD44 binds the COOH-terminal heparin-binding domain of fibronectin*. *J Cell Biol*, 1992. 116(3): p. 817-25.
337. Tsang, E., et al., *Molecular mechanism of the Syk activation switch*. *J Biol Chem*, 2008. 283(47): p. 32650-9.
338. Cheng, S., et al., *BTK inhibition targets in vivo CLL proliferation through its effects on B-cell receptor signaling activity*. *Leukemia*, 2014. 28(3): p. 649-57.
339. Muzio, M., et al., *Expression and function of toll like receptors in chronic lymphocytic leukaemia cells*. *Br J Haematol*, 2009. 144(4): p. 507-16.
340. Tomlinson, M.G., et al., *Expression and function of Tec, Itk, and Btk in lymphocytes: evidence for a unique role for Tec*. *Mol Cell Biol*, 2004. 24(6): p. 2455-66.
341. Ringshausen, I., et al., *Constitutive activation of the MAPkinase p38 is critical for MMP-9 production and survival of B-CLL cells on bone marrow stromal cells*. *Leukemia*, 2004. 18(12): p. 1964-70.
342. de Toter, D., et al., *The opposite effects of IL-15 and IL-21 on CLL B cells correlate with differential activation of the JAK/STAT and ERK1/2 pathways*. *Blood*, 2008. 111(2): p. 517-24.
343. Furman, R.R., et al., *Modulation of NF-kappa B activity and apoptosis in chronic lymphocytic leukemia B cells*. *J Immunol*, 2000. 164(4): p. 2200-6.
344. Lutzny, G., et al., *Protein kinase c-beta-dependent activation of NF-kappaB in stromal cells is indispensable for the survival of chronic lymphocytic leukemia B cells in vivo*. *Cancer Cell*, 2013. 23(1): p. 77-92.
345. Cuni, S., et al., *A sustained activation of PI3K/NF-kappaB pathway is critical for the survival of chronic lymphocytic leukemia B cells*. *Leukemia*, 2004. 18(8): p. 1391-400.
346. Amrein, L., et al., *The phosphatidylinositol-3 kinase I inhibitor BKM120 induces cell death in B-chronic lymphocytic leukemia cells in vitro*. *Int J Cancer*, 2013. 133(1): p. 247-52.
347. Johnson, A.J., et al., *Characterization of the TCL-1 transgenic mouse as a preclinical drug development tool for human chronic lymphocytic leukemia*. *Blood*, 2006. 108(4): p. 1334-8.
348. Kraman, M., et al., *Suppression of antitumor immunity by stromal cells expressing fibroblast activation protein-alpha*. *Science*, 2010. 330(6005): p. 827-30.
349. Santos, A.M., et al., *Targeting fibroblast activation protein inhibits tumor stromagenesis and growth in mice*. *Journal of Clinical Investigation*, 2009. 119(12): p. 3613-25.